Université catholique de Louvain

Earth and Life Institute - *Agronomy,* Crop physiology
and plant breeding

and

Ghent University

Faculty of Sciences, Department of Plant Biotechnology
and Bioinformatics, VIB - Plant Systems Biology

Comparative study of molecular mechanisms underlying *Arabidopsis* and cereals root architecture

This thesis is submitted as fulfilment of the requirements for the degrees of Docteur en Sciences agronomiques et Ingénierie biologique (UCL) and of Doctor in Sciences (UGent).

Beata Orman-Ligeza

Promoters: Prof. Xavier Draye

Prof. Tom Beeckman

Orman-Ligeza, B. (2015) “Comparative study of molecular mechanisms underlying *Arabidopsis* and cereals root architecture”. PhD Thesis, Université catholique de Louvain, Louvain-la-Neuve and Ghent University, Ghent, Belgium

The authors and promoters give the authorization to consult and copy parts of this work for personal use only. Every other use is subject to the copyright laws. Permission to reproduce any material contained in this work should be obtained from the author.

Beata Orman-Ligeza was supported by FWO (Flanders Research Foundation, project G0273.13N), a short-term COST Action TD0801 and the FRIA (Fonds pour la Recherche dans l’Agriculture et l’Industrie)

Promoters

Prof. Xavier Draye

Earth and Life Institute – Agronomy, Université catholique de Louvain, Belgium

Prof. Tom Beeckman

Department of Plant Biotechnology and Genetics, Ghent University

Promotion commission

Prof. Bruno Delvaux **(chair)**

Earth and Life Institute – Agronomy, Université catholique de Louvain, Belgium

Prof. Malcolm Bennett

The Plant and Crop Sciences Division, The University of Nottingham, UK

Prof. Henri Batoko

Institut des Sciences de la Vie, Université catholique de Louvain, Belgium

Prof. François Chaumont

Institut des Sciences de la Vie, Université catholique de Louvain, Belgium

Prof. Sofie Goormachtig

Department of Plant Biotechnology and Genetics, Ghent University, Belgium

Prof. Ive de Smet

Department of Plant Biotechnology and Genetics, Ghent University, Belgium

SUMMARY

Plant roots are required to anchor the plant in the soil and to acquire water and nutrients. Root branching contributes largely to the morphological plasticy of the root system in response to various biotic and abiotic stimuli. Our current understanding of lateral root (LR) formation stems largely from studies of the plant *Arabidopsis thaliana (L)*. Now is the time to transfer this knowledge to economically important crops, such as *Hordeum vulgare* (barley).

Auxin is an important plant hormone involved in LR development and root gravitropism. In this thesis, an *in silico* translational approach was employed to identify selected auxin-related genes in barley (*Hordeum vulgare L.*). We focused our work on auxin transporters that are involved in plant response to environmental stimuli. *AUX1* and *LAX3* were identified in barley and subsequently characterised. These experiments revealed the maintenance of AUX/LAX developmental function between highly divergent plant species.

Abscisic acid (ABA) is another plant hormone known to modulate LR development and to regulate responses to environmental stimuli. We demonstrated that ABA response pathways act downstream of water deficit in the LR formation root zone, that ABA is likely to mediate LR repression through auxin-dependent pathways and that it attenuates the oscillatory network operating in the basal meristem. Those results can be interpreted as root branching adaptation to local soil porosity.

Reactive oxygen species (ROS) were recently proposed to contribute to auxin-mediated LR formation, however the nature of their involvement remains elusive. We show that hydrogen peroxide (H_2O_2) and superoxide (O^{2-}) are repeatably present within emerging LR. Subsequently, we show that H_2O_2 accumulates in middle lamellae of cells overlying LR primordia and progressively creates a fine layer around the emerging primordia. Our results lead us to propose that ROS contribute to LR emergence by influencing cell wall plasticity. We finally show that the *Respiratory burst oxidase homologs* (*Rboh*) gene family are likely contributors to a fine-tuned extracellular ROS balance during LR emergence.

ACKNOWLEDGEMENTS

I would first like to express the deepest appreciation to my PhD advisors. To Prof. Xavier Draye, who has an attitude and the substance of a genius. Equally, to Prof. Tom Beeckman, whose spirit of adventure and enthusiasm for the “underlying mechanisms” had lasting effect. Without their guidance and support this thesis would not have been possible.

I am also grateful to Prof. Malcolm Bennett from The Plant and Crop Sciences Division (The University of Nottingham, UK) for his support, advice and great ideas. A special thank to Dr Ranjan Swarup for his help and kindness.

I wish to express my sincere thanks to past and present ECAV and ISV lab members for the nice atmosphere during all those years. In particular, Prof. Marc Boutry, Prof. Francois Chaumont and Prof. Henri Batoko for their kind support and access to their endless resources. I have to offer a special thanks to Benjamin Lobet who was instrumental to my PhD during the last days.

I would also like to thank The Root Group at VIB. It has been an incredible experience to be a part of such an international community within the group and the PSB department. Particularly, special thanks to Dr Boris Parizot for his continued enthusiasm and encouragement.

I am extremely grateful to Robbie Waugh, David Marshall and Jennifer Stephens from The James Hutton Institute, UK. The time I spent working there was invaluable to my PhD.

I also thank the FRIA (FNRS), IAP (BELSPO) and FWO founding at The Gent University for funding this PhD.

Lastly I thank my family and friends for being supportive during my PhD adventure.

I dedicate all my work to my daughter Olivia who was born during my PhD.

TABLE OF CONTENTS

2,4-D 2,4-Dichlorophenoxyacetic acid

ABA Abscisic acid

ARF Auxin response factor

AUX1 Auxin resistant 1

bp Base pair

DNA Deoxyribonucleic acid

GFP Green fluorescent protein

hpt hours post transfer

hag hours after gravistimulation

IAA Indole-3-acetic acid

LAX3 Like AUX1 3

LRP Lateral root primordia

LRE Lateral root emergence

MS Murashige and Skoog medium

mRNA messenger RNA

NAA 1-Naphthaleneacetic acid

°C Degree Celsius

ROS Reactive oxygen species

RSA Root system architecture

RT-PCR Reverse transcriptase PCR

RZ Repressed zone

WD Water deficit

The **first chapter** is an introduction to cereal root development with a special emphasis given to lateral root (LR) formation.

The **second chapter** presents the *in silico* translational approach of gene identification in monocots. The components of the key pathways of auxin-mediated LR formation that were described in *Arabidopsis* were investigated.

The **third chapter** is devoted to detailed description and functional characterisation of auxin influx carriers in barley. The special emphasis was given to *AUX1* and *LAX3* in barley, as they were shown to be essential for generation of auxin gradients during LR formation in *Arabidopsis*.

The **fourth chapter** describes a branching behaviour of barley seedlings exposed to transient treatment with ABA in aeroponics. This plant hormone is proposed as an intrinsic messenger of LR repression upon water deficit, that affects early stages of LR development.

The **fifth chapter** focuses on the role of ROS during LR development in *Arabidopsis* and monocots. Extracellular accumulation of H_2O_2 around LR primordia is proposed to contibute to LR emergence.

The **sixth chapter** summarizes the main findings and presents perspectives for future research.

Owing to the presentation of the chapters of this thesis in a publication format, a number of repetitions could not be avoided.

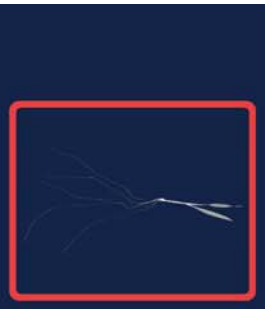
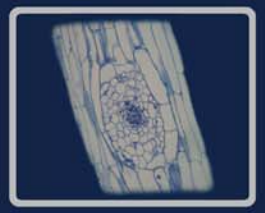
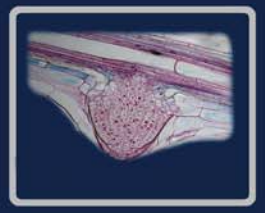

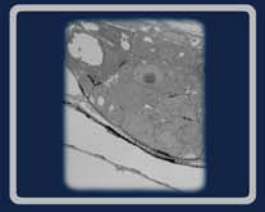
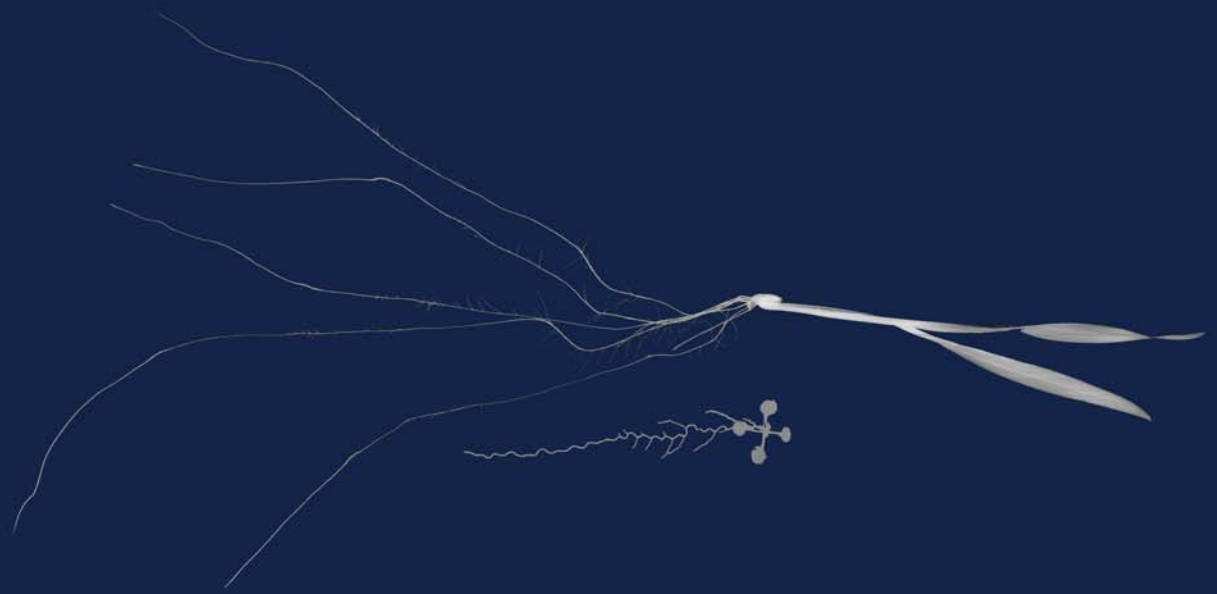

Chapter ٦

CHAPTER 1

Introduction

Adapted from:

Orman-Ligeza, B., Parizot, B., Gantet, P.P., Beeckman, T., Bennett, M.J., and Draye, X. **2013**. Post-embryonic root organogenesis in cereals: branching out from model plants. *Trends in plant science* 18, 459-467.

Orman-Ligeza, B., Civava, R., De Dorlodot, S., Draye, X. **2014**. Root System Architecture, in: *Root Engineering*„ Basic and Applied Concepts, A. Morte and A. Varma, Editors. Springer: Berlin Heidelberg, pp. 39-56.

Context

Root system architecture

Definition and description

The root system architecture is a composite notion that encapsulates aspects of root structure and of root shape. On the one hand, the structure of root systems, which defines the assembly and properties of the different root segments, is bound to the developmental processes that lead to the expansion, direction and senescence of roots, and to the production of new roots. On the other hand, the shape of root systems describes the spatial distribution of roots and relates to major functions of the root system such as resource capture, anchorage and plant hydraulics (Gregory et al. 2003). The importance of RSA lies in the fact that major soil resources are heterogeneously distributed in the soil, so that the spatial deployment of roots substantially determines the ability of a plant to secure and transport edaphic resources (Lynch 1995). In addition, the structure and spatial configuration of the root system are important aspects of the mechanical soil-root system responsible for plant anchorage (Fitter 2002). Finally, RSA determines largely the extent of the contacts and interactions between the plant and the rhizosphere.

Interestingly, RSA does not bear specific functions by itself. Instead, it carries the spatial and temporal dimensions that are needed to analyze many functions at the plant scale. Resource uptake, for example, is primarily realized at the root surface by multiple cellular or apoplastic transport mechanisms that have little connections with RSA. The placement of the roots, however, determines the maximum amount of resource that can be absorbed (King et al. 2003). Similarly, water transport through cells and in the apoplast are driven by local water potential gradients and regulated by local conductivities (i.e. aquaporins, cell wall decorations and xylem diameter) which do not depend primarily on RSA. The complete structure of the root system is needed, however, to consider how the negative water potentials at

the leaf surface propagate throughout the plant and the soil environment (Sperry et al. 2002).

As a consequence of its composite nature and of the multiplicity of functions where it is involved, RSA has become a topic on its own in many research communities (i.e. ecologists, geneticists, molecular biologists, crop physiologists, microbiologists) with contrasting interests, investigation scales, experimental strategies, observation techniques or modes of description. A major problem that results from this situation is the coexistence of very different ways to describe RSA. Beyond the fact that developmental biologists and breeders are looking at different aspects of RSA, different constraints apply to the RSA description of *Arabidopsis* (*Arabidopsis thaliana*) seedlings in a Petri dish and of cereal plants in soil columns or in the field. The ingeniosity of researchers have led to an arsenal of phenotyping methods, from 1D to 3D, static or dynamic, direct or indirect, partial (Fitter 1982) or exhaustive (Lobet and Draye 2013) and with a variety of culture systems (de Dorlodot et al. 2007; Dhondt et al. 2013; Smit et al. 2000). This situation could be seen as an opportunity to generate complementary information on common genetic resources, especially given the amplitude of environmental influence on RSA. However, we have not been successful in developing a unified framework to exchange and discuss concepts and data on RSA.

Organisation of cereal root system

Higher plants exhibit an amazing diversity of root architectures at both the systems and anatomical level. Many dicot species such as *Arabidopsis* have a primary root that iteratively branches to generate several orders of lateral roots (LRs), whereas the root system of cereal crops such as barley, maize (*Zea mays*) and rice (*Oryza sativa*) is predominantly composed of many shoot-borne crown roots that branch sequentially to form a herringbone-like structure (Coudert et al. 2010b; Hochholdinger et al. 2004b; Rebouillat et al. 2009) that are exemplified here by the schematic representation of a maize seedling (Figure 1-1).

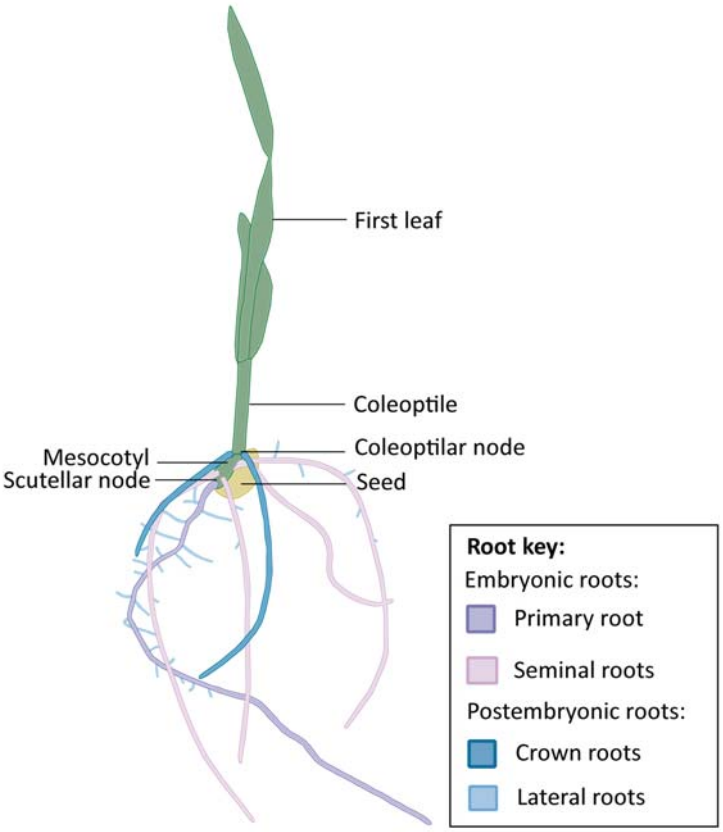

Figure 1-1. Organization of cereal root system.

Adapted from Orman-Ligeza, B. et al., 2013, with modifications.

The primary root (termed 'radicle' in rice) emerges from the seed quickly after germination. In the next few days, seminal roots emerge from the scutellar node in maize, whereas five embryonic crown roots emerge from the coleoptilar node in rice. These roots constitute the embryonic root system, which is essential during plant establishment and sometimes remains functional over the whole life cycle. The largest part of the root system is made up of shoot-borne post-embryonic roots that are produced sequentially from the successive shoot nodes, starting at the coleoptilar node. These adventitious roots, which are part of the normal development plan of cereals, are designated crown roots or nodal roots. Adventitious emerging above the soil surface are designated brace roots (e.g., in maize). In rice,

hundreds of crown roots are formed within 6 weeks after germination. Depending on the genotype, crown roots have a relatively large diameter and elongation rate, an indeterminate growth type, and positive gravitropism. Over their entire life, primary, seminal, and crown roots initiate LRs in a regular acropetal sequence, although branching patterns are often obscured in field conditions by growth responses to local soil conditions (Drew 1975). LRs in cereals vary in terms of diameter, growth rate and duration, branching angle, and tropism. In rice, the LR population comprises long and thick LRs (lLRs) with gravitropic and indeterminate growth and short and tiny LRs (sLRs) with agravitropic and determinate growth (Coudert et al. 2010b), whereas maize and barley produce a continuum of LR types (Babe et al. 2012). Strong LRs (or lLRs in rice) also have the ability to produce LRs and it is not uncommon to observe third and fourth order branches on cereal roots roots (Coudert et al. 2010b; Rebouillat et al. 2009).

Over the past decade, it has become apparent that the developmental pathways of the different root types of cereals are at least partly distinct. In both rice and maize, for example, crossing a crown rootless (CRL) mutant with a primary rootless mutant produces a double mutant with an additive phenotype (no crown roots and no primary root) (Hochholdinger and Tuberosa 2009; Kitomi et al. 2011b). Two classes of LR mutants have also been identified: the first class affects both crown root and LR initiation, whereas the second class specifically affects LR initiation (Coudert et al. 2010b; Rebouillat et al. 2009). Finally, the effect of several abiotic factors on LR formation also supports the existence of LR specific pathways (Babe et al. 2012; Drew 1975; Huang et al. 1991; Jansen et al. 2012; Li et al. 2012; Liu et al. 2010; Wang et al. 2002b), some of which are being exploited to repress LR formation at a predictable stage (Babe et al. 2012; Jansen et al. 2012) and move the study of LR formation forward in cereals (Smith and De Smet 2012).

Developmental processes underlying root system architecture

Root growth

Several mutants with a reduction in seminal root growth and gravitropism have been described in cereals (Gowda et al. 2011a; Hochholdinger et al. 2004b), however most of these genes have not been identified. Genetic mechanisms regulating root growth rate as an output of meristem activity and cell elongation rate in *Arabidopsis* are just beginning to be revealed. Several plant hormones act in concert to govern root growth through complex interactions at multiple levels, including biosynthesis, metabolism, transport and signalling. This includes auxin, cytokinin, ethylene, abscisic acid (ABA), gibberellin and jasmonate (Brady et al. 2003; Monroe-Augustus et al. 2003; Werner et al. 2003). Cytokinin, for example, antagonizes auxin action in root growth and apical meristem (RAM) size determination. Cytokinin is perceived by family of AHK histidine kinase receptors and the *ahk2 ahk3 ahk4* triple mutant shows inhibition in root and shoot growth (Nishimura et al. 2004). Its deficiency results in the increased growth of the primary root in *CYTOKININ OXIDASE/DEHYDROGENASE (CKX)* overexpressing plants (Werner et al. 2003). Mutations in genes responsible for cytokinin biosynthesis, e.g. *ATP/ADP ISOPENTENYL TRANSFERASES 3, 5* and *7 (IPT3, IPT5, IPT7)* and signalling, e.g. *AHK3* and *ARABIDOPSIS RESPONSE REGULATOR 1* and *12* (*ARR1 and ARR12)* decrease root-meristem cell number and root growth rate (Dello Ioio et al. 2007). Interestingly, the double mutant *arr1-3 arr12-1* shows reduced sensitivity to salt due to the increase in a high-affinity K(+) transporter responsible for sodium removal from the root xylem. Thus, cytokinin-regulated pathways may be used to improve root length and salinity tolerance (Mason et al. 2010).

Root gravitropism

The gravistimulus regulates the root growth angle through the concerted action of auxin efflux and influx carriers which modulate the distribution of auxin in the elongation zone. The efflux carrier PIN-FORMED 3 (PIN3) protein initiates the assymetric auxin

transport in the columella, driving more auxin to concave side of the root while PIN2 and auxin influx carrier AUX1 transmits the signal through the LR cap to the epidermal cells in the elongation zone (Michniewicz et al. 2007). There, auxin receptors, including TRANSPORT INHIBITOR RESPONSE 1 (TIR1), induce auxin-signalling machinery (Dharmasiri et al. 2003) resulting in assymetric cell elongation and, most likely, LR branching. Interestingly, few mutants were described that are impaired in LR gravitropism, but not in primary root gravitropism (Mullen and Hangarter 2003). On the opposite, both primary and LRs of the *long hypocotyl 5 (hy5)* mutant shows reduced gravitropism. Those results suggest that the lateral and or primary root angle could be potential engineering targets. Computer simulations showed the influence of root angle on inter-root competition and on the efficiency of nutrient acquisition (Guyomarc'h et al. 2012).

Root morphology and structure

Root hairs

Water and nutrient uptake is often restricted by a limited contact area between the root surface and the soil particles, especially where roots clump within pores and cracks that are larger than the root diameter (White and Kirkegaard 2010). Both the length and the density of root hairs contribute to maintain the soil-root contact. Longer root hairs improve phosphorus acquisition (Bates and Lynch 2000; Lynch 2011a) and likely water uptake (Segal et al. 2008), although their actual contribution has been recently revisited (Keyes et al. 2013). Several root hair mutants have been described in cereals (Hochholdinger et al. 2004b; Zuchi et al. 2011), yet the genetic background of hoot hair formation has been best described in *Arabidopsis*. Root hairs mutants display variation in hair density (Bernhardt et al. 2003; Hauser et al. 1995; Ohashi et al. 2003; Schiefelbein and Somerville 1990; Walker et al. 1999), hair length (Cernac et al. 1997) and hair development (Grierson et al. 1997; Parker et al. 2000; Ryan et al. 1998). In *werewolf (wer), enhancer of glabra 3 (egl3), transparent testa glabra 1 (ttg1)* and *glabra 2 (gl2)*

mutants, root hairs are formed on nearly all root epidermal cells (Ohashi et al. 2003; Walker et al. 1999). In fact, the transcriptional complex of WER, EGL3 and TTG1 proteins promotes *GL2* expression, which prevents root hair formation in nonhair cells and regulates the density of root hairs at the root surface. In this process, CAPRICE protein (CPC), a positive regulator of root hair development, competes with WER protein for binding to this transcriptional complex (Tominaga-Wada et al. 2011).

Root vasculature

Early experiments indicated that xylem diameter in wheat influences grain yield in rain-fed environments (Richards and Passioura 1989). In fact, the number and size of xylem vessels are important determinants of the water flow capacity, the axial hydraulic conductivity and the cavitation susceptibility of roots (Bramley et al. 2009; Sperry and Ikeda 1997) which, in combination with RSA, affect the spatial and temporal patterns of water uptake in the soil (Draye et al. 2010). Mutagenesis in *Arabidopsis* revealed numerous regulators of radial tissue development, mutations of which disrupts the spatial organization of vascular tissue, endodermis and cortex, such as *phloem intercalated with xylem (pxy)* (Fisher and Turner 2007), *woodenleg (wol), shortroot (shr), gollum (glm), fass* (Close et al.), *scarecrow (scr) and pinocchio (pic)* (Scheres et al. 1995). Recently, several regulatory mechanisms that control the specification of xylem and phloem have been uncovered. These include class III HD-ZIP and KANADI gene family members that control the establishment of the spatial arrangement of phloem, cambium and xylem (Ilegems et al. 2010) and *ALTERED PHLOEM DEVELOPMENT (APL)* that encodes a MYB-coiled-coil transcription factor responsible for phloem differentiation. The phenotypes of the mutants indicate that small-scale changes in root anatomy may impact whole plant physiology and growth.

Cell-wall modifications

Roots respond to different external stimuli by various cell-wall modifications such as lignification of the schlerenchyma layer and

suberization of the rhizodermis, exodermis or endodermis (Hose et al. 2001). For example, the suberization of the sclerenchyma is thought to reduce water uptake in flooded conditions while that of the endodermis seems to help the root to retain water under drought (Henry et al. 2012). In addition, suberization of endodermis and thickened cell walls restrict the water uptake to the distal region of the roots (Bramley et al. 2009), hence their obvious link with RSA. Increased suberin content in *Arabidopsis enhanced suberin 1 (esb1)* mutant causes enhanced hydraulic resistance to radial transport of water and results in decrease in transpiration and in shoot biomass accumulation. However, this reduction is smaller than the reduction in transpiration, leading to an overall increase in water use efficiency of *esb1* (Baxter et al. 2009). Increased root suberin content may therefore open new opportunities for enhancing drought resistance in crops.

Cell wall modifications also occur during LR development, when the LR primordia penetrates the endodermis, cortex and epidermis of the parental tissue (Vilches-Barro and Maizel 2014). Interestingly, two different mechanisms seem to operate in endodermis and in the other two, more outer cell layers. (Gonzalez-Carranza et al. 2007; Neuteboom et al. 1999; Swarup et al. 2008; Lewis, 2013). In endodermal cells in front of the forming LR primordia, the Casparian strip, a lignin-reach structure sourrounding cells of this layer, is locally degraded (Vermeer et al. 2014), which eases the "safe" passage of the LR primordia through the endodermal cell without cell wall separation event. In cortex and epidermal cells overlaying the emerging LR primordia, putative cell wall remodeling enzymes are proposed to facilitate LR emergence by weakening or modification of the cell walls belonging to the parental tissue (Gonzalez-Carranza et al. 2007; Neuteboom et al. 1999; Swarup et al. 2008; Lewis et al. 2013). The activity of an auxin influx carrier LAX3 in cortex and epidermis was proposed to regulate the auxin-induced expression of cell wall remodelling genes that degrade the pectin-rich middle lamella. In agreement with this, LR emergence through cortex and epidermis is hampered in *Atlax3* mutants (Swarup et al. 2008). In addition, defects in genes involved in cell wall formation increase the rate of LR

primordia emergence, as shown recently by screening the mutants impaired in cell wall biosynthesis (Roycewicz and Malamy 2014) and further supports the hypothesis that cell wall remodelling in LR primordia overlaying cells is an important component of LR emergence. In parallel to the above, the symplastic connectivity between LR primordia and the overlaying tissues decreases gradually through callose deposition at the plasmodesmata (Benitez-Alfonso, 2013). Interestingly, there are also other differences in cell wall properties between the developing LR primordia and the overlaying tissues, such as pectin demethylesterification in the middle lamella. It has been shown that pectin is largerly methylated in LRP and mostly demethylated in the LR primordia overlaying tissues, which makes them prone to degradation. This difference is proposed to restrict cell separation events to the outer tissues (Laskowski et al. 2006).

Root aerenchyma

Modelling studies indicate that the production of so called „cheap roots“ with extensive root cortical aerenchyma might increase root growth up to 70% under phosphorus deficient conditions and thus tackle nutrient deficiencies (Lynch 2011a; Postma and Lynch 2011). In addition, large intercellular spaces in cortex could also speed up an exchange of gases between aerobic shoot to the anaerobic root and serve as an important adaptation to flooding conditions (Jackson and Armstrong 1999). Therefore, this phenomena driven by non-apoptotic programmed cell death (Joshi and Kumar 2012), has been extensively studied on cereals and is known to be stimulated by several stress factors, such as drought, transient nutrient and oxygen deficiencies and mechanical impedance (Drew et al. 1989; Jackson and Armstrong 1999; Postma and Lynch 2011; Whalen 1988; Yang et al. 2012). Moreover, the process of aerenchyma formation is tightly regulated, where ethylene, calcium, H_2O_2 and abscisic acid orchestrate to produce it in a predictable pattern (Drew et al. 2000; Siyiannis et al. 2012) and can be therefore targeted in plant breeding programs. On the contrary, it has been shown that aerenchyma could impede the radial transport of water (Yang et al. 2012) or affect the mechanical

strength of the roots and their susceptibility to root collapse (Mostajeran and Rahimi-Eichi 2008). To date, studies have shown that *Arabidopsis* seedlings do not form root aerenchyma in response to hypoxia, yet *LESION SIMULATING DISEASE 1* (*LSD1), ENHANCED DISASEASE SUSCEPTIBILITY 1 (EDS1)*, and *PHYTOALEXIN-DEFFICIENT 4 (PAD4)* control aerenchyma formation in *Arabidopsis* leaves and hypocotyls (Muhlenbock et al. 2007).

Post-embryonic root formation in cereals

Root formation is an essential complement to root growth. It contributes to widen the volume of soil explored, increase the extension capacity of the root system, and compensate for root death. Post-embryonic root formation includes the production of adventitious roots and LRs that have specific physical and physiological properties, uptake behaviours, construction costs and survival rates. Hence, adventitious and LRs contribute in sensibly different ways to the multiple functions of root systems and to the efficiency of the root system (defined as a ratio of resource captured : carbon invested). Similarly, the processes of adventitious and LR formation are likely to be coordinated in order to achieve an optimal performance at the whole plant scale.

Lateral root development in cereals

LR primordia originate from a subset of cells (called founder cells) at the periphery of the stele of the parent root. In maize, rice, barley, and wheat (*Triticum aestivum*), founder cells originate from pericycle and endodermis cells located opposite phloem poles (Casero et al. 1996; Demchenko and Demchenko 2001; Hochholdinger et al. 2004a). This contrasts with many dicots, such as *Arabidopsis*, where LR primordia originate exclusively from pericycle cells opposite protoxylem poles (Casimiro et al. 2003) with some exceptions (Lloret et al. 1989). Given the polyarch stelar organisation of cereal roots, which consists of several phloem poles alternating with the same number of xylem poles, LRs appear in several longitudinal files (also referred to as ranks or rows) (Bell and McCully 1970; Draye et al.

1999), the number of which is roughly proportional to the stele diameter (Draye 2002). Within each file, LR primordia formation follows an acropetal sequence, with the youngest primordia appearing closest to the root tip (Casimiro et al. 2003), often at a predictable distance (Dubrovsky et al. 2006a; Mallory et al. 1970). Few studies in maize (Bell and McCully 1970; MacLeod 1990) and wheat (Bingham and Blackwood 1997; Huang et al. 1991) have reported deviations from this strictly acropetal rule. However, the acropetal sequence can easily be obscured when LR primordia developmentally arrest before emergence (Babe et al. 2012; Dubrovsky et al. 2006a) or in rice when thick, long LRs arise between fine, short LRs (Clark et al. 2011; Coudert et al. 2010a). However, nothing is known about the control of inter-lateral distance in cereals, or whether the pattern is the result of a spatial or temporal control mechanism, as in *Arabidopsis* (Dubrovsky et al. 2006a).

Similar to the situation in *Arabidopsis*, LR formation in cereals follows a succession of developmental steps comprising initiation, growth through the cortex, and emergence through the epidermis (Figure 1-2). The first morphological events of LR initiation are observed on the proximal side of the elongation zone, for example, at 10–15 mm from the root tip in maize (Casero et al. 1995; Jansen et al. 2012) and at 15–20 mm from the root tip in wheat (Demchenko and Demchenko 2001). Two longitudinally adjacent pericycle cells undergo asymmetric transverse divisions opposite a protophloem element (stage I in Figure 1-2). In barley, such paired divisions occur synchronously in four to six neighbouring pericycle cell files (Demchenko and Demchenko 2001), compared with three files in *Arabidopsis* (Malamy and Benfey 1997). The resulting two short cells expand radially (stage II in Figure 1-2) and undergo asymmetric periclinal divisions, giving rise to two inner and two outer cells, approximately 21–24 mm from the maize root tip (Bell and McCully 1970). The two outer daughter cells (in each file) then engage in a long succession of anticlinal and periclinal divisions (spanning stages III–VII in Figure 1-2). Unlike *Arabidopsis*, endodermal cells adjacent to the dividing pericycle cells divide anticlinally just after

stage III and contribute an additional cell layer to the new LR primordium (Figure 1-2). Later on, few cells at the forefront of the primordium divide synchronously and periclinally to generate an inner layer of root cap initials and an outer layer of root cap cells. When the primordium has progressed half-way through the cortex (stage VI in Figure 1-2), a morphologically distinct meristematic zone and root cap can be observed (Bell and McCully 1970). During LR formation, overlying cortical and epidermal layers of the parent root are reprogrammed to facilitate the emergence of the new organ. In maize as in *Arabidopsis*, loosening of cortical cell walls occurs at early stages of LR primordium development and involves cell wall enzyme action (Bell and McCully 1970) Swarup, 2008). In cereals, this loosening is preceded by divisions of the cortical cells directly overlaying LR primordia (Figure 1-2) and (Bell and McCully 1970; Casero et al. 1996; Sreevidya et al. 2010). These cells re-enter the cell cycle very early as mitotic figures are observed from stages II or III in barley, approximately 10–12 h after the first asymmetric division of the founder pericycle cells (A. Babé, unpublished). Therefore, whereas separation of cell files seems to be sufficient to allow the emergence of LR primordia through the three overlying endodermal, cortical, and epidermal cell layers in *Arabidopsis*, cell division appear to be required for the penetration of the large LR primordia of cereals through a much larger number of cortical layers, and implies a profound reorganisation of the overlying cells.

Genetic and hormonal control of LR development in cereals

LR development in cereals is controlled by many extrinsic (environmental) and intrinsic signals. Plant hormones represent key regulators of plant developmental processes, as reviewed in (Depuydt and Hardtke 2011; Garay-Arroyo et al. 2012; Vandenbussche et al. 2010), including LR initiation, patterning and emergence of LRs (Peret et al. 2009). Besides the classical phytohormones, peptide hormones such as members of the CLE-Like/GOLVEN family (Yamada and Sawa 2012), small molecules such as nitrite oxide (Wang et al. 2012) and (Chen et al. 2012), or reactive oxygen species (Causin et al. 2012) also have regulatory effects on different aspects

of root development and branching. However, most of the knowledge on hormonal control of root branching has been acquired from studies using *Arabidopsis* or other dicot plants, and it is only recently that efforts have been made to understand LR formation in monocots and is reviewed in (Ghanem et al. 2011; Kitomi et al. 2012). In monocots, most LR mutants also affect the development of crown roots, and a minor number specifically affect LR or crown root formation, revealing that both specific and common hormonal and developmental pathways are involved in post-embryonic root formation in cereals. Because many LR mutants have been initially analyzed in the context of crown root formation, parts of our review will cover both processes. An updated schema of the regulatory pathway controlling crown root and/or LR initiation in rice compared with corresponding steps for LR initiation in *Arabidopsis* is presented in Figure 1-3.

Auxin

To date, the majority of mutants reported to be affected in LR and crown root initiation, patterning, and emergence have been auxin-related (Coudert et al. 2010b; Hochholdinger and Tuberosa 2009; Rebouillat et al. 2009). Auxin is a common regulator for all monocot root types. Studies have reported a positive correlation between auxin biosynthesis and crown root initiation frequency in rice (Yamamoto et al. 2007), a positive effect of auxin treatments on LR formation in rice, maize, and barley (Babe et al. 2012; Jansen et al. 2012; Sreevidya et al. 2010), as well as a negative effect of blocking auxin transport in rice and maize (Jansen et al. 2012; Sreevidya et al. 2010; Zhang et al. 2012).

Over the past decade, several genes orthologous to the *Arabidopsis* auxin transport/signalling cascade have been characterised in monocots. Although it is often unclear whether these act in a root cell type-specific manner or have a more generic contribution in all root cell types, many of the components belonging to the canonical auxin signalling pathway involved in LR initiation in *Arabidopsis*, from transport to downstream responses, have also been identified in monocot species. The differential distribution of auxin throughout the

various root tissues and cell types is at the core of its mode of action during all developmental processes. Such distribution is achieved through tightly orchestrated polar transport mechanisms, which result in the local induction of an auxin response in specific cell types at defined time points. Reporter constructs containing the synthetic promoter DR5 (Ulmasov et al. 1997) have been instrumental in helping to visualise local auxin responsive gene expression and have revealed a role for auxin in LR initiation (Casimiro et al. 2001) and patterning in *Arabidopsis* (Benkova et al. 2003). Similar reporters have been used in monocots such as rice and maize (Gallavotti et al. 2008b; Scarpella et al. 2003; Sreevidya et al. 2010) to monitor auxin responses during LR initiation (Sreevidya et al. 2010; Jansen et al. 2012; Kitomi et al. 2012; Zhu et al. 2012) and during crown root initiation in rice (Inukai et al. 2005). In the primary root of maize, a detailed survey of DR5 expression at the tissue level revealed the involvement of auxin in vascular element differentiation, pericycle specification, and LR initiation (Jansen et al. 2012). Interestingly, an auxin response maximum at the phloem poles precedes the first divisions of the pericycle in monocots, which is reminiscent of the priming of the xylem pole pericycle cells reported in *Arabidopsis* (De Smet et al. 2007). Similar observations have been made in rice using another auxin responsive reporter employing the soybean GH3 promoter (Liu et al. 1994; Sreevidya et al. 2010).

Auxin transport

Both PIN and AUX1 classes of auxin efflux and influx carriers are involved in LR formation in cereals. PIN auxin efflux carriers, such as *ETHYLENE INSENSITIVE ROOT (EIR)* (Luschnig et al. 1998; Paponov et al. 2005), and *AUX1* influx carriers are expressed in specific areas of the root in relation to LR formation, in rice (Wang et al. 2009). The maize homologue of *AUX1* is also highly expressed during brace root initiation (Li et al. 2011). In *Arabidopsis*, the intracellular trafficking of PIN1 is regulated by GNOM1, a membrane-associated guanine nucleotide exchange factor of the ADP-ribosylation factor G protein (ARF-GEF) (Steinmann et al. 1999).

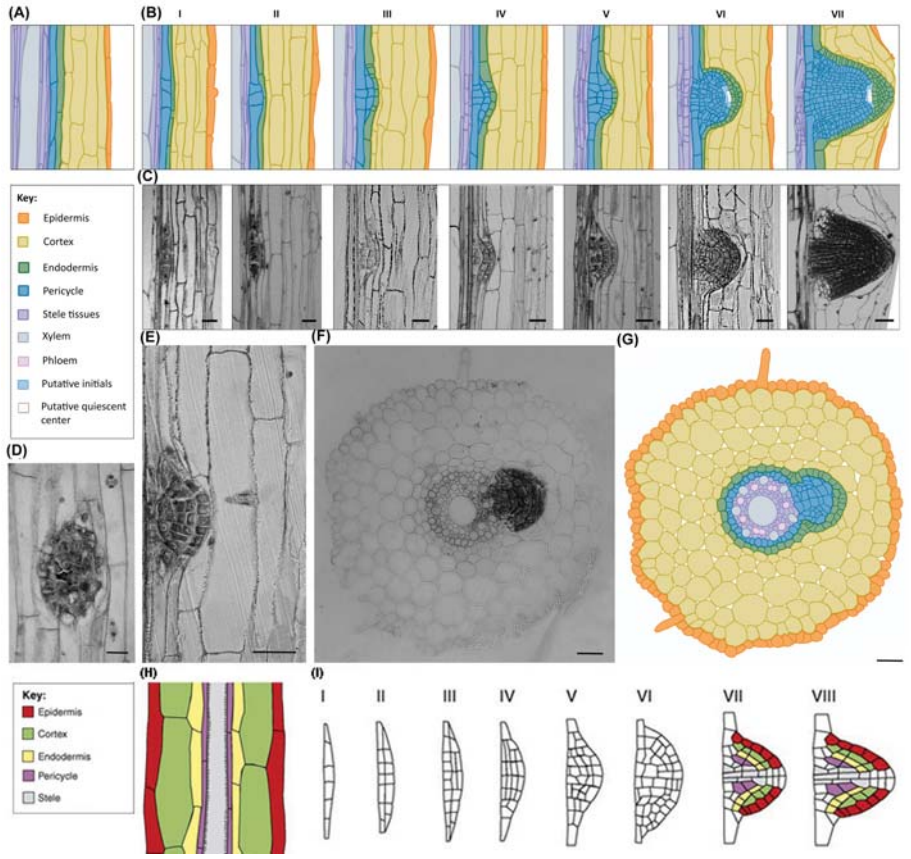

Figure 1-2: Lateral root development in barley and *Arabidopsis*.

(A) Illustration of a longitudinal section showing the typical tissue organisation of cereal roots. The number of cortex layers that have to be penetrated by the developing meristem is much larger than in *Arabidopsis*. **(B)** Succession of morphological stages during LR development and emergence (arbitrary stages). **(C)** Original toluidine blue stained sections used for illustrations in **(B)**. **(D)** Periclinal and **(E)** anticlinal longitudinal sections of the growing LRs. The sections show an extensive cortical region around the primordium where divisions are taking place. **(F)** Radial tissue organisation of cereal roots (toluidine blue staining). **(G)** Illustration of the section in **(F)** to highlight the deformation of the cortex that occurs during LR penetration. **(H)** Illustration of a longitudinal section showing the typical tissue organisation of *Arabidopsis* root. **(I)** The eight stages of LR primordium development in *Arabidopsis* (Scale bars = 50 µm). Adapted from Orman-Ligeza, B. et al., 2013 and Peret, B. et al., 2009 with modifications.

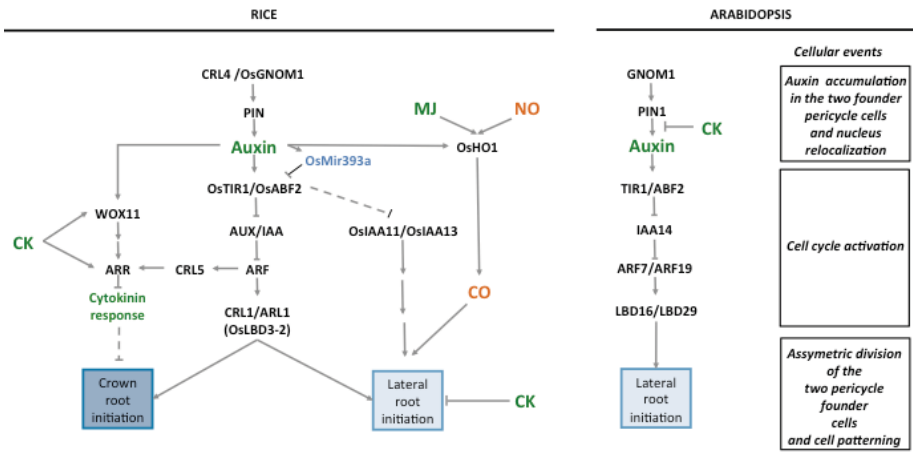

Figure 1-3: Gene regulatory networks controlling crown root and/or lateral root initiation in rice and in *Arabidopsis*.

The corresponding early cellular events of root initiation in *Arabidopsis* are noted. Arrows represent the positive regulatory action of one element of the network on another one. Genes are denoted in black, hormones in green, miRNA in blue, and regulatory molecules in red. A line ending with a trait represents the negative regulatory action of one element of the network on another one. Dotted lines represent hypothetical links between two elements. Abbreviations: AFB2, auxin signalling F-box2; ARF, Auxin Response Factor; ARL, adventitious rootless; ARR, type-a response regulator2; AUX/IAA, auxin/indole-3-acetic acid; CK, cytokinin; CO, carbon monoxide; CRL, crown rootless; GNOM1, membrane-associated guanine nucleotide exchange factor of the ADP-ribosylation factor G protein (ARF-GEF); HO1, heme oxygenase 1; LBD, lateral organ boundaries domain; MJ, methyl jasmonate; NO, nitric oxide; PIN, pin-formed auxin efflux carrier proteins; TIR1, transport inhibitor response 1; WOX11, WUSCHEL-Related Homeobox 11. Adapted from Orman-Ligeza, B. et al., 2013, with modifications.

GNOM1 is required for the first asymmetrical division of pairs of pericycle cells, which triggers LR initiation in *Arabidopsis* (Geldner et al. 2004; Peret et al. 2009). Mutations in the rice gene orthologous to *GNOM1, crown rootless 4 (crl4)* (Kitomi et al. 2008) and *Osgnom1* (Liu et al. 2009), exhibit no crown roots and a reduced number of LRs (Liu et al. 2009). In addition, the expression of *OsPIN2, OsPIN5b*, and *OsPIN9* is altered in *Osgnom1*, indicating that polar auxin transport involving OsPIN auxin carriers and regulated by CRL4/OsGNOM1 is required for crown root and LR initiation in rice.

Interestingly, some monocot PIN sequences do not cluster with dicot sequences, suggesting the existence of clade-specific pathways (Paponov et al. 2005). An extensive characterization of PIN, AUXIN1/LIKE-AUX1 (AUX/LAX), and P-GLYCOPROTEIN (PGP) classes of auxin transport proteins has been initiated in sorghum (Sorghum bicolor) (Shen et al. 2010; Wang et al. 2010) and suggests their involvement in root development, but a direct link with LR initiation has yet to be investigated.

Auxin perception

AUXIN/INDOLE-3-ACETIC ACID (Aux/IAA) proteins are key regulators of the nuclear auxin response pathway and several of them have been shown to modulate LR formation in *Arabidopsis* (Goh et al. 2012b). These short-lived nuclear proteins function as auxin co-receptors with TRANSPORT INHIBITOR RESPONSE 1 (TIR1) and closely related AUXIN SIGNALLING F-BOX (AFB) proteins (Calderon Villalobos et al. 2012). Aux/IAA proteins also function as transcriptional repressors by interacting with members of the AUXIN RESPONSE FACTORS (ARF) transcription factor family. In the presence of auxin, Aux/IAA proteins are degraded via ubiquitination by the E3 ligase Skp1–Cullin–F-box protein $(SCF)^{TIR1/AFB}$ complex, thereby derepressing ARF activity. Several components of this nuclear auxin response pathway have been identified in cereals that regulate LR formation.

Mutations in Aux/IAA proteins such as *OsIAA13* (Kitomi et al. 2012) in rice and *ROOTLESS WITH UNDETECTABLE MERISTEMS 1 (RUM1)* in maize (von Behrens et al. 2011; Woll et al. 2005) that block their auxin-mediated degradation confer LR defects. The *rum1-R (rootless with undetectable meristems)* mutant is deficient in polar auxin transport and lacks embryonic seminal roots and post-embryonic LRs in the primary root. *RUM1-R* encodes a truncated *ZmIAA10* sequence that lacks the auxin degron sequence. ZmIAA10 can interact with ZmARF25 and ZmARF34 (von Behrens et al. 2011), suggesting that an auxin–AUX/IAA-ARF pathway regulates lateral and seminal root initiation in maize.

The gain-of-function mutant *Osiaa13* contains a single amino acid substitution in the degron sequence required for the auxin-triggered turnover of the OsIAA13 protein (Kitomi et al. 2012). *Osiaa13* exhibits a LRless phenotype, yet crown root initiation and development are not modified, suggesting that the stabilised OsIAA13 protein specifically inhibits the auxin transduction pathway involved in LR initiation. This is also supported by the specific expression of *OsIAA13* in the pericycle and endodermis, in regions where LRs are initiated (Sato et al. 2011; Takehisa et al. 2012). Furthermore, root transcriptome laser dissection analysis revealed that 71 genes could be associated with LR initiation in rice, of which 21 have a functional annotation (Takehisa et al. 2012). Nine of these 21 genes are differentially regulated in *Osiaa13* relative to the wild type (Kitomi et al. 2012), and seven of them contain an auxin response element in their promoter sequences that can function as binding sites for ARF. This list of genes includes transcription factors (Coudert et al. 2012), cell wall modification enzymes, and Cdc2 protein kinases (Kitomi et al. 2012). However, further analysis is required to confirm their functional importance during LR initiation in rice.

OsIAA11 and *OsIAA30* show sequence and expression pattern similarities with *OsIAA13* (Jain et al. 2006; Sato et al. 2011). Interestingly the gain-of-function mutant *Osiaa11* also has a LR defect (Zhu et al. 2012), suggesting that *OsIAA11, OsIAA13*, and perhaps *OsIAA30* have redundant functions controlling LR initiation in rice. Other components of the auxin response pathway have also been shown to control LR development in cereals. In rice, mutations in *Cyclophilin 2 (OsCYP2)* and *Cullin-associated Nedd8-dissociated protein 1 (OsCAND1)*, which are involved in the assembly of the E3 ubiquitin ligase $SCF^{TIR1/AFB}$ complex, cause the cell cycle to arrest at the G2/M transition, resulting in defects in LR initiation (Kang et al. 2013) and crown root emergence (Wang et al. 2011), respectively.

miRNAs OsMir393a and OsMir393b, negative regulators of the messenger RNAs *OsTIR1* and *OsAFB2,* the rice orthologues of *Arabidopsis* auxin co-receptors TIR1 and AFB2 (Bian et al. 2012; Xia

et al. 2012), also appear to be involved in LR initiation in rice. Overexpression of 35S:Mir393 leads to a reduced number of crown roots and a strong auxin-resistant phenotype (Bian et al. 2012). The GUS reporter gene controlled by the OsMir393a promoter sequence is expressed in the crown root and at LR initiation sites. GUS staining accumulates transiently in the pericycle cells during the early stages of LR formation, suggesting that OsMir393a may be involved in a feedback regulatory loop of auxin signalling during LR initiation.

Auxin response

Aux/IAA protein degradation releases ARF transcription factors, thereby activating a set of downstream target genes, including *LATERAL ORGAN BOUNDARIES DOMAIN (LBD)*. In *Arabidopsis*, the positive regulation of *LBD16* and *LBD19* by ARF7 and ARF19 proteins, is essential for LR initiation and occurs just after auxin perception by TIR1/ABF auxin receptors that mediate the degradation of Aux/IAA (Okushima et al. 2007; Wang et al. 2007; Wilmoth et al. 2005). In rice, OsARF16, the orthologue of ARF7 and ARF19 in *Arabidopsis*, binds auxin response elements located in the *CROWN ROOTLESS 1 (CRL1)* promoter (Inukai et al. 2005). *CRL1* encodes OsLBD3-2 protein, which is closely related to LBD16 and LBD19 in *Arabidopsis* (Coudert et al. 2012). Two mutants of *OsLBD3-2, crl1* (Inukai et al. 2005) and *adventitious rootless 1 (arl1)* (Liu et al. 2005), are devoid of crown roots and present a reduced number of LRs (70% reduction in crl1 compared with the wild type). The induction of *CRL1* expression by auxin is disrupted in plants overexpressing an ubiquitin-insensitive mutated AUX/IAA protein. A comparative transcriptome analysis of *crl1* versus wild type stem bases revealed the existence of CRL1-dependent auxin-regulated genes but further functional analysis is required to determine if these are downstream targets of CRL1 involved in crown and LR initiation (Coudert et al. 2011).

In maize, mutations in genes that encode LBD proteins such as *ROOTLESS CONCERNING CROWN AND SEMINAL ROOTS*

(RTCS) (Taramino et al. 2007), orthologous to the rice gene *ARL1*/*CRL1*, interfere with the initiation of crown and seminal, but not LRs (Hetz et al. 1996; Hochholdinger et al. 2004b). *RTCS* and its duplicated homologous gene *RTCS-LIKE (RTCL)* could share functional redundancy and co-regulate LR initiation (Taramino et al. 2007). RTCS and RTCL can form heterodimers and bind to an LBD motif present in the promoter of *ZmARF34*. In turn, ZmARF34 binds with the auxin response elements present in *RTCS* and *RTCL* promoters (Majer et al. 2012). In maize, inorganic phosphate (Pi) starvation was exploited to experimentally interfere with LR initiation and a gene expression study comparing the LR initiation zone of the seminal root of plantlets cultivated with or without Pi revealed that *ZmLBD17* and several genes encoding auxin biosynthesis enzymes or involved in auxin transport were found to be upregulated in response to Pi deprivation (Li et al. 2012).

Cytokinins

Cytokinin and auxin have antagonistic effects on root development in *Arabidopsis*. In particular, cytokinins disrupt LR formation and patterning by influencing auxin transport and homeostasis (Benkova and Hejatko 2009; Dello Ioio et al. 2008; Laplaze et al. 2007; Peret et al. 2009). In rice, treatment with cytokinin or an inhibitor of cytokinin oxidase (CPPU) leads to inhibition of lateral and crown root initiation and stimulation of LR elongation (Kitomi et al. 2011b; Rani Debi et al. 2005). Inhibiting the cytokinin signalling pathway by downregulation of *type-A RESPONSE REGULATORS (OsRR2 and OsRR1)* known to function as repressors of cytokinin signalling (Hirose et al. 2007; Tsai et al. 2012) also leads to a reduction in crown root initiation, as shown in the mutants *wuschel-related homeobox 11 (wox11)* (Zhao et al. 2009) and *crl5* (Kitomi et al. 2011a). However, *crl5* does not impair LR initiation, suggesting that a different genetic pathway is involved in regulating LR initiation by cytokinin.

Jasmonic acid, nitric oxide, and carbon monoxide signals

Jasmonic acid has been proposed to act independently of auxin to induce LRs in rice (Wang et al. 2002a). Methyl jasmonate, nitric

oxide, and auxin induce LR initiation in rice and it is hypothesised that this occurs via the induction of *HEME OXYGENASE 1 (OsHO1)* expression, through a calcium- and calmodulin-dependent signal transduction pathway (Chen et al. 2012; Hsu et al. 2013). OsHO1 can produce carbon monoxide, a molecule known to promote LR initiation in different species. A similar pathway exists in maize and the overexpression of *ZmHO1* in *Arabidopsis* impacts on the expression of different *Arabidopsis* cyclin-dependent kinases involved in LR initiation (Han et al. 2012). This suggests that *HO1* genes and carbon monoxide production may constitute a key relay in the promotion of LR initiation by different signals and hormones in monocots.

Ethylene

As yet, there is only limited knowledge about the role of the gaseous hormone ethylene during the formation of LRs in monocots. In *Arabidopsis*, ethylene has been reported to inhibit LR formation because ethylene-insensitive mutants form more LRs (Ivanchenko et al. 2008; Negi et al. 2008). The downregulation of *ETHYLENE-INSENSITIVE 3 (EIN3)* transcription (a key transcription factor promoting ethylene regulated gene expression) during maize brace root initiation may indicate a role for this pathway in monocots (Li et al. 2011). By contrast, stimulation of crown root emergence by ethylene in deep-water rice upon flooding is much better studied (Bailey-Serres et al. 2012; Ma et al. 2010). In these roots, ethylene promotes the growth of the primordium (Steffens et al. 2006; Zhang et al. 2012) and the breakdown of surrounding epidermal cell layers (Zhang et al. 2012; Steffens et al. 2006; Steffens et al. 2012). In addition, crown root emergence is facilitated by H_2O_2-mediated cell death, weakening the epidermal cell barrier (Steffens et al. 2012; Steffens and Sauter 2005; Steffens and Sauter 2009). This role of ethylene is not exclusive to monocots because it has also been shown to promote the growth of adventitious roots in other dicotyledonous species (Peeters et al. 2002) and insensitivity to ethylene has been shown to result in slower growth of adventitious roots (Clark et al. 1999).

Objectives of the thesis

The general objective of this thesis is to improve our understanding of the process of LR formation in plants. To achieve this goal, components of hormonal and environmental cues that define the final shape of a root system were investigated in cereals and *Arabidopsis*.

This thesis addresses four specific questions.

What is the level of conservation between dicots and monocots for a key auxin gene regulatory pathway involved in LR formation?

Many studies underlined the crucial role of plant hormone auxin in virtually every step of LR formation in the dicot plant *Arabidopsis* (Benkova et al. 2003; Casimiro et al. 2001). This was then followed by decades of molecular work that revealed the genetic background of this process and the network organisation of its main components (Lavenus et al. 2013). On the contrary, little is known on genes involved in this process in monocot plant species (Orman-Ligeza et al. 2013) and it remains elusive if we can successfully translate the knowledge from *Arabidopsis* to cereal crops. Therefore, the first step of the thesis was devoted to the *in silico* prediction of corresponding genes in *Arabidopsis*, barley, maize and rice.

Auxin transporters AUX1 and LAX3 are patterning auxin distribution in *Arabidopsis*. What is the function of corresponding genes found in cereals?

In *Arabidopsis* shoot, regular priming is achieved by the generation of dynamic auxin gradients by both auxin influx and efflux carriers (Bainbridge et al. 2008). In root, local accumulation or local auxin gradients seems to determine which cells become LR founder cells (Dubrovsky et al. 2006a) and auxin carriers, namely AUX1 and LAX3, were shown to be crucial for auxin-dependent stages of LR formation (Marchant et al. 2002; Swarup et al. 2008). Thus, it is essential to know if the strategic components that enable to generate auxin maxima on a cellular- and a tissue-wide scale in *Arabidopsis* are maintained in monocots. Therefore, the second step of the thesis was

devoted to the functional characterisation of auxin influx carriers in barley and rice.

What are the mechanisms that drive the adjustment of root branching in response to transient or local water deficit?

Plant roots that grow in soil have to face and adapt to changes in external conditions (Drew 1975). Adjustment of root branching has been proposed as one of the major responses to environmental cues (Lynch 2007). However, studying LR plasticy in soils remains challenging and may be hampered not only by technical difficulties, but also by the spatial and temporal heterogeneity of the soil environment. On the contrary, root system architecture can be easily described and exposed to treatments in artificial systems. Previous studies reported that transient water depletion (WD) in aeroponics triggers a repression of LR formation at early stage (Babe et al. 2012). We used this system to depict the mechanisms of response to water deficit and interpreted our results in views of similar branching behaviours that have been observed in soil, e.g. when roots enter macropores (White and Kirkegaard 2010).

What is the role of ROS in LR formation?

Reactive oxygen species (ROS) are produced as byproducts of normal aerobic metabolism, such as membrane-associated electron transport, redox cascades and stress responses. Recently, several reports underlined the possible contribution of ROS to auxin-mediated LR formation, yet still their exact spatial localisation during this developmental process remained ellusive. Thus, we employed ROS-visulalisation techniques during root branching and investigated the possible sources of ROS during LR emergence.


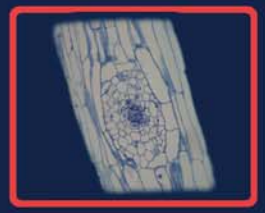
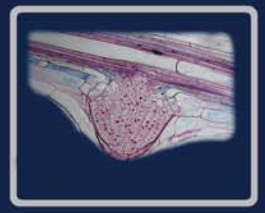

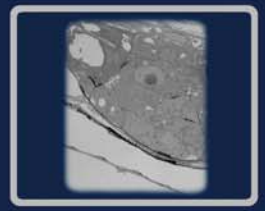

Chapter 2

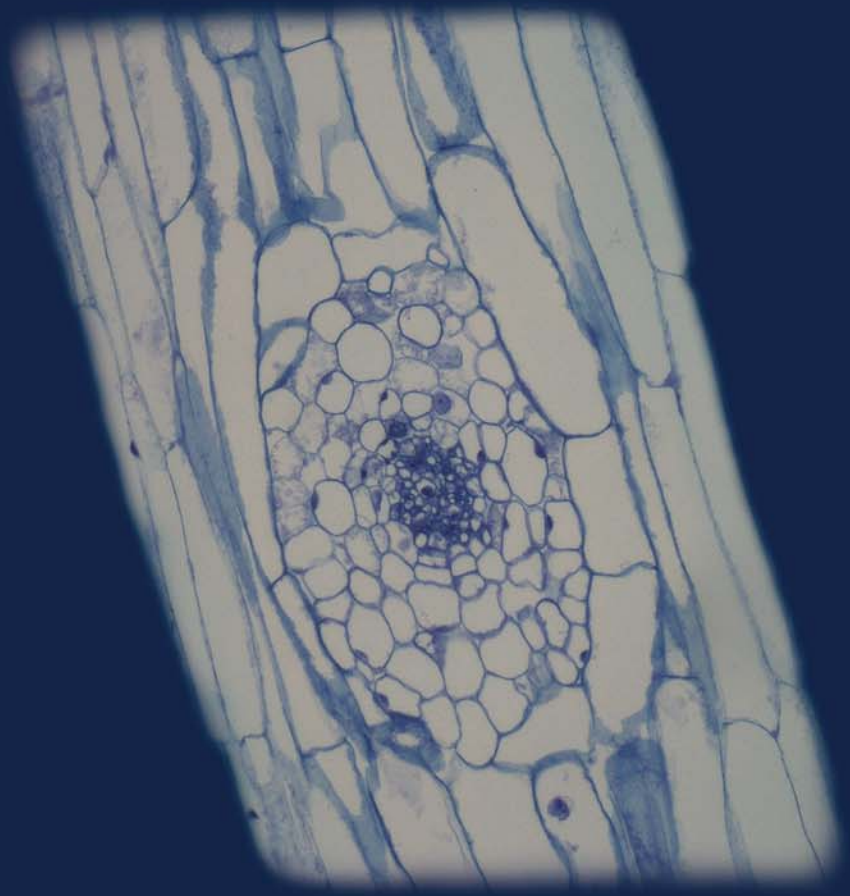

CHAPTER 2

Identification of auxin-related genes involved in lateral root formation in barley (*Hordeum vulgare*)

Abstract

Auxin-dependent gene networks are known to operate during LR formation in *Arabidopsis thaliana*. In this chapter, a transcriptional approach was used to identify in the barley genome candidate genes crucial for root branching.

Six genes were selected from *Arabidopsis* and homologs in barley and in other cereals were identified by using a basic local alignment search tool (BLAST). To ensure accurate predictions of equivalent genes in barley, evolutionary relationships of *Arabidopsis* and monocot gene families of interest were established through phylogenetic analyses. The exon/intron boundaries of putative orthologs in *Arabidopsis*, rice *(Oryza sativa)* and barley were then analysed. Subsequently, the chromosomal positions of the identified genes in barley were projected on consensus barley genetic maps. Finally, a candidate-based QTL meta-analysis for one of the candidate genes, namely *AUX1*, was performed in rice, maize (*Zea mays*) and soy bean (*Glycine max*). The latter analysis revealed the intra-species conservation of QTLs linked to root development and phosphorus uptake in the region that spans the chromosomal position of putative *AUX1* in those three plant species.

We conclude that (1) components of auxin-dependent pathway of LR formation are likely to be conserved between eudicots and monocots, (2) the translational approach can be used to identify putative orthologs of *Arabidopsis* genes in monocots and (3) the candidate-based approach may be potentially used to target genes behind known QTLs.

Key words: translational approach, auxin, lateral root, LR, *Arabidopsis*, barley, cereal crops

Introduction

Little is known about the molecular basis of root system formation and architecture in barley. The large amount of data that has been released for *Arabidopsis*, highlighting the role of auxin-related genes in root development, should be instrumental for comparative and translational genomics. However, the divergence of plant lineages was usually preceded by whole-genome duplications (WGD) followed by the reciprocal loss of duplicated genes. Therefore, proper matching of the homologs between *Arabidopsis* and cereals can be hampered by evolutionary events. Homologs are the genes or genomic regions derived from a common ancestral gene. This general term refers to (i) paralogs, which derive from a duplication event within a lineage, (ii) orthologs that derive from the divergence of lineages and (iii) homeologs, that represent a subset of paralogs created by whole-genome duplication event(s) (Schnable et al. 2012). The orthologs in cereals are often expected to have equivalent function as they fulfil in *Arabidopsis* (Haga et al. 2005; Waters et al. 2012; Campoli et al. 2012; Huffaker et al. 2011; Kojima et al. 2002; Zou et al. 2006).

In this study, six auxin-related genes previously described as key players in LR development have been selected for *in silico* identification in barley. In *Arabidopsis*, those genes are involved in auxin influx [*AUX1(AUXIN-RESISTANT 1)* and *LAX3 (LIKE AUX1)*], in maintenance of PIN polarity essential for polar auxin transport [*GN (GNOM)*] and in auxin signalling [*TIR1 (TRANSPORT INHIBITOR RESPONSE), ARF7* and *ARF19 (AUXIN RESPONSE FACTOR 7/19)*] (Okumura et al. 2013; Okushima et al. 2007; Parry et al. 2009; Swarup et al. 2008; Swarup et al. 2001).

As auxin is involved in virtually every aspect of eudicot and monocot root development (Lavenus et al. 2013; Orman-Ligeza et al. 2013), changes in those genes are expected to influence root system efficiency (see Chapter 1) and crop performance under various conditions. For example, mutations leading to agravitropic root behaviour in *Arabidopsis*, like in *aux1-22* (Marchant et al. 1999), may

improve nutrient uptake and/or reduce the risk of nutrient leaching. Furthermore, auxin signalling in plants is widely used by various biotic pathogens during infection. For example, mutations in the *TIR1* family increase the susceptibility to biotic agents (Jahn et al. 2013) and auxin influx carriers are involved in actinorhizal nodule formation in *Casuarina glauca* (Peret et al. 2007).

Aims of the study

This chapter aims to answer the following question: What is the level of conservation between dicots and monocots for a key auxin gene regulatory pathway involved in LR formation? The three specific objectives of this chapter are given below:

(1) Detailed phylogenetical analysis of barley gene (sub)families with the purpose of establishing their homology to selected *Arabidopsis* genes.

(2) Virtual mapping of these selected genes on commonly used genetic map(s), which will be needed for future comparative QTL analysis.

(3) QTL meta-analysis for one of the chosen genes based on publicly available QTL data.

Results and discussion

Sequence-based search for homologs in barley

The protein sequences of selected *Arabidopsis* genes were first used in a tBLASTn search for putative homologs in sorghum (*Shorghum bicolor*) and rice, whose genomes have been recently released (International Rice Genome Sequencing 2005; Paterson et al. 2009). We included the monocot protein family sequences into the analysis and not only putative equivalent genes to improve the accuracy of the predictions and to verify if any of the barley sequence is missing due to the incompleteness of current barley expression databases. *Brachypodium distahyon* was also considered in this analysis as it is a close relative of barley and as the size of gene families is likely to be smaller than in barley, sorghum and rice (Wei et al. 2014). Those monocot sequences also made the backbone of a temporal phylogeny analysis (data not shown).

In order to pull out possible representatives of selected gene families in barley, the protein sequences from *Arabidopsis* and chosen monocots were used to query the publicly available barley sequence databases. In the framework of our long-standing collaboration with the JHI (James Hutton Institute, UK), we could also access the most recent barley sequence resources that included barley cv. Bowman genomic assemblies and confidential barley expression datasets. Barley consensus sequences from expression and genomics data were used to predict the putative coding sequences that were then introduced into the final phylogenetic analysis. The size of gene families was consistent between barley and chosen monocots, except for amino acid/auxin permeases (AAAP) protein family, were the initial BLAST search returned only four AUX/LAX sequences, in contrast to rice and maize, where AUX/LAX protein family contains five members. Therefore, by using a pair of degenerated primers, we made an attempt to amplify an additional member of AUX/LAX family from barley cDNA synthetized from the root tissue. This molecular approach revealed the existence of one more expressed

AUX/LAX member in barley which was not found in the initial BLAST search. Based on its highest sequence similarity to AtLAX3 protein, we named it HvLAX3_1H. Thereafter, a full mRNA sequence obtained by using 5'- and 3'-RACE PCR revealed that short fragments of this barley gene were present in databases, but were misaligned with other members of AUX/LAX protein family during the automatic creation of contigs, possibly due to high sequence similarity. This cloned sequence was thereafter included in the subsequent analyses.

Therefore, based on sequence-similarity searches in cereal databases including those of barley that are not yet publicly available, we were able to gather the expressed members of the selected gene families in barley.

Phylogenetic analysis of selected protein families

Phylogenetic analysis at the protein level was employed to establish the relationship between the selected protein sequences from *Arabidopsis*, barley, rice, sorghum or maize.

The phylogenetic studies of the transport inhibitor response1-like family (TIR1-like family) revealed that proteins fall into two clades, containing six TIR1-like members in *Arabidopsis* and five members from each monocot species (Figure 2-1). The top cluster contains the selected *Arabidopsis* TIR1 protein sequence and four other closely related AFB auxin receptors (Parry et al. 2009). Barley HvTIR1_1H falls into a small clade that contains one gene from *Brachypodium*, rice and sorghum and two genes from *Arabidopsis*, that are TIR1 and AFB1. It is likely that the presence of one additional member in *Arabidopsis* is a result of a gene duplication event after eudicot-monocot split (Wang et al. 2006). The functional analysis of TIR1/AFB clade has been reported and suggests that TIR1 and not AFB1 contributes to auxin response in the root (Parry et al. 2009).

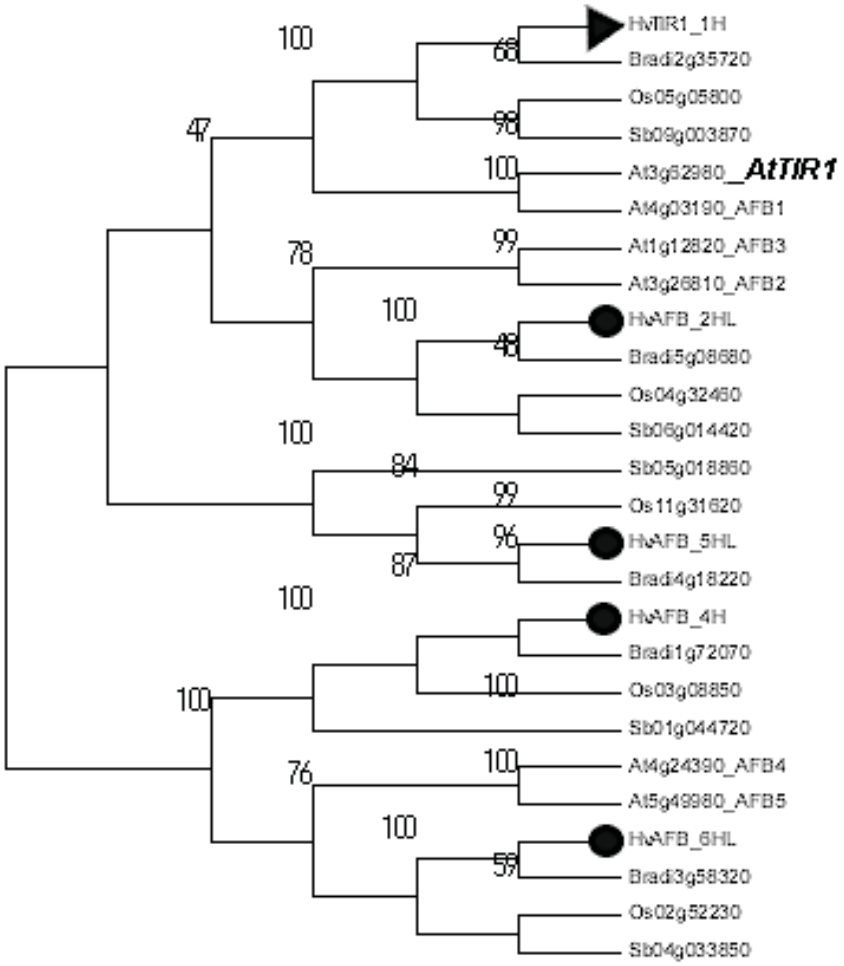

Figure 2-1: Evolutionary relationships of selected *Arabidopsis* and grasses proteins belonging to TIR1-like family.

The evolutionary history was inferred using the Neighbor-Joining method and the optimal unrooted tree of the transport inhibitor response1-like family is shown. The predicted homologous protein sequences belonging to the TIR1-like family in barley are marked with rounds and represent their previously uncharacterized members. The triangle marks a putative TIR1 protein in barley. Chromosomal location of each barley gene is shown after its name, where S = short arm, L = long arm. The percentage of replicate trees in which the associated taxa clustered together in the bootstrap test (1000 replicates) is shown next to the branches. Evolutionary analyses were conducted in MEGA6.

In the guanine nucleotide exchange factor (GEF) subfamily, the phylogenetic analysis shows that the proteins fall into two clades in

the probed species (Figure 2-2). This analysis revealed that one barley protein sequence, HvGNOM_4S, is closely related to *Arabidopsis* GNOM protein (At1G13960) and to one rice, one shorgum and one *Brachypodium* protein.

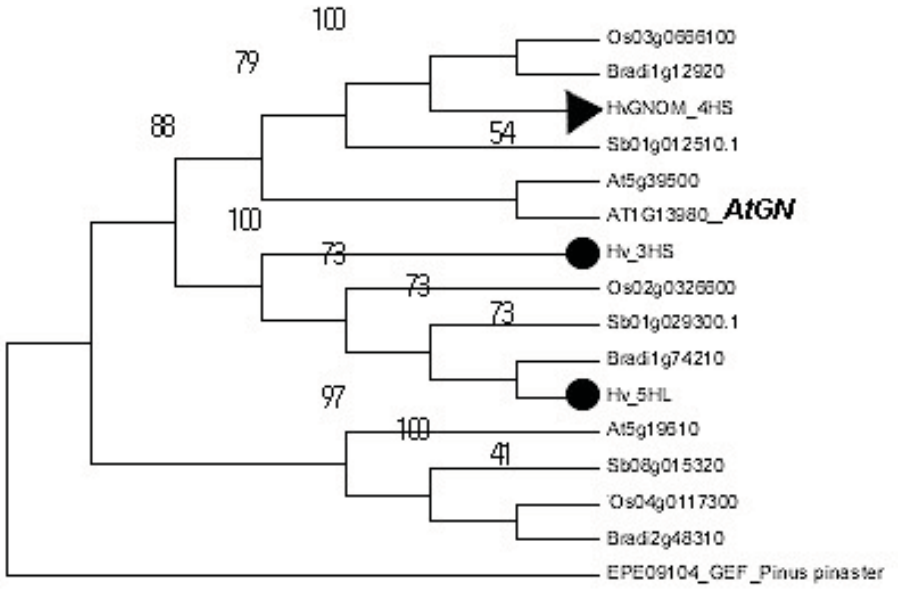

Figure 2-2: Evolutionary relationships of selected *Arabidopsis* and grasses proteins belonging to GNOM-like subfamily.

The evolutionary history was inferred using the Neighbor-Joining method and the optimal tree of the guanine nucleotide exchange factor subfamily is shown. The predicted homologous protein sequences belonging to the GNOM-like protein (sub)family in barley are marked with rounds and represent their previously uncharacterized members. The triangle marks a putative GNOM protein in barley. Chromosomal location of each barley gene is shown after its name, where S = short arm, L = long arm. The percentage of replicate trees in which the associated taxa clustered together in the bootstrap test (1000 replicates) is shown next to the branches. GEF protein sequence from *Pinus pinaster* was used as an outgroup. Evolutionary analyses were conducted in MEGA6.

In the auxin response factor (ARF) subfamily, the phylogenetic analysis showed two major clades that are further divided into several smaller ones (Figure 2-3). Surprisingly, only one barley protein sequence, HvARF7HS.1, clusters together with *Arabidopsis* ARF7 and ARF19 sequences, which is in agreement with rice and *Brachypodium*.

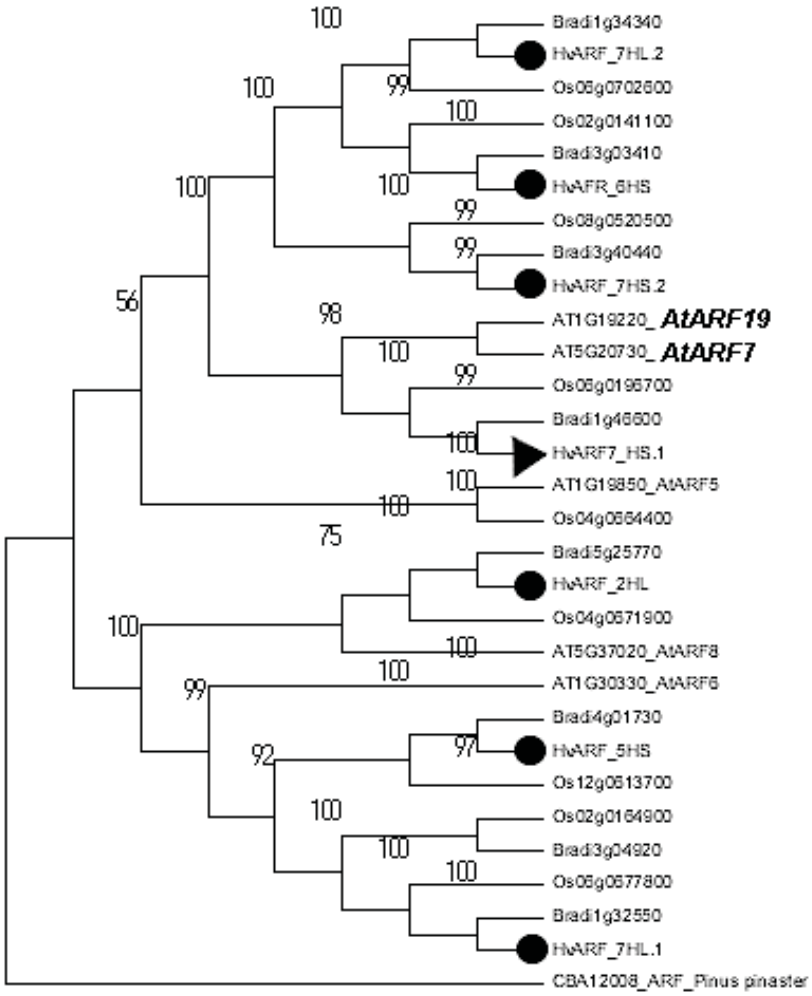

Figure 2-3: Evolutionary relationships of selected *Arabidopsis* and grasses proteins belonging to ARF family.

The evolutionary history was inferred using the Neighbor-Joining method and the optimal tree of auxin response factor subfamily is shown. The predicted homologous sequences belonging to the ARF protein subfamily in barley are marked with rounds and represent their previously uncharacterized members. The triangle marks a putative barley protein equivalent to *Arabidopsis* ARF7 and ARF19 proteins. Due to the size of the ARF family, sorghum sequences are not shown. Chromosomal location of each barley gene is shown after its name, where S = short arm, L = long arm. The percentage of replicate trees in which the associated taxa clustered together in the bootstrap test (1000 replicates) is shown next to the branches. ARF protein sequence from *Pinus pinaster* was used as an outgroup. Evolutionary analyses were conducted in MEGA6.

Therefore, on the basis of phylogenetic analysis, the presence of two *Arabidopsis* ARF genes may suggests that they have arisen from gene duplication that occurred after eudicot and monocot split followed by subfunctionalisation in eudicots (Rastogi and Liberles 2005).

Phylogenetic studies revealed that members of AAAP subfamily family of AUX/LAX fall into two clades (Figure 2-4).

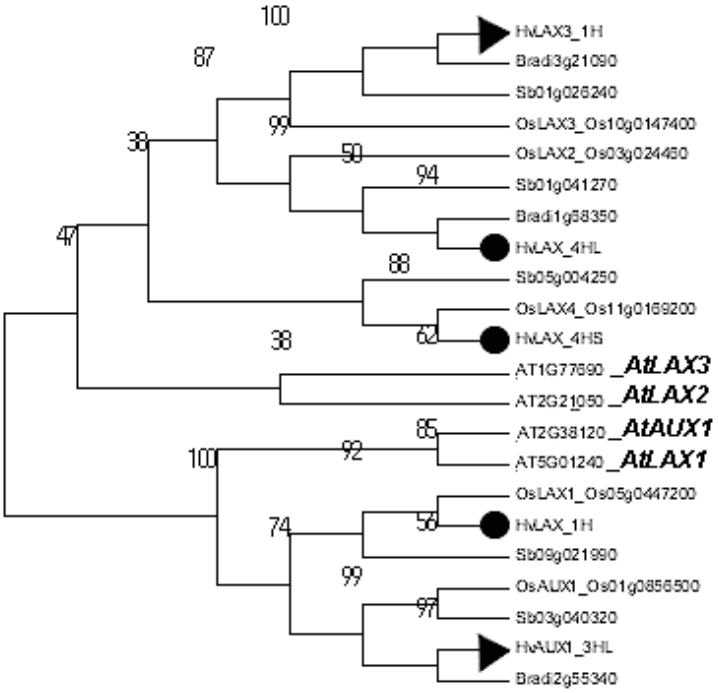

Figure 2-4: Evolutionary relationships of selected *Arabidopsis* and grasses proteins belonging to AUX/LAX family.

The evolutionary history was inferred using the Neighbor-Joining method and the optimal unrooted tree of amino acid/auxin permeases subfamily of AUX/LAX is shown. The predicted homologous protein sequences belonging to the AUX/LAX protein subfamily in barley are marked with rounds and represent their previously uncharacterized members. The triangles mark the putative AUX1 and LAX3 proteins in barley equivalent to *Arabidopsis* AUX1 and LAX3 proteins. AUX/LAX family members in maize (Buchanan et al.) are also shown. Chromosomal location of each barley gene is shown after its name, where S = short arm, L = long arm. The percentage of replicate trees in which the associated taxa clustered together in the bootstrap test (1000 replicates) is shown next to the branches. Evolutionary analyses were conducted in MEGA6.

The top cluster further separates into a cluster that contains AtLAX2 and AtLAX3 and three distinguishable monocot clusters, containing three AUX/LAX genes for rice and maize, respectively. It is likely that one additional AUX/LAX gene in monocot species is a result of a gene duplication event after the eudicot-monocot divide (Wang et al. 2006). The bottom cluster illustrates the relationship between *AUX1* and *LAX1* in *Arabidopsis* and selected monocot species. Again, monocot sequences fall in two clades separately from *Arabidopsis* sequences. Barley *HvAUX1_3HL* and *HvLAX3_1CH* sequence ware assigned as putative orthologs of *OsAUX1* and *OsLAX3* and will be named *HvAUX1* and *HvLAX3* thereafter, respectively.

It is difficult to unambiguously assign homolog to the *Arabidopsis* sequences on the basis of the phylogenetic tree alone. However, this study revealed that members of selected gene families fall into distinguishable clades with a similar number of genes from each plant species. Therefore, it is likely that major components of the auxin regulatory network involved in LR formation were conserved across plant lineages.

Analysis of exon/intron arrangement

The comparison of exon/intron arrangement can help further to reveal the type of relationship between candidate genes from divergent plant species (Schnable et al., 2012). This is in agreement with the hypothesis that the number, size and location of exons should be largely conserved between orthologs in cereals and to a lesser extent with *Arabidopsis* (Schnable et al. 2012). Therefore, the gene models of *Arabidopsis TIR1, GNOM* and *ARF7/ARF19* were aligned with rice and barley models (Figure 2-5A). For the two members of *AUX/LAX* family investigated in detailes, this comparison is shown in a next chapter, on Figure 3-4.

Although barley genomic sequences were not complete at that time, this approach revealed a general conservation of exon boundaries in selected genes and indicated that those genes are likely to share a common ancestor sequence.

Synteny analysis and virtual mapping of chosen barley genes

Arabidopsis, rice and barley shared a common angiosperm ancestor about 240 million years since these three species diverged. Rice and barley have diverged for approximately 50 million years from a common grass ancestor (Gale and Devos 1998). The comparative genetics in grasses revealed a remarkable conservation of gene content and gene order (Gale and Devos 1998). Therefore, the identification of syntenic blocks of genes is one of the methods for ortholog/homeolog classification in grasses (Schnable et al. 2012). To gain a better inside into the evolution of the selected gene families and to improve bioinformatic predictions, we performed a synteny analysis in cereals using the Strudel software. This analysis was restricted to the genes of interests and revealed broad synteny blocks between barley, *Brachypodium* and rice (Figure 2-5B through D).

To determine map positions of selected barley genes, the "Genome Zipper" files that contain barley genes in a putative linear order along each barley chromosme (Mayer et al. 2011) has been combined with Steptoe x Morex (SxM) consensus genetic map (Close et al. 2009) in agreement with the chromosome arm location established by the IPK Gatersleben group (Figure 2-6). The Genome Zippers in barley were developed by chromosome sorting, next-generation sequencing, array hybridization, and systematic exploitation of conserved synteny with model grasses to assign ~86% of the estimated ~32,000 barley genes to individual chromosome arms (Mayer et al. 2011). The putative final locations of the genes of interest on barley Steptoe x Morex Rec-Bin genetic map are summarized in Table 2-1.

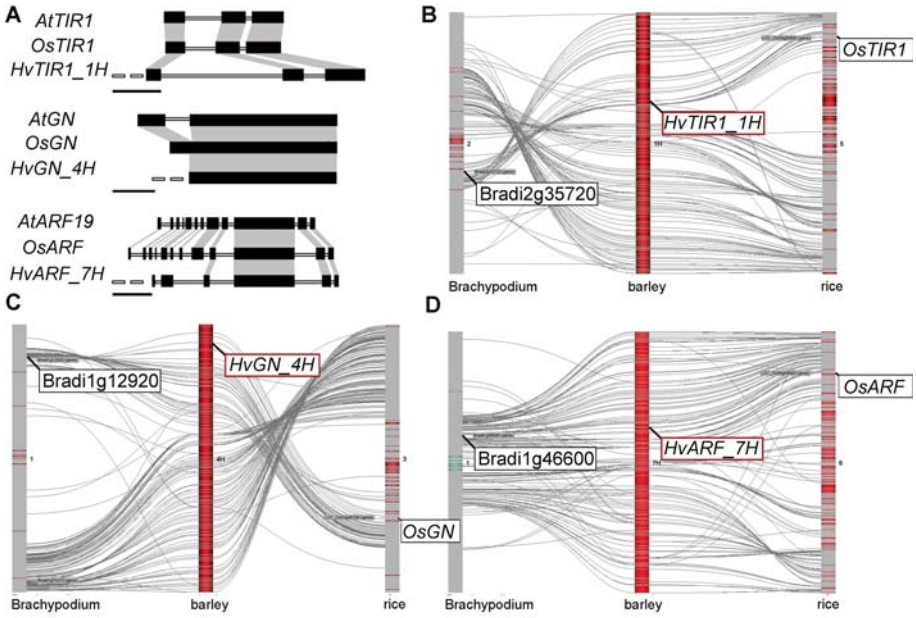

Figure 2-5: Exon/intron arrangement of putative orthologs in *Arabidopsis*, rice and barley and synteny analysis in *Brachypodium*, barley and rice.

Black boxes in **(A)** represent coding sequences of exons and are connected via white lines that correspond to introns. The corresponding regions between *Arabidopsis,* rice and barley gene models are shaded grey. Barley coding sequences were obtained from barley expression databases and were compared with barley cv. Morex and cv. Bowman genome assemblies. The truncated sequence of barley is shown as a dashed line. *Arabidopsis* and rice coding and genomic sequences were obtained from the NCBI database. *AtARF7* is not shown, as it resembles *AtARF19*. All sequences were aligned with the Spidey sequence alignment software (NCBI) for exon/intron boundary visualisation and processed in Powerpoint (Microsoft). Bar = 1 kbp. **(B** through **D)** Synteny analysis between *Brachypodium,* barley and rice performed in Strudel software. The positions of corresponding genes are pointed out by white boxes and synteny between chromosomes is marked with gray lines.

Because the Derkado x B83 (DxB) mapping population is heavily used in our lab for QTL analysis, the estimated position of the genes of interest has also been transferred into a DxB consensus map (Bill Thomas, pers. comm.) based on corresponding markers (Table 2-1). Taken together, this genome-wide analysis pointed out the putative orthologs in barley, rice and *Brachypodium* genomes. The chosen

genes were then virtually mapped onto barley chromosomes, based on a recently released Genome Zippers.

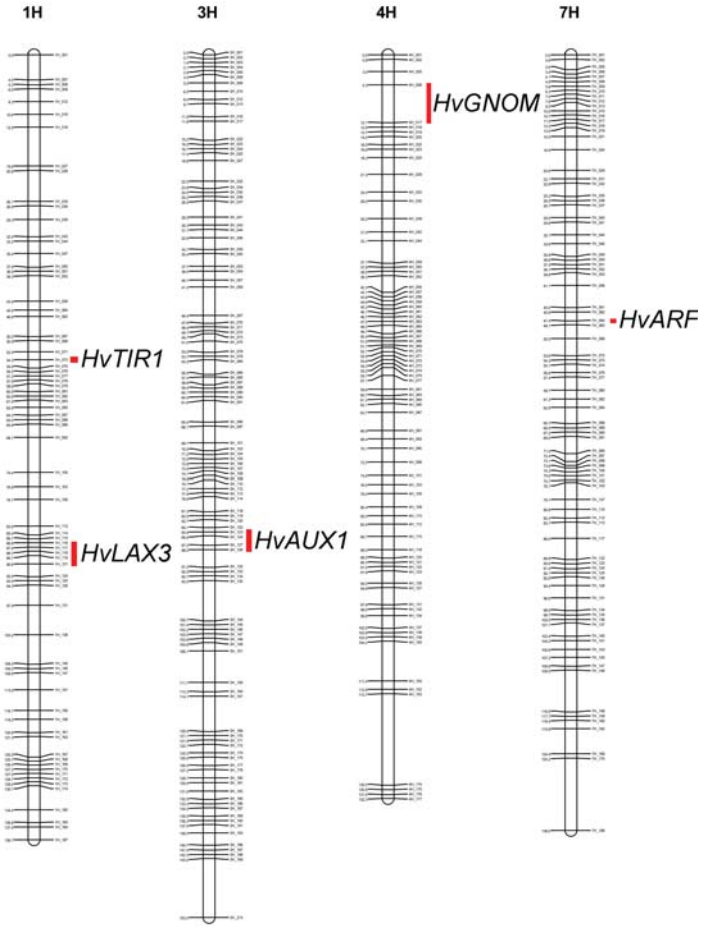

Figure 2-6: Positions of putative *HvTIR1, HvLAX3, HvAUX1, HvGNOM* and *HvARF* genes on barley Steptoe x Morex recbin map.

Red frames indicate putative position of chosen barley genes.

The virtual mapping on the chromosomes alongside sequence information could be instrumental for barley TILLING (Targeting Local Lesions IN Genomes), using the selected candidate genes as a probe. TILLING is a resource for high-throughput gene discovery that was successfully used in barley (Gottwald et al. 2009; Weil 2009). Therefore, we used a phenotypic screen on the barley cv. Morex TILLING population developed at JHI (TILLMORE) to search for

mutants in selected genes by using aeroponics and filter-based systems (data not shown). Unfortunately, the TILLING platform was not operational anymore by the end of our experiments.

Table 2-1: Summary of putative position of chosen genes on used maps.

Alias	Flanking Rec-Bin markers, Steptoe x Morex	Distance [cM]	Flanking Zipper markers, Morex	Distance [cM]	Old Steptoe x Morex marker name	Derkado x B83 map	Distance [cM]
HvAUX1	3H_124 3H_128	85.6-88	2_1381 1_0344	102.21-104.53	8984-579 2660-678	8020-87 10114-1946	94.9-120.8
HvLAX3	1H_075 1H_077	55.8-57.2	2_1217 3_0478	54.73-55.49	2401-1028 5297-796	6081-850 3675-2615	53-62.3
HvTIR1	1H_073	54.3	1_0235 1_1301	47.47-49.34	21412425 ABC12550-1-3-276	6081850 3675-2615	53-62.3
HvGNOM	4H_008 4H_018	5.3-12.9	1_1345 3_0140	5.55-7.06	ABC14522-1-8-350 ABC12449-1-3-227	13301-90 2055-947	0-20.4
HvARF	7H_064	47.4	2_0031 2_0113	50.65-53.88	304-194 4767-1374	5467-1663 5028-1261	84.9-88.2

QTL meta-analysis of *AUX1*

Several research studies support the notion that an increase in topsoil root penetration might be beneficial for phosphorus uptake (Gowda et al. 2011b; Guyomarc'h et al. 2012; Trubat et al. 2012). This can be achieved, among the other possible ways, by altering root angle (Guyomarc'h et al. 2012). Therefore, the *AUX1* locus that is known to govern primary root gravitropic response in *Arabidopsis* was chosen for comparative QTL analysis. In this meta-analysis, a special emphasis was given to morphological root traits and phosphorus uptake.

The sequence-based search and phylogenetic analysis of *AUX/LAX* family members in soybean, maize and rice were used to point out the

putative orthologs of *AtAUX1* (Figure 2-4). In soybean, a putative ortholog of *AtAUX1* is located on third chromosome with physical coordinates 3: 67956412-67962071, under the locus name SB03G040320. In maize, *ZmAUX1* is localised within bin3.06 on the third chromosome (3:178002561-178009059) with the locus name LOC100285200. In rice, *OsAUX1* was found on the first chromosome (1:36997295-37003753) with a locus name LOC_Os01g63770. Using this information, the *AUX1* genes were projected on public genetic linkage maps along with reported QTL for root traits that coincide with positions of putative orthologs of *AtAUX1* in eudicot soybean and monocot rice and maize (Figure 2-7 and Suplementary Materials, Tables S-1 through S-3).

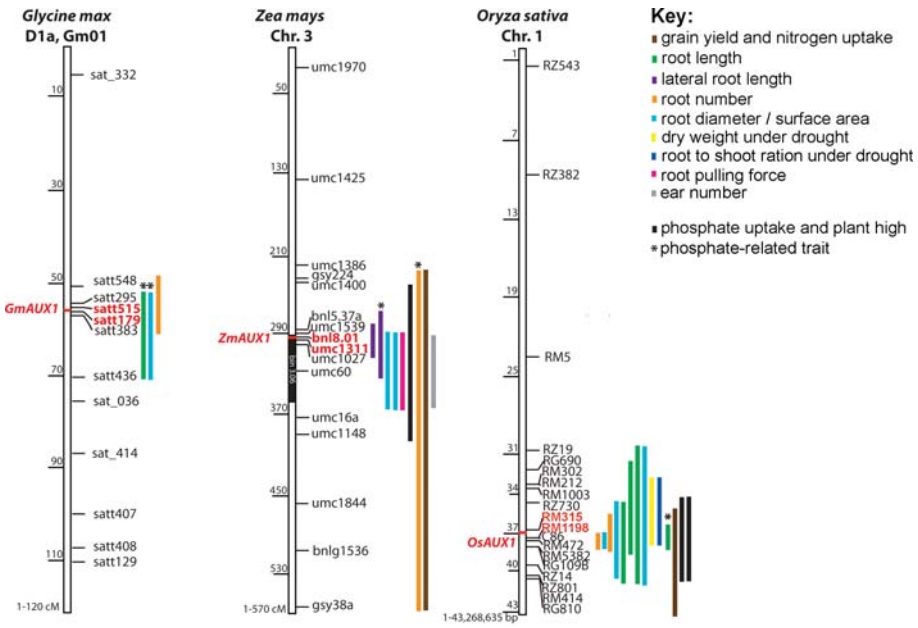

Figure 2-7: *In silico* QTL analysis of putative AUX1 in soybean, maize and rice.

The information of soybean *SbAUX1*, maize *ZmAUX1* and rice *OsAUX1* positions and morphological root traits were collected and projected on the public genetic linkage maps.

This meta-analysis revealed that *AUX1* position in soybean, maize and rice match QTL intervals for a number of traits that might relate with

root gravitropism. In addition, the *AUX1* position in soybean, maize and rice also coincide with QTLs for phosphorus uptake. The presence of several QTLs within different mapping populations and among plant species suggests that this chromosomal region carries important loci for RSA that are evolutionary well conserved.

Taken together, the QTL meta-analysis in three different plant species revealed the possible link between morphological root traits, phosphorus uptake and *AUX1* chromosomal location.

Conclusions

Using an *in silico* strategy, we have been able to identify the main components of auxin-dependent LR gene regulatory pathways in barley. The combination of sequence-based and phylogenetic methods provided a good tool for investigating evolutionary history of gene families in diverged plant species.

First, all members of the six selected gene families from *Arabidopsis*, barley, rice, sorghum and *Brachypodium* were analysed by employing sequence-based and phylogenetic approaches. The sequence similarity-based searches reveal that the overall number of gene family members is similar in *Arabidopsis* and in chosen monocots. Incorporating other plant species in the analysis has proved to be substantial when addressing a plant species like barley, for which sequence data were not yet complete. The phylogenetic studies showed that members of equivalent gene families in *Arabidopsis* and selected monocots fall into distinguishable clades with a similar number of genes from each plant species. Interestingly, this analysis also demonstrated that the evolutionary history of these plant gene families was accompanied by gene duplication and/or gene loss events.

Secondly, a more detailed bioinformatic analysis of predicted orthologs from *Arabidopsis* and chosen monocots was performed. The comparison of exon/intron arrangement allowed observing a conservation of general gene structures among equivalent genes in *Arabidopsis*, rice and barley. Subsequently, a genome-wide analysis

of barley, rice and *Brachypodium* genomes revealed the presence of the synteny blocs in close proximity to selected barley genes.

By using both gene- and genome-wide approaches that mirror the evolutionary evens at different scale, we concluded that those genes are likely to share a common ancestral gene.

The QTL meta-analysis performed for three different plant species revealed the possible link between chromosomal location of *AUX1*, morphological root traits and phosphorus uptake. It is likely that, according to its functional description in *Arabidopsis*, the cereal equivalent of *AUX1* may be used to improve plant performance in low-phosphorus content soils. Furthermore, the candidate-based approach may be potentially used to target genes behind known QTLs.

Taken together, it is likely that major components of a gene network involved in LR formation are conserved across plant lineages. Further studies should focus on functional characterisation of these selected genes in barley. This could be achieved by reverse complementation assay in *Arabidopsis* and transcriptional studies in cereals. Coupled with characterisation of available mutants and/or gene silencing lines, this could help to understand the molecular background behind post-embryonic root formation in plants.

Materials and methods

Chemicals

The chemicals used were obtained from Sigma (Sigma-Aldrich Co. LCC, Diegem, Belgium), WVR (VWR International Europe BVBA, Leuven, Belgium) and Fisher (Fisher Co. Ltd., Erembodegem – Aalst, Belgium) unless otherwise mentioned.

The gene evolution analysis

This work was partially carried out using the MIPS (Munich Information Center for Protein Sequence; mips.helmholtz-muenchen.de) and Maize sequence databases (www.maizesequence.org). Barley sequences were obtained from barley cv. Bowman genomics assemblies at The James Hutton Insitute,

UK (confidential), barley cv. Morex genomics assembly generated by IPK Garersleben (confidential), recently produced expression data through a second-generation (2G) sequencing platform (Solexa) at The James Hutton Institute, UK (confidential), the released expression data form Harvest#32, TIGR (http://www.jcvi.org/cms/research/groups/plant-genomics/) and #35 in PLEXDB (www.plexdb.org).

The prediction of the new putative barley coding sequences and exon/intron arrangements was done using on-line *in silico* tools: Softberry (http://linux1.softberry.com), Spidey (http://www.ncbi.nlm.nih.gov) and CAP3 (http://pbil.univ-lyon1.fr/cap3.php). The similarities on protein levels were determined using ClustalW. BLOSUM62 scoring matrices were computed in order to determine similarity scores that reffers to the sum of functionally similar aminoacids for all aligned pairs of characters minus the gap penalties introduced in either sequences. N-terminal analysis was performed by motif scan (http://myhits.isb-sib.ch/cgi-bin/motif_scan). Evolutionary analyses were conducted in MEGA5 (Tamura et al. 2007). The evolutionary history of gene families was inferred using the Neighbor-Joining method using a bootstrap test (1000 replicates) and the evolutionary distances were computed using the Poisson correction method. MapViewer (www.harvest-web.org) was used to analyse the conservation of gene order along chromosomes of *Brachypodium*, barley and rice.

Identification of *HvLAX3* in barley

Identification strategy

The pair of degenerated primers AF2 and AF3 (Peret et al. 2007) was used to amplify fragments of *AUX1* and *LAX3* cds from barley cv. Golden Promise cDNA based on sequence similarity. The two amplicons obtained were extracted from the gel and sequenced. One amplicon matched the *HvAUX1* present in barley expression databases, whereas the second amplicon corresponded to *HxLAX3*, which was not found in the initial BLAST search. Based on the two sequences obtained, RACE primers were designed and are listed in Table 2-2. 5'- and 3'-RACE PCRs were done for both *HvAUX1* and *HvLAX3*, based on barley cv. Golden Promise cDNA using RACE PCR kit (Clontech) according to the manufacturer's instructions.

Table 2-2: Primers used to identify *HvLAX3* in barley.

Name	Primer name	Sequence
AUX/LAX	F_AF2	CCACAT6GCRTGCATDATYTC
	R_AF3	TGGAC6TAYATHTTYGG6GC6TGY
HvLAX3	3'LAX3RACE	TCATGACCACCTACACCGCCTGGTA
	5'LAX3RACE	GGTACCAGGCGGTGTAGGTGGTCAT
HvAUX1	3'AUX1RACE	GGAACCAGTACTGTTGCTTGCT
	5'AUX1RACE	CAGGAATTTACTGTGCGATTGA

RT-PCR analysis

Extraction of total RNA from plant tissues was carried out using the Tri Reagent (Sigma) according to the manufacturer instructions. The RNA was then stored at -80°C. Synthesis of cDNA was carried out using 1µg or total RNA measured with a spectrometer (NanoDrop) and treated for 30 min with DNase RQ1 (Promega). The cDNA was subsequently prepared from a minimum of 250 ng RNA using a SuperScript II reverse transcriptase kit and Oligo(dT)12–18 primers (Invitrogen), according to the manufacturer's instructions. The cDNA was then stored at -20°C. PCR were carried out using a PTC-100 thermocycler (MJ Research INC). The PCR mix was made on ice with the following solutions: 1µl of cDNA template (0.2 µg), 1 µl of 10 mM forward primer, 1 µl of 10 mM reverse primer, 0.6 µl of 10 mM dNTPs, 4 µl of 5 x PCR green Phire buffer, 0.4 µl of Phire polymerase (Thermo Scientific) and SDW up to a final volume of 20 µl. The primers used in this study are listed in Table 2-1. PCR were carried out with the following standard conditions: initial denatutation 98°C for 15 s min, 36 cycles of 98°C for 5 s, 60°C for 15 s and 72°C (30 s per 1 kb fragment) and then 72°C 5 min. Agarose (1.5% w/v) was dissolved in 0.5xTris-Borate-EDTA (TBE) buffer in a microwave oven. Ethidium bromide (EtBr) was added to give a final concentration of 0.1 µg / ml. The agarose was then poured into the electrophoresis tray and after 15 min, the gel was transferred to a gel electrophoresis tank containing 0.5 x TBE buffer. Samples and 10 kb ladder were loaded into the wells of the gel and run for 90 V for 90 min. The gel was then exposed to UV light transillumiator and photographed.

QTL meta-analysis

The information of morphological root trait and AUX1 positions in soybean, maize and rice were collected from: Gramene (http://www.gramene.org/), MaizeGDB (http://www.maizegdb.org/), SoyBase (http://soybase.org/), JGI (http://jgi.doe.gov/), PGROP (http://www.plantgdb.org/) and NCBI (http://www.ncbi.nlm.nih.gov/). These positions were aligned on the public genetic linkage maps and consensus maps were generated.

Plant growth materials and growth conditions

Seeds of *Hordeum vulgare* cv. Golden Promise kindly provided by Dr Jennifer Stephens (The James Hutton Institute, UK) were used in this study. Seeds were wetted in 70% (v/v), placed in 5% (v/v) sodium hypochlorite for 15 min on a shaker and were washed several times with SDW (steril destilled water). Seeds were then stratified at 4°C for 2 d on a filter paper and were partially covered in SDW. Then, seeds were attached to a filter paper on a vertical plexi-glass plate with a sterile tape (Milipore, 3M) and left to germinate for two days in a dark, humid and closed box. Seedlings were then transferred to the aeroponics system where roots were sprayed with nutrient solution for 15 s every 5 min. Half-strength Hewitt solution (Hewitt 1966) was used for barley and consist of 2 mM Ca(NO3)2 · 4H2O, 2 mM KNO3, 0.75 mM MgSO4 · 7H2O, 0.67 mM NaH2PO4 · 2H2O, 0.05 mM FeEDTANa, 0.03 μM (NH4)6Mo7O24 · 4H2O, 50 μM NaCl, 25 μM H3BO3, 5 μM MnCl2 · 4H2O, 0.5 μM CuSO4 · 5H2O, 0.5 μM ZnSO4 · 7H2O, 0.6 mM Na2SiO3 · 5H2O; pH 5.8). Seedlings were scanned on a customized (21 x 60cm) flatbet transparency scanner with a resolution of 300 DPI.


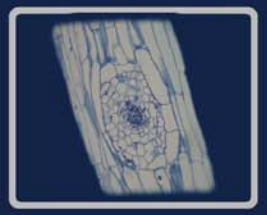
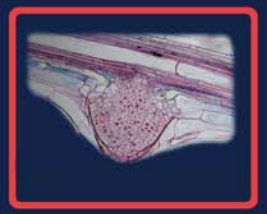


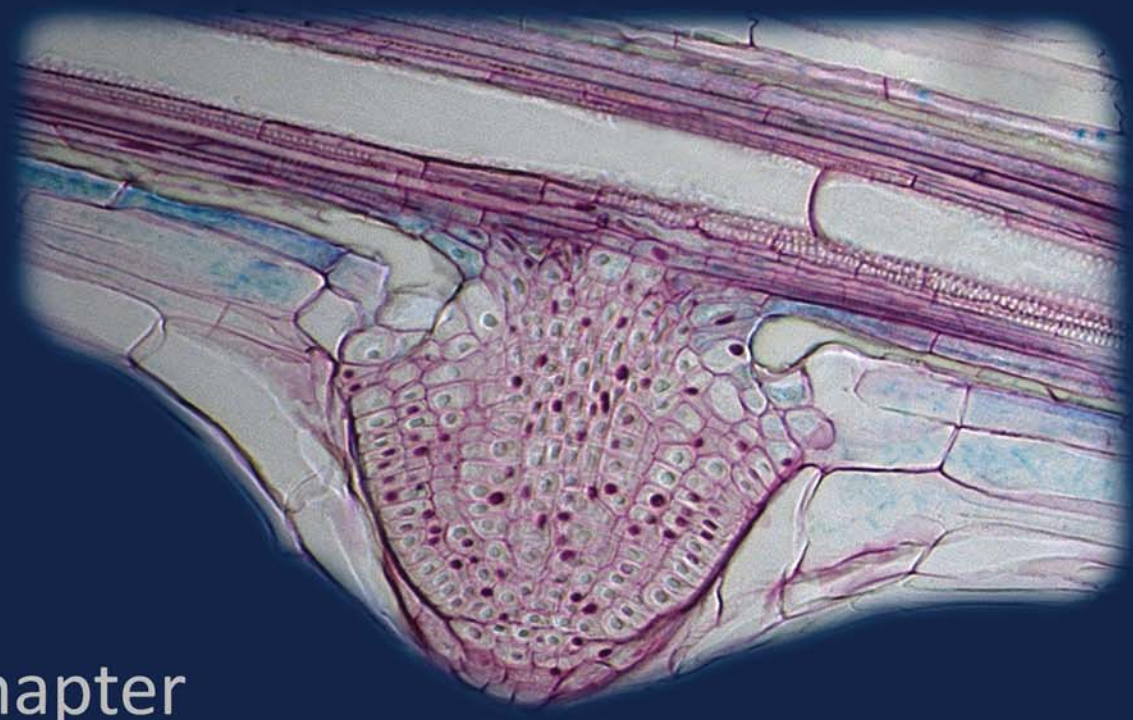

Chapter 3

CHAPTER 3

Characterisation of auxin influx carriers in cereals

Manuscript in preparation

Beata Orman-Ligeza[1,2,3], Benjamin Lobet[1], Malcolm J. Bennett[4], Tom Beeckman[2,3] and Xavier Draye[1]

[1]Universite catholique de Louvain, Earth and Life Institute, Louvain-la-Neuve, Belgium.
[2]Department of Plant Biotechnology and Bioinformatics, Ghent University, B-9052, Ghent, Belgium.
[3]Department of Plant Systems Biology, VIB, B-9052, Ghent, Belgium.
[4]Centre for Plant Integrative Biology, School of Biosciences, University of Nottingham, Sutton Bonington, LE12 5RD, UK.

Author Contributions

X.D., T.B., M.B. and B.O.-L. designed the research; B.O.-L. performed the research and wrote the manuscript, B.L. selected and confirmed barley HvLAX3:GUS and HvLAX3 RNAi homozygous lines, performed GUS staining of *HvLAX3:GUS* lines and characterised HvLAX3 RNAi lines in barley.

Abstract

Auxin carriers are largely responsible for the generation of local auxin gradients and are therefore involved in the spatial regulation of several developmental events, including different steps of LR formation. This chapter reports on a translational candidate gene approach between the model *Arabidopsis thaliana* and barley *(Hordeum vulgare)*, and on the subsequent characterisation of two members of the *AUX/LAX* gene family in barley.

In an initial search, a basic local alignment search tool (BLAST) was used to identify the members of *AUX/LAX* family in barley, followed by molecular analyses and phylogenetic analyses at the protein level. Further insight into the evolution *AUX/LAX* family in barley was gained by exon/intron arrangement, expression patterns and genetic map location. Two auxin carriers have been selected for further characterisation in barley. Reverse complementation assays in *Arabidopsis* indicated that *HvAUX1* and *HvLAX3* are functionally equivalent to *AtAUX1* and *AtLAX3*. Both influx carriers are expressed during LR development, but their expression patterns suggest that their function might have diverged from *Arabidopsis*. These results suggest that *HvAUX1* and *HvLAX3* are orthologous to *AUX1* and *LAX3* described in *Arabidopsis*.

Key words: translational research, lateral root, LR, gravitropism, barley, cereal, auxin influx carriers, *AUX1*, *LAX3*.

Introduction

Auxin influx and efflux carriers in *Arabidopsis* mediate together the formation of local auxin gradients that are crucial for many aspects of root growth and development (Band et al. 2014). However, how these regulatory processes translate in crop species remains widely unexplored. Members of the AUX/LAX family belongs to amino acid transmembrane permeases. Their topological structure and protein activity as auxin influx carriers have been well described in *Arabidopsis* (Swarup et al. 2008; Yang et al. 2006; Peret et al. 2012b). AtAUX1 has 11 predicted transmembrane domains and functionally important residues between the transmembrane regions and in N-terminus (Swarup et al. 2004; Yang et al. 2006). The other members of AUX/LAX family share high sequence similarity along the predicted transmembrane regions and are estimated to have a similar number of such domains (Peret et al. 2012b). Despite their sequence similarity, members of *AUX/LAX* family exhibit nonredundant, complementary expression patterns (Figure 3-1) and orchestrate together distinct auxin-dependent developmental processes (Peret et al. 2012b). In aerial tissues, AUX1 and LAX3 are involved in apical leaf phyllotaxy and apical hook development (Bainbridge et al. 2008; Vandenbussche et al. 2010), LAX2 regulates vascular development and LAX1 and LAX2 are both required for correct leaf phyllotaxy (Bainbridge et al. 2008; Peret et al. 2012b). In root tissues, mutations in *AtAUX1* cause roots to become agravitropic (Delbarre et al. 1996) and lead to a 50% reduction in LR number (Marchant et al. 2002), whereas the other members of the *AUX/LAX* family exhibit normal gravitropic response (Peret et al. 2012b). Early studies showed that *AtAUX1* is expressed in the root cap and epidermis of the elongation zone (Marchant et al. 1999) and that both tissue are essential for its proper functioning (Swarup et al. 2005). Subsequently, *AtAUX1* has been shown to be a high affinity auxin carrier protein in a *Xenopus* oocyte expression system (Yang et al. 2006).

AtLAX3 has also been shown to be a high affinity auxin transporter using heterologous expression in *Xenopus* oocyctes and human U20S

cells (Swarup et al. 2008). Mutations in *AtLAX3* do not influence root gravitropism, but impair LR emergence. Expression studies revealed that *AtLAX3* is expressed in cortical and epidermal cells directly overlaying developing LR primordia (Swarup et al. 2008). The LAX3 activity in those cells is proposed to induce cell-wall-remodelling enzymes, which are likely to promote cell separation and ease the progression of the developing LR primordia (Swarup et al. 2008).

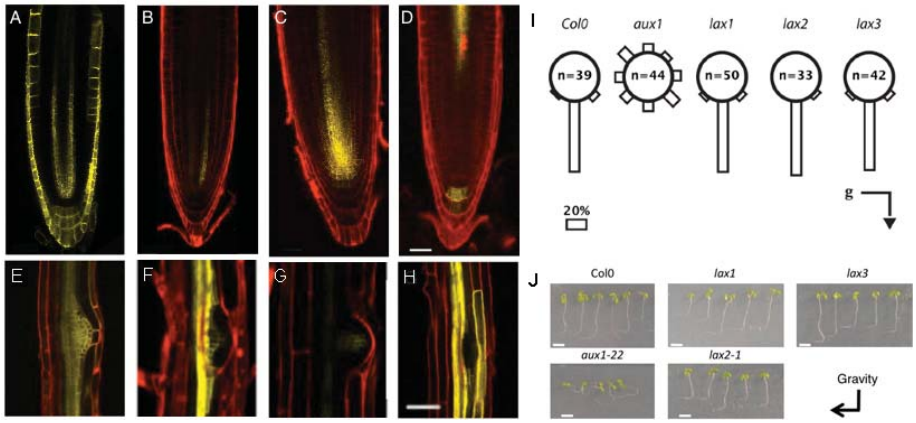

Figure 3-1: *AUX/LAX* genes exhibit complementary expression patterns and *lax1, lax2* and *lax3* mutants exhibit normal gravitropic response in *Arabidopsis*.

(A, E) Expression profile of *ProAUX1:AUX1-YFP,* **(B, F)** *ProLAX1:LAX1-VENUS,* **(C, G)** *ProLAX2:LAX2-VENUS* and **(D, H)** *ProLAX3:LAX3-VENUS* in the primary root apex and LRs, respectively. Wheel diagrams **(I)** and images **(J)** showing gravitropic responses of wild-type (Col0), aux1-22, lax1, lax2-1 and lax3 seedlings. Plates were rotated at 90° and root angles were determined 3, 6, 9 and 12 h after gravistimulation and grouped into 8 classes of 45° **(I)**. Scale bars 50 µm (**J**); 40 µm **(E-H)**. Bars sizes represent percentage of plants according to scale. Photographs were taken 24 hrs after the gravistimulus (n=20). Adapted from (Peret et al. 2012b) with modifications.

The LR phenotypes of *AUX1* and *LAX3* mutants suggest that there is a link between LR formation and auxin accumulation upstream of auxin response pathways. Interestingly, the other members of *AUX/LAX* family, when expressed under the *AtAUX1* promoter, are unable to rescue *Ataux1* (Peret et al. 2012b). It has also been proposed that regulatory and coding sequences of *AUX/LAX* genes have

undergone subfunctionalization (Peret et al. 2012b). These elements stimulate the identification *AtAUX1* and *AtLAX3* orthologs in barley.

Aims and objectives

The objectives of this study were (1) a detailed *in silico* analysis of barley *AUX/LAX* family with the special emphasis given to *HvAUX1* and *HvLAX3* and (2) functional characterisation of *AUX1* and *LAX3* in barley.

Results and discussion

In silico analysis of the *AUX/LAX* gene family in barley

AtAUX1 and *AtLAX3* function in two different developmental events of LR formation. *Arabidopsis* AtAUX1 operates upstream of LR initiation and root gravitropism (Marchant et al. 2002; Marchant et al. 1999), whereas AtLAX3 facilitates LR emergence (Swarup et al. 2008). Therefore, those two genes were chosen as primary targets of characterisation of potential orthologs in barley.

The protein sequences of barley AUX/LAX family were aligned with *Arabidopsis* AUX/LAX protein sequences using ClustalW software (Figure 3-2). A similarity score was calculated as the sum of scores given for similar aminoacids for all aligned pairs of characters minus the gap penalties introduced in either sequences (Table 3-1). According to the sequence similarity scores computed with four members of *Arabidopsis* AUX/LAX family, barley protein sequences can be divided into two groups, where HvAUX1 and HvLAX_1CH proteins are the most similar to AtAUX1 and AtLAX1, whereas HvLAX_4CHL, HvLAX3 and HvLAX_4CHS are the most similar to AtLAX2 and AtLAX3. The similarity scores with *Arabidopsis* did not allow to confirm earlier predictions of putative orthologs of *AtAUX1* and *AtLAX3* in barley. Therefore, we align the AUX/LAX barley sequences with rice *(Oryza sativa)* AUX/LAX family members (Table 3-1). This approach produced more reliable similarity scores

and suggests that *HvAUX1* is a candidate for the functional ortholog of *AUX1* in rice, whereas *HvLAX3* is most likely an ortholog of *OsLAX3*.

The structure-function analysis of *AtAUX1* revealed that several of the *aux1* mis-sense alleles result from amino acid substitutions at highly conserved residues (Swarup et al. 2004). Those residues are also maintained in the AUX/LAX proteins in barley (Figure 3-2, black arrowheads).

Recent domain swapping studies suggest that the N-terminal end of AUX/LAX family members may be essential for correct protein localization and function (Peret et al. 2012b). A special emphasis was thus given to the N-terminal ends of each AUX/LAX family members in barley. The alignment reveals an insertion of 15 amino acids at the N terminal end of *Hv*LAX_4HS that produces a glycine-rich motif that is absent in the A*t*LAX3 sequence or within any other member of the AUX/LAX sequences (Figure 3-2).

This motif has been proposed to be involved in protein-protein interactions (Bocca et al. 2005). Interestingly, C terminal ends of barley HvLAX3 and HvLAX_4HL proteins both possess a histidine-rich motif, that also may affect protein functionality (Hernandez et al. 2014). We concluded that *HvLAX3* and *HvLAX_4HL* might be the functional orthologs to *AtLAX3*.

A more detailed synteny analysis visualized the presence of syntenic relationships between chromosomal maps of *Brachypodium*, barley and rice that contain *AUX/LAX* family members (Figure 3-3). In barley, five *AUX/LAX* family members were *in silico* located on three chromosomes, namely on first, third and fourth. Only three *AUX/LAX* family members can be found in *Brachypodium* and these were assigned to *OsAUX1, OsLAX2* and *OsLAX3* based on synteny and phylogenetic analyses. Thus, it is likely that the remaining two *AUX/LAX* genes in barley and rice may have arisen from the duplication or retrotransposition events (Schnable et al. 2012).

We then considered the general gene structure (exon number, size and

location) to refine our view of the evolutionary history of the *AUX/LAX*. The available genomic sequences of *AUX/LAX* members in barley were analysed using the exon prediction software Softberry. In parallel, the sequence alignment software Spidey was employed to match expressed barley sequences with available barley genomic sequences. The manually curated gene structures are shown below (Figure 3-4).

The analysis revealed that general gene structure is largely conserved between rice and barley and to a lesser extent with *Arabidopsis*. The members of *AUX/LAX* family contain usually six to nine exons in these plant species.

Table 3-1: Protein similarity scores of *Arabidopsis* and rice in compare to barley sequences.

The protein sequences of AUX/LAX family members in barley, rice and *Arabidopsis* were compared to each other with ClustalW (EMBL). The red-shaded cells represent high similarity rates.

	HvAUX1 3HL	HvLAX 1H*	HvLAX 4HL	HvLAX3 1H	HvLAX 4HS
AtAUX1	85	81	74	69	72
AtLAX1	82	79	80	72	75
AtLAX2	73	72	81	73	75
AtLAX3	73	75	81	80	79
OsAUX1	90	83	74	68	70
OsLAX1	82	88	74	69	72
OsLAX2	72	77	91	75	77
OsLAX3	71	73	80	80	75
OsLAX4	70	72	75	70	85

* Truncated protein sequence

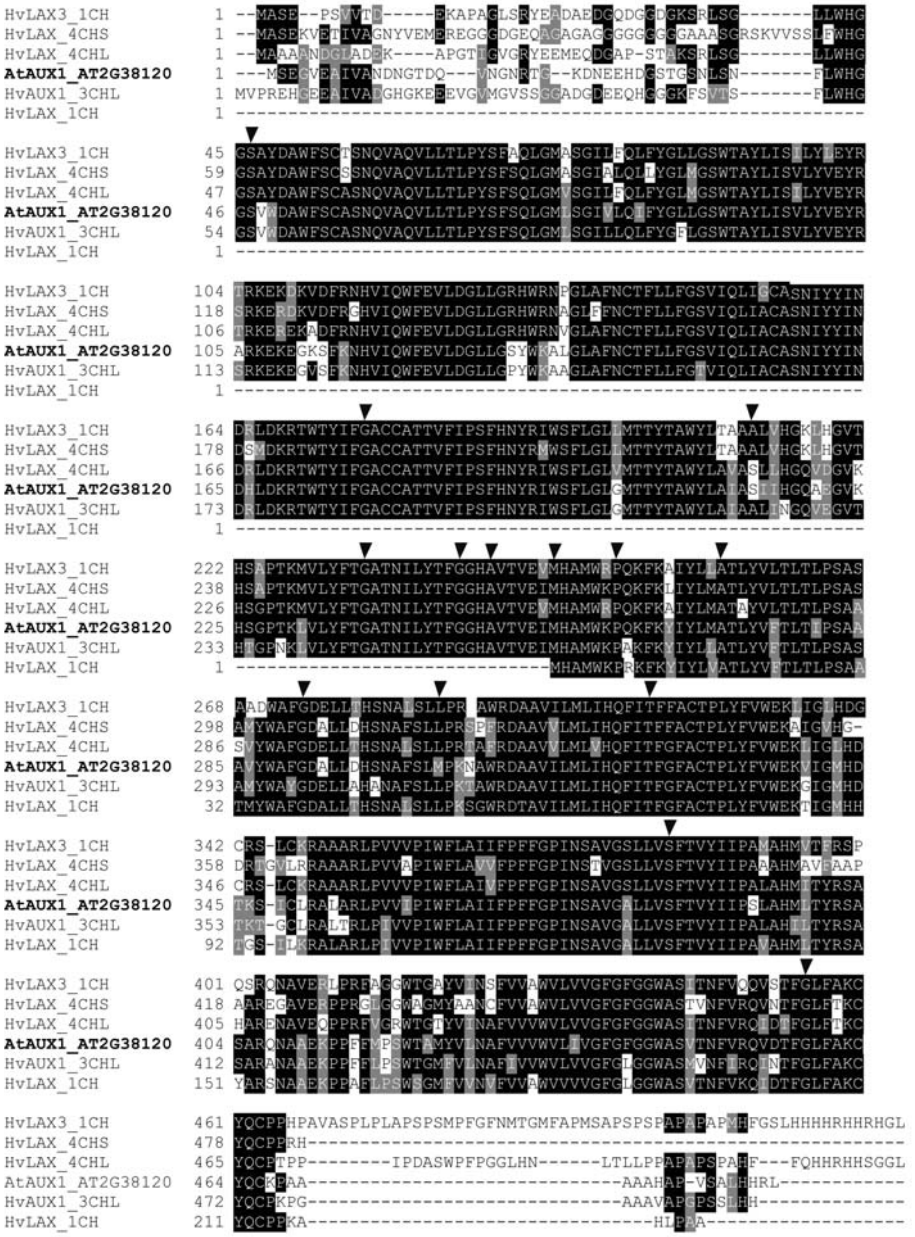

Figure 3-2: Comparative protein sequence alignment of AtAUX1, AtLAX3 and barley AUX/LAX protein sequences.

The sequences of AUX/LAX family members were aligned using the ClustalW alignment software (EMBL) and visualised with the BoxShade tool (ExPASy). Black arrowheads points to the functionally important residues substituted in missense *aux1* alleles, as described in Swarup et al. (2004).

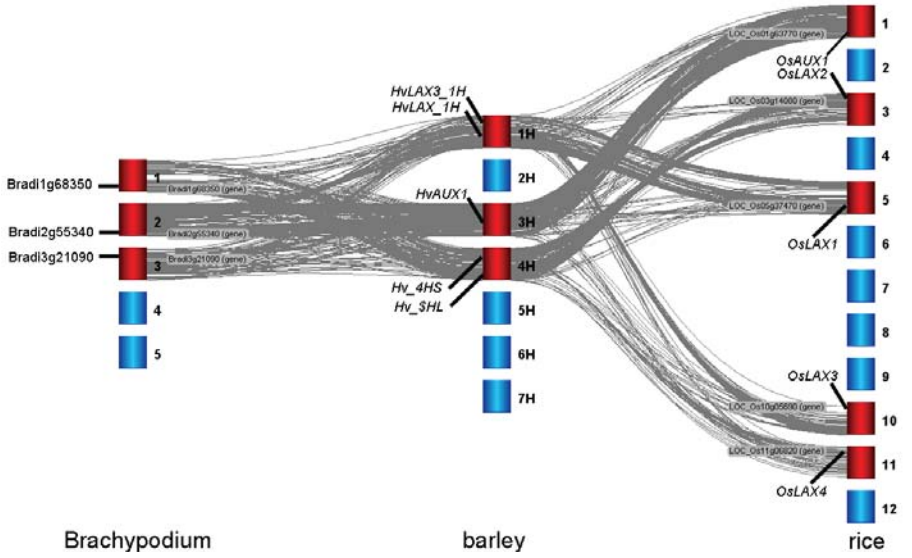

Figure 3-3: The syntenic relationships between maps of *Brachypodium*, barley and rice.

The conservation of gene order was limited to chosen chromosomes of *Brachypodium*, barley and rice that contain *AUX/LAX* genes and those chromosomes are highlighted in red. The grey lines connect the corresponding genes among the three plant species. The analysis was performed in Mapviewer.

In agreement with previous studies, the positions and lengths of introns are not well conserved and might be explained by the evolutionary distance between lineages followed by re-arrangements involved cis events like inversions, duplications, or deletions (Dubcovsky et al. 2001). Gene models were then grouped based on a similarity of exon/intron arrangement between the selected species (Figure 3-4), based on the assumption that exon/intron arrangement should be similar in orthologs (Schnable et al. 2012). Only a partial alignment was obtained for the truncated *HvLAX_1H* sequence from barley cv. Morex and cv. Bowman genome assemblies and therefore, is not shown here. Interestingly, *HvLAX_4HS* is the most similar to *OsLAX4* and appears to have evolved in a different way than the other members of the *AUX/LAX* family, likely via retroposition (Wang et al. 2006).

Taken together, these results suggest that barley genome contains five *AUX/LAX* family members, for which putative orthologs can be predicted in rice and *Arabidopsis* genomes. The detailed sequence, synteny and gene structure analyses supports the selection of *HvAUX1* and *HvLAX3* for a molecular characterization.

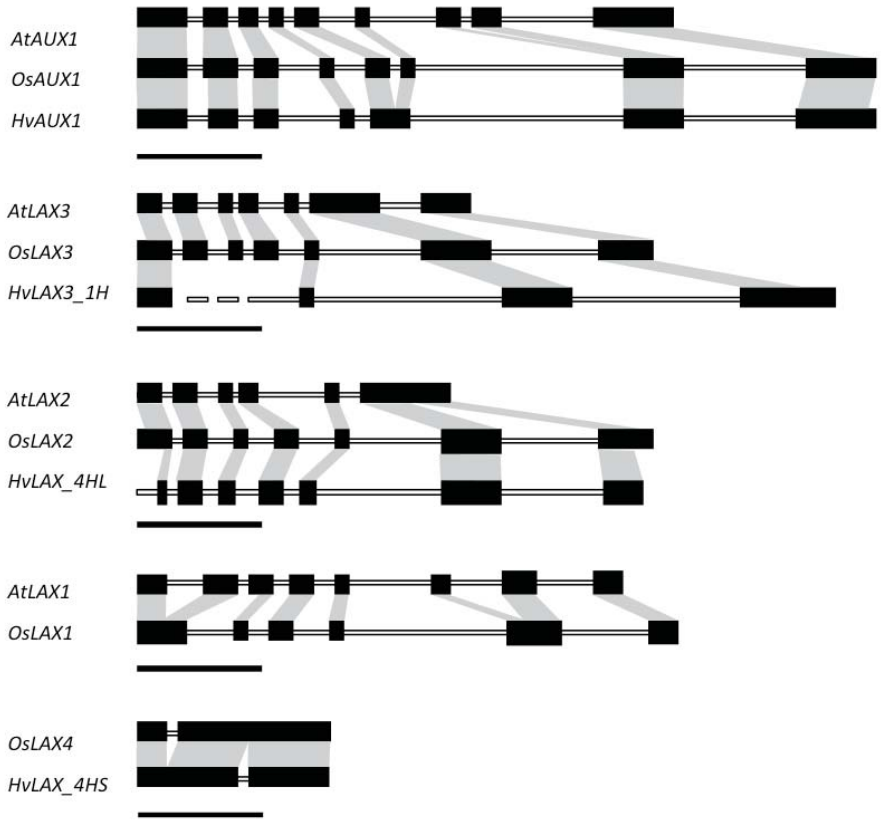

Figure 3-4: Exon/intron arrangement in *AUX/LAX* families in *Arabidopsis*, rice and barley.

The black boxes indicate exons and are connected via white lines that correspond to introns. The corresponding regions are shaded gray. Barley mRNA sequences were obtained from barley expression databases and were compared with barley cv. Morex and cv. Bowman genome assemblies. The truncated sequence of barley *HvLAX_1H* is not shown. *Arabidopsis* and rice mRNA and genomic sequences were obtained from the NCBI database. All sequences were aligned with the Spidey sequence alignment software (NCBI) for exon/intron boundary visualisation and processed in the Powerpoint (Microsoft). Bar = 1 kbp.

AUX/LAX gene expression analysis in barley by RT-PCR

A semi-quantitative RT-PCR was employed to determine transcript abundance of each member of *AUX/LAX* family in leaves and roots of 5 dag barley seedlings (Figure 3-5A). The analysis showed that *AUX/LAX* genes are expressed abundantly in leaf and root tissue with the exception of *HvLAX_4HS* that was not expressed in leaves. In addition, the expression in leaves and roots differ between members of *AUX/LAX* family. In leaves, *HvLAX_4HL* was the most abundant when compared to the other *AUX/LAX* members, whereas in roots, *HvAUX1, HvLAX_4HL* and *HvLAX3* are the most abundant.

Transcript abundances of *HvAUX1* and *HvLAX3* within root tissues was then analyzed (Figure 3-5B). Semi-quantitative RT-PCR revealed that both genes are expressed in all of the different root samples.

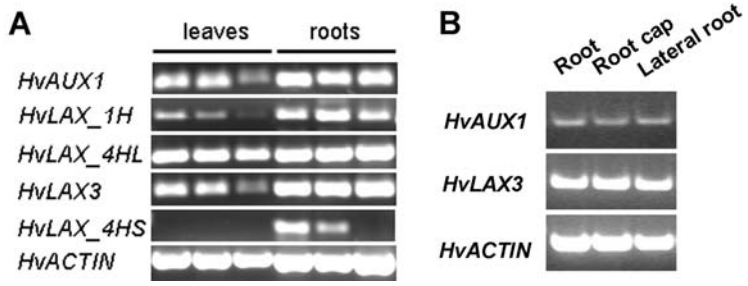

Figure 3-5: *AUX/LAX* expression analysis by RT-PCR in barley.

(A) Transcript abundance of *AUX/LAX* family members in leaves and roots of 7 d-old barley seedlings (n = 3). **(B)** *HvAUX1* and *HvLAX3* expression levels in 3 cm-long apical segments of three roots, 3 mm-long root cap zones from ten seminal roots and twenty emerged LRs from three seedlings, respectively. Barley actin signal was used as an equal loading control.

Functional characterisation of *HvAUX1* and *HvLAX3*

Reverse complementation assay of *Ataux1* with barley *HvAUX1*

A complementation assay has been performed in *Arabidopsis* to determine whether the *HvAUX1* encodes a functional auxin influx protein. The coding sequence (cds) of *HvAUX1* has been cloned into a pMOG binary vector between the native *AtAUX1* promoter and terminator. As a positive control, the *AtAUX1* coding sequence was

also cloned in the same configuration. The transformations were performed in the *aux1-22* mutant background (loss of function mutant) that exhibits a reduced number of LRs by 50% in comparison to wild-type seedlings (Marchant et al. 2002). The expression of *HvAUX1* and *AtAUX1* (positive control) both fully restored the *aux1-22* LR phenotype and had no effect on primary root growth (Figure 3-6A).

The root elongation of *aux1* mutants displays auxin resistance after 2,4-D treatment (Marchant et al. 1999) compared to wild-type plants in the Columbia ecotype which show inhibition of root growth at 0.1 μM 2,4-D and at 4μM 1-naphthaleneacetic acid (1-NAA). These two forms of auxin can thus be used to distinguish between passive and active transport, as NAA enters cells predominantly via diffusion and exits through efflux carriers while 2,4-D enters through influx carriers and exits passively (Delbarre et al. 1996). Therefore, we checked whether the introduction of *HvAUX1* into *aux1-22* is able to restore auxin sensitivity (Figure 3-6B). Treatments with both auxins were found to inhibit root elongation of Pro_{AtAUX1}*:AtAUX1/aux1-22* and Pro_{AtAUX1}*:HvAUX1/aux1-22* transformed plants as in wild-type plants. We therefore concluded that *HvAUX1* is able to facilitate the uptake of carrier-dependent auxin.

In *Arabidopsis* (Peret et al. 2012b) and *Casuarina glauca* (Peret et al. 2007), *AUX1* is the only member of the *AUX/LAX* family that can rescue the agravitropic phenotype of *Ataux1-22*. A gravitropic assay was therefore employed to determine the ability of the root to respond to the changes in gravity. The plates were turned from their initial vertical position by 90° to the right. After 24 h, root angles were scored as plants responding to the gravitropic stimulus would bend by 90°. We found that *HvAUX1* restore the function of the native *AUX1* to mediate the gravitropic response, similarly to the native AtAUX1 protein (Figure 3-7). These converging results indicate that *HvAUX1* can restore *aux1-22* and proves its functionality as an auxin-influx carrier.

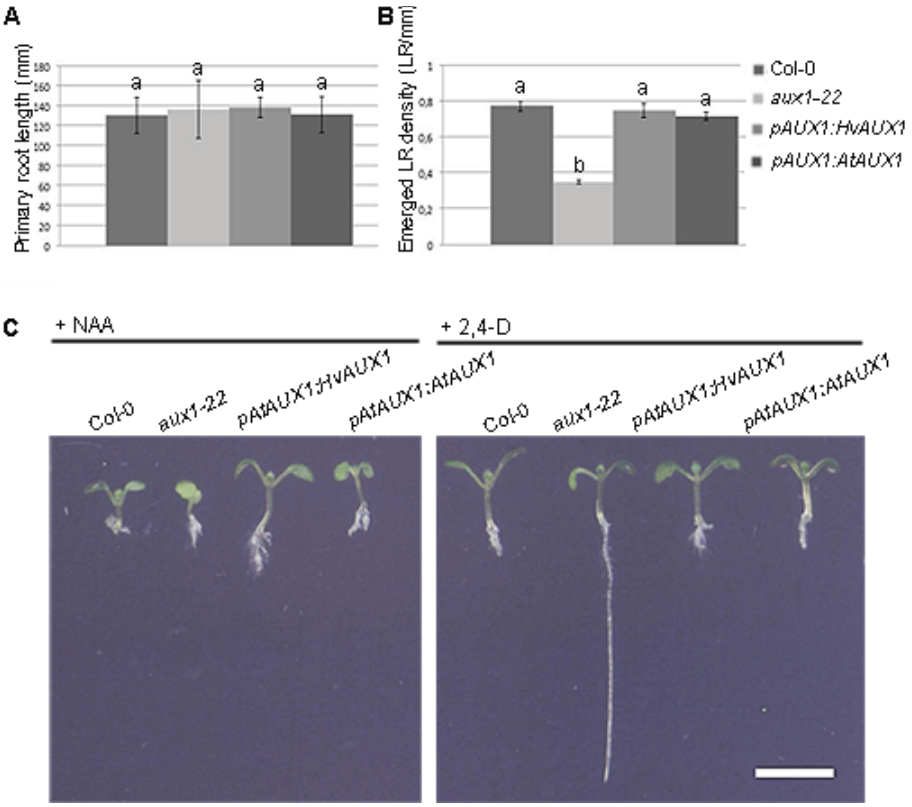

Figure 3-6: Root phenotype and auxin sensitivity of *HvAUX1* in *aux1-22* complementation assay.

(A) Primary root length and **(B)** LR density of 12 day old wild-type (Col-0), *aux1-22*, Pro_{AtAUX1}*:AtAUX1/aux1-22* and Pro_{AtAUX1}*:HvAUX1/aux1-22* seedlings. **(C)** Auxin sensitive root elongation phenotype of 7 day old transformed plants. Seedlings were aligned on a fresh plate for photography. Left to right: wild-type (Columbia), aux1-22, Pro_{AtAUX1}*:AtAUX1/aux1-22* and Pro_{AtAUX1}*:HvAUX1/aux1-22* for NAA and 2,4-D, respectively. Bars are means ± CI, with different letters indicating significant differences with $p < 0.001$ according to Tukey's HSD test after ANOVA. Scale bar = 5mm.

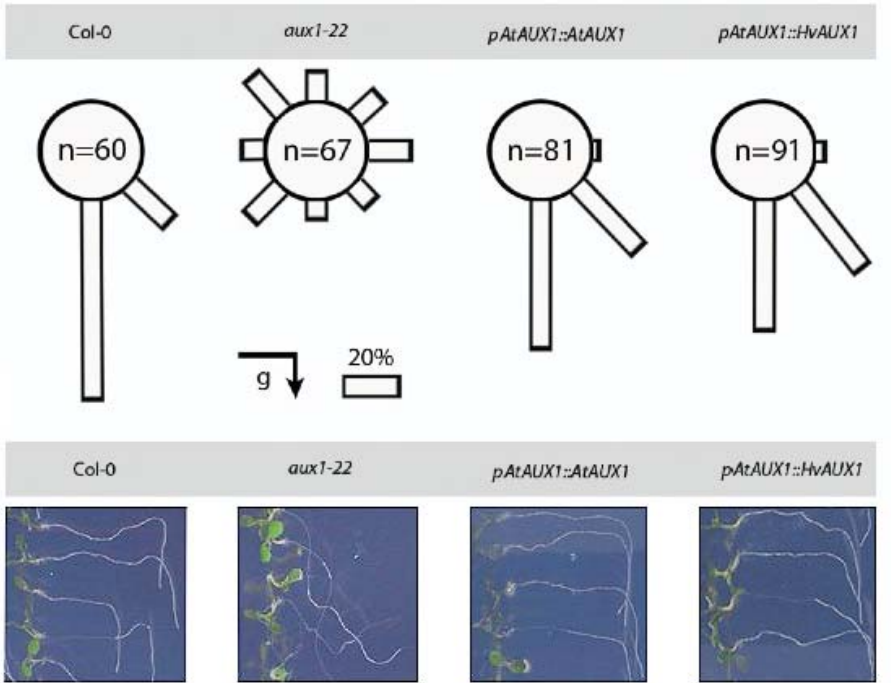

Figure 3-7: The rescue of *aux1-22* gravitropic defect by *HvAUX1*.

HvAUX1 and *AtAUX1* coding sequences were expressed under the control of *AtAUX1* native promoter and terminator. The n number of homozygous kanamycin-resistant T2 transgenic plants from three independent lines were screened in this assay on vertical plates with standard Murashige and Skoog (MS) growth medium. Root angles were determined 24h after gravistimulation by 90°. Wild-type (Col-0) plants responded to gravitropic stimuli in contrast to *aux1-22* plants. The *aux1-22* plants transformed with *AtAUX1* or with *HvAUX1* under the control of its native promoter display a gravitropic phenotype. Arrows indicate direction of gravistimulus.

Reverse complementation assay of *Ataux1lax3* with barley *HvLAX3*

A complementation strategy in *Arabidopsis* has been employed to determine whether *HvLAX3* encodes a functional auxin influx protein that can complement *Atlax3*. It is likely that, as for *AUX1* (Peret et al. 2012b), only a true *LAX3* ortholog would complement *lax3* in *Arabidopsis*. Therefore, the *HvLAX3* cds has been cloned into the paux3131 binary vector (Navarre et al. 2011) between the native

AtLAX3 promoter and terminator. As positive control, the *AtLAX3* cds has also been cloned under its native promoter. The transformations were performed in the *aux1lax3* mutant background (loss of function mutant). *Atlax3* mutants normally produce three times as many LR primordia as a wild type, but the majority of them fail to emerge, leading to a 40% reduction in LR number (Swarup et al. 2008; Peret et al. 2012b). The double mutant of *Atlax3* and *Ataux1* does not produce LRs until 14 d after germination (Swarup et al. 2008) and is therefore more convenient to use in a complementation assay than a single *lax3* mutant. In a *aux1lax3* complementation assay, plants with a restored functional LAX3 protein would have emerged LRs at 10 dpg, but would exhibit agravitropic root phenotype due to *aux1* backgound. The expression of *HvLAX3* under *AtLAX3* promoter restored LR phenotype of *lax3* mutation in *aux1lax3* background and had no effect on primary root gravitropism, similarly to *AtLAX3* coding sequence, that remained agravitropic (Figure 3-8).

These results therefore indicate that *HvLAX3* can restore *lax3* and prove its functionality as an auxin-influx carrier.

Analysis of transcriptional regulation of *HvAUX1* and *HvLAX3*

Expression data provide essential information on how genes function *in planta*. In *Arabidopsis* root tissue, *AtAUX1* is expressed within the root apex and inside LR primordia (Figure 3-1) where it is involved in the acropetal auxin unload from protophloem to the root apex, the generation of auxin maxima in LR and the basipetal auxin transport towards the shoot (Marchant et al. 2002; Marchant et al. 1999; Swarup et al. 2001). On the other hand, *AtLAX3* is expressed in cortex cells surrounding emerging LR primordia (Figure 3-1) where it supports the LR emergence process. Although *AtLAX3* is also expressed in the stele and in root columella cells, its exact function there is unknown (Swarup et al. 2008). *In situ* reverse transcriptase-mediated PCR (RT-PCR) method was first employed to analyse the expression pattern of *HvAUX1* and *HvLAX3* in barley roots. *HvAUX1* signals were observed in the lateral root cap, within the root meristem

and inside LR primordia at early and late stages of development (Figure 3-9), similarly to *Arabidopsis*. This expression pattern of *HvAUX1* further confirms that *HvAUX1* is orthologous to *AtAUX1*.

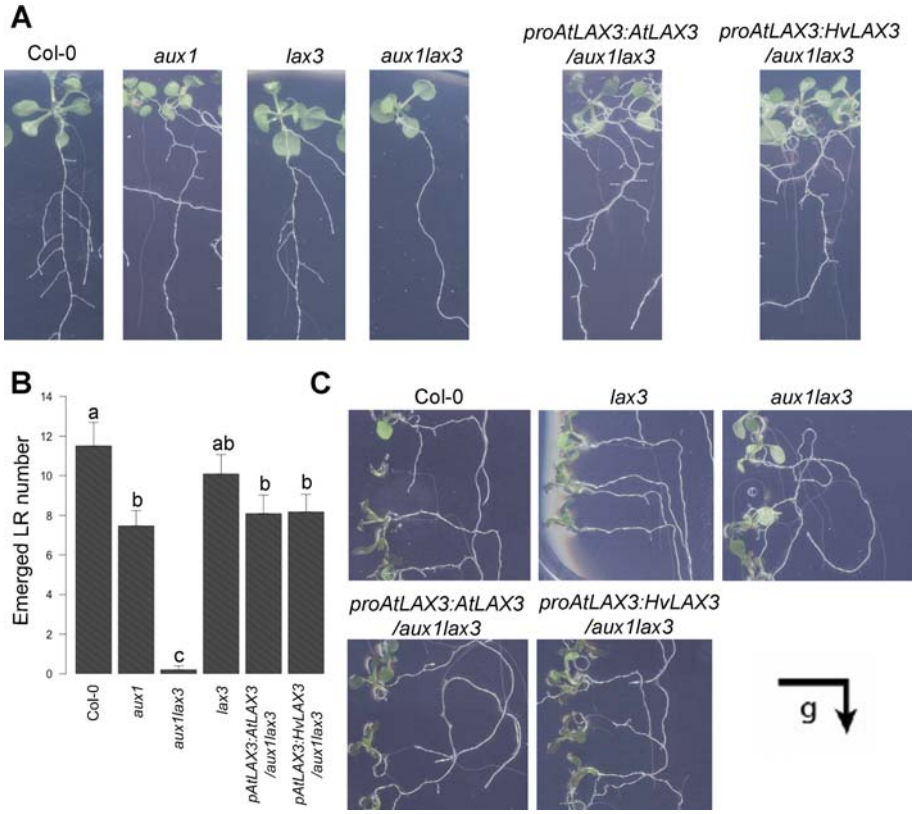

Figure 3-8: The rescue of *lax3* by *HvLAX3* in *aux1lax3* background.

AtLAX3 and *HvLAX3* coding sequences were expressed under the control of *AtLAX3* native promoter and terminator. **(A, B)** *aux1lax3* plants do not form LR at 10 dpg, in contrast to *lax3* plants that have less LR in compare to the wild-type (Col-0). The *aux1lax3* plants transformed with *AtALAX3* or with *HvLAX3* under the control of *AtLAX3* promoter display *aux1*-like root phenotype, that is, less LRs. The LR number was determined 10 dpg ($n > 10$). **(C)** Root angles were determined 24h after gravistimulation by 90° on homozygous kanamycin-resistant T2 transgenic plants ($n > 10$). The *aux1lax3* plants transformed with *AtLAX3* or *HvLAX3* remain agravitropic. Bars are means ± CI, with different letters indicating significant differences with $p < 0.05$ according to Tukey's HSD test after ANOVA.

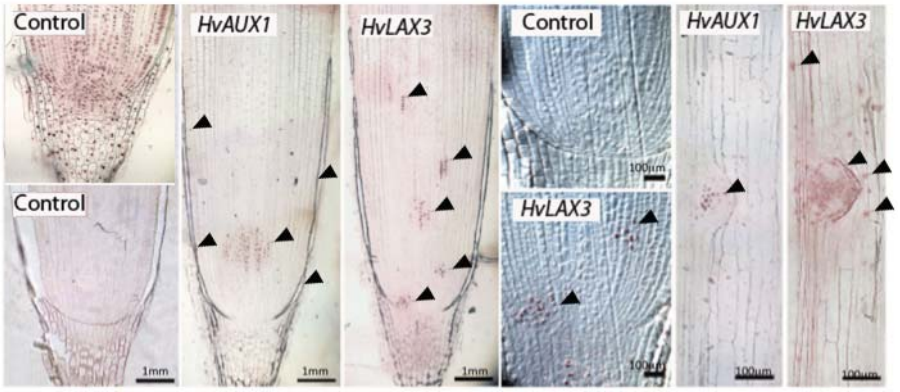

Figure 3-9: Expression patterns of *HvAUX1* and *HvLAX3* by *in situ* RT-PCR.

Black arrowheads points to the expected nuclear-localised purple precipitates of NBT/BCIP, that mark the cells where the gene is expressed. *HvAUX1* expression was observed in the meristematic zone and LR cap in barely crown root tip. *HvLAX3* expression was observed in the LR columela, root vasculature and endodermis/cortex cell files at specific positions in crown root. This is also visible using Normaski optics with comparison to the control. *HvAUX1* and *HvLAX3* expression was detected inside LR primordia. Moreover, *HvLAX3* seems to be also expressed in cortex cells in front of developing LR primordia. The control samples are: positive control (no DNAse, top left) and negative control (no Polymerase, bottom left).

In the case of *HvLAX3*, positive signals were detected in the vasculature and in cortex cells flanking an emerging LR in the crown (Figure 3-9) and primary roots (data not shown), as observed for *AtLAX3* in the *Arabidopsis* primary root.

Surprisingly, we also observed patches of *HvLAX3* expression in the apical root segment (in barley crown roots) and a positive signal inside LR primordia (in both, primary and crown roots of barley) that have not been reported for *AtLAX3* in the primary root of *Arabidopsis*.

A promoter-reporter analysis was therefore used to further examine the expression pattern of *HvLAX3*. The 1.7-kb of *HvLAX3* promoter fragment was cloned and fused with GUS reporter sequence to create a *HvLAX3:GUS* construct. This construct was then introduced in *Arabidopsis* and in barley via *Agrobacterium*-mediated transformation.

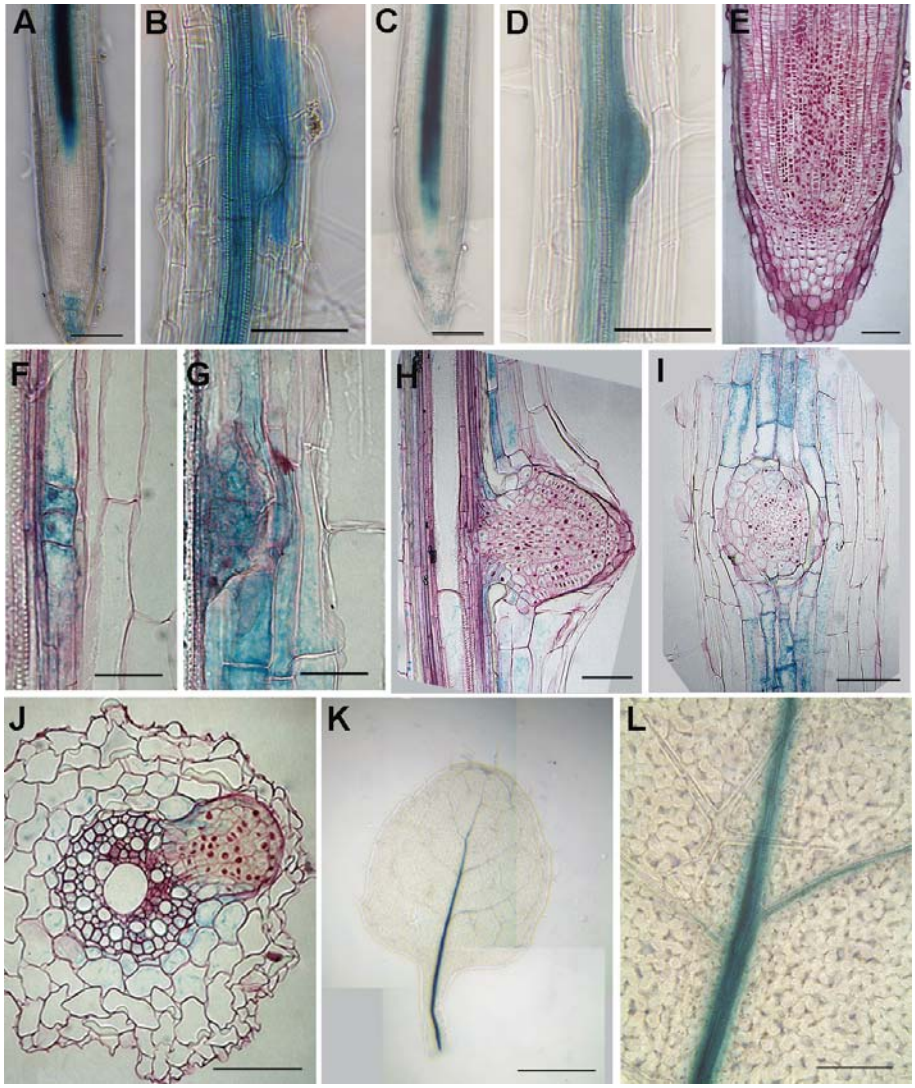

Figure 3-10: Promoter-reporter analysis of *HvLAX3* in *Arabidopsis* and barley.

(A, B) *AtLAX3:GUS* expression in the root tip and during LR emergence in *Arabidopsis*. **(C, D)** *HvLAX3:GUS* expression in root tip and during LR emergence in *Arabidopsis* (n = 5 independent transformation events analysed). **(E)** *HvLAX3:GUS* expression in barley crown root tip and **(F-J)** during sequential stages of LR formation in barley (n = 3 independent transformation events analysed). **(K, L)** *HvLAX3:GUS* expression in *Arabidopsis* leaf. Size bars: (A-J): 50 µm, (K): 1 mm, (L): 100 µm.

In *Arabidopsis*, *AtLAX3* is expressed in the leaf and root vasculature, root tip columella cells and in cortex cells sourounding LR primordia

during LR development (Figure 3-10A and Figure 3-10B). The heterologous expression of *HvLAX3:GUS* in *Arabidopsis* revealed expression domains in the leaf vasculature (Figure 3-10K and Figure 3-10L) and in the root vasculature (Figure 3-10C), in agreement *AtLAX3* expression. However, it was also expressed inside LR primordia until its emergence from a parental root (Figure 3-10D). The *Arabidopsis* line that showed the strongest GUS staining also displayed the *HvLAX3* expression in patches in the *Arabidopsis* primary root meristematic zone, but *HvLAX3* was not expressed in the cells surrounding the LR primordia (Figure 3-10C and Figure 3-10D).

In barley, we found that *HvLAX3* is expressed in cells surrounding the emerging LR primordia (Figure 3-10E through J), similarly to *AtLAX3* in *Arabidopsis*. In addition, *HvLAX3* was also expressed inside developing LR primordia at early stages until its emergence from the parental tissues. The expression of *HvLAX3* during subsequent steps of LR development is summarised in Figure 3-11.

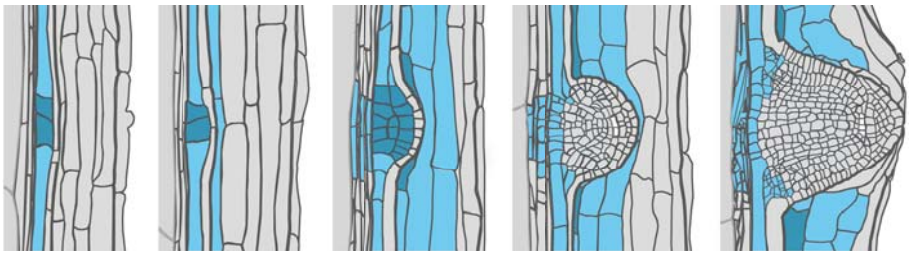

Figure 3-11: Summary of *HvLAX3* expression pattern during LR development in barley.

HvLAX3 expression is shown in blue colour on schematic representation of LR developmental stages in barley. Darker-blue points to more intense staining. The barley LR developmental stages used as a backgroung for visualisation of *HvLAX3* promotor activity were adapted from (Orman-Ligeza et al. 2013), with modifications.

When GUS-stained root samples were processed with a resin-based histology method and cut by a microtome, no patches of *HvLAX3* expression were observed within the primary and crown meristems of barley roots. It is possible that the promoter activity and/or the GUS staining method were not sufficient to visualize the activity of

HvLAX3 promoter in the thick barley crown roots. It is in agreement with the previous reports, which showed that *in situ* RT-PCR enables detection of low copy mRNA sequences with greater sensitivity than the other methods (Bates et al. 1997). In addition, it is unlikely that other members of *AUX/LAX* family were amplified during the *in situ* RT-PCR, as the primer pairs were designed in the way that ensured specificity and were checked for unspecific bands by a standard RT-PCR reaction with the same settings prior to *in situ* RT-PCR experiments. Interestingly, the expression of *HvLAX3* inside the LR primordia overlaps with the expression pattern of *HvAUX1*. This overlap is not found in *Arabidopsis* for *AtAUX1* and *AtLAX3*. However, *AtLAX1* and *AtLAX2* are both expressed inside LR primordia in *Arabidopsis* (Figure 3-1). This suggest that, at some extend, members of AUX/LAX family may have diverged differently in eudicots and monocots and provide evidence as to the complex roles of *AUX/LAX* within the plant. We can therefore not rule out the possibility that other members of AUX/LAX family in barley would also accompany developing LR primordia during emergence.

The expression of *AtLAX3* in the cells surrounding LR primordia is crucial for LR emergence (Swarup et al. 2008). Therefore, based on the positive signal in those cells shown in both, *in situ* and promoter-reporter studies, we conclude that *HvLAX3* encodes a potential auxin influx carrier equivalent to *AtLAX3*.

Characterisation of *HvLAX3* RNAi lines in barley

The down regulation of gene expression by stable RNA interference (RNAi) has been successfully used in cereals as a tool to determine the function of a gene or to obtain a desired phenotype (Mikkelsen et al. 2012; Regina et al. 2010; Zalewski et al. 2010; Wu and Messing 2012). Here, a silencing cassette containing fragments of *HvLAX3* gene in the sense and antisense orientations were cloned into the pBRACT207 binary vector and used in *Agrobacterium*-mediated transformation of barley cv. Golden Promise. This fragment spanned the 3' end region of the *HvLAX3* coding sequence and 3' untranscribed region (3'UTR) to avoid silencing of the other

members of *AUX/LAX* family. 15 lines out of 22 regenerated seedlings segregated 3:1 and were considered as separate single-insertion events. A semi-quantitative expression analysis of *HvLAX3* in root tissue of homozygous T3 and heterozygous T2 seedlings was performed (data not shown). However, the expression levels were similar to those of the wild type Golden Promise. In addition, homozygous lines grown for 7 d in aeroponic system did not show any root phenotype.

The efficiency of RNAi-mediated knockdown appears to be highly dependent on the identity and nature of the target gene and therefore, may lead to a low rate of silencing (Terenius et al. 2011). In addition, the susceptibility of different genes to RNAi also shows considerable variation in model species and some of them were even proved to be completely refractory to suppression as observed in most of the neuronal expressed genes in *C. elegans* (Kennedy et al. 2004). To our knowledge, there are no RNAi lines described for *AUX/LAX* family members. We concluded that RNAi-mediated silencing of *HvLAX3* was not successful.

Characterisation of *Osaux1* lines

Phenotype of *Osaux1* lines

It has been suggested that an increase in topsoil root penetration may potentially affect plant capacity to withstand water shortage (Trubat et al. 2012) and that deep root penetration and steeper root angles may be valuable in water-limited environments (Trubat et al. 2012; Zhu et al. 2011). *Osaux1-1* and *Osaux1-2* represent two independent insertional events in *OsAUX1,* kindly provided by Prof. M. J. Bennett (UNottingham) and are expected to show perturbed gravitropism. We characterised rice wild type cv. Dongjin and these two *Osaux1* lines in rhizotron and aeroponic systems. Thereafter, the water uptake dynamics during a progressive 5 d-long drought episode was assayed in rhizotrons.

The 30 dpg wild type rice cv. Dongjin root system grew 25 - 30 cm deep down into the rhizotrons. On the contrary, *Osaux1-1* and *Osaux1-2* plants showed shallow root systems located within the

upper 15 - 20 cm (Figure 3-12A and Figure 3-12B) and therefore, is considered as an agravitropic. The root system of *Osaux1-1* tended to be more agravitropic than *Osaux1-2,* suggesting that *Osaux1-1* is a more severe allele of *Osaux1* in rice. The horizontal deviation between the actual trajectory and a midline trajectory was estimated along each root (n=149, Figure 3-13), and the 60% interquartile range of that deviation (difference between percentiles 20 and 80) was computed as a measure of the amplitude of directional variation of individual roots. A mixed model ANOVA revealed highly significant differences ($P<0.005$) between aux1 and the control, with a nearly two-fold range difference.

Thereafter, a detailed analysis revealed that there were no differences in the total length of seminal and crown root systems between wild type and *Osaux1-1* line. The average total seminal root system length of wild type (n = 6) and *Osaux1-1* (n = 6) plants was respectively 74 ± 32 cm and 63 ± 17 cm (ns, T-test) and the average total crown root system length was 79 ± 24 cm and 83 ± 14 cm (ns, T-test).

The wild-type rice roots that penetrate the mixture of sand and clay of the rhizotrons showed wavy growth behaviour. Such small waves are also observed when root is growing in soil and on agar (Mochizuki et al. 2005; White and Kirkegaard 2010). Interestingly, both *Osaux1-1* and *Osaux1-2* also produced “large” waves, probably due to the horizontal space limitation in rhizotrons. Therefore, it is likely that *Osaux1* lines would grow closer to the surface in soil conditions compared to wild type plants.

The aeroponic system was also employed to determine if the mutation in *Osaux1* lead to decrease in LR number, similarly to *Ataux1* in *Arabidopsis*. However, there was no difference in LR number on the primary seminal roots at 10 dpg (P = ns, Tukey HSD test after Anova). The LR densities per cm for the wild type, *Osaux1-1* and *Osaux1-2* were respectively 12.8 ± 3.6, 11.4 ± 1.75 and 12 ± 1.8 (Means ± SD, $n > 10$).

Taken together, these results revealed that mutation in *OsAUX1* lead to agravitropic seminal and crown root phenotype without affecting either LR formation or length of seminal and crown roots.

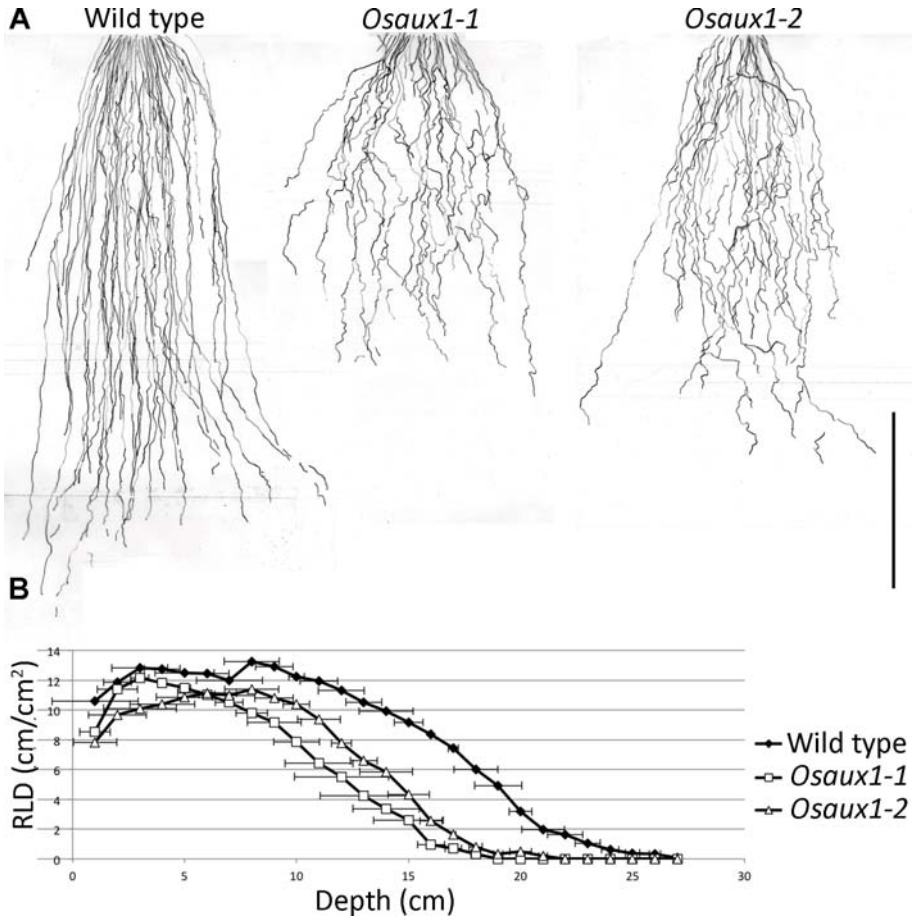

Figure 3-12: Characterisation of rice wild type cv. Dongjin, *Osaux1-1* and *Osaux1-2* root systems.

(A) The seminal and crown roots of rice plants were drawn every day on a transparent sheet that was scanned each day. Drawings at day 30 are shown. Bar = 10 cm. **(B)** Root length density profile of 30 d-old rice plants grown in rhyzotrons. Points are means ± SE (n = 6 plants).

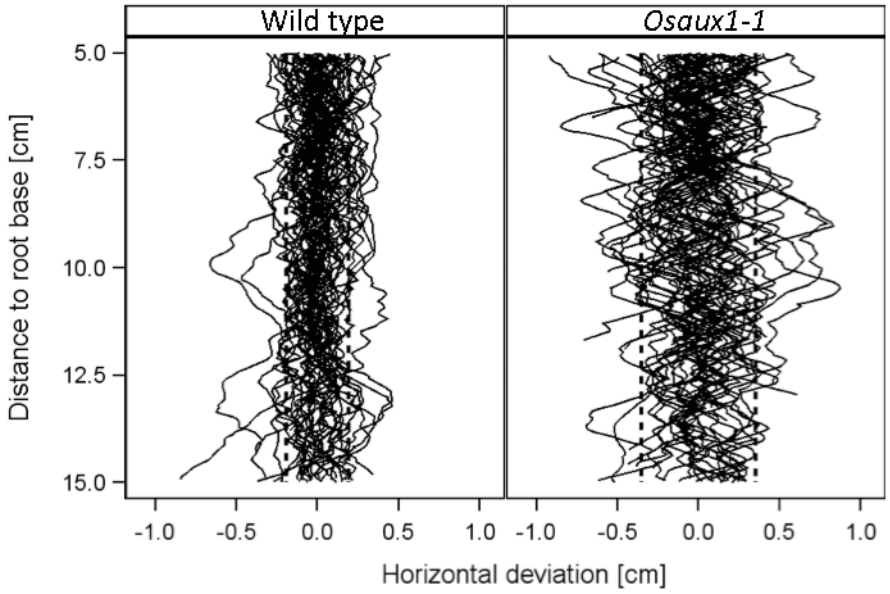

Figure 3-13: Horizontal deviation between the actual root trajectory and an estimated trend line, as a function of the distance to the root base.

The midline was estimated for each root (n = 149) using a degree-2 polynomial regression through the actual trajectory. Dotted lines correspond to 20 and 80% percentiles, estimated as least-square means of the corresponding percentiles for each root (mixed model ANOVA).

Osaux1 response to water shortage episode

After 4 weeks of growth in rhizotrons, plants were exposed to a 5 d-long drought episode. Wild type plants were shown to take up water from deep layers, whereas Os*aux1* lines from layers closer to the surface (Figure 3-14). The water uptake areas at the fifth day of water shortage were wider for the wild type than for *Osaux1* mutants and were 777 ± 31 cm^2 for the wild type, 338 ± 56 cm^2 for *Osaux1-1* and 532 ± 29 cm^2 for *Osaux1-2*. However, there were no significant differences in transpiration rates between wild type and *Osaux1* mutants (P = ns, Tukey HSD test after Anova).

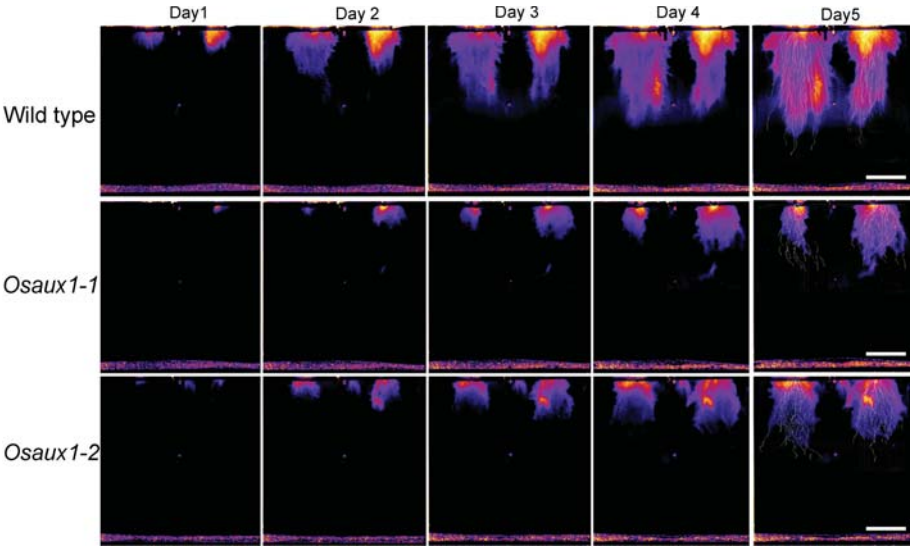

Figure 3-14: Evolution of soil water content distribution during 5 d-long drought episode

Using the light transmission imaging technique, the soil water content distribution in the rhizotrons was recorded four times per day and the results for 7 pm are shown. Bar=10cm.

The mixture of sand and clay used in these experiments is characterized by a high hydraulic conductivity when the mixture is wet, which allows a rapid capillary movement of the water from the bulk mixture in the direction of the root zone where water uptake occurs. However, the conductivity of the subtrate decreases rapidly when the water content decreases, as a result of the lack of micropores. Therefore, water uptake in the root zone will be possible as long as it does not exceed the rhizosphere supply from the bulk soil. Where uptake exceed supply, the substrate conductivity becomes limiting and further uptake at that location is prevented, even if water is available in the bulk soil. It is therefore likely that the tortuosity of the agravitropic roots of *Osaux1-1* leads to a spatial distribution of roots that leaves ample bulk soil space between roots and allows mainained supply of water in the root zone. Comparatively, the wild type displays a higher concentration of roots in a narrow zones that probably accelerates the drop of substrate conductivity in the central root zone, so that the water supply is only secured by the periphery of

the root system convex hull. This is in agreement with the observation that starting from day 3, *Osaux1-1* plants seemed to transpire even more per leaf area than the wild type plants (Figure 3-15). It is therefore likely that, in a longer experiment, *Osaux1-1* would have been able to maintain its transpiration rate longer than the wild type, because it exploits better the ability of the substrate to conduct water from the bulk soil to the root zone.

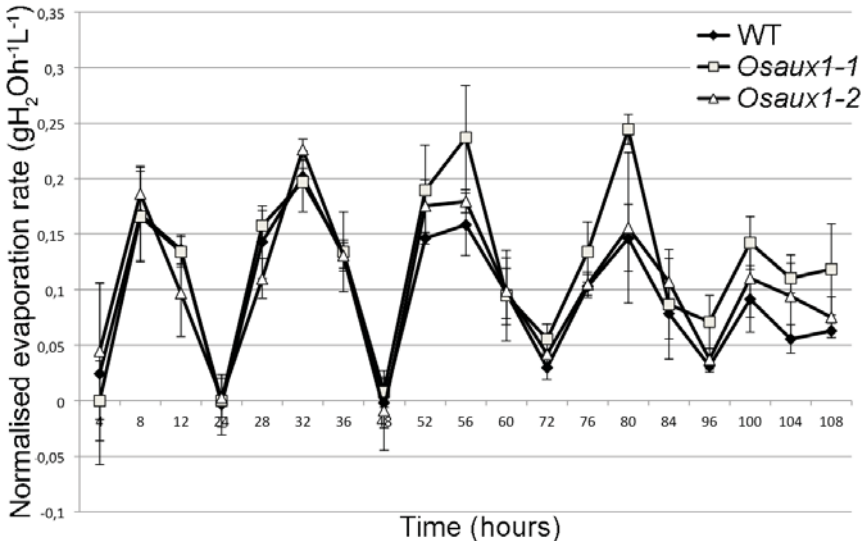

Figure 3-15: Evolution of transpiration rates during 5 d-long drought episode.

The rhyzotrons were saturated with nutrient solution prior to the beginning of a drought experiment. The weights of the rhyzotrons were determined every four hours by weighting the rhizotrons and the control rhyzotrons without any plants. The evaporation rates were calculated as a difference in weights compare to the control rhyzotrons and normalised by a plant leaf area in each rhyzotron (P = ns, Tukey HSD test after Anova).

Conclusions

The objective of this study was to characterize in barley the homologs of two *Arabidopsis* auxin influx carriers, involved in LR initiation (*AUX1)* and LR emergence (*LAX3)*. Bioinformatic and molecular tools were used to achieve this objective.

AUX/LAX family members in *Arabidopsis*, barley and rice, genomes were first characterised by a detailed *in silico* analysis, which enabled to select two candidates for a functional characterisation. *HvAUX1* and *HvLAX3* were then shown to maintain the amino acid residues pointed as important for the activity of auxin influx carriers (Swarup et al. 2004) and to rescue respectively, *aux1-22* and *lax3,* when expressed under native *Arabidopsis* promoter sequences. Transcriptional regulation studies further showed that the expression of auxin influx transporters in barley occurs during all stages of LR development in barley, at a similar extent to *Arabidopsis*. Finally, the roots of *Osaux1* lines – *Hvaux1* and *Osaux1* display 90% similarity – showed a shallow root phenotype consistent with agravitropic primary root phenotype of *aux1* loss of function mutant in *Arabidopsis*.

Therefore, based on bioinformatics, expression and functional analyses, we concluded that *HvAUX1* and *HvLAX3* are functional orthologs of *Arabidopsis AtAUX1* and *AtLAX3*.

The expression pattern of *HvLAX3* differ, at some extent, from the *Arabidopsis* equivalent. In barley, *HvLAX3* is also expressed inside LR primordia starting from the very early steps of LR development and overlaps with the expression pattern of *HvAUX1*. In line with that, *Osaux1* lines did not show any LR phenotype, suggesting that most likely other members of *AUX/LAX* family have an overlapping function. It is therefore possible that *AUX/LAX* family members in cereals have diverged partially differently from those of the dicot *Arabidopsis*. This is also supported by the fact that the *AUX/LAX* family in cereals counts one more member than *Arabidopsis*. This would probably allow the process of subfunctionalization, when the ancestral gene function is divided between duplicated genes and/or neofunctionalization, when a duplicated gene acquires a new function (Duarte et al. 2006). This notion is further supported by the fact that the fibrous cereal root system architecture visibly differs from the taproot system of *Arabidopsis* and intuitively, the underlying molecular mechanisms might have been modified.

Recently, Sreevidya and co-workers (2010) described the patterns of auxin distribution in rice by using soybean *GH3* promoter fused to *GUS*. Those results indicated that auxin maxima within the pericycle cells at the beginning of the maturing zone of cereal root tissue correspond to the future positions of LR. The auxin-responsive promotors can be particularly utilized to monitor already established auxin maxima. Thus, the auxin influx carriers that are able to generate such auxin gradients are good candidates behind these observations. It is therefore tempting to speculate that in barley, the process of LR initiation in crown roots involves *HvLAX3*. The patches of expression of *HvLAX3* visualised by *in situ* RT-PCR suggests that LR initiation in crown roots may take place already within the meristematic zone, but this pattern could not be confirmed by the promoter-reporter assay.

During LR emergence, cell divisions occur in cortical layers facing the emerging LR, in barley, rice (Sreevidya et al. 2010), white clover (Larkin et al. 1996), onion (Casero et al. 1996), soybean (Byrne et al. 1977), but not in *Arabidopsis* (Swarup et al. 2008). In barley, those dividing cortex cells specifically express *HvLAX3*. Expression of *HvLAX3* may contribute to cell divisions in front of the growing primordia in plants with several cortex layers, however further studies are needed to confirm this hypothesis. In addition, what triggers the spatial-specific expression of *HvLAX3* remains to be elucidated.

Acknowledgments

I would like to thank Dr Jennifer Stephens, Prof. Robbie Waugh, Dr David Marshall, Dr Bill Thomas and all the members of The James Hutton Institute Genetic Group for helpful discussions during my stay in UK. I thank also Prof. Marc Boutry, Prof. Francois Chaumont and Prof. Henri Batoko (Institute of life sciences, UCL) and their teams for the access to their resources and their kind support. My gratitude to Benjamin Lobet, who helped me characterise the barley transformants.

Materials and methods

Chemicals

Laboratory chemicals used were obtained from Sigma (Sigma-Aldrich Co. LCC, Diegem, Belgium), WVR (VWR International Europe BVBA, Leuven, Belgium) and Fisher (Fisher Co. Ltd., Erembodegem – Aalst, Belgium) unless otherwise mentioned.

Arabidopsis plant growth materials and growth conditions

The *Arabidopsis aux1*-22 and *aux1lax3* seeds were kindly provided by Prof. M.J. Bennett and Dr Ranjan Swarup (Plant and Crop Sciences Division, The University of Nottingham, UK).

Seeds were stratified at 4°C for 2 d in SDW. After cold treatment, seeds were sown over solid half-strength MS growth medium (per litre: 2.15 g MS salts, 0.1 g *myo*-inositol, 0.5 g MES, 10 g sucrose, 8 g plant tissue culture agar; pH = 5.7 with KOH) and grown vertically under continuous light (110 μE m^{-2} s^{-1} photosynthetically active radiation, supplied by cool-white fluorescent tungsten tubes, Osram) for 4 - 5 d. Seedlings were analysed in details with BX53 microscope (Olympus) equipped with DS-Fi1 (Nicon) camera and scans of the plates were taken with V700 (Epson) unless stated otherwise. Figures were arranged in Photoshop CS3 without modifications. In all experiments with *Arabidopsis*, seeds were sterilized with sodium hypochloride. Seeds were incubated in 70% (v/v) ethanol for 1 min and mixed several times. Then, seeds were placed in 50% (v/v) sodium hypochlorite for 15 min, inverted several times and after that, washed four times with SDW.

Rice plant growth materials and growth conditions

The wild type rice seeds (*Oryza sativia* L. *japonica* cv. *Dongjin)* and two *Osaux1* mutant lines were kindly provided by Prof. M.J. Bennett (Plant and Crop Sciences Division, The University of Nottingham, UK). Disinfected seeds were stratified at 4°C for 2 d on filter paper in darkness and were partially covered in water. Then, seeds were allowed to germinate on a wet filter paper for two days in 28°C in petri dish covered with an aluminium foil. Seedlings were then transferred to an aeroponic growth system containing 10 L of the rice nutrient solution sprayed for 15 s every 5 min, or to rhizotrons

(Lobet et al. 2014). Nutrients for rice aeroponics and rhizotrons were adapted from (Yoshida et al. 1976). The composition of nutrient solution (pH = 5.8) was as follows: 4.38 mM NH_4NO_3, 1.54 mM K_2SO_4, 0.6 mM KH_2PO_4, 1 mM $CaCl_2$, 3.27 mM $MgSO_4$, 0.04 mM $MnCl_2$, 0.2 µM $(NH_4)_6Mo_7O_4$, 0.6 µM $ZnSO_4$, 0.6 µM $CuSO_4$, 0.076 mM H_3BO_3, 0.026 mM $FeSO_4$. In all experiments, rice grains were rinsed in 70% (v/v) and placed in 5% (v/v) sodium hypochlorite for 15 min on a shaker. Then, seeds were washed several times with SDW.

Semi-quantitative RT-PCR analysis

The protocols for extraction of total RNA from plant tissue, RT-PCR and gel electrophoresis are described in Materials and Methods in chapter 2.

Fast DNA extraction protocol

For fast DNA extraction, two buffers are needed: Extraction Buffer, 10x (EB): 1.21 g Tris-HCl, 0.73 g NaCl, 0.47 g EDTA and 2.5 ml 10% SDS, pH = 7.5, for 50ml and TE buffer: 0.12 g Tris-HCl and 0.04 g EDTA, pH = 8, for 100 ml

Plant tissue (small fragment, about 5 mg) was freezed in liquid nitrogen in 1.5 ml eppendorf tube. 200 µl of cold EB was added on ice and tissue was crushed with a pastille. After that, 180 µl of cold TE buffer was added and samples were centrifuged (15 s, 1500 x g) to remove the debris. 1 µl of the extract was then used for PCR reaction.

Generation of PCR products

All amplicons were obtained respectively from plant DNA or cDNA by using a proof reading Phire polymerase (Thermo Scientific), with the standard conditions and the primers listed in Table 3-3 The names of the primers include restriction enzymes for which overhangs were added at 5' ends.

The PCR products were separated on agarose gel by electrophoresis and then amplicons of correct size were extracted form the gel by a Gel extraction kit (Macherey-Nagel) according to the manufacturer's instructions.

Table 3-2: Primers used in semi-quantitative RT-PCR of *AUX/LAX* family in barley.

Gene name	Primer name	Sequence
HvLAX_1H	F_179	TGATCCTCATGCTCATCCAC
	R_504	ACACGTTCACCACGAACATC
HvLAX_4HS	F_34	GGGAACTACGTGGAGATGGA
	R_243	CGAGCTGCGAGAAGGAGTAG
HvLAX_4HL	F_1155	CGTCAGCTTCACCGTCTACA
	R_1385	GCACTGGTAGCACTTGGTGA
HvLAX3_1H	F_1712	GGTCTCTAGTCGATCGGAAGG
	R_1975	CCTCCCTCGGGTTACATTAGTT
HvAUX1_3H	F_135	TCCGTGTAGCACACCATTACTT
	R_342	CAGGAATTTACTGTGCGATTGA
Hv_ACTIN	F_1056	CCATCCTAGCCTCACTCAGC
	R_1056	CAAATCAAGCCAACCCAAGT

DNA extraction from a gel

DNA extraction was carried out from a gel using a QIAquick minielute kit (Qiagen, Germany), as per the manufactures instruction.

DNA sequencing

DNA was verified by spectrophotometry (NanoDrop) and the final concentration of 50 ng/µl (for PCR amplicons) or 100 ng/µl (for plasmid DNA) was used alongside a 1 µl of primer (25 µM) in 10µl of total sample volume. DNA sequence was determined by the ISV sequencing service (UCL).

Plasmid DNA extraction

Plasmid DNA was extracted using the High Pure Plasmid Isolation kit (Roche) according to the manufacturer's instructions.

Table 3-3: Primers used to generate *pHvLAX3:GUS, HvLAX3 RNAi* and constructs used in the reverse complementation assays in *Arabidopsis*.

Fragment name	Primer name	Sequence
pHvLAX3	F_HindIII	AAGCTTAGCATTGGAAACACGCCAGA
	R_KpnI	GGTACCCGATCTTTGGGTGCTCTGCT
pAtLAX3	F_EcoRI	cgGAATTCCAAACCGAAACGAATTGGCA
	R_EcoRI	cgGAATTCCGCCATTTTTCTCTTCTTCT
cds_HvLAX3	F_EcoRI	ccgGAATTCTCCGAGCCGAGCGTCGTCAC
	R_PstI	CCAATGCATTGGTTCTGCAGCTAGAGACCGTGGCG ATGGT
cds_AtLAX3	F_EcoRI	cgGAATTCGCAGAGAAAATAGAGACAGT
	R_PstI	CCAATGCATTGGTTCTGCAGTCATGGCTTGTGAGGA GGGC
3'UTR_AtLAX3	F_PstI	CCAATGCATTGGTTCtgcaCTGCAGTATACAAATTTGC CATTCAA
	R_NotI	atagtttaGCGGCCGCTTTCTTGAGCTATAGAAGAA
cds_HvAUX1	F_XhoI	CCGCTCGAGCGGGTGCCGCGCGAGCATGGGGA
	R_BamHI	CGGGATCCGGTGGTGCAACGAGGAGGGGC
HvLAX3 RNAi	F*	TGGCGATTATTGCTCAGTTG
	attL1-tailed GS_F	AGGCTcctgcaggACGTGATCAACTCGTTCGTG
	attL1-universal	ccccGATGAGCAATGCTTTTTTATAATGCCAACTTTGT ACAAAAAAGCAGGCTcctgcaggACCATG
	R*	GAGCAATAATCGCCAATGCT
	attL2-tailed GS_R	GAAAGCTGGGTctcgagCTACACGAATCAAACAGGCA GCA
	attL2-universal	ggggGATAAGCAATGCTTTCTTATAATGCCAACTTTG TACAAGAAAGCTGGGTctcgagCTA

* Designed based on intron sequence

Restriction digestion

Plasmid DNA and PCR products were all digested using NEB or Roche restriction enzymes as per the manufactures protocols. The DNA, restriction enzyme, the appropriate buffer were added together up to 40 µl total reaction volume and the reaction was carried out from 2h to overnight at 37°C. The concentration of the digested DNA was then estimated by running 5 µl of the restriction reaction on a 1.5% agarose gel alongside a 10 kb ladder of known concentration. The DNA was then used in ligation reactions.

Ligation

In a total volume of 10 µl ligation reaction, about 30-50 ng of vector and amplicon (3:1 vector to insert ratio), SDW, 1.0 µl of T4 ligation buffer (Roche) and 1.0 µl of T4 DNA ligase (1 U/µl) were added together and then left overnight at 4^0C.

Preparation of competent *Escherichia coli*

5 ml of pre-culture of *E.coli* in standard LB was grown overnight at 37°C with shaking and then was added into 1000 ml LB. Culture was inoculated until OD_{600} = 0.5 – 0.9 and placed on ice for 20 min. The culture was then centrifuged (4000 rpm for 10 min at 4°C). The pellet was washed two times with 100 ml ice-cold SDW and centrifuged (4000 rpm for 10 min at 4°C). Then, cells were gently suspended in 20 ml ice-cold 10 % glycerol (w/v) and centrifuged (4000 rpm for 10 min at 4°C). Finally, cells were gently suspended in 3 ml ice-cold 10 % glycerol (w/v) and 40 µl aliquots were prepared and freezed immediately in liquid N_2 and stored at -80°C.

LB media: 10 g Bacto-tryptone, 5 g yeast extract, 10 g NaCl, pH = 7.5 with NaOH, per 1000 ml.

***E.coli* transformation via electroporation**

The JL109 *E.coli* competent cells were initially allowed to thaw on ice. During that time, 10 µl of ligation mixture was dialyzed for about 10 min on nitrocellulose filter (0.025 µm, Milipore) floating on SDW and then added to 40 µl of *E.coli* cells. The cells and ligation mixture were then transferred to cold electroporation cuvette (0.1 cm, Bio-Rad). The electroporation was done as per the manufacture protocol (1.65 kV, 25 µF, 200 Ω; Bio-Rad Gene Pulser™). After transformation into

E.coli, the cells were spread over LB agar plates containing: 50 μg/ml of Ampicillin for pAUX3131 and pBluescript II SK (+) or 100 μg/ml Spectinomycin for a binary vector pMODUL3408 and 100 μg/ml of Kanamycine for pMOG402.

Preparation of competent *Agrobacterium tumefaciens*

5 ml of pre-culture of *A. tumefaciens* in 2YT medium (rif, gent) was grown overnight at 28°C with shaking and then 300 μl was added into 500 ml 2YT (rif, gent) and left overnight on a sharer. Culture was inoculated until OD_{600} = 0.5 – 1 and placed on ice for 20 min. The culture was then centrifuged (4000rpm for 15 min at 4°C). The pellet was washed three to four times with 50 ml ice-cold 1 mM HEPES (pH = 7) and centrifuged (4000rpm for 10 min at 4°C). Then, cells were gently resuspended in 10 ml ice-cold 10% glycerol (w/v) and centrifuged (4000rpm for 10 min at 4°C). Finally, cells were gently suspended in 2.5 ml ice-cold 10% glycerol (w/v) and 50 μl aliquots were prepared and freezed immediately in liquid N_2 and stored at -80°C.

2YT (rif, gent) media were prepared as follows: 1.6 g Bacto-tryptone, 0.5 g yeast extract, 1 g NaCl, 0.02 g $MgSO_4$, 0.1 g glucose, per 100 ml, pH = 7.5 with NaOH. For plates, include 2 g agar (2%). After autoclaving, selection agents were added: Gentamycin (40 mg/l, stock: 20 mg/ml in SDW, stored at -20°C) and Rifampicin (20 mg/l, stock: 20 mg/ml in DMSO, stored at -20°C). For plant destination binary vectors used in this study, additional selective agents were added: Kanamycine (100 μg/ml, stock: 100mg/ml in SDW, stored at -20°C) for pMOG402 or Spectinomycin (100 μg/ml, stock: 100 mg/ml in SDW, stored at -20°C) for pMODUL3408 and Hygromycin (50 μg/ml, stock: 50mg/ml in SDW, stored at -20°C) for pBRACT202 and pBRACT207.

***A. tumefaciens* transformation via electroporation**

The GV3101 *A. tumefaciens* competent cells were initially allowed to thaw on ice. During that time, 10 μl of ligation mixture was dialyzed for about 10 min on nitrocellulose filter (0.025 μm, Milipore) floating on SDW and then added to 50 μl of *A. tumefasciens* cells. The cells and ligation mixture were then transferred to cold electroporation cuvette (0.1 cm, Bio-Rad). The electroporation was done as per the

manufactures protocols (1.25 kV, 25 μF, 400 Ω; Bio-Rad Gene Pulser™).

Generation of *pHvLAX3* ß-Glucuronidase (GUS) fusion vector

The promoter region from -1.7 kb from the start (ATG) codon was amplified from barley cv. Golden Promise genomic DNA with primers listed in Table 3-3. Restriction sites of HindIII and KpnI were added into 5' ends of the primers and were used to digest the amplified promoter fragments. The promoter was first ligated into the pAUX3131 vector (2712 bp) called pAUXM vector (Figure 3-16) as it contained GUS-Venus coding sequence (2553 bp) behind HindIII and KpnI sites (Navarre et al. 2011) and then used to transform JL109 competent *E.coli* cells. Confirmation of cloning was carried out by restriction digestion and agarose gel electophoresis. Inserts with a correct size from two vectors were then sequenced.

For barely transformation, the promoter-GUS fusion (4794 bp) was then transferred with NotI-XmaI restriction digestion into BRACT202 barley destination vector kindly provided by Dr Jennifer Stephens (The James Hutton Institute, UK). This construct was then used to transform JL109 competent *E.coli* cells (Figure 3-16). Confirmation of cloning was carried out by restriction digestion with NotI and XmaI and agarose gel electophoresis. Inserts with a correct size from two vectors were then sequenced. One chosen vector was then used to transform GV3103 competent Agrobacterium cells and subsequent barley transformation.

For *Arabidopsis* transformation, I-SceI restriction sites that flank *pHvLAX3:GUS* in pAUXM vector were used to transfer the insert into pMODUL3408 (8306 bp) binary vector (Navarre et al. 2011). This construct was then used to transform JL109 competent *E.coli* cells. Confirmation of cloning was carried out by restriction digestion with I-SceI and agarose gel electophoresis. Inserts with a correct size from two vectors were then sequenced. One chosen vector was then used to transform GV3103 competent Agrobacterium cells and subsequent *Arabidopsis* transformation.

Generation of *pAtLAX3:AtLAX3* and *pAtLAX3:HvLAX3* vectors

For genetic complementation of *lax3* in *aux1lax3*, *Arabidopsis LAX3* promoter (1920 bp) was amplified with primers listed in Table 3-3 and

fused by the use of EcoRI to pAUX3131 vector. The insert orientation was checked by restriction digestion with BamHI and agarose gel electrophoresis. *AtLAX3* (1407 bp) and *HvLAX3* (1574 bp) coding sequences were PCR amplified with primers listed in Table 3-3 and fused by the use of EcoRI and PstI to pBluescript II SK (+) (Agilent Technologies, Inc.) independently. Confirmation of cloning was carried out by restriction digestion and agarose gel electophoresis. Inserts with a correct size from two vectors were then sequenced. *AtLAX3* 3'UTR region (291 bp) was PCR amplified with primers listed in Table 3-3 and fused behind *Arabidopsis* and barley *LAX3* coding sequences in pBluescript II SK (+) with PstI and NotI. Confirmation of cloning was carried out by restriction digestion and agarose gel electophoresis. Inserts with a correct size from two vectors were then sequenced. Next, *AtLAX3cds:3'UTR* and *HvLAX3:3'UTR* were transferred by using EcoRI and NotI behind *Arabidopsis LAX3* promoter in pAUX3131 vector (Figure 3-16). Confirmation of cloning was carried out by restriction digestion and agarose gel electophoresis. Inserts with a correct size from two vectors were then sequenced. Finally, I-SceI restriction sites that flank inserts in pAUX3131 vector were used to transfer the inserts into pMODUL3408 binary vector (Navarre et al. 2011). pMODUL3408 binary vectors carrying *pAtLAX3:AtLAX3:3'UTR* and *AtLAX3:HvLAX3:3'UTR* were then used to transform GV3103 competent Agrobacterium cells and subsequent *Arabidopsis* transformation.

Generation of *pAUX1:HvLAX3* vector

pMOG402 binary vector (MOGEN International) carrying *pAtAUX1* promoter (1.7 kb), *AtAUX1* cds and terminator (0.3 bp) and an empty vector without *AtAUX1* cds were kindly rovided by Dr Ranjan Swarup (Plant and Crop Sciences Division, The University of Nottingham, UK) and were preiously described (Peret et al. 2007). For genetic complementation of aux1, barley *HvAUX1* coding sequence was amplified by the use of the primers listed in Table 3-3 and fused between *Arabidopsis AUX1* promoter and terminator sequences in pMOG402. Confirmation of cloning was carried out by restriction digestion and agarose gel electophoresis. Inserts with a correct size from two vectors were then sequenced. pMOG402 binary vectors carrying *pAtAUX1:AtAUX1* and *pAtAUX1:HvAUX1* were then used to transform GV3103 competent Agrobacterium cells and subsequent *Arabidopsis* transformation.

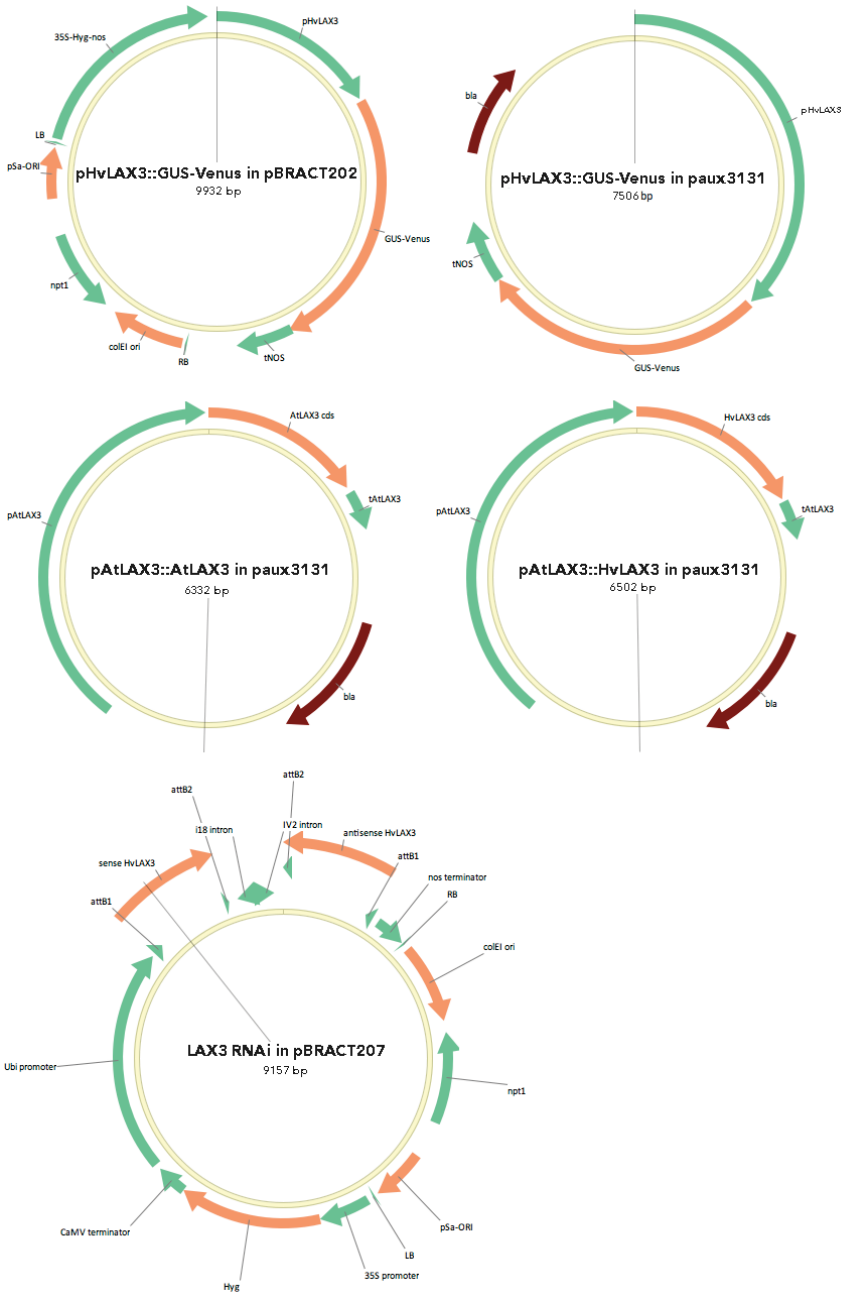

Figure 3-16: Schematic representation vectors used in this study.

pBRACT vectors were used to transform barley plants. Inserts from paux3131 were transferred into binary vector pMODUL3408 that was used to transform *Arabidopsis*. *In silico* cloning was made in Vector NTI Express v1.0.0.

Generation of *LAX3 RNAi* vector

The 3'end fragment of *HvLAX3* mRNA was amplified by PCR from barley cv. Golden Promise with F and R primer listed in Table 3-3 This 662 bp-long region spanned the end of the *HvLAX3* cds and the beginning of *3'UTR*. In order to use a rapid one-step recombination cloning method that do not require BP reaction (Fu et al. 2008), two more PCR amplifications were needed. In the first PCR, attL1-tailed gene specific (GS) primers were used, creating overhangs needed for the universal primers. In the second PCR, attL1 universal primers generated overhangs sufficient to perform LR reaction. Final PCR product of correct size was visualised by agarose gel electrophoresis and confirmed by sequencing. The insert was then cloned into pBRACT207 vector for barley RNAi (Figure 3-16) that was kindly provided by Dr Jennifer Stephens (The James Hutton Institute, UK) by using Gateway cloning (Life technologies) according to the manufacturer's instructions.

Barley transformation

Transformation of barley cv. Golden Promise has been done at The James Hutton Institute, UK. Fifteen and twenty-two independent transformation events were obtained for *pHvLAX3:GUS* and *LAX3 RNAi*, respectively. From each of T1 line, twenty seeds were sown on round petri plates (Ø 5 cm) that contained 25 ml of 0.7 % agar and 50 µg/ml of hygromycine and then vernalized in dark for 7 days at 4°C. Plates were then transferred for five days to growth room with 16h photoperiod at 18°C. After that time, seven and fifteen T2 lines showed 3:1 segregation on hygromycine. Those seedlings were then upscaled so that several T3 and T4 homozygous lines were obtained and used for experiments.

The protocol for barley transformation

This protocol was kindly provided by Dr Jennifer Stephens from The James Hutton Institute.

Day 1: Collect barley grains, approx 14 days post-anthesis. Sterilise by rinsing in 70% (v/v) ethanol, followed by 5 min in 50% (v/v) Sodium hypochlorite with 5 rinses of SDW. Isolate immature embryos (1.5 – 2 mm diameter) from the grains, remove axis and transfer to callus induction medium, scutellum side up and incubate in the dark at

24°C. Prepare an overnight *Agrobacterium* broth by adding a standard inoculum of *Agrobacterium* to 10 ml of liquid MG/Lmedium - no antibiotics. Incubate for 20 h at 28°C, on a shaker (180 rpm).

Day 2: Using a pipette, drip full strength *Agrobacterium* suspension onto each embryo. Drag the embryo (gently!) across the surface of the medium to remove any excess *Agrobacterium* and transfer to fresh callus induction medium, scutellum side down. Incubate in the dark at 24°C and co-cultivate for 3 days. Discard any damaged embryos.

Day 5: Transfer embryos to callus induction medium + 150 mg l-1 Timentin + selective agent and incubate in the dark at 24°C. Subculture the developing calli every 14 days, for a period of 12 - 24 weeks, following a suitable shoot regeneration programme. Only transfer resistant embryogenic lines to regeneration medium and discard any material stained with oxidised polyphenols. Immediately discard any explants which become overgrown with *Agrobacterium*.

Barley regeneration media: Four types of media are required, which may be grouped into two pairs for ease of production. Barley callus induction and rooting media are essentially of the same composition, differing only in the presence or absence, respectively, of growth regulator. Shoot initiation and regeneration media are also similar (although different from the above) differing only in the presence or absence, respectively, of growth regulators and copper. Appropriate selective agents and/ or antibiotics should be included for transformation experiments.

Barley callus induction (BCI): 4.3 g l-1 Murashige & Skoog plant salt base, 30 g l-1 Maltose, 1.0g l-1 Casein hydrolysate, 350 mg l-1 Myo-inositol, 690 mg l-1 Proline, 1.0 mg l-1 Thiamine HCl, 2.5 mg l-1 Dicamba, pH = 5.8, 3.5 g l-1 Phytagel

Shoot initiation/ transition: 2.7 g l-1 Murashige & Skoog modified plant salt base (without NH_4NO_3), 20 g l-1 Maltose, 165 mg l-1 NH_4NO_3, 1.25 mg l-1 $CuSO_4.5H_2O$, 750 mg l-1 Glutamine (reduce to 50 mg l-1 if using Bialaphos as selective agent), 100 mg l-1 Myo-inositol, 0.4 mg l-1 Thiamine HCl, 2.5 mg l-1 2,4D, 0.1 mg l-1 BAP, pH = 5.8, 3.5 g l-1 Phytagel

Shoot regeneration: 2.7 g l-1 Murashige & Skoog modified plant salt base (without NH4NO3), 20 g l-1 Maltose, 165 mg l-1 NH_4NO_3,

750 mg l-1 Glutamine (reduce to 50 mg l-1 if using Bialaphos as selective agent), 100 mg l-1 Myo-inositol, 0.4 mg l-1 Thiamine HCl, pH = 5.8, 3.5 g l-1 Phytagel

Rooting: 4.3 g l-1 Murashige & Skoog plant salt base, 30 g l-1 Maltose, 1.0 g l-1 Casein hydrolysate, 350 mg l-1 Myo-inositol, 690 mg l-1 Proline, 1.0 mg l-1 Thiamine HCl, pH = 5.8, 3.5 g l-1 Phytagel

Agrobacterium medium MG/L: 5.0g l-1 Tryptone, 5.0g l-1 Mannitol, 2.5g l-1 Yeast extract, 1.0g l-1 L-glutamic acid, 250 mg l-1 KH_2PO_4, 100 mg l-1 NaCl, 100 mg l-1 $MgSO_4.7H_2O$, 10 µl Biotin (0.1mg/ml stock), pH = 7.0, 15 g l-1 agar (for plates).

Selecting homozygous transformed barley lines

The selection of single insertion homozygous lines was based on Hygromycin resistance. 20 sterile grains (T1) were sown on agar plates (0.7 % agarose) that contained 50 µg/ml Hygromycin (stock: 50 mg/ml in SDW). Grains were vernalized for 7 d in 4°C in darkness and then transferred to growth room (18°C, 16h photoperiod). Lines that segregated 3:1 (resistant : sensitive) were considered as single insertion events and healthy, green T2 seedlings were upscaled. Again, grains from T2 were sterilized and sown on agar plates with Hygromycin (50 µg/ml), vernalized for 7 d in 4°C in darkness and then transferred to growth room (18°C, 16h photoperiod). From T3 lines, only homozygous (all resistant) or segregating 3:1 were upscaled. The same procedure was repeated for T4 lines and all homozygous lines were used in experiments.

***Arabidopsis* transformation**

Arabidopsis Col-0 plants were transformed by using floral-dip method (Bent 2006).

Selecting homozygous transformed *Arabidopsis* lines

The selection of single insertion homozygous lines was based on Kanamycin resistance. At least 100 seeds (T1) were sterilised and sown on MS plates that contained 50 µg/ml Kanamycin (stock: 50 mg/ml in SDW). Seeds were vernalized for 2 d in 4°C in darkness and then transferred to growth room. Lines that segregated 3:1 (resistant : sensitive) were considered as single insertion events and five healthy, green seedlings were upscaled. The procedure was

repeated until homozygous lines (resistant to Kanamycine) for three independent transformation events were obtained.

Arabidopsis GUS expression analyses

Seedlings were grown for one week in standard conditions and were transferred to 24 well square plates with 90% acetone and left overnight in in 4°C. After two washes with 500mM phosphate buffer (pH = 7), a GUS-solution was added [1 mM X-Gluc, 0.5% (v/v) dimethylformamide (DMF), 0.5% (w/v) Triton X-100, 1 mM EDTA (pH 8), 0.5 mM potassium ferricyanide ($K_3Fe(CN)_6$), 0.5% potassium ferrocyanide ($K_4Fe(CN)_6$), 500 mM phosphate buffer (pH = 7)] and plates were incubated for 4 h at 37°C for GUS staining, and finally washed in 500 mM phosphate buffer (pH = 7). For microscopic analysis, samples were cleared in chloral hydrate at 4°C overnight. Clearing solution that was prepared by adding 12 g of chloral hydrate to 5 ml of 30% glycerol (w/v). The solution was then allowed to dissolve at room temperature, as described in (Berleth and Jurgens 1993). Samples were analyzed by differential interference contrast microscopy with Primo Vert equiped with moticam 2300 (Zeiss).

Barley GUS expression analyses

The barley seedlings were grown in aeroponics for two weeks and primary seminal and crown roots were cut into approximately 1 cm sections. Seedlings were pre-fixed for 1h at 4^0C in pre-fixation solution [0.3% (v/v) formaldehyde, 0.1 % (w/v) Triton X-100 in 50 mM phosphate buffer, pH = 7], washed several times in 50 mM phosphate buffer, pH = 7, transferred to a GUS staining-solution [1mg/ml X-Gluc, 0.1% (w/v) Triton X-100, 10mM EDTA (pH = 8), 1mM potassium ferricyanide ($K_3Fe(CN)_6$), 50mM phosphate buffer (pH = 7)] and incubated overnight at 37°C for GUS staining and finally washed in 50mM phosphate buffer (pH = 7). For microscopic analysis, samples were embedded in resin Technovit 7100 (Kulzer) according to the manufacturer's instructions. The resin blocks were cut into 12 µm-thick sections with a microtome (Leitz 1512, Leica) and allow to dry on a microscopy slide in a drop of dejonized water at 40°C on a standard heating plate. Ruthenium red counterstaining was used (0.1% (v/v) for 90 s) and slides were mounted with a neutral medium (Klinipath). Samples were analyzed by optic microscopy with SM-LUX (Leitz) equiped with DFC320 camera (Leica).

Water uptake experiment in rhizotrons

Rice seeds (wild type *Oryza sativa L. japonica* genotype Dongjin, Os*aux1-1* and *Osaux1-2)* were kindly provided by Prof. M.J. Bennett (Plant and Crop Sciences Division, The University of Nottingham, UK). Seedlings were germinated on filter paper for 5 days. The plants where then transferred into thin rhizotrons (50x50x0.4 cm) filled with a substrate made of white sand (98.5%) and clay (1.5%) and saturated with Yoshida's nutrient solution prior to the beginning of the experiement. Two seedlings per rhizotron and three rhizotrons by genotype were used in this study and Yoshida's nutrient solution was applied during the whole experiment. In order to increase the number of roots growing along the rhizotron surface, rhizotrons were stored at an angle of ≈ 35 degrees. Plants were grown during 30 days without any stress applied and the seminal and crown roots of the plants were drawn every day on a transparent sheet that was scanned each time. Secondary roots could not be traced (too thin).

After 30 days, the nutrient solution supply was stopped for all the rhizotrons. During the next five days, rhizotrons were weighted every four hours (7 am, 11 am, 3 pm, 7 pm). The 2D soil water content distribution was obtained by placing each rhizotron between a light source (light tubes, 36W, Sylvania Standard F36W/33-640-T8) and a regular CCD camera (Canon EOS 450D with a lens Canon EF 50mm 1:1.8). Using this technique, time series of light transmission images every four hours during five days were obtained for each rhizotron [as described in (Lobet et al. 2014)]. Daily temperature (°C) and relative humidity (RH, %) were also measured with a data logger near the rhizotrons. The relative transpiration rate was calculated as a difference between the weight of the rhizotron with plants and the mean weight of three control rhizotrons without plants at a given time point. Because the plants subjected to soil drying varied in size, it was useful to further normalize the relative transpiration rate data. Therefore, all leaves from two plants per rhizotron were scanned and leaf area was measured in ImageJ (v. 1.43u). The total leaf area of two plants in a given rhizotron was then used to normalize the relative transpiration rate.

***In situ* RT-PCR**

The specificity of the primer pairs used in this study has been verified by RT-PCR on barley cDNA from cv. Golden Promise.

Several primer pairs were used per barley gene and only the chosen ones are shown in Table 3-4.

Table 3-4: Primers used in expression analysis by *in situ* RT-PCR.

Gene name	Primer name	Sequence
HvAUX1	AUX_135_F	TCCGTGTAGCACACCATTACTT
	AUX_342_R	CAGGAATTTACTGTGCGATTGA
HvLAX3	LAX_1712_F	GGTCTCTAGTCGATCGGAAGG
	LAX_1975_R	CCTCCCTCGGGTTACATTAGTT

The barley seedlings were grown in aeroponics for two weeks and primary seminal and crown roots were cut into approximately 0.5 – 1 cm sections. This sections were then precceeded as described in (Hachez et al. 2006; Fetter et al. 2004). Briefly, root segments were fixed and embedded in Technovit 7100 (Kultzer) as for manufacture instructions and sectioned into 5 µm slices with a microtome (Leitz 1512, Leica). The slides were pre-treated before RT-PCR: with 0.02M HCl for 20 min, washed with 2xSSC buffer for 30 min, incubated with 2% pectinase (Calbiochem) for 8 min at 37°C, washed for 10 min with PBS buffer, treated with proteinse K (2µg/ml) for 8 min at 37°C, then transferred into 2 mg/ml Glycine (in PBS) for 1 min, washed in PBS for 5 min, then in SDW for 5 min and finally, left to air-dry for 30 min. DNAse treatment was then performed on slides in a humid chamber overnight at 37 °C [for 50 µl:8 µl Dnase RQ1 (Promega), 1 µl RNAse inhibitor (Invitrogen), 5 µl 0.5 M sodium acetate and 36 µl DEPC-treated SDW]. Slider were then washed (10 min in 0.5 EDTA, 10 min in 2xSSC, 10 min in 1xSSC, 10 min DEPC-treated SDW) and RT was performed by using SuperScript II reverse transcriptase kit (Invitrogen), in humid chamber at 42°C for 1h [for 20 µl: 1 µl MMLV (40 U/5µl, Life Technologies), 0.2 µl RNAse Inhibitor (20 U/µl), 0.2 µl forward primer (100 µM), 0.2 µl reverse primer (100 µM) 1 µl dNPs (10mM) and 17.4 µl DEPC-treated SDW] and then a PCR reaction [for 50 µl: 0.6 µl Dynazyme polymerase (2 U/µl, Thermo Scientific), 1 µl dNTPs (10 mM), 0.25 µl DIG-11-dUTPs, 0.5 µl forward primer (100 mM), 0.5 µl reverse primer (100 mM), 5 µl Dynazyme buffer and 42.1 µl SDW]. The PCR conditions were as follows: 94°C for 2 min, 94°C for 30 s, 56°C for 30 s, 72°C for 30 s for 30 cycles and 72°C for 2 min. Signals were detected with

NBT/BCIP detection kit (Life Technologies) following the manufacture's instructions. Briefly, samples were rinsed with washing buffer and were first incubated for 30 min in blocking solution and then transferred into antibody solution for 30 min. Then, samples were washed two times in washing buffer for 15 min. and incubated for 5 min in detection buffer. Finally, samples were incubated for 2h in colour substrate solution in humid, dark container. Samples were then rinsed with water and pictures were taken using an optic microscope SM-LUX (Leitz) equiped with DFC320 camera (Leica). Several buffers were used in this method and are listed below. In all buffers before PCR reaction, DEPC-treated SDW was used. (1) 0.02 M HCl: 403.55 µl HCl and 250 ml H_2O. (2) 0.5 M sodium acetate: 4.1015 g sodium acetate and up to 100 ml H_2O, pH = 4.8 with glacial acetic acid. (3) 1.5 % pectinase in pectinase buffer: 0.8203 g sodium acetate, 0.14612 g EDTA per 100 ml, pH = 4. Working solution: 0.015 g pectinase / 1 ml of pectinase buffer. (4) 2 µg/ml proteinse K in proteinse buffer: 1.211 g Tris-HCl, 1.4612 g EDTA, pH = 8. Working solution: 3 µl of pectolyase (0.9 U/mg, Sigma) / 20 ml of proteinase buffer. (5) PBS (10x): 8 g NaCl, 0.2 g KCl, 1.15 g $NaH_2PO_4.4H_2O$, 0.2 g KH_2PO_4, for 100 ml, pH = 7.4. (6) Glycine in PBS: 0.2 g Glycine, 10 ml 10xPBS, 90 ml H_2O. (7) 0.5 M EDTA: 14.612 g EDTA for 100 ml, pH = 8. (8) Washing buffer: 0.1607 g maleic acid, 0.877 g NaCl, 0.3 ml Tween 20 and H_2O up to 100 ml, pH = 7.5. (9) Blocking solution: 0.2 ml of 10 % blocking stock solution (2 g blocking reagent up to 20 ml maleic acid buffer) and 20 ml maleic acid buffer (freshly prepared). (10) Maleic acid buffer: 1.1607 g maleic acid, 0.877 g NaCl up to 100 ml with H_2O, pH = 7.5). (11) Detection buffer: 1.16 g NaCl, 2.52 g Tris-HCl up to 200 ml with H_2O, pH = 9.5. (12) Color substrate solution: 15 µl NBT, 15 µl BCIP and 4 ml detection buffer. (13) Antibody solution: 2 µl antibody (anti-digoxigenin-AP) in 1 ml blocking solution.

Statistical analyses

All data analyses were performed with R software package, v. 2.15. Bars are means ± CI, with different letters indicating significant differences according to Tukey's HSD test.

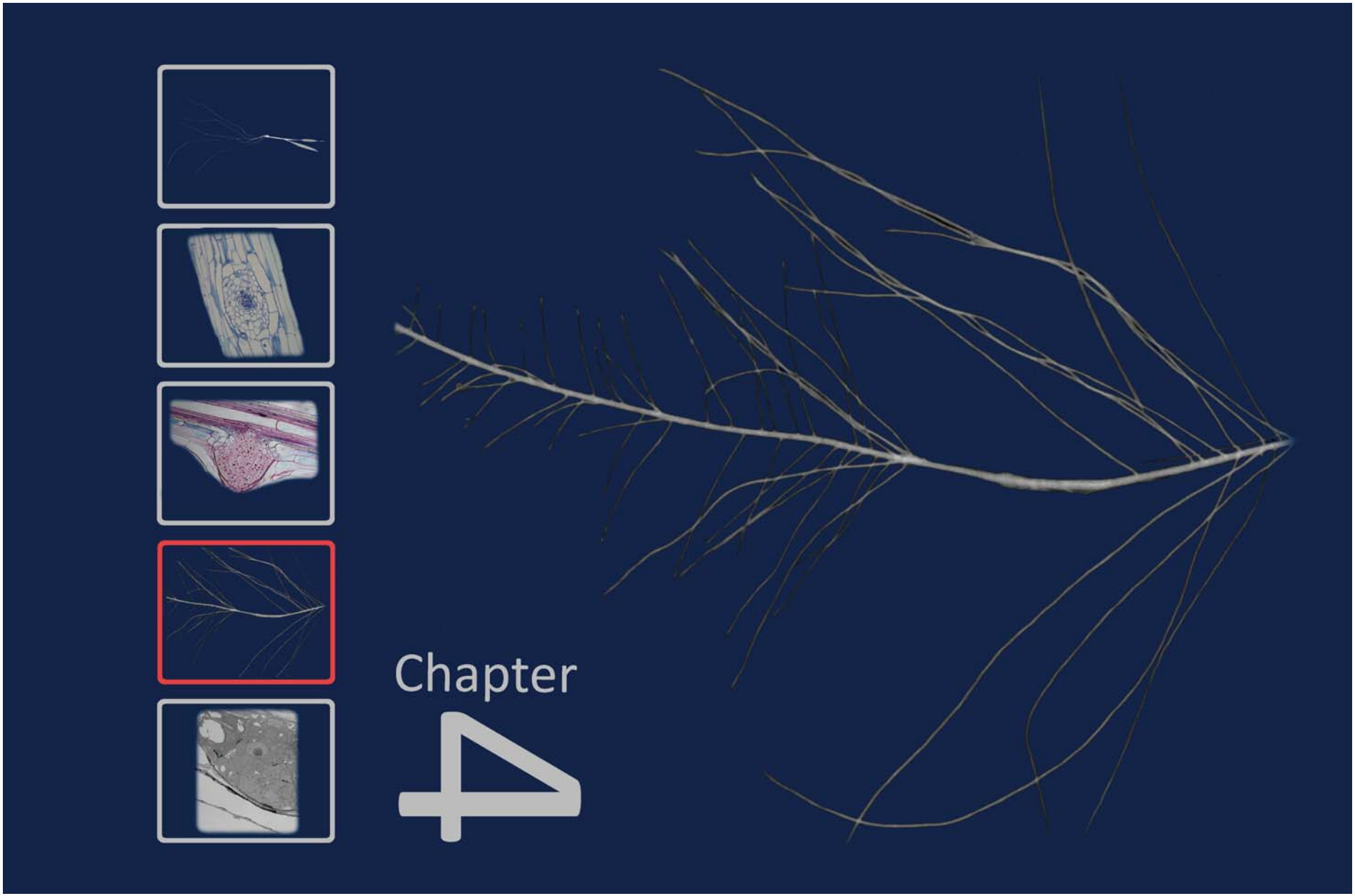
Chapter
4

CHAPTER 4

Transient water deficit triggers ABA response pathway to repress lateral root development in cereal crops and *Arabidopsis*

Manuscript in preparation

Beata Orman-Ligeza[1,2,3], Tristan Lavigne[1], Boris Parizot[2,3], Aurelie Babé[1], Jean-Philippe Séverin[1], Wei Xuan[2,3], Ian C. Dodd[4], Karin Ljung[5], Ondrey Novak[5,6], Bart Roman[7], Thomas Heugebaert[7], Malcolm J. Bennett[8], Tom Beeckman[2,3] and Xavier Draye[1]

[1]Université catholique de Louvain, Earth and Life Institute, Louvain-la-Neuve, Belgium.
[2] Department of Plant Biotechnology and Bioinformatics, Ghent University, B-9052, Ghent, Belgium.
[3] Department of Plant Systems Biology, VIB, B-9052, Ghent, Belgium.
[4]The Lancaster Environment Centre, Lancaster University, LA1 4YQ, UK.
[5]Umeå Plant Science Centre (UPSC), Department of Forest Genetics and Plant Physiology, SLU, SE-901 83 Umeå, Sweden.
[6]Laboratory of Growth Regulators, Centre of the Region Haná for Biotechnological and Agricultural Research, Palacký University and Institute of Experimental Botany AS CR, Šlechtitelů 11, CZ-78371 Olomouc, Czech Republic.
[7]Department of Sustainable Organic Chamistry and Technology, Ghent University, B-9052, Ghent, Belgium.
[8]Centre for Plant Integrative Biology, School of Biosciences, University of Nottingham, Sutton Bonington, LE12 5RD, UK.

Author Contributions

X.D., T.B., M.B. and B.O.-L designed the research; B.O.-L. performed the research and wrote the manuscript; T.L. conducted the microarray experiment; B.P. analyzed the microarray data; A.B and J.P made the initial morphological experiments on barley and maize; W. X. preformed the DR5 assays; O. N. and K.L. made the IAA quantification; A.B. and I.D. did the ABA quantification; B.R. and T.H. synthetized AbamineSG.

Abstract

Transient water deficit has been previously shown to repress LR formation in barley (*Hordeum vulgare*) and maize (*Zea mays*). However, the molecular bases of this phenomenon have not been uncovered. Here, we demonstrate that ABA response pathways are involved in the LR repression that occurs during water shortage in the root zone. Expression studies in barley revealed that transient water deficit conditions trigger components of ABA response pathways. We then showed, in barley, maize and *Arabidopsis*, that exogenous ABA treatments are sufficient to mimic the repression of LR formation at or before the founder cell division that was initially observed under transient deficit in barley and maize. IAA mediates this ABA response as pre-treatments with auxins could partially prevent the LR repression. Further experiments revealed that auxin transport, signalling and homeostasis are all altered during this process.

We therefore propose a model in which transient water deficit triggers ABA response pathways that subsequently alter auxin metabolism [general term] to repress LR formation in both monocots and dicots. This raises ABA as a major downstream intrinsic messenger of environmentally induced repression of LR development to quickly adapt root branching to local variations of soil water content.

Keywords: Lateral root, repression, abscisic acid, auxin, transient drought episode, transient ABA treatment, abscisic acid response, auxin response, cereal crops, barley, maize, *Arabidopsis*

Introduction

The spatial distribution of roots in soils is one of the determinants of water uptake by plants (Draye et al. 2010; Lynch 2007). It results from several processes, including growth, tropisms, (post-)embryonic root formation and senescence, that plants are able to modulate in response to their environment (de Dorlodot et al. 2007; Drew 1975). Among those processes, the post-embryonic formation of LR makes the largest contribution to the production of root meristems throughout the soil profile and is therefore a major driver of morphological plasticity (Drew 1975; Williamson et al. 2001; Lopez-Bucio et al. 2003; Desnos 2008).

LR formation was extensively studied in model *Arabidopsis* and cereal crops during the past decades (see recent reviews: (Lavenus et al. 2013; Orman-Ligeza et al. 2013)). This process involves a definite succession of developmental events, namely: priming, initiation, emergence and meristem activation, subsequently giving rise to autonomous LR that grows outside the parental tissues. There is a growing body of evidence that hormonal signalling mediates root developmental plasticy in response to environmental stimuli (Duan et al. 2013; Geng et al. 2013).

Abscisic acid (ABA) has been proposed as an intrinstic mediator acting downstream of several environmental cues (Schroeder et al. 2001; Oztur et al. 2002; Shinozaki et al. 2003; Buchanan et al. 2005; Young and Gallie 2000). In particular, plants rely on ABA signalling to regulate LR formation in response to nitrate availability (Signora et al. 2001), osmotic stress (Deak and Malamy 2005), salt stress (Duan et al. 2013) and water deficit (Shkolnik-Inbar and Bar-Zvi 2010; Brady et al. 2003; Deak and Malamy 2005).

We previously showed in cereals that transient drought exposure (Babe et al. 2012) does not alter LR formation in the same way as prolonged exposure to drought (Vartanian et al. 1994), ABA (De Smet et al. 2003) or osmotic stress (Deak and Malamy 2005) in *Arabidopsis*. While the latters reversibly inhibit LR development between the

emergence and the activation of the LR meristem, the former irreversibly represses the first stage of LR formation. From an evolutionary perspective, specific responses to transient and prolonged exposure to water deficit could be interpreted as, respectively, the response to the localized water deficit experienced by a root growing into a soil pore without soil contact (Bao et al. 2014; White and Kirkegaard 2010) and the adaptation to whole plant water shortage in slowly drying soils.

Here, we report a previously uncharacterized function of ABA in cereal root responses to water deficit and we support our results with *Arabidopsis*. We first show in barley roots that ABA levels increase transiently and that several ABA-regulated genes modify their expression shortly after the onset of a water deficit episode. We then show in cereals and *Arabidopsis* that this phenomenon can be partially explained by alterations in auxin transport, auxin metabolism and signalling. Finally, we show that transient ABA treatment also irreversibly represses the transition between LR priming and initiation in an auxin-independent manner, which is different from the previously reported response to long term ABA exposure in *Arabidopsis*.

Results

Transient water deficit induces ABA-responsive genes in barley roots

Gene expression during 2 to 6 h-long water deficit treatments was profiled using Barley1 GeneChip Genome Arrays (22,782 contigs) on segments of the primary seminal root containing the LR repression window described previously by Babe et al. (Babe et al. 2012). We found 755 genes with significant treatment x time interaction and significant regulation over the drought treatment (respectively Two-Way ANOVA p-value ≤ 0.01 and FC≥1.5 FDR p-value ≤ 0.01). This list surprisingly showed a higher number of genes having gene ontology related with ABA response pathways in comparison with

auxin response pathways (39 VS 21) and other hormone response pathways (data not shown). The enrichment in genes involved for these both hormone pathways is significant but also higher for ABA related genes in comparison with auxin related genes (2.3 VS 1.8, p-value ≤ 0.01). A survey of these genes shown that corresponding *Arabidopsis* homologues have been described to be involved in ABA response and display a LR mutant phenotype such as *xbat32* (Prasad et al. 2010), *hkl1* (Karve and Moore 2009) or *pad4* (Kim et al. 2012). We therefore decided to investigate further the involvement of ABA response pathways in the intrinsic LR repression by transient WD in barley and *Arabidopsis*.

Among the 755 genes, we could generate a list of 36 putative transcription factors based on gene ontology with *Arabidopsis* homologues (see Suplemental Table S-4). One of these transcription factors, Contig10961 that belong to the basic-leucine zipper (bZIP) transcription factor family protein and is a close homologue of AT1G58110 *AtbZIP*, displays altered root growth dynamics upon ABA and NaCl treatments (Suplementary Materials, Figure S-1).

Since we could find putative *Arabidopsis* orthologues for 506 out of the 755 selected genes, we also decided to investigate whether these genes are significantly regulated during different steps of the lateral root formation related processes in *Arabidopsis*. For this purpose, we gathered different datasets dedicated to (i) SOLITARY-ROOT/IAA14 dependant NAA response during the course of the lateral root induction system (Vanneste et al. 2005; Himanen et al. 2004), (ii) NAA response in the lateral root initiation competent xylem pole pericycle tissue during the same treatment (De Smet et al. 2008), (iii) similar NAA or naxillin non-auxin-like molecule response during the course of a 2 h-long lateral root induction (De Rybel et al. 2012), (iv) IBR1 IBR3 IBR10 dependant IBA response during the course of a 6 h-long lateral root induction (Xuan and Audenaert, unpublished), and (v) oscillating expression concomitant with the DR5 oscillations observed in the root apical meristem (Moreno-Risueno et al. 2010). Interestingly, we observed the highest

enrichments for the naxillin and the IBA datasets (respectively 2.6X and 2.7X, p-value ≤ 0.01), which are related with the priming of the pericycle cell to insure the subsequent formation of lateral roots. We could also notice a significant, but lower, enrichment for the two datasets related to the lateral root initiation itself (1.5X for both SLR and xylem pole pericycle, p-value ≤ 0.01), but no significant enrichment could be observed for the oscillation dataset. The fact that the above microarray experiments were designed to target transcriptional events that occur during early stages of LR formation in *Arabidopsis*, we hypothesize that transient WD episode interfere with LR initiation stage or earlier, assuming that such developmental process is conserved in these two species.

ABA levels increase in response to WD in barley roots

We previously found in our experimental conditions that a 4 h-long WD is sufficient to trigger a clear repression zone (RZ) along the root (Babe et al. 2012). To explore the possibility that ABA would drive the response to transient WD, we quantified active ABA levels in barley roots during the WD episode. Compared to control plants, WD triggered an increase in active pools of ABA in root tissue, within 4 h of the treatment. The ABA levels were respectively, 377 ± 11 ng/g FW and 1384 ± 167 ng/g FW in control condition and upon WD ($P < 0.001$). This biologically active ABA pool is likely to be released from conjugates (Lee et al. 2006), as inhibition with AbamineSG of the 9-cis-epoxycarotenoid dioxygenase (NCED), a key regulatory enzyme in the major ABA biosynthesis pathway in plants, did not rescue LR formation under WD (Figure 4-1, Lee et al. 2006). We therefore concluded that an active pool of ABA increases in the root tissue under WD, likely through hydrolysis of ABA conjugates.

Transient ABA treatment mimics branching responses to transient WD

To test if an increase in ABA levels alone is sufficient to mimic WD-induced LR repression in cereals, we exposed 5 dpg barley and 4 dpg maize seedlings to 8 h of transient ABA treatment in the aeroponic conditions used by Babé et al (2012). We observed clear

RZs in both barley (Figure 4-2A and 4-2B) and maize (data not shown).

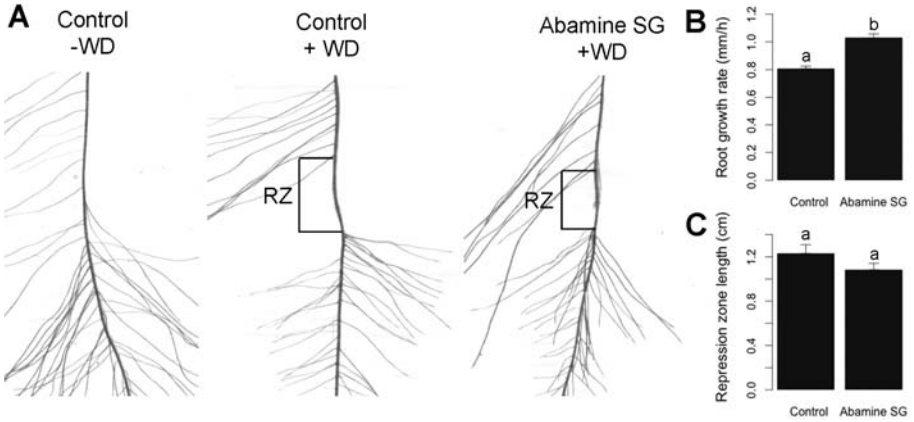

Figure 4-1: Effect of AbamineSG pretreatment in LR repression experiments.

(A) to **(C)** 3-d-old barley seedlings were transferred on agar plates with DMSO (Control) or 100 µM AbamineSG and plates were scanned. After 1 d plates were scanned again and plants were transferred to the aeroponics and soaked in standard nutrient solution (NS) or in NS with AbamineSG prior to 8 h of WD. Plants were photographed after 7 d of growth in aeroponics **(A)**, root growth rate on plates with DMSO or AbamineSG was measured **(B)** and the length of repression zone was measured **(C)**. Bars are means ± CI, with different letters indicating significant differences according to Tukey's HSD test after ANOVA ($n > 15$).

The length of the RZs were 0.94 ± 0.06 and 1.08 ± 0.35 cm in barley and maize, respectively. We then confirmed this response using an agar-based square plate system (Figure 4-3). Barley seedlings in this system formed RZ when treated with 50 µM ABA, which supports that ABA, independently from the aeroponic conditions, is sufficient for RZ formation. The validation of the ABA response in agar plates allowed us to compare the ABA response of *Arabidopsis* with that of barley. The duration of the ABA treatment had to be increased for *Arabidopsis* in such a way that the treatment produced a distinguishable RZ lacking at least 4 LRs. As for cereal experiments, *Arabidopsis* seedlings treated with ABA during 2 d lacked LRs in close proximity to the root segment that grew in the presence of ABA (Figure 4-2C and 4-2D). This response was observed under ABA concentrations ranging from 5 to 50 µM (Figure 4-2E).

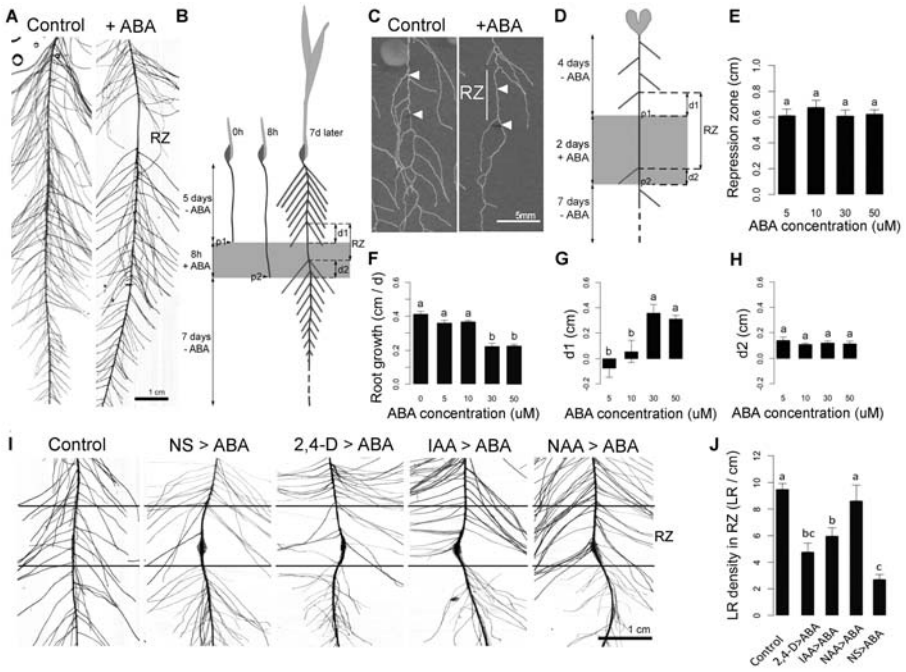

Figure 4-2: Effect of transient ABA treatment on root branching.

(A) Morphology of 12 dag barley root systems treated with DMSO (Control) or 50 µM ABA (+ABA) for 8 h in LR repression experiments. The basal and apical zones are not shown. **(B)** Diagram illustrating our experimental design for studying repression of LR formation by ABA in cereal crops. **(C)** Branching pattern of 13 dag *Arabidopis* root system exposed to DMSO (Control) or 50 µM ABA (+ABA) for 2 d in LR repression experiments. The basal and apical zones are not shown. **(D)** Principle of the experimental approach used to study repression of LR by ABA in *Arabidopsis*. **(E)** RZ length in *Arabidopsis* seedlings grown for 2 d with various ABA concentrations and then transferred for 7 d to standard media (n > 15 seedlings). **(F)** Average *Arabidopsis* root growth rate during 2 d of treatment with given ABA concentrations (n > 10 seedlings). **(G)** Average d1 offset between the position of the root tip at the beginning of ABA treatment and the last emerged LR (n > 10 seedlings). **(H)** Average d2 offset between the position of the root tip at the end of ABA treatment and the first emerged LR (n > 10 seedlings). **(I)** and **(J)** Branching pattern of barley roots in auxin complementation assay. Plants were exposed for 1 h to nutrient solution (NS), or to 75 µM of 2,4-D, IAA or NAA and then treated for 6 h with 50 µM ABA in aeroponics. Roots were imaged after 7 d of growth **(A)** and the average number of LRs within the RZs was calculated **(B)**, and compared to control conditions (Control) when no pre-treatment was applied (n > 16). Bars are means ± CI., Different letters indicate significant differences with $p < 0.001$ according to Tukey's HSD test after ANOVA.

In addition, the length of the RZ was not affected within the ABA concentrations tested (F-test, P = 0.5). We finally quantified the root growth response during the ABA treatment. In agar conditions, 50 µM ABA reduced the root growth rate by 40 and 45 %, in barley and *Arabidopsis*, respectively (Figure 4-2 F; Figure 4-3) and by about 40% in barley in aeroponic conditions. Interestingly, low ABA concentrations did not reduce the root growth rate in *Arabidopsis*, suggesting that the root growth response might be independent from the LR repression. Taken together, these results suggest that transient ABA treatment mimics the morphological responses to WD episode and, in particular, represses LR formation.

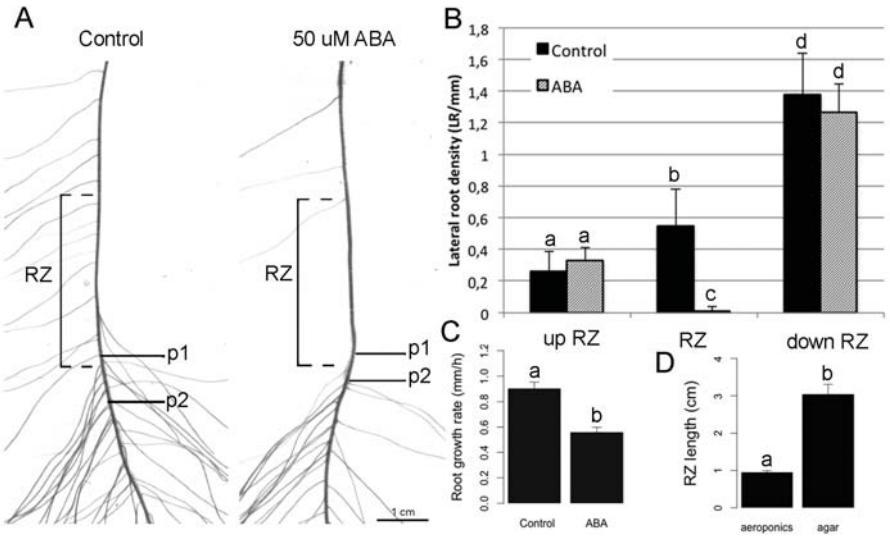

Figure 4-3: Effect of agar on ABA-mediated LR repression.

(A) to **(D)** 3 d-old plants were transferred on agar plates with DMSO (Control) or 50 µM ABA (+ABA) for 6 h. Positions of root tips were marked before and after the ABA treatment. After 7 d of growth in aeroponics, plants were imaged **(A),** the number of LRs in three indicated zones was counted **(B)**, root growth rate during 6 h of treatment was estimated **(C)** and the length of RZ was measured **(D).** Bars are means ± CI. Different letters indicate significant differences according to Tukey's HSD test after ANOVA (n > 20).

ABA targets a well-defined LR developmental window

We first analysed at which stage of lateral root formation the repression occurred in ABA-treated cereal seedlings. In barley and

maize control plants, the root segment spanning the region where the RZ appears in ABA-treated plants contains ca. 10 emerged LR (Babe et al. 2012). In the presence of 50 μM ABA treatment, no LR primordia were observed in the RZ, with a few exceptions where a maximum of two to three arrested primordia were present (n = 20). In agreement with previous experiments Babe et al. (2012), these few primordia were arrested at the first asymmetric division stage in barley, or at more advanced stages in maize.

In *Arabidopsis* control seedlings, the root segment corresponding to the region where the RZ appears in treated plants contains ca. four emerged LRs (n = 10). In the presence of 5 and 10 μM ABA, the RZ of about 60% of the seedlings comprised 1 - 2 LRs that were arrested between stage 5 and soon after emergence, whereas that of the remaining seedlings did not comprise any LR primordia (n > 10 seedlings). Similarly, the RZ observed at 30 and 50 μM ABA did not contain any visible LR primordia, except for 15% of the 30 μM-treated seedlings for which the RZ contained one LR primordium arrested at stages 1 (n > 10 seedlings for each condition) close to the proximal boundary of RZ.

By virtue of their position, the LR primordia arrested at advanced stages that were found occasionally in the RZ were initiated during the ABA treatment. However, the stage at which these are arrested is normally reached several days after LR initiation in both species. We can therefore conclude that those few LR primordia that were able to escape the early repression during the ABA treatment were ultimately repressed well after the end of the treatment.

Using the time-lapse approach that was described for WD experiments (Babe et al. 2012), we estimated the position along the primary root where ABA represses LR formation. According to this method and by virtue of the acropetal nature of LR formation, the proximal boundary of the RZ should be offset from the position of the root tip at the onset of the ABA treatment by a distance (d1) equal to the position of the most advanced LR stage repressed by ABA (Figure 4-2B and 4-2D). Similarly, the distal boundary of the RZ should be offset from the position of the root tip at the end of the ABA treatment by a distance

(d2) equal to the position of the earliest LR stage that is affected by ABA.

Subsequently, we estimated the timing of ABA repression along the course of the LR formation. In barley, d1 and d2 offsets were, respectively, 14.4 ± 0.11 and 12 ± 0.32 mm. We found that LR primordia are typically at stage 1 or before, up to 15 mm from the root tip (Babe, A., pers. comm.). In *Arabidopsis*, d1 and d2 values (Figure 4-2G and 4-2H) at 5 and 10 µM ABA were both close to 1 mm, which falls within the 0.2 - 1.2 mm region where likely LR priming occurs (Dubrovsky et al. 2006b; De Smet et al. 2007; De Rybel et al. 2010; De Smet 2011)). At both 30 and 50 µM ABA, d1 and d2 were respectively close to 3.4 and 1.1 mm, which spans the transition from founder cell specification and primordium initiation that occur 4.2 mm from the tip (Dubrovsky et al. 2006b). This time-lapse analysis in barley and *Arabidopsis* therefore indicates that the ABA repression occurs before the first asymmetric division and, according to the *Arabidopsis* results, presumably as early or before the founder cell specification.

IAA partially overcomes ABA-mediated LR repression

Given its well-established role in LR formation (Lavenus et al. 2013; Benkova et al. 2003; Himanen et al. 2002), we investigated whether auxin is able to rescue ABA-mediated LR repression (Figure 4-2I and 4-2J). 5 dpg barley seedlings were exposed for 1 h to 75 µM NAA, IAA or 2,4-D prior to a 6 h long ABA treatment in the same aeroponic system. These three auxins were used to distinguish between passive and active transport, as NAA enters cells predominantly via diffusion and exits through efflux carriers, 2,4-D enters through influx carriers and exits passively, while IAA moves in and out via passive and active transport systems (Delbarre et al. 1996). Pre-treatments with NAA and IAA restored LR formation fully and partially, respectively. Based on LR counts in the RZ, the 2,4-D pre-treatment was not significantly different from the mock ABA treatment (Figure 4-2I and 4-2J). Interestingly, the restoration of LR formation by auxins did not occur on barley seedlings that were post-treated with the same auxins (data not shown).The inability of

auxin post-treatment to restore LR formation suggests that pericycle cells affected by a transient ABA treatment lose irreversibly the competence to respond to auxin and to engage into LR formation, suggesting that ABA targets a narrow LR developmental window.

The ability of auxins that can be actively exported from the cell to overcome the ABA-mediated repression therefore indicates that IAA synthesis, efflux transport and/or signalling are affected by ABA. We therefore investigated the major components of auxin metabolism in LR repression experiments.

Transient ABA treatment decreases free IAA levels in roots

IAA profiling was performed along the 2 cm long distal region of maize roots treated with ABA during 2 to 6 h. The profiling focused on levels of free IAA, several IAA precursors (Trp (Tryptophan), Tra (Tryptamine), IpyA (Indole-3-pyruvic acid)) and several products of IAA inactivation (oxidative intermediate oxIAA (2-oxindole-3-acid acid), and IAA conjugates to Asp (Aspartate) and Glu (Glutamate)) (Ludwig-Muller 2011; Novak et al. 2012). The ABA treatment progressively decreased free IAA levels by 80 % in the proximal part of the analysed region (Figure 4-4A).

A very large transient increase of free IAA occurred after 4 h of treatment in the distal part. As LR repression already occurs in 2 h long treatments (Draye, personal observation), this free IAA increase might be a downstream effect. In parallel to the free IAA decrease, the amounts of IAA conjugates increased in root segments after 2 h of treatment (Figure 4-4C), while only a minor impact on auxin biosynthesis was observed (Figure 4-4B).

These results indicate that ABA decreases auxin levels above the root meristem, which fits the rescue effect of external auxin application reported above. They also suggest that the IAA decrease might be related, at least partly, with the formation of auxin conjugates.

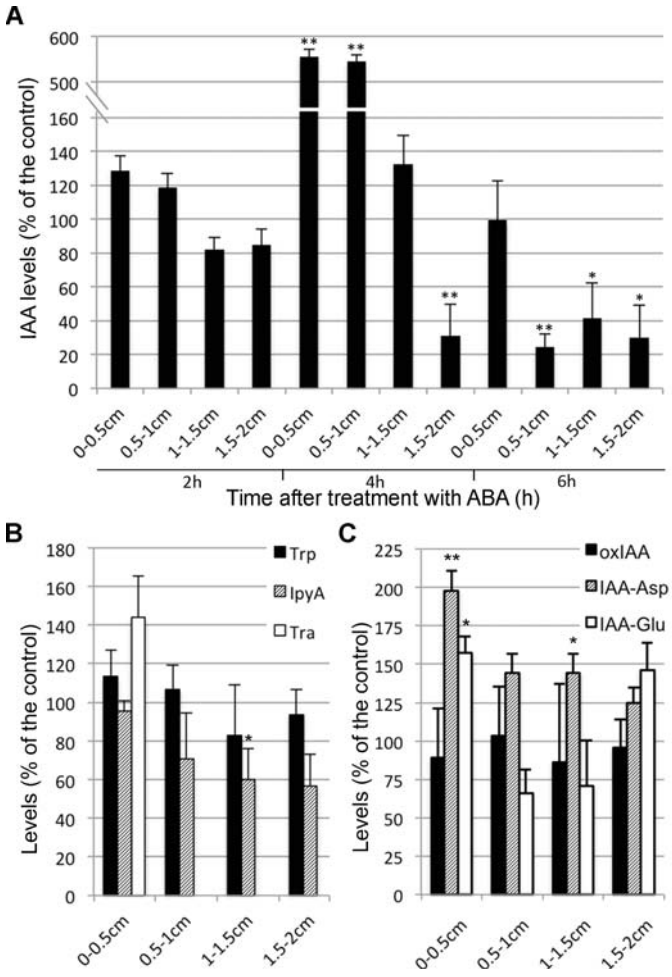

Figure 4-4: The effect of transient ABA treatment on auxin metabolism.

Changes in levels of given auxin metabolites in maize B73 root segments in LR repression experiments were quantified by LC-MRM-MS (liquid chromatography/multiple reaction monitoring/mass spectrometry), (n = 3). **(A)** Levels of free IAA**. (B)** Levels of IAA precursors upon 2 h-long ABA treatment: Tryptophan, Trp, Tryptamine, Tra, Indole-3-pyruvic acid, IpyA. **(C)** Levels of IAA conjugates upon 2 h-long treatment: oxindole-3-acetic acid, oxIAA, indole-3-acetyl-aspartate, IAA–Asp, and indole-3-acetyl-glutamate, IAA–Glu. Asterisks indicate statistically significant difference in the treated plants versus the control plants in an ANOVA analysis (Student's *t* test; * and ** correspond to P value of $0.05 > p > 0.01$ and $0.01 > p > 0.001$, respectively).

ABA alters abundance of auxin transport proteins

We then investigated the effect of transient ABA treatments on auxin transport proteins. We first analysed the effect of ABA on root gravitropism, given the well-documented dependence of gravitropism on auxin influx and efflux carriers (Baster et al. 2013). In our experimental conditions, ABA-treated barley seedlings showed significantly faster bending response (Figure 4-5).

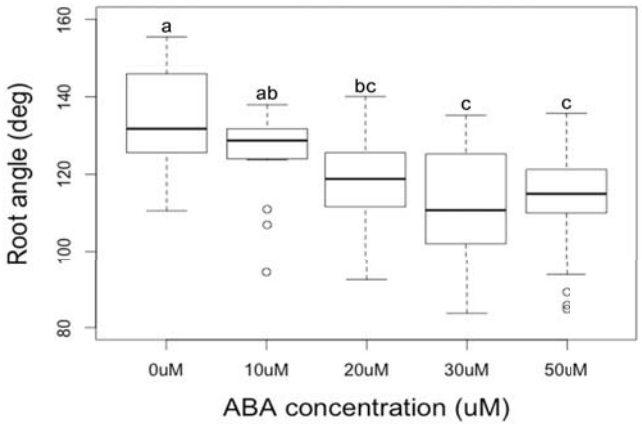

Figure 4-5: Effect of transient ABA treatment on the root bending response.

Barley 3-4-d-old seedlings were transferred to Petri plates with solidified standard nutrient solution (NS) with DMSO (Control) or indicated ABA concentrations and the plates were turned by 90 degrees. Plates were scanned before and after 18 h of gravistimulus ($n > 20$). Bars are means ± 95% CI, with different letters indicating significant differences according to Tukey's HSD test after ANOVA.

We next quantified the effect of ABA treatment on auxin carriers on transcriptional level. No changes in expression were observed upon ABA treatment in maize (Figure 4-6A; see Suplementary Materials, Figure S-2) in agreement with our WD microarray experiment in barley.

We then investigated whether transient ABA treatments affect auxin carriers protein levels. In maize, using a PIN1 reporter line (Gallavotti et al. 2008a), we showed that PIN1 protein abundance transiently

increases within 1 h and then drops back to control levels upon 50 µM ABA treatment (Figure 4-6B and 4-6C).

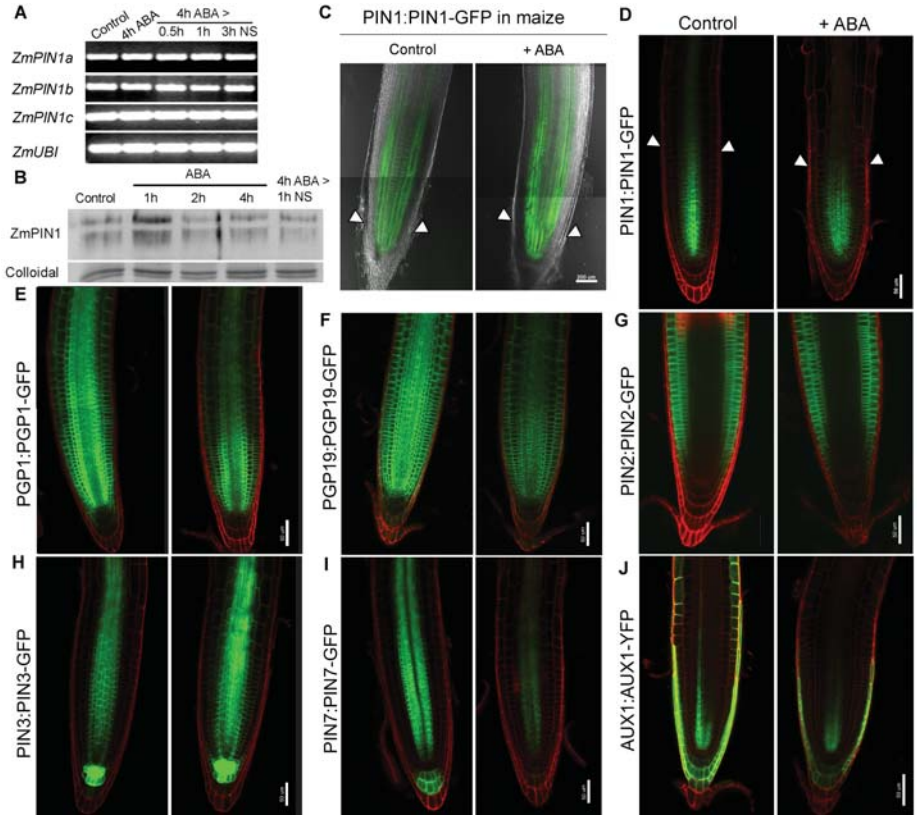

Figure 4-6: Effect of transient ABA treatment on the abundance of auxin transport proteins.

(A) *PIN1a, PIN1b* and *PIN1c* transcript abundances as determined by RT-PCR analysis from B73 wild-type plants in LR repression experiments. Maize ubiquitin signal was used as an equal loading control. **(B)** PIN1a protein levels in LR repression experiments as determined by western blots performed on microsomal extracts from maize PIN1:PIN1-YFP seedlings using anti-YFP antibody. Colloidal blue staining was used as a loading control. **(C)** Representative YFP fluorescence of the PIN1:PIN1-YFP in maize in LR repression experiments, n > 5. White arrowheads indicate the ends of the lateral root cap. **(D)** to **(J)** Representative GFP fluorescence of auxin transport proteins in LR repression experiments as indicated on the left side. Propidium iodide was used as a counterstain.

In the absence of other marker lines for auxin carriers in cereals, we examined the abundance of proteins responsible for acropetal (PIN1, PIN3, PIN7, PGP1 and PGP19) and basipetal (AUX1 and

PIN2) auxin transport Figure 4-6D to 4-6J) in *Arabidopsis*. Under 6 h-long 30 μM ABA treatments, auxin carriers protein abundance and localization remained constant (data not shown). However, 1 d-long treatment with 30 μM ABA caused a decrease of PGP1 abundance above the meristematic zone, an overall loss of PIN7 and PGP19 and only a moderate decrease in PIN1 and an overal loss of AUX1, especially in epidermis. Interestingly, PGP mutant phenotypes often display a decrease number of LR and faster gravitropic response (Strohm et al. 2012).

These results suggest that auxin transporters involved in root gravitropic response (AUX1 and PIN2) in the root tip are not affected by transient ABA treatment and that PGP's might be the main targets of ABA response pathways.

ABA targets auxin signalling

Finally, we investigated whether auxin signalling is affected by transient ABA treatment using available auxin-signalling reporters. In barley seedlings exposed to 2 to 6 h-long ABA treatments, DR5:RFP fluorescence in collumella cells decreased in a time-dependent manner and was partially restored when ABA was removed (Figure 4-7A and 4-7B) A similar decrease of fluorescence was confirmed in DR5:RFP maize (Suplementary Materials, Figure S-3). However, fluorescence of DR5 and DII in the *Arabidopsis* collumella did not decrease upon ABA treatment (Figure 4-7C and 4-7D).

A more advanced analysis was thus performed in *Arabidopsis* using *in vivo* time-lapse imaging of DR5pro:NLS3xVENUS (Figure 4-8). Upon a 24 h ABA treatment, the overall fluorescence level above the root tip slightly decreased in time compared to control conditions. In particular, typical new DR5 fluorescence maxima did not form during the 30 μM ABA treatment and similar response was then observed upon 10 μM ABA (not shown).

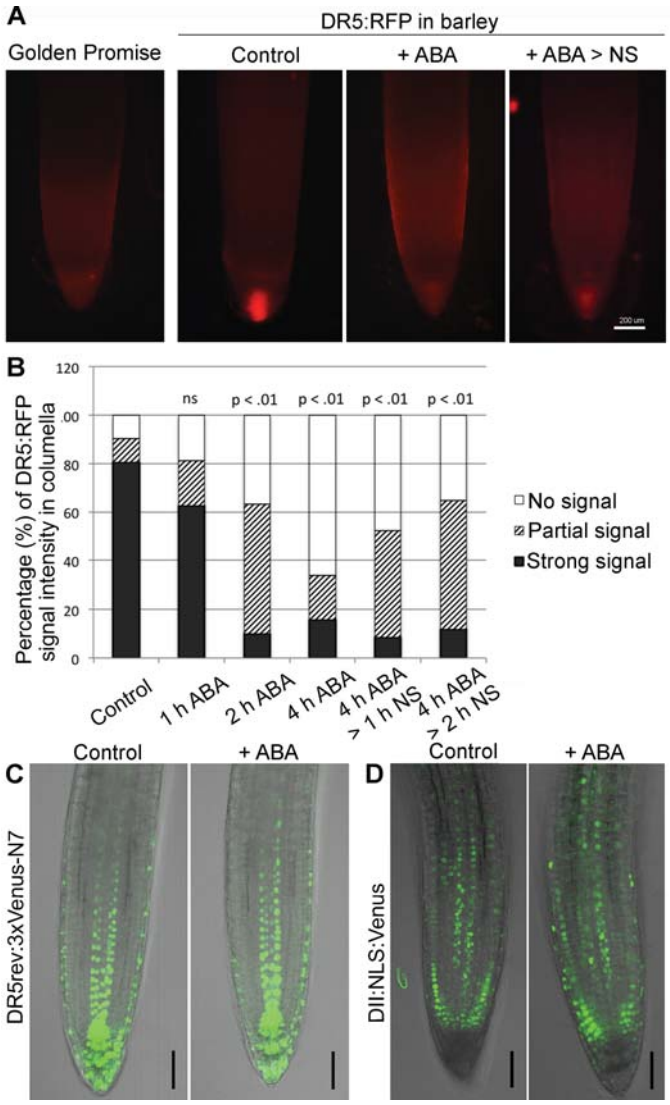

Figure 4-7: Effect of transient ABA treatment on DR5 fluorescence in the root tips of cereal crops and *Arabidopsis*.

(A) and **(B)** DR5:RFP fluorescence in the root tip of barley in LR repression experiments. **(A)** Roots were imaged with fluorescence binocular and a wild-type Golden Promise was used as a background signal control and **(B)** the proportion (%) of root tips with strong, partial and no fluorescence signal in root tip was calculated from > 20 seedlings in each treatment. P values are given for pair-wise comparisons to the Control (Student *t* test). **(C)** and **(D)** Expression pattern in the *Arabidopsis* root tip of auxin response markers DR5 **(C)** and DII **(D)** in LR repression experiment. 5 dag seedlings or were transferred to standard media with DMSO (Control) or 30 μM ABA (+ABA) and imaged after 1 d (DR5) or 30 min (DII), n>20.

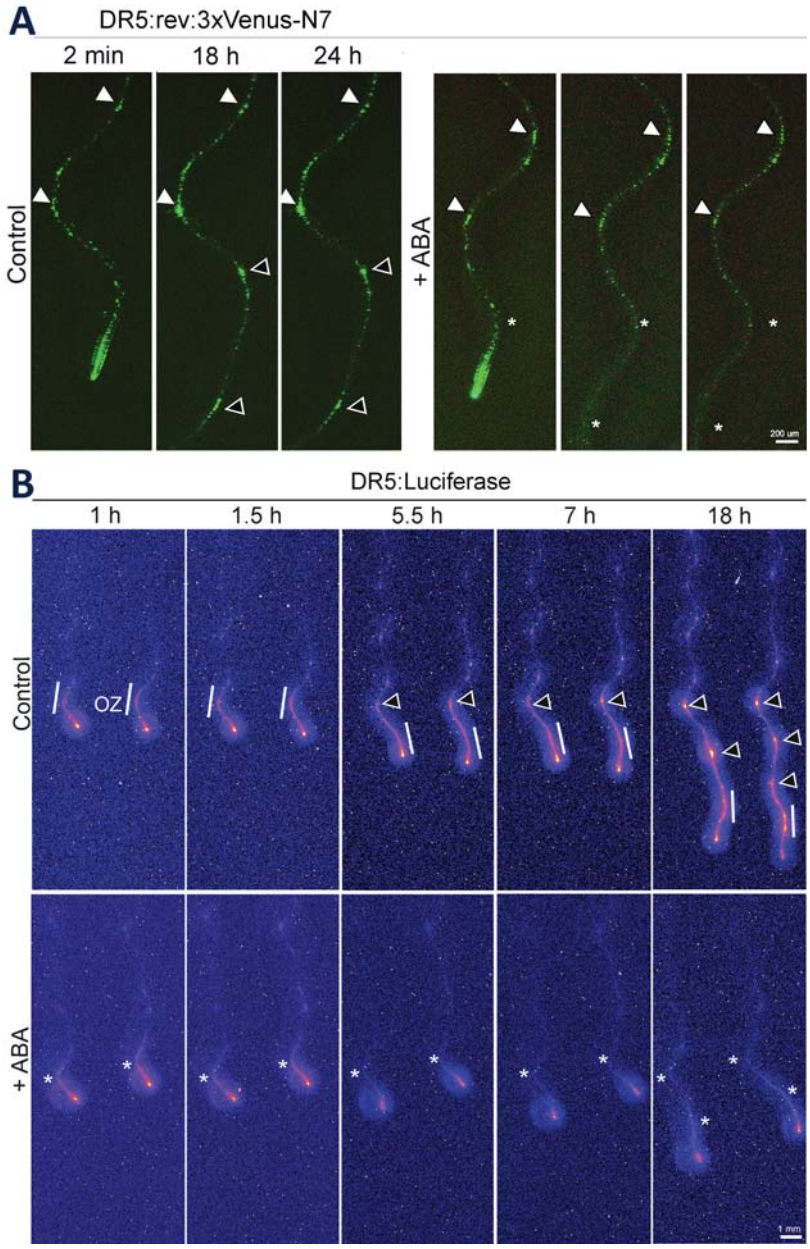

Figure 4-8: Transient ABA treatment alters the emergence of DR5 maxima during the formation of LR primordia and affects DR5 oscillations in the root oscillation zone.

(A) **R**epresentative DR5rev:3XVENUS-N7 fluorescence in LR repression experiments viewed using time-lapse imaging. 4 dag *Arabidopsis* seedlings grown

on standard media were transferred to standard media with DMSO (Control) or 30 μM ABA (+ABA) and imaged every 2 min during 24 h in a dark imaging chamber (n = 9). White arrowheads mark the position of DR5 maxima present at the time of transfer. Black-filled arrowheads indicate the position of DR5 maxima that appear during the time-lapse imaging. **(B)** Representative DR5:luciferase luminescence in the LR repression experiments viewed by using time-lapse imaging. 4 dag *Arabidopsis* seedlings grown on standard media were transferred to standard media with DMSO (Control) of 30 μM ABA (+ABA) and imaged every 10 min up to 18 h in the dark imaging chamber (n = 10). Black-filled arrowheads indicate the position of pre-branched sites that appear during the time-laps imaging and subsequent formation of DR5 maxima that indicates the position of future LR primordia. White line indicates the position of oscilation zone (OZ). White stars mark the position where DR5 maxima **(A)** or oscillation pulses **(B)** should be present by the virtue of the position along root.

The latter observation was further investigated using DR5:Luciferase whose pulses close to the root tip correlate with and mark the future position of LRs (Moreno-Risueno et al. 2010). We found that the DR5:Luciferase pulses are lost upon 30 μM ABA treatment (Figure 4-8), what was not observed in the presence of 0.5 μM ABA (Van Norman et al. 2014), indicating that high ABA concentration attenuates the oscillatory network located in the basal meristem.
These results indicate that ABA targets very early LR formation stages and presumably affects the oscillatory mechanism that triggers root branching. Altogether, our results suggest that transient ABA treatment can alter auxin response in early LR initiation events and prevent new ones from taking place.

Discussion and conclusions

WD-induced ABA increase is likely responsible for LR repression

In this study, we have shown that a WD episode, which was previously shown to repress LR formation, targets several genes involved in ABA response and transiently increases ABA levels in roots. We also showed that exogenous ABA application leads to LR repression before the initiation stage, which fully mimics the developmental response to WD. We therefore speculated that WD triggers rapid ABA response pathways in roots, as it does in leaves during stomata closure (Schroeder et al. 2001; Geiger et al. 2011).
The origin of the ABA increase remains unknown. However, a similar

increase was also observed in sunflower in detached and droughted apical root fragments, without access to shoot-borne ABA (Ruiz-Sola et al. 2014; Robertson et al. 1985). The ABA increase could therefore involve alternative root-borne source of ABA. We can also not exclude the possibility that WD induces the release of ABA from the glucosyl ester form, as previously suggested (Lee et al. 2006). Upon prolonged drought, however, ABA levels have been shown to decrease in roots (De Diego et al. 2013) and the LR phenotype is similar with that of seedlings exposed to long term ABA treatments (De Smet et al. 2003; Xiong et al. 2006). In particular, the long term exposure to ABA inhibits lateral root meristem activation by promoting quiescence of the quiescent center in a reversible fashion and does not affect early stages of LR formation (De Smet et al. 2003; Zhao et al. 2014; Zhang et al. 2010). The repression of LR formation early after the onset of WD or of an ABA treatment appears therefore to be distinct from the consequence of ABA signalling in response to prolonged water deficit (Moriwaki et al. 2012; Bahrun et al. 2002; De Diego et al. 2013).

ABA-mediated LR repression involves auxin

The ability to restore LR formation by exogenous application of IAA in barley indicated that an auxin-dependent pathway is involved in the repression of LR formation by ABA as by transient water deficit. Two to four hours after the start of the ABA treatment, IAA and IAA precursors decreased in proximal root segments and IAA conjugates increased simultaneously. After one day, the abundance of auxin carriers PGP1, PGP19 and PIN7 decreased in ABA-treated seedlings. Furthermore, auxin response (DR5pro:NLS3xVENUS fluorescence) decreased in initiated sites (Fig 8, closed symbols) and was lacking in putative primed sites (Fig 8, open symbols) in *Arabidopsis*, and it decreased already in the root columella cells in cereal crops. We therefore propose that the LR repression observed upon transient water deficit and ABA treatment might be achieved through IAA content, spatialization and signalling.

This auxin-dependent pathway is expected to interfere with auxin dependent steps of LR formation (Benkova et al. 2003; Casimiro et al.

2001; Himanen et al. 2002). Since auxin is not sufficient to drive DR5 pulses in the oscillation zone that trigger LR branching (Moreno-Risueno et al. 2010), this pathway should act on LRP that had been primed just before the onset of the treatment, leading to founder cell specification or stage 1 repression, as we observed at high ABA concentrations in barley, maize and *Arabidopsis*. This is further supported in *Arabidopsis* by their being located at the proximal part of the repression zone.

LR repression occurred similarly at different ABA concentrations in *Arabidopsis*. A notable difference was that some of the auxin-dependent repression events at low ABA were delayed until stages 5 or 6, before meristem activation. Similar delayed events occurred sometimes in maize. In these delayed events, the repression occurred after the end of the treatment. This may suggest that the transient ABA signal triggers some modification to the IAA metabolism that leads to irremediable repression, at an ABA concentration-dependent rate.

The response to long term osmotic or ABA treatments also leads to the suppression of lateral root development (Deak and Malamy 2005; Zhao et al. 2014; De Smet et al. 2003). This suppression has been interpreted at least as a consequence of auxin signaling modification under ABA. As for transient treatment, long term suppression can be overcomed by exogenous application of auxin. Prolonged ABA also leads to growth recovery of some of those LR, through an auxin-dependent cascade that involves activation of MYB77 that binds to ARF7 and promotes the expression of ARF7-induced genes during LR recovery phase (Zhao et al. 2014). However, several elements suggest that the underlying mechanism of transient and long term treatments are different. In particular, in long term treatments LR initiation is not affected, and LR are only blocked soon after emergence.

ABA attenuates an endogenous oscillatory mechanism that triggers root branching

The suppression of DR5:Luciferase pulses in the oscillation zone located in the basal meristem during the transient ABA treatment indicates that ABA also represses LR formation by altering an

endogenous mechanism that triggers root branching (Moreno-Risueno et al. 2010; Van Norman et al. 2014). The exact mechanism of these oscillatory pulses of gene expression remains to be uncovered, but it is likely that they are driven by self-sustaining or autonomous oscillations (Moreno-Risueno et al. 2010). It appears that auxin itself is not sufficient to drive these pulses of DR5 expression, as additional pre-branch sites were not specified by auxin application (Moreno-Risueno et al. 2010). Furthermore, the oscilations of DR5 expression seem to dependent on uncharacterised carotenoid-derived molecule (Van Norman et al. 2014), in addition to their dependence on TIR1–AFB, ARF7- and IAA28 (De Rybel et al. 2010; Moreno-Risueno et al. 2010). Interestingly, several alternative transcriptional regulators have been found to oscillate in frame or in opposite phase with DR5 in the oscillation zone (Moreno-Risueno et al. 2010). The ABA-mediated repression of DR5 pulses in the oscillation zone is further supported by the facts that the RZ comprises many more potential sites than the number of auxin-dependent repression events (i.e. stage 1 LRP), and that IAA post-treatment does not complement the effect of ABA.

ABA response pathways coordinate LR repression

Our results leads to a general model where ABA response pathways are involved in the repression of LR formation (Figure 4-9). The obtained evidence suggest that this model is valid for *Arabidopsis* and cereals, and describes both ABA and WD response.

On the one side, ABA response pathways cause a reduction of auxin levels, by altering auxin transporters (PGP1, PGP19, PIN7), increasing auxin conjugate formation (IAA-Aspartate) or decreasing auxin biosynthesis (IAA precursor), which ultimately attenuates DR5 auxin response. This pathway leads to the repression of initiated LRP between stage I and meristem activation. It is therefore likely to be the same mechanism that locks LRP at the meristem activation under 10-12 d-long ABA treatment (De Smet et al. 2003; Zhao et al. 2014; Zhang et al. 2010).

On the other side, ABA also affects the endogenous clock-like mechanism that triggers root branching. This ABA pathway operates rapidly and leads to the early repression and fast restoration of LR

formation. It is also equally observed upon transient WD (Babe et al. 2012). However, this second pathway is not repressing LR initiation under 12 d-long exposure and low ABA concentrations, where LRP are formed at a normal density and remain locked at the meristem activation phase (De Smet et al. 2003).

Physiological and evolutionary significance

Roots growing through soil macropores often display reduced LR numbers and enhanced root hair formation (Figure 4-9) and see also (White et al., 2010; Bao et al. 2014). These observations suggest that local adjustments of root architecture take place when roots experience the rapid loss of soil contact and the drop of external water potential which both occur while entering macropores. The fact that LR repression in aeroponics under transient water deficit (Babe et al. 2012) or ABA (this study) reproduces those local adjustments suggests that our experimental setup mimics the conditions to which roots are exposed in macropores. This would imply that the low external water potential in a macropore is sufficient to induce the repression of LR.

From a logical point of view, the immediate adjustments of LR density that occur at the boundaries of the macropore and that ensure the perfect match of the RZ with macropore boundaries could be achieved by a switch-type mechanism operating in a small developmental window. Such mechanism would switch the repression on and off whenever the window is exposed to, respectively, the air when the root enters the pore or the soil when the root leaves the pore. The endogenous clock-like mechanism that triggers root branching (Figure 4-9) features a switch behavior operating in a small window and appears therefore as a candidate mechanism of LR repression in macropores. In addition, as the LR “priming” region will be exposed to the change of conditions at macropore boundaries before the LR initiation zone, the LR initiation should not be triggered in macropores. On the contrary, it has been reported in *Arabidopsis* that system-wide decrease of soil water content or osmotic stress leads to the reduction of lateral root formation throughout the whole root system (Babe et al. 2012; Xiong et al. 2006; Deak and Malamy 2005).

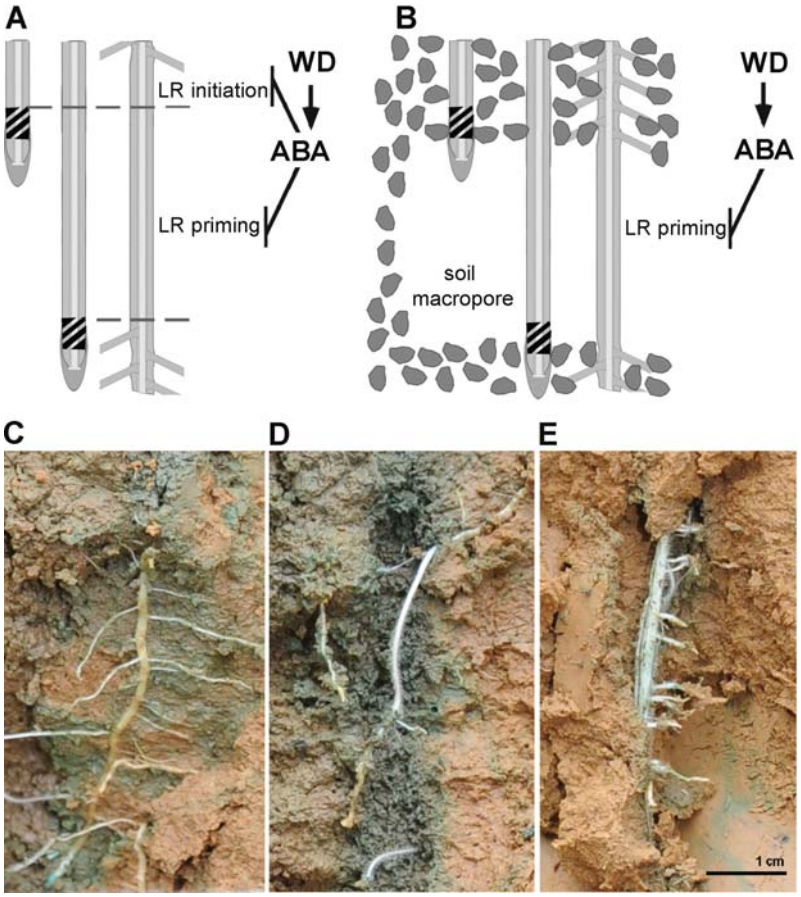

Figure 4-9: Different ABA response pathways operates downstream of water deficit in LR repression.

(A) In aeroponics conditions, a whole root is exposed to transient water deficiency (Babe et al. 2012) or ABA (this work) for several hours. According to the model, the IAA-dependent pathway causes LR repression at the initiation stage (for site that were primed before the treatment) and indices repression at the priming stage (in the segment that is formed during the treatment). As a result, offsets are observed between the repressed zone boundaries and tip positions at the onset and the end of the treatment. **(B)** In soil conditions, when a root enters a macropore, LR repression occurs only in the part of the root that is exposed to the macropore environment. LR repression occurs at the priming stage immediately after the developmental window of LR priming enters the macropore. **(C – E)** Distribution of maize LR on roots growing **(C)** in soil, **(D)** within a macropore and **(E)** at the side of a macropore. Photographs were taken in a trench profile made after a dye aspersion above the canopy. The areas infiltrated by dye and stained with a dark blue colour represent the fastest and accessible way to bring water in the deep soil and likely point out the soil macropores that are connected with the surface. Photographs provided by Dr Laure Beff.

The IAA-dependent pathway that we described here could be the mechanism triggering this gradual response, as was proposed earlier (De Smet et al. 2003). Interestingly, the simultaneous observation of the two pathways in the aeroponics and agar-based experiments appears as an artifact of the systems, in which the water deficit or ABA treatments are applied in an on/off mode and simultaneously to the whole root, which triggers both pathways.
This report may thus provide the first glimpse into the intrinsic mechanisms standing behind the immediate plant responses to local depletions of soil-water content such as occur when a root meristem enters a macropore. The conservation of this process across the monocot – dicot split suggests that this mechanism of root plasticity was an early adaptation to sessile plant life.

Aknowledgements

We would like to thank J. Friml and S. Vanneste for DR5rev:GFP, PIN1:PIN1-GFP, PIN2:GFP, PIN3:GFP, PIN7:GFP, PGP1:PGP1-GFP and PGP19:PGP19-GFP constructs, M. J. Bennett for AUX1:AUX1-YFP and DII:VENUS constructs.

Materials and methods

Cereal plant material and growth conditions

Seeds of barley (*Hordeum vulgare)* cv. Derkado and of maize (*Zea mays)* B83 inbred line were used in this study. Seed sterilization and growth conditions were as previously described (Babe et al. 2012a). The maize *DR5rev*:*mRFPer* and PIN1a:YFP were previously described (Gallavotti et al. 2008a). The DR5rev:mRFPer in barley was obtained by cloning the maize DR5rev:mRFPer with primers:
DR5_F: ggactagtccTCGACGGTATCGCAGCCCAG,
DR5_R: CCCCCCGGGGGGgcatgcctgcaggtcac,
using a Gateway system (Invitrogen) in the pBRACT202 vector for barley transformation. Transformation of barley cv. Golden Promise has been done at The James Hutton Institute, UK. Twenty-one independent transformation events were obtained, from which twelve lines showing 3:1 segregation on hygromycine in T2 generation were

analyzed for expression of DR5rev:mRFPer. Several T3 and T4 homozygous lines were selected and used for experiments.

In abscisic acid (ABA) experiments in aeroponic system, 4 dpg (barley) or 3 dpg (maize) seedlings were transferred to the aeroponics filled with 5 L of nutrient solution (pH = 5.8) and the root system of barley was reduced to a single seminal root, preferably the most vertical one. After one or two d, seedlings were sprayed for up to 8 h with a fresh nutrient solution with or without 50 µM ABA (stock: 50 mM ABA (Alfa Aesar) diluted in *dimethyl sulfoxide (*DMSO, Sigma-Aldrich). In auxin pretreatment assays, seedlings were exposed to auxin for 1 h before the start of 6 h of ABA treatment in nutrient solution (pH = 5.8) supplemented with increasing concentrations (0, 1, 10, 50, 75, 100 and 500 µM) of different auxins: α-Naphthalene acetic acid (NAA, Sigma-Aldrich), indole-3-acetic acid (IAA, Sigma-Aldrich) and 2,4-Dichlorophenoxyacetic acid (2.4D, Sigma-Aldrich) and washed briefly before 6 h of ABA treatment. Only results for 75 µM are shown.

Arabidopsis plant material and growth conditions

In all experiments with *Arabidopsis*, seeds were sterilized with chlorine gas and stratified at 4°C for 2 d in water. After cold treatment, seeds were sown over solid half-strength MS growth medium (per litre: 2.15 g MS salts, 0.1 g *myo*-inositol, 0.5 g MES, 10 g sucrose, 8 g plant tissue culture agar; pH = 5.7 with KOH), later called "growth medium" and grown vertically under continuous light (110 μE m^{-2} s^{-1} photosynthetically active radiation, supplied by cool-white fluorescent tungsten tubes, Osram) for 4 - 5 d. Seedlings were analyzed in details with BX53 microscope (Olympus) equipped with DS-Fi1 (Nicon) camera and scans of the plates were taken with V700 (Epson) unless stated otherwise. Figures were arranged in Photoshop CS3 without modifications.

For confocal experiments, 4 dpg seedlings were transferred to fresh growth medium with DMSO or with 30 µM ABA for 6 h up to 1 d. Prior imaging, seedlings were shortly incubated in darkness in 10 µg/ml propidium iodide (stock: 10 mg/ml in water). Photographs were acquired with LSM5 (Axiovert, Zeiss). All *Arabidopsis thaliana* GFP reporter lines used in this study were previously described and are in Col-0 background : DR5rev:3xVENUS-N7 (Heisler et al. 2005), DII-VENUS (Brunoud et al. 2012), PIN1:PIN1-GFP (Benkova et al. 2003),

PIN2:PIN2-GFP (Xu and Scheres 2005), PIN3:PIN3-GFP (Zadnikova et al. 2010), PIN7:PIN7-GFP (Blilou et al. 2005), AUX1:AUX1-YFP (Swarup et al. 2004), PGP1:PGP1-GFP/pgp1 and PGP19:PGP19-GFP/pgp19 (Mravec et al. 2008). For DII-Venus imaging, 4-5 dpg seedlings were immobilized in confocal chambers by a block of solidified growth medium with or without 30 µM ABA prior imaging for 30 min.

For transient ABA treatments in *Arabidopsis*, 5 dpg seedlings were transferred on square Petri plates with or without increasing concentrations of ABA and the exact positions of root tips were marked. After 2 d, plates were scanned and seedlings were transferred on new plates without ABA in the same order. After 7 d, positions of emerged LRs were marked under binocular (S6D, Leica) and plates were scanned again. Each data point represents a mean from at least 10 seedlings. Images were analyzed with ImageJ software to estimate the lengths of RZs and the longitudinal position of individual LR flanking RZ preceding statistical analysis.

Microscopy analysis in cereals

For HvDR5rev:RFP experiments in barley, apical root segments were fixed in 4 per cent para-formaldehyde in phosphate buffer for 1 h at 4°C, mounted with distilled water and photographed with a Leica epi-fluorescence binocular with a filter set for rhodamine. Images were taken with an AxioCam (Zeiss).

For ZmPIN1:PIN1-YFP, apical root segments were fixed as above and then embedded in 6 per cent agarose with 0.5 per cent gelatine and hand-made sections were mounted with distilled water and immediately observed and imaged with LSM 710 (Zeiss).

Expression studies in barley

The sampling strategy was designed in order to monitor LR formation specific gene expression during the first asymetric cell division in barley. From previous work, we considered that this division occurs on average 12 mm proximal from the root tip, while the next divisions occur at 20 mm from the tip. Based on this, a sample length of 5 mm was chosen, as a compromise between maximising the amount of RNA per sample and minimising the probablity to capture cells undergoing the second round of divisions. As a « no-LR » control,

we relied on a described LR repression system (Babé et al. 2011). In this system, the first asymetric divisions are repressed within 2 hours of a water deficit treatment. The treatment can be applied as long as 8 hours. In the conditions of these experiments, barley roots grow at ca. 1 $mm.hr^{-1}$. During an 8 hour-long treatment, a 8-mm long root segment is formed where LR formation has been repressed. The sampling strategy was designed to monitor gene expression at -4, -2, 0, 2 and 4 hours relative to the first asymetric division, in conditions that enable (A) or repress (B) LR formation. 5-mm long segments were sampled such that the first sampling (-4h position) targets a region distal to the first asymetric divisions, and the last sampling (+4h position) targets a region proximal to the first asymetric division.

The following indicates the likely number of formative divisions in each sample, assuming a LR density of 1 $LR.mm^{-1}$. At the -4h position, the samples in A and B conditions do not contain any first asymetric divisions. At the -2h position, A samples are likely to contain one LR initiation engaged in asymetric divisions, against zero in the B samples where these sites have been repressed. At the -0h position, A samples are likely to contain two-three LR initiation engaged in asymetric divisions, against zero in the B samples where these sites have been repressed. At the +2h position, A samples are likely to contain four LR initiation engaged in asymetric divisions, against zero in the B samples where these sites have been repressed. At the +4h position, A samples are likely to contain five LR initiation engaged in asymetric divisions, against zero in the B samples where these sites have been repressed.

Preliminary tests indicated that a 6-cm long fragment would give the required amount of RNA for one chip hybridization. We therefore collected 12 independent biological samples for each chip. The whole procedure was repeated three times, amounting to a total of 36 independent biological samples (three chips) per condition and time point.

RNA was isolated from frozen root segments according to the SV Total RNA Isolation Systems (Promega). After DNAse treatment (Promega), RNA samples were quantified by using Nanodrop spectrophotometer (Nanodrop Technologies) and then confirmed by RNA electrophorese. 5.3 µg of total RNA was used for cDNA

synthesis, labelling and fragmantation acocrding to One Cycle Target Labelling kit (Affymetrix), as for manufacture protocol. The samples were hybridized to the arrays for 16 h at 45°C, washed on GeneChip Fluids Station (Affymetrix) and imaged on GeneChip Scanner (Afftmetrix). The resulting data were processed for a quality assurance in MAS 5.0 (Affymetrix). The expression values have been normalized using the robust multi-array average method (Irizarry et al. 2003). Differential analysis was performed using linear models and empirical Bayes methods within affy and limma R packages (www.r-project.org, Gautier et al. 2004; Smyth 2004; Smyth et al. 2005). Raw p-values were adjusted using the Benjamini-Hochberg method to control the FDR (Benjamini and Hochberg 1995). Affymetrix probesets annotation was retrieved from Affymetrix website (Affymetrix_Barley1.na34.annot, http://www.affymetrix.com/) and genes that are controls of the microarray were discarded. Two-factor ANOVA p-values were computed using the MultiExperiment Viewer (http://www.tm4.org/mev/). Raw and processed microarray data have been deposited in the Gene Expression Omnibus (http://www.ncbi.nlm.nih.gov/geo/) under the accession number (in preparation). Genes have been selected if they could satisfy the following criteria: significant regulation upon drought treatment in at least one of three pairwise comparisons (Drought T2 VS T0, Drought T4 VS Drought T2, Drought T6 VS Drought T4) an dependant on the treatment, the time and the interaction in comparison to control time points without drought treatment (FC≥1.5, FDR corrected pvalue ≤0.01, two factor Anova pValue ≤0.01). The homologous equivalence between probesets contigs and *Arabidopsis* AGI gene models was realized using the genelist suite on PLEXdb (http://www.plexdb.org/modules/glSuite/) with default parameters. Gene ontologies were retrieved from the *Arabidopsis* homologues using the "ATH_GO_GOSLIM" repository available at TAIR (www.arabidopsis.org). A Fisher test was realized to estimate the statistical significance of the enrichment analysis.

Arabidopsis datasets compendium analysis

Datasets corresponding to the experiments published by (i) Vanneste et al. (2005), (ii) De Smet et al. (2008) and (iii) De Rybel et al. (2012), were retrieved from the following respective Gene Expression Omnibus (http://www.ncbi.nlm.nih.gov/geo/) accessions GEO (i)

GDS1515, (ii) GSE6349 and (iii) GSE42896 and and were independently analyzed using the same procedure as previously described for the barley microarray. The dataset corresponding to the IBA treatment is a kind gift of the Root Development Laboratory (Tom Beeckman, Root Development, VIB Gent, Belgium), and the data corresponding to the oscillation datasets were extracted from Moreno-Risueno et al. (2010).

Genes were considered to be significantly regulated in each independent experiment if they could satisfy the following respective conditions: (i) absolute fold change FC ≥1,5, adjusted p-value ≤0.01, between 0 and 6 hours upon lateral root inducible system in the control plants, and a TWO-WAY ANOVA p-value ≤0.01 for the interaction of the treatment and the genotype (*slr*), (ii) absolute FC ≥2, adjusted p-value ≤0.01 between 0 and 6 hours upon lateral root inducible system in the sorted pericycle cells, (iii) absolute FC ≥2, adjusted p-value ≤0.01 between 0 and 2 hours upon treatment with both compound (NAA and naxillin) during the time course upon lateral root induction system, (iv) absolute fold change FC ≥1,5, adjusted p-value ≤0.01, between 0 and 6 hours upon IBA treatment in the control plants, and a TWO-WAY ANOVA p-value ≤0.01 for the interaction of the treatment and the genotype (*ibr1 ibr3 ibr10*), (v) expression in phase or anti-phase with DR5 oscillations. A Fisher test was realized to estimate the statistical significance of the enrichment analysis.

Validation of barley microarray experiment in *Arabidopsis*

For overexpression studies, 5 dpg seedlings were transferred on fresh square Petri plates containing 50 ml of growth medium with DMSO or with increasing concentrations of ABA for 7 d. Root lengths and LR number were estimated with ImageJ software (Suplementary Materials, Figure S-1). In short-term overexpression studies, seeds were sown over round plates with 25 ml of solid growth medium with DMSO or with increasing concentrations of ABA for 3 d. The full length of *bZIP* (At1g58110), coding sequence was obtained from root cDNA of *Arabidopsis* with the following primers :
bZIP_F:ccgCTCGAGTCCAACTGGCAAGGGTGACA, bZIP_R:cgcGGATCCAG TGGGTAGAGAGACATTTA
and was introduced to pEN50PMA4 (Zhao et al. 1999) with

XhoI/BamHI restriction sites. Constructs were transformed in Col-0 using floral dip (Clough and Bent 2008).

RT-PCR analysis

For semi-quantitative RT-PCR analysis of PIN1a, PIN1b and PIN1c, maize RNA was isolated from five 1 cm-long root apical zones in two biological replicates using a Plant RNeasy Kit (Qiagen, Germany) according to the manufacturer's instructions. cDNA was prepared using the Invitrogen synthesis kit SuperScript II, with Phusion High-Fidelity DNA Polymerase (Fisher Scientific) from 1 μg of total RNA. RT-PCR was performed by using primers previously described in (Forestan et al. 2012; Gallavotti et al. 2008a) and are listed in (Suplementary Materials, Table S-5) Ubiquitin transcript accumulation was used as an internal control in each RT-PCR reaction. The PCR amplification cycle was: 98°C for 30 s (one cycle); 98°C for 5 s, 58°C for 15 s, 72°C for 30 s (35 cycles); and 72°C for 5 min (one cycle). The entire amplified sample was loaded onto an agarose gel and visualised.

SDS-PAGE and Western blot analysis

1cm-long apical root segments from 10 roots per sample from PIN1:PIN1-YFP maize line were frozen in liquid nitrogen and then homogenized with glass beads in 800 μl of extraction buffer (250 mM sorbitol, 60 mM Tris-HCl, 2 mm EDTA, pH = 8 with HCl, 20 mm dithiothreitol, 0.6% polyvinylpolypyrrolidone (Polyclar AT; Serva), 10 mM PMSF, and a cocktail of peptidase inhibitors from Sigma [1 μg mL^{-1} each of leupeptin, pepstatin, aprotinin, antipain, and chymostatin]). The homogenate was centrifuged two times and the supernatant was transferred into a new tube each time (9700 rpm, 5 min, 4°C; 9700 rpm, 10 min, 4°C). The supernatant was centrifuged again (54000 rpm, 15 min, 4°C) and the pellet was suspended in 30 μl of suspension buffer (3 mM KCl, 5 mM KH_2PO_4, pH = 7.8, 10 mM PMSF and a cocktail of peptidase inhibitors from Sigma as above) and sonicated in ice-bath (2 x 30 s with 30 s pause). Microsomal fraction was quantified with a standard Bradfort method. Then, microsomal fraction (20 μg) was solubilized in Laemmli buffer (2% SDS, 0.125 mM Tris-HCl, pH = 6.8, 10% glycerol, 0.002% bromphenol blue, and 60 mM dithiothreitol) for 30 min at 37°C and subjected to electrophoresis on 8% SDS-polyacrylamide gel. Bottom line of a gel was cut off, stained with Coomassie Brilliant Blue G250 and used as

a loading control. Western blotting was performed according to standard procedures using rabbit anti-YFP antibodies (1:2000 for 1h) and peroxidase-coupled anti-rabbit IgG antibodies (1:10000 for 1h) in two biological replicates.

Quantification of IAA metabolites

3 dpg maize seedlings were transferred to aeroponic box containing nutrient solution. After one d, half of the seeds were subjected to ABA treatment, where 50 μM ABA was added to nutrient solution for varying lengths of time. Small fragments of roots, 0.5 cm each up to 2 cm from the root tip from at least three roots per sample were harvested and immediately frozen in liquid nitrogen. IAA metabolites were quantified from 20 mg of frozen tissue at the Umea Plant Science Centre, Sweden, using LC-MRM-MS (liquid chromatography/multiple reaction monitoring/mass spectrometry), as described in (Novak et al. 2012). Three biological replicates were performed per sample type.

Quantification of ABA content

Barley seedlings were grown in aeroponics as described above up to 12 d, when half of the seeds were subjected to a transient WD treatment. The treatment was applied by interrupting the nutrient supply for 4 and 8 h, respectively, during the night phase. Each sample type represents five complete root systems. ABA content was quantified at Lancaster Environment Centre. The peak corresponding to ABA was quantified by ELISA with an anti-ABA antibody using immunolocalisation, as described in (Dodd and Davies 2006).

Kinematic analysis

Root growth rates were estimated as described previously (Babe et al. 2012a).

In vivo imaging

For DR5rev:3xVENUS-N7 imaging experiments, 4-5 dpg seedlings were transferred directly on growth medium with DMSO or 30 μM ABA and imaged according to a protocol developed by Xuan et al. (Manuscript in Preparation). Photographs were taken every 2 min up

to 24 h for DR5rev:3xVENUS-N7 line. The picture series were saved as TIFF format for further analysis.

In Luciferase experiments, before the transfer of plant material, the plates with DMSO or 30 μM ABA were sprayed with 400 μl of 1 mM luciferine (Duchefa Biochemie) using a pump spray and left in darkness to dry. The Luciferase images were taken by a Lumazone machine carrying a charge-coupled device (CCD) camera (Princeton Instruments, Trenton, NJ, USA). The CCD camera that is controlled by a WinView/32 software took movies of the DR5:Luciferase expression automatically every 10 minutes (exposure time, 10 minutes) for up to 24 hours. The picture series were saved as TIFF format for further analysis. The picture series were saved as TIFF format for further analysis.

Statistical analyses

All data analyses were performed with R software package, v. 2.15 or SAS/STAT software, v. 9.2. Bars are means ± CI, with different letters indicating significant differences according to Tukey's HSD test after ANOVA.

GUS expression analysis

For GUS expression analyses, 5 dpg seedlings were transferred on square Petri plates containing 50 ml of growth medium with DMSO or 10 μM ABA for 1 d. pbZIP:GUS construct was created by cloning the promoter fragment (3503 bp) in front of the *GUSVENUS* (*GV*) coding sequence in pAUX3131 (Navarre et al. 2011) using *Not*I site with primers:
F:ataagaatGCGGCCGCAGAATAGAGAGCTAAAAGAG,
R: atagtttaGCGGCCGCTGTCACCCTTGCCTGACAAA.
Then, the fusion construct was excised using *I-Sce*I and inserted into the pMODUL plant expression vector. Construct was transformed in Col-0 using floral dip (Clough and Bent 2008).

Seedlings were put overnight in 90% acetone, then transferred to a GUS-solution [1 mM X-Glc, 0.5% (w/v) dimethylformamide (DMF), 0.5% (w/v) Triton X-100, 1 mM EDTA (pH = 8), 0.5mM potassium ferricyanide ($K_3Fe(CN)_6$), 0.5% potassium ferrocyanide ($K_4Fe(CN)_6$), 500mM phosphate buffer (pH = 7)] and incubated for 4 h at 37 °C for GUS staining, and finally washed in 500mM phosphate buffer (pH = 7). For microscopic analysis, samples were cleared in chloral

hydrate solution as described in (Berleth and Jurgens 1993). Samples were analyzed by differential interference contrast microscopy with Primo Vert equiped with moticam 2300 (Zeiss).

Repression zone formation in cereals on agar plates and banding assay

In ABA experiments on agar square plates, 3 dpg barley seedlings were transferred from filter paper (Waterman) to the square Petri plates with 50 ml of nutrient solution (pH = 5.8) supplemented with 1.5% of agarose alone or with ABA to the final concentration of 50 μM (RZ experiment) or with increasing concentrations of ABA (bending assay) with 10 seedlings per each plate. The same amount of DMSO was added to the control solution. Positions of root tips were marked. In RZ formation assay, seedlings were grown vertically for 6h, scanned and then transferred to the aeroponics with nutrient solution. After 7 d in aeroponics, seedlings were scanned again and images were processed with ImageJ software. In bending assay, after 1 h of growing in vertical orientation, positions of root tips were marked seedlings were gravistimulated by 90° rotation. After 18 h, plates were scanned and root angles were measured with ImageJ software. Mean values were determined from two biological replicates.

RNA extraction, cDNA synthesis, and qRT-PCR analysis

Barley RNA was isolated from seedlings at 7 d after germination using a Plant RNeasy Kit (Qiagen, Germany) according to the manufacturer's instructions. cDNA was subsequently prepared from a minimum of 250 ng RNA (determined by UV spectrophotometry) using a SuperScript II reverse transcriptase kit and Oligo(dT)12–18 primers (Invitrogen, USA), according to the manufacturer's instructions. Quantitative real-time PCR (qRT-PCR) was performed in a 384-well white dish format using a LightCycler 480 (Roche Applied Science, USA) with 40 PCR amplification cycles using SYBR Green I fluorescent dye (Invitrogen, USA) and primers: bZIP_F:GATGAACTTGGGGCAGAGAG, bZIP_R:TGTTTAGCACGGTTGGTG TC,
EF_F:ATGGTTGTGGAGACCTTTGC, EF_R: CATGTCACGGACAGCAAAAC.

Expression was determined from a minimum of three biological replicates, each with three technical repeats, and normalized against *EF1α*.

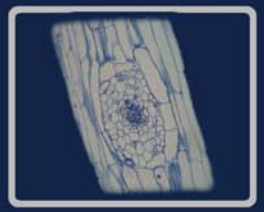

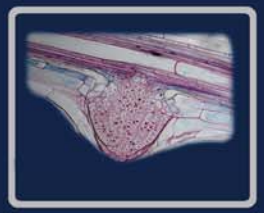

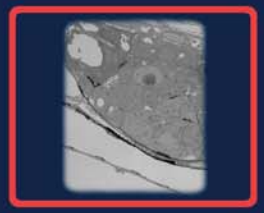

Chapter 5

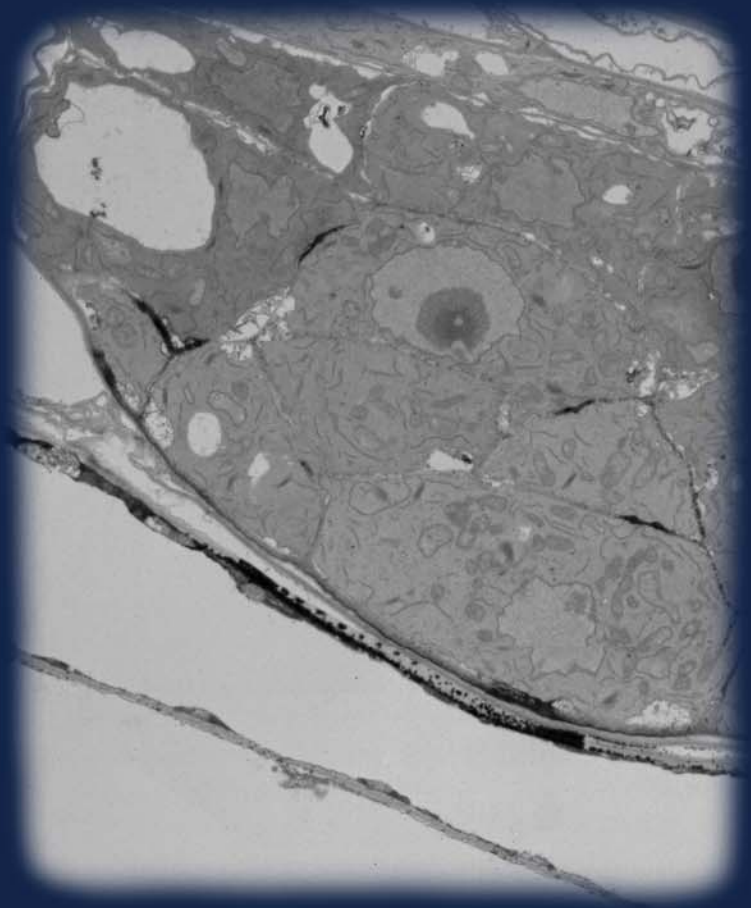

CHAPTER 5

Interplay of auxin and ROS during LR formation

Manuscript in preparation

Beata Orman-Ligeza[1,2,3] Riet De Rycke[4], Boris Parizot[2,3], Malcolm J. Bennett[5], Tom Beeckman[2,3], and Xavier Draye[1]

[1]Université catholique de Louvain, Earth and Life Institute, Louvain-la-Neuve, Belgium;
[2]Department of Plant Biotechnology and Bioinformatics, Ghent University, B-9052, Ghent, Belgium; [3]Department of Plant Systems Biology, VIB, B-9052, Ghent, Belgium;
[4]TEM-Core Facility, Inflammation Research Center, VIB, Ghent, Belgium; Department of Biomedical Molecular Biology, Ghent University, Ghent, Belgium
[5]Centre for Plant Integrative Biology, School of Biosciences, University of Nottingham, Sutton Bonington, LE12 5RD, UK.

Author Contributions

X.D., T.B., M.B. and B.O.-L. designed the research; B.O.L. performed the research and wrote the manuscript; B.P. analyzed the microarray data; R.D.R. performed the TEM observations.

Abstract

Lateral root (LR) development emerges as a tightly regulated process in which plant hormones make the core of a sophisticated signalling network. Reactive oxygen species (ROS) have been proposed to function as second messengers in auxin signalling during LR formation, however their role is still poorly understood. Here, we report the localization of ROS during LR development in *Arabidopsis* and maize. We show that a fine layer of H_2O_2 is deposited to the middle lamellae as the LR primordium (LRP) emerges through the parental tissue and progressively covers the entire LRP. In parallel, H_2O_2 is observed in the middle lamellae of cortex cells adjacent to LRP and in peripheral cells inside of LRP. We next provide chemical and genetic evidence that H_2O_2 contributes to the LR emergence through the parental tissue, presumably by modulating cell wall dynamics. Finally, a detailed analysis of the *Respiratory burst oxidase homologs* (*Rboh)* gene family of extracellular ROS donors, suggests that these operate upstream of peroxidases to ensure a fine-tuned extracellular redox balance during LR formation.

Keywords: Lateral root, auxin, ROS, hydrogen peroxide, superoxide, *Respiratory burst oxidase homologs*

Introduction

Plants growing in the field are exposed to environmental constraints that affect their potential growth rate, biomass production, yield and other agricultural traits. Precise and fast perception of and reaction to various stimuli are crucial for the physiological and morphological adaptation to these constraints. Virtually all biotic and abiotic stresses induce the burst of reactive oxygen species (ROS) or involve oxidative stress at some extent (Shapiguzov et al. 2012). The term ROS defines a set of more active derivatives of molecular oxygen (Figure 5-1A), such as superoxide (O_2) and hydroxyl radical (OH) as well as non-radical compounds including singlet oxygen ($^1O_2$) and hydrogen peroxide (H_2O_2) (Mhamdi et al. 2010; Mittler 2002; Bhattacharjee 2012). Several cellular components (e.g. peroxisomes, mitochondria and chloroplasts) produce ROS in plants and extracellular sources have been described, like cell wall- and plasma membrane-located enzymes comprising transmembrane flavoproteins, respiratory burst oxidase homologs (RBOH) and cell wall class III peroxidases. ROS are known to react with proteins, DNA and membrane lipids and affect several important processes. They reduce photosynthesis, increase electrolyte leakage and accelerate senescence, programmed cell death or necrosis (Bhattacharjee 2012; Pitzschke et al. 2006). Antioxidant systems have evolved in plants and in other aerobic organisms (Figure 5-1A). Enzymes, such as superoxide dismutase (SOD), catalase (CAT), peroxidase (POX), glutathione reductase (GR) and ascorbate peroxidase (APX) and non-enzymatic antioxidants such as ascorbic acid (AA) and glutathione (GSH) orchestrate the detoxification of ROS, presumably to counteract their effects on plant senescence. Interestingly, the cellular ability to maintain their redox equilibrium appears to be correlated with plant stress tolerance (Levine et al. 1994; Gill and Tuteja 2010; Lamb and Dixon 1997).

Aside from the sensing of changes in the surrounding environment, there is compelling evidence that ROS also function as signalling molecules in plant development. It has been clearly demonstrated that

they modulates gene expression (Dalton et al. 1999; Vandenabeele et al. 2003; Vanderauwera et al. 2005) and interfere with several hormonal signal transduction pathways (Mori et al. 2001; D'Haeze et al. 2003; Ishibashi et al. 2012; Joo et al. 2001), stomata closure (Zhang et al. 2001), xylem differentiation and lignification (Ros Barcelo 2005), root gravitropism (Joo et al. 2001), adventitious root formation (Wei-Biao 2012) and root-to-shoot coordination (Passaia et al. 2013).

Due to its relative stability, an increasing evidence points to the vital role of H_2O_2 among other ROS in the regulation of specific biological processes. H_2O_2 has a relatively long half-life (1 ms) under the physiological conditions in comparison with the other ROS. It can diffuse some distance (1 μm) from its site of production, cross membranes via diffusion or through aquaporins and modulate enzymes by oxidization (Bhattacharjee 2012; Bienert and Chaumont 2014). Alltogether, this supports the hypothesis that ROS play a signalling role in both stress response and developmental processes.
It has been proposed recently that ROS are involved in lateral root (LR) formation ((Li and Jia 2013; Correa-Aragunde et al. 2013; Manzano et al. 2014) and, more precisely, in auxin response during LR formation (Correa-Aragunde et al. 2013; Ma et al. 2014). In *Arabidopsis,* LRs are formed at a predictable distance from the root tip and have their origin inside the parental root from xylem pole pericycle cells that are activated to form a lateral meristem (Dubrovsky et al. 2006b; Himanen et al. 2002; Malamy and Benfey 1997; Jansen et al. 2013). During LR development, rapid cell wall remodelling processes occur within the emerging lateral root primordia (LRP) and in cortex cells overlying LRP (Swarup et al. 2008; Vilches-Barro and Maizel 2014; Benitez-Alfonso et al. 2013), including callose deposition, lignification and a decrease in flow through plasmodesmata (Benitez-Alfonso et al. 2013).

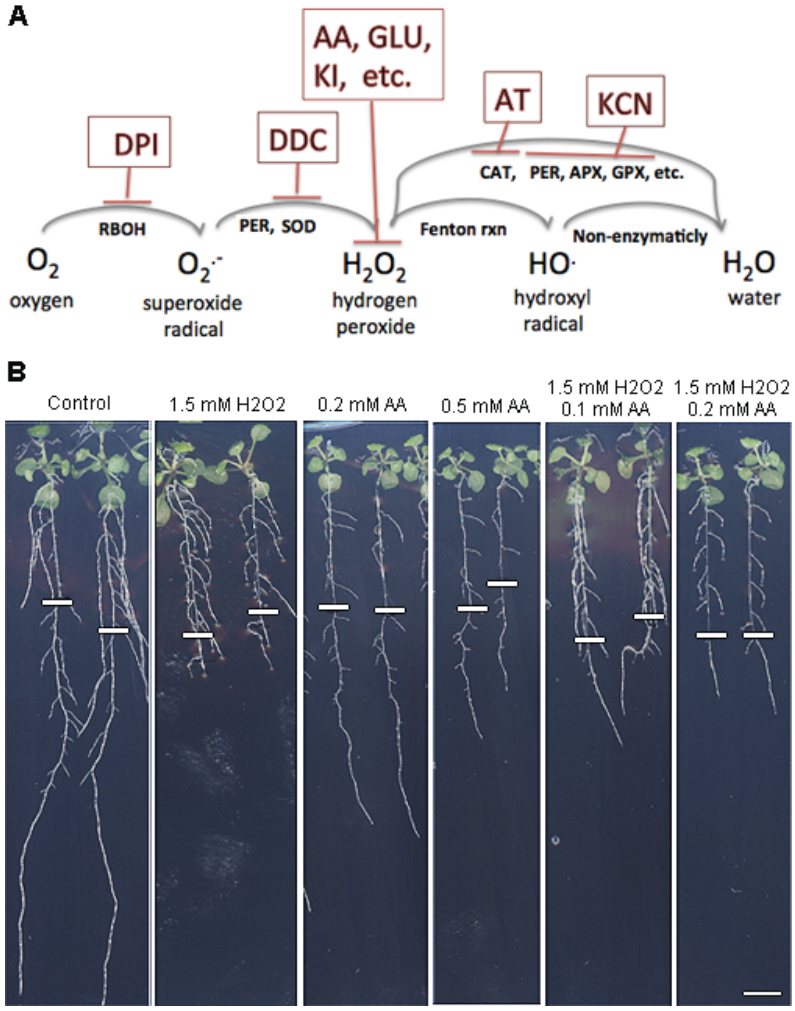

Figure 5-1: Dissecting ROS metabolism in plants.

(A) Schematic representation of ROS metabolism in plants. The respiratory burst oxidase homologs (Rboh) are transmembrane flavoproteins that oxidize cytoplasmic NADPH and translocate electrons across plasma membrane. Subsequently, the extracellular ambient (triplet)oxygen is reduced and gives rise to $O^{\bullet -2}$ in the cell wall. Then, as this short-lived ROS is unable to passively cross the lipid bilayer due to its charge, $O^{\bullet -2}$ remains in the apoplast, where it is rapidly converted into more stable ROS species, H_2O_2. This can be acheieved either spontaneously or in a reaction catalyzed by the superoxidedismutase (SOD) or peroxidase (PER). H_2O_2 is then metabolised spontaneusly or through enzymatic scavengers. Ascorbic acid (AA, H_2O_2 scavenger), ascorbate peroxidase (APX, H_2O_2 scavenger), 3-aminotriazole (AT, catalase inhibitor), catalase (CAT, H_2O_2 scavenger), diethyldithiocarbamate (DDC, SOD inhibitor), diphenylene iodonium (DPI, Rboh inhibitor), glutathione (GLU, H_2O_2 scavenger), glutathione peroxidase (GPX, H_2O_2 scavenger), peroxidase (PER, H_2O_2 scavenger or donor), potassium cyanide (KCN, peroxidase inhibitor),

potassium iodide (KI, H_2O_2 scavenger), respiratory burst oxidase homologs (Rboh, superoxide producer), superoxide dismutase (SOD, H_2O_2 producer). **(B)** Effect of H_2O_2 and AA on root system architecture of *Arabidopsis*. 5 dpg seedlings were transferred for 7 d on standard MS media supplemented with H_2O_2, and/or AA, as indicated. Representative images of seedlings from two biological replicates are shown. White lines indicate the position of root tip at the time of transfer. Bar = 0.5 cm.

Similar modifications have been previously attributed to O_2^- and H_2O_2 during other developmental processes. O_2^- has been shown to contribute to cell expansion (Foreman et al. 2003; Carol et al. 2005; Monshausen et al. 2007), while H_2O_2 appears to strengthen the cell wall by cross-linking lignification (Ros Barcelo 2005), also affecting the conductivity of plasmodesmata (Rutschow et al. 2011; Petrov and Van Breusegem 2012). Whether ROS are involved in the auxin signaling cascade leading to cell-wall remodelling during LR formation remains an ongoing debate.

The production of ROS in extracellular spaces depends on several classes of enzymes, including Rboh and class III peroxidases (Figure 5.1A). Interestingly, these enzymes seem to act on root branching through different pathways from auxin (Manzano et al. 2014). Our study analyses the connections between Rboh mediated ROS production and auxin signal transduction during LR formation. Using available microarray datasets, we validated a crosstalk between ROS and auxin at the transcriptional level. Subsequently, we localized ROS during LR formation and determined the effect of ROS on the LR formation in *Arabidopsis* mutants defective in auxin transport and signalling. A special emphasis was given to RBOH enzymes and to the producers of extracellular ROS in plant cells.

Results and discussion

Crosstalk between auxin and ROS responses in root tissue

Exogenous auxin application (Himanen et al. 2002; Jansen et al. 2013) or endogenous auxin overproduction (Boerjan et al. 1995) are able to induce *de novo* LR formation and auxin is known to facilitate LR

emergence (Swarup et al. 2008). We first show that treatment with H_2O_2 increases emerged LR number in *Arabidopsis*, whereas seedlings exposed to ascorbic acid (AA), a membrane-permeable scavenger of H_2O_2, display impaired LR growth (Figure 5-1B). Furthermore, the H_2O_2-mediated increase in LR number is repressed when H_2O_2 and AA are applied together, which is in agreement with recent reports (Ma et al. 2014; Correa-Aragunde et al. 2013). Interestingly, auxin treatment increases H_2O_2 levels in root tissue, as visualised by a whole-mount diaminobenzidine (DAB) staining (Figure 5-2A). These preliminary observations indicate potential overlap of auxin and ROS signalling pathways during LR formation.

In order to validate a possible crosstalk between auxin and ROS at the transcriptional level, we explored available datasets from published microarray experiments (Affymetrix ATH1 arrays) that targets auxin-mediated LR formation (two datasets) or ROS responses (two datasets). The experiments on auxins employed a LR inducible system (LRIS, (Himanen et al. 2002; Jansen et al. 2013)) and allowed us to focus on genes potentially involved in fast transcriptional response to auxin and most likely involved in LR formation. In the LRIS system, seedlings are grown for 3 d on NPA and were then treated for a short time (2 hours) with NAA or naxillin to trigger synchronous LR formation in pericycle cells (De Rybel et al. 2012; Vanneste et al. 2005). In the experiments on ROS, 5 d-old seedlings were treated for one hour with 20 mM H_20_2 (Davletova et al. 2005) or 2 weeks-old seedlings were sprayed for 3 h with 20 mM H_20_2 (Ng et al. 2013). From our meta-analysis, we could select a list of 108 overlapping genes presenting an absolute Fold Change ≥2 and a p-value ≤0.05 out of 489 genes from the two auxin experiments and 414 genes from at least one of the two H_20_2 experiments (Figure 5-2B; Suplementary Materials, Table S-6). The phenotypic analyses of T-DNA insertion lines for some of these 108 genes, including genes involved in response to stress, transcription factors, kinases, cell wall remodelling enzymes and in oxidation-reduction, is currently in progress.
From those 108 genes, 87 % are simultaneously induced in auxin and H_2O_2 datasets while only 2% were repressed in both. A large number

of the auxin-induced genes relate to signal transduction and redox activity, suggesting that a fine-tuned control of redox balance may be needed in LR formation. Interestingly, we also found a number of genes related to auxin response and auxin-mediated LR formation like *PID-BINDING PROTEIN 1* (Benjamins et al. 2003), *ARGOS* (Hu et al. 2003), *JAZ1* (Grunewald et al. 2009), to cell wall plasticy, like *SKU5* (Sedbrook et al. 2002), *MUR4* (Roycewicz and Malamy 2014) or *ADC2* (Perez-Amador et al. 2002) and to plasma membrane transport, like *PHO1* (Hamburger et al. 2002), *NRT1.5* (Lin et al. 2008) or *ZIFL1* (Remy et al. 2013).
These results at the transcriptional level support the hypothesis of connections between auxin and ROS.

Localization of ROS during LR formation

Using DAB and blue formazan (NBT) staining, we investigated the spatial localization of ROS in *Arabidopsis* and maize (Figure 5-3) roots during LRP development.
In *Arabidopsis*, dark-purple precipitates of oxidized DAB indicate the presence of H_2O_2 inside LRP from early stages of development throughout LR emergence (Figure 5-3A). Occasionally, DAB precipitates were also observed in cortex and epidermis cells overlying LRP. NBT precipitates indicate that O_2^- accumulation overlaps with H_2O_2 localization within the LRP (Figure 5-3B).
These results suggested that H_2O_2 and O_2^- are both present inside LR during their early development.
Next, we investigated the distribution of ROS during LR formation in maize (Figure 5-3C through F). The larger root diameter of this monocot species allowed us to access the longitudinal and radial distribution of ROS without tissue-cleaning step. As for *Arabidopsis*, H_2O_2 and O_2^- in maize accumulated within the LRP at early stages of development. Remarkably, at later stages of LRP emergence through the multi-layer cortex of maize, H_2O_2 and O_2^- co-localized within the border cells of the emerging LRP and O_2^- seemed to be present in the outer cells of the primordium, whereas H_2O_2 was also found in the center of LRP, at the position where vasculature would typically form.
The distribution of ROS of *Arabidopsis* and maize were also studied

(Figure 5-4) and showed different distribution of H_2O_2 and O_2^- in the root tips.

These results suggest that ROS, on the one side, are not equally distributed within LR primordia during their emergence but that, on the other side, they display a common trend toward cells that are in contact with with parent root tissues.

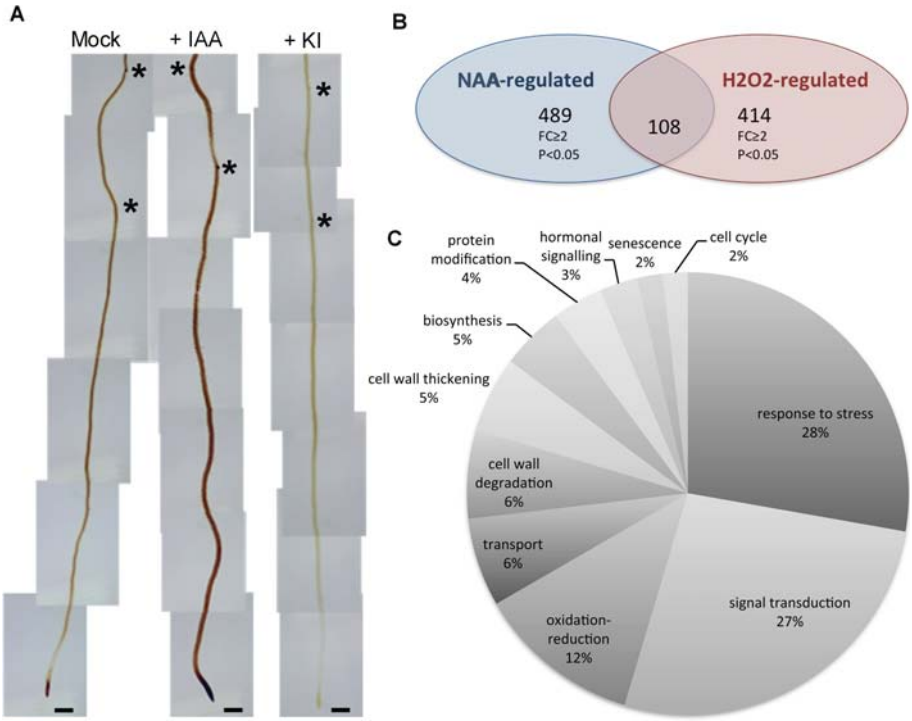

Figure 5-2: Crosstalk between auxin and ROS during root development in *Arabidopsis*.

(A) DAB staining that visualise H_2O_2 accumulation in *Arabidopsis* primary root after 1 h-long treatment with water (Mock), 10 µM of IAA, and 10 mM KI. The positions of emerging LRP are marked with black stars. Bar = 200 µm. **(B** and **C)** The meta-analysis of two LR, auxin-related (Vanneste et al., 2005; Rybel et al., 2012) and two ROS-related (Ng et al., 2013; Davletova et al., 2005) microarrays. **(B)** The overlap of 108 genes between auxin and ROS transcriptionally regulated genes was found and **(C)** those 108 genes were further classified according to their function.

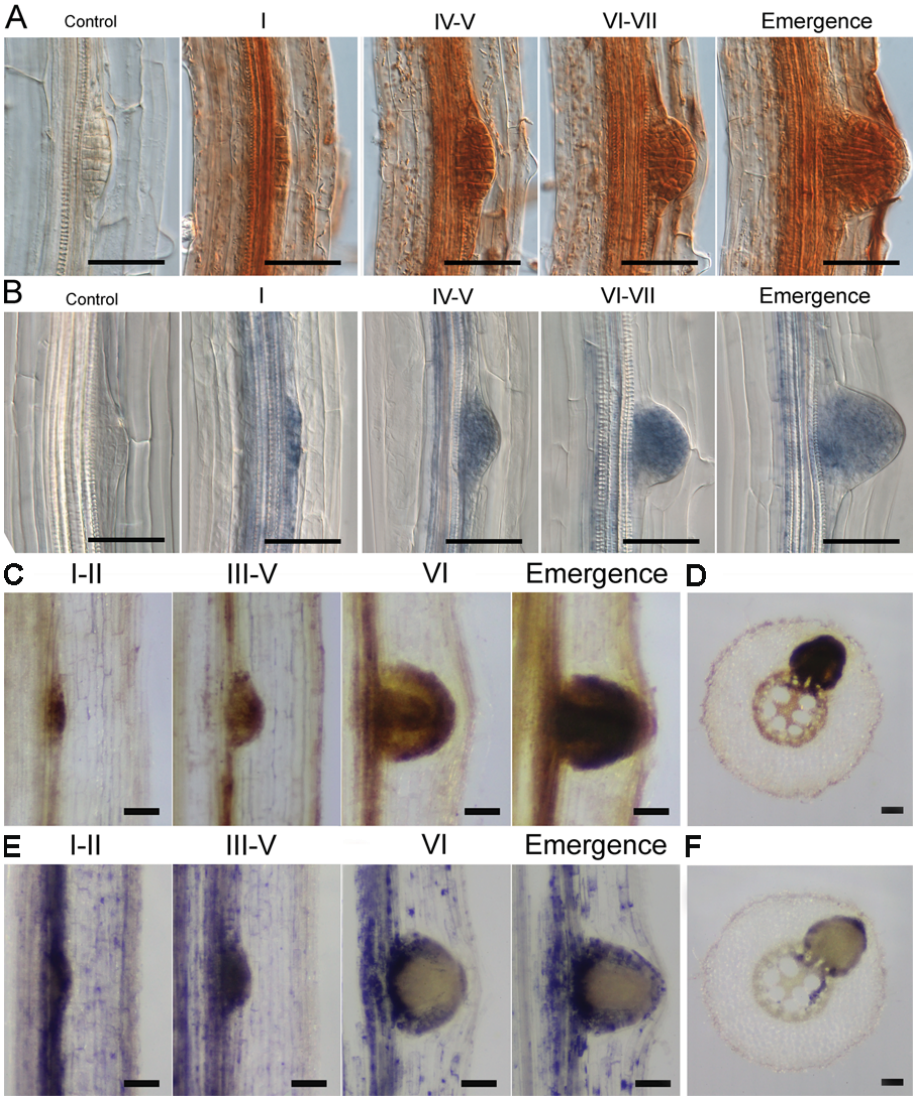

Figure 5-3: ROS localization during LRP formation in *Arabidopsis* and maize root tissue.

(A) DAB staining indicates the presence of H_2O_2 (dark-purple precipitates) in LRP of *Arabidopsis*. Photographs show LRPs from an initial stage of development to an organized primordium growing across the cortical tissues of the primary root (stage I to emergence) and a young LRP (control) pretreated for 1 h with H_2O_2 scavenger, 10 mM potassium iodide before DAB staining. Bars = 1 mm. **(B)** NBT staining (dark-blue precipitates) indicates the presence of O_2^- in LRP of *Arabidopsis* seedlings. Photographs show developmental stages of LRP formation stained with NBT (stage I to emergence) and a control root pretreated with for 1 h with $O_2^{\bullet-}$ scavenger, 10 mM propyl gallate before NBT staining (adapted from (Manzano et al.

2014), with modifications. **(C)** DAB staining indicating the presence of H_2O_2 in LRP of maize (dark-purple precipitates). Photographs show LRPs from an initial stage of development (stage I-II) to an organized primordium growing across the cortical tissues of the primary root (stage VI) and through epidermis (Emergence). **(D)** DAB staining on a radial section through developing LRP. **(E)** NBT staining indicating the presence of superoxide in LRP of maize seedlings (dark-blue precipitates). Photographs show developmental stages of LRP formation stained with NBT, from stage I to Emergence. **(F)** NBT staining on a radial section through developing LRP. Bars = 100 μm. Sections were made on vibratome.

Figure 5-4: ROS localisation in *Arabidopsis* and maize root tips.

(A-B) DAB staining that indicates the presence of H_2O_2 in root tips of **(A)** *Arabidopsis* and **(B)** maize (dark-purple precipitates). **(C-D)** NBT staining that indicates the presence of superoxide in root tips of *Arabidopsis* **(C)** and **(D)** maize seedlings (dark-blue precipitates). Bars = 50 μm (*Arabidopsis*) and 150 μm (maize).

We then employed transmission electron microscopy (TEM) to investigate the localization of H_2O_2, the most stable ROS species, at a sub-cellular level (Figure5-5). Cerium precipitates were located within the middle lamella, a pectin-based layer that cements the cell walls of adjacent cells together (Figure5-5D). H_2O_2 accumulation was observed in the middle lamella of cortex and endodermis cells in contact with LRP (Figure5-5A through Figure5-5C). In addition, cerium precipitates were found in the middle lamella between emerging LRP and parental tissues and this fine layer of H_2O_2 covering the entire LRP was present in all samples tested ($n > 10$ LRP) and clearly distinguished it from parental tissue.

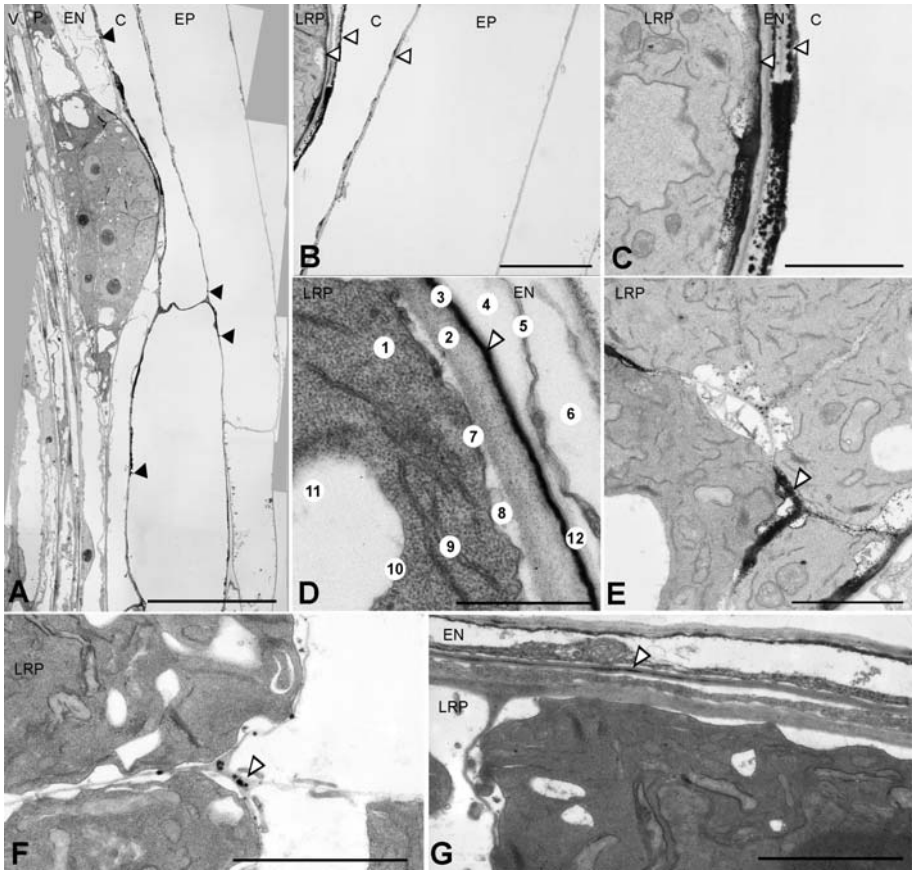

Figure 5-5: Representative transmission electron microscopic images of *Arabidopsis* LRP treated with cerium chloride to visualize localization of H_2O_2 by black cerium depositions.

(**A** through **E**): H_2O_2 localization during LR emergence. **(F** and **G)** H_2O_2 localization in LRP at stage II of development in **(F)** middle lammelae of outer cells inside of LRP and in **(G)** middle lamellae between outer cell of LRP and endodermis, as LRP is passing through endodermis. V indicates vasculature, LRP - Lateral root primordium, P - Pericycle, EN -Endodermis, C - Cortex, EP – Epidermis; Numbers in **(D)** points to 1 – Cytoplasm, 2 - Cell wall of outer LR cell, 3 - Middle lamella, 4 - Periplasmatic space, 5 - Remnants of endodermis protoplast, 6 – Vacuole, 7 - Plasma membrane, 8 - Periplasmatic space, 9 – Endoplasmic reticulum, 10 – Tonoplast, 11 – Vacuole and 12 - Cell wall of endodermis cell. Bars, 20 um **(A)**, 6 um **(B)** and 2 um **(C-G)**; Magnifications, 1200 **(A)**, 4000 **(B)**, 12000 **(C** through **G);** black arrowheads in **(A)** indicates the spatial end of a strong H_2O_2 signal in cortex cells overlying LRP; white-filled arrowheads **(B** through **G)** points to the cerium depositions.

Interestingly, this ROS-containing coat seems to develop progressively, as weaker and intermittent signals were observed at early stages of development (n = 5), before the LRP passes through endodermis (Figure5-5F and Figure5-5G), this is, stage II of LR formation. Inaddition, H_2O_2 accumulation was observed in the outer cells inside of LRP (Figure5-5A and Figure5-5E). We also inspected ROS localisation during LR development using confocal microscopy and 2'-7'-dichlorodihydrofluorescein diacetate (DCFH-DA) staining (Aranda et al. 2013). We could not get the stain penetrating the LR, however the staining revealed a strong ROS signal in cortex cells in touch with LR primordia (Figure 5-6).

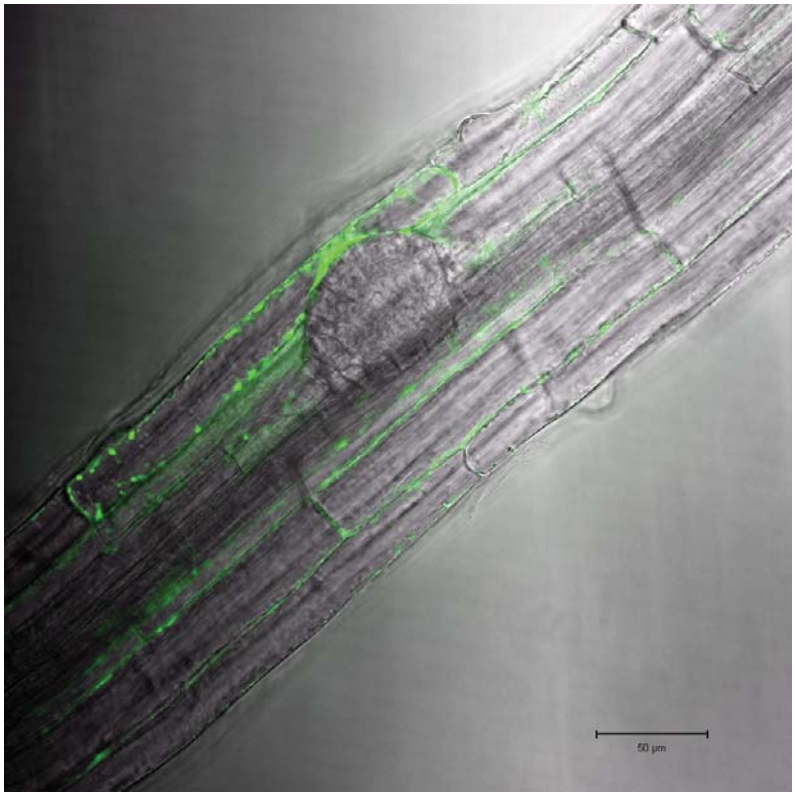

Figure 5-6: ROS localisation in *Arabidopsis* using a fluorescence probe.

5 dpg seedlings were stained for 15 min in 50µM DCFH-DA in 50 mM phosphate buffer in darkness, as indicated by the light-green colour. Seedlings were washed briefly in phosphate buffer alone before imaging upon confocal microscopy. Bar = 50 µm.

Taken together, these observations indicate that H_2O_2 is progressively deposited from early stages of LRP development in the middle lamellae between the outer cell layer of the LRP from the endodermis and cortex cells in contact with the LRP, ultimately covering the entire LRP. In parallel, H_2O_2 is also observed in the middle lamellae around endodermis and cortex cells adjacent to LRP and in outer cells inside of LRP.

ROS balance affects LR emergence

In order to investigate how extracellular ROS contribute to LR development, we used two experimental setups commonly used to study the kinetics of LR initiation and emergence.

In the first one, LR initiation was synchronized by gravistimulation (Peret et al. 2012b) and the stages of synchronized LRP were counted at 20 and 44 h after gravistimulation (hag). The experiment was upon treatments with H_2O_2, paraquat (O_2^- donor), KI (ROS scavenger), DDC (inhibitor of an intra- and extracellular enzyme involved in the conversion of O_2^- into H_2O_2) and DPI (inhibitor of the Rboh family of extracellular O_2^- producers) (Figure 5-7). The activity of peroxidases that produce and degrade H_2O_2 during LR formation was studied elsewhere (Manzano et al. 2014).

At 20 hag, control roots accumulated mainly LRP at stage I. Seedlings treated with ROS donors showed higher percentage of stage II and III in comparison to the control, while KI- and inhibitor-treated seedlings showed a decrease in stage I LRP. At 44 hag, control plants accumulated mainly stage V, VI and VII LRP. Seedlings treated with ROS donors were more advanced than control and showed stage VII LRP and emerged LR, while inhibitor-treated seedlings accumulated LRP between stages IV and VI (KI) and stage II (DPI). Interestingly, no remarkable differences were observed upon treatment with DDC.

We complemented this observation using the LRIS experimental setup (Himanen et al. 2002; Jansen et al. 2013), where LR formation is synchronised by germinating the seedlings for 3 d in the presence of NPA and then transferring them on media supplemented with 10 uM NAA. The treatments considered here were 1.5 mM H_2O_2, 0.01 mM KI or H_2O_2 + KI. Samples were collected at 6 h, 12 h, 18 h and 24 h

post-transfer (hpt). In control conditions and upon KI treatment, the first DR5 maxima appeared within 12 hpt, whereas in 86% of seedlings grown in the presence of H_2O_2, DR5 maxima were already observed within 6 hpt (Suplementary Materials, Figure S-4).

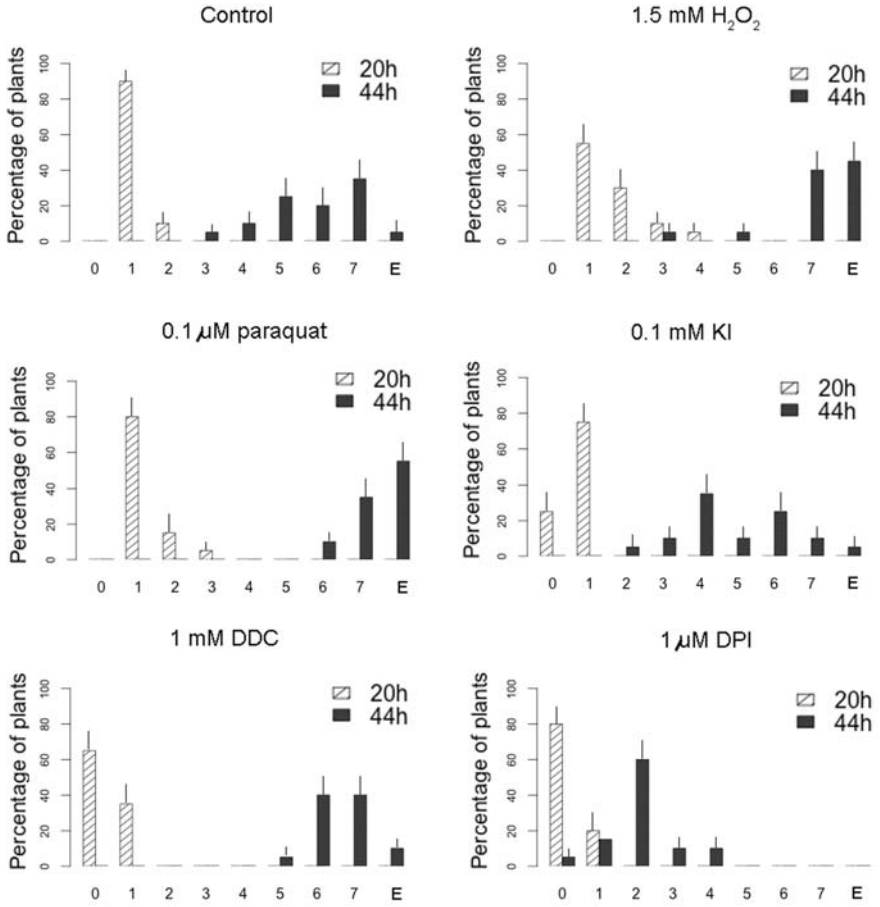

Figure 5-7: Effect of ROS and ROS scavengers on LR emergence phenotype.

5 dpg seedlings were transferred on standard MS media supplemented with various compounds, as indicated above each graph. After 1 h, seedlings were gravistimulated by 90 degrees to achieve synchronization of LR formation. Primordia were grouped according to developmental stages at 20 h (grey bars) and 44 h (black bars) after the onset of gravistimulation (n = 20). Data points represent averages ± SE.

We also analysed the CYCB1;1 promoter activity that marks early cell divisions in developing LRP. The promoter activity was observed in at

least 80% of the seedlings within 18 hpt in control conditions, 12 hpt upon H_2O_2 treatment and 24 hpt upon KI.
Altogether, these results support the hypothesis that a fine-tuned redox balance is maintained during LR formation and might be important to regulate the rate of cell divisions. Our results also suggest that DPI-sensitive (extracellular) and DDC-insensitive (intra-and extracellular) enzymes may be involved in this regulation.

H_2O_2 bypasses impaired auxin influx

To determine if H_2O_2 function in an auxin-dependent process, we exploited the fact that inhibitors of auxin influx (1-NOA), efflux (NPA, TIBA) and response (PCIB) afcects the auxin pathways involved in LR formation and lead to impaired LR development. We simultaneously exposed 5 dpg seedlings for 7 d to inhibitors of auxin metabolism with increasing concentrations of H_2O_2 (Figure 5-8). In control conditions, seedlings exposed to H_2O_2 showed an increase in LR number. They did not respond to H_2O_2 in the presence of KI. Interestingly, the inhibitory effects of inhibitors of auxin transport and response were bypassed by the H_2O_2 treatment. The LR density was fully restaured to the control level by 1-NOA and PCIB, though only partially by NPA and TIBA. These observations suggested that H_2O_2 may overcome the absence of auxin gradients and/or response during LR formation.

We next analysed the effects of H_2O_2 treatment on the LR phenotype of loss-of-function mutations in auxin influx carriers. Lateral root number, but not root gravitropism, was rescued in *aux1* and *aux1lax3* backgrounds upon 7 d-long treatments (Figure 5-9). This suggest that H_2O_2 treatment does not influence the basipetal auxin transport driven by *AUX1* that is required for gravitropism, but rather overcomes the absence of auxin gradient inside the LR founder cells and/or LRP that is required for early stages of LR formation. In agreement with this, the H_2O_2 treatment did not affect *AUX1* nor *LAX3* promoter activities (Figure 5-10). The H_2O_2 treatment also resulted in a large reduction of the primary root growth rates in wild-type and loss-of-function mutants, with a more pronounced response in auxin influx mutants

(Figure 5-9). We observed in wild-type seedlings an overall decrease in the size of root meristem and a drop in cell divisions, as visualised by *LAX3:GUS* and *CYCB1;1:GUS* promoter activities (Figure 5-10) which suggests that the root growth reduction by H_2O_2 is likely to result from a reduction in meristem activity.

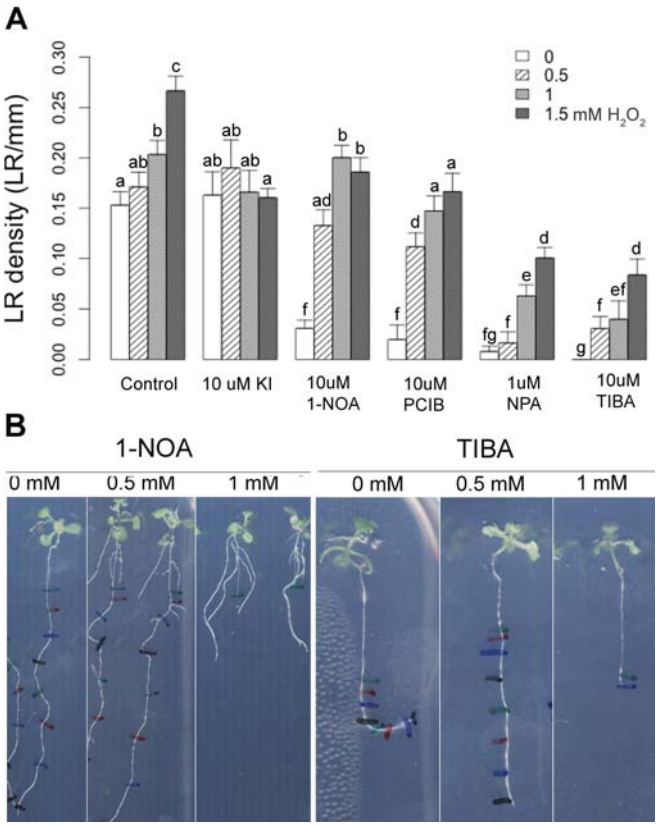

Figure 5-8: Effect of ROS on LR phenotype mediated by auxin inhibitors.

(A) 5 dgp Col-0 seedlings grown vertically were transferred into a fresh agar plates containing various concentrations of H_2O_2 and/or 10 µM KI, 10 µM 1-NOA, 1 µM NPA, 10 µM TIBA and 10 µM PCIB and were incubated vertically for additional 7 d. The total number of lateral roots (the sum of LRP and emerged LR) per mm of dissected transferred region was calculated for each seedling (n = 15) after tissue cleaning. Data points represent averages ± confidence interval. Means not sharing subscripts differ at $p < 0.05$ according to Tukey HSD comparison. **(B)** Representatives of root phenotypes observed when 5 dgp Col-0 seedlings were grown for 7 d on standard MS media supplemented with 10 µM 1-NOA or 20 µM TIBA and H_2O_2, as indicated.

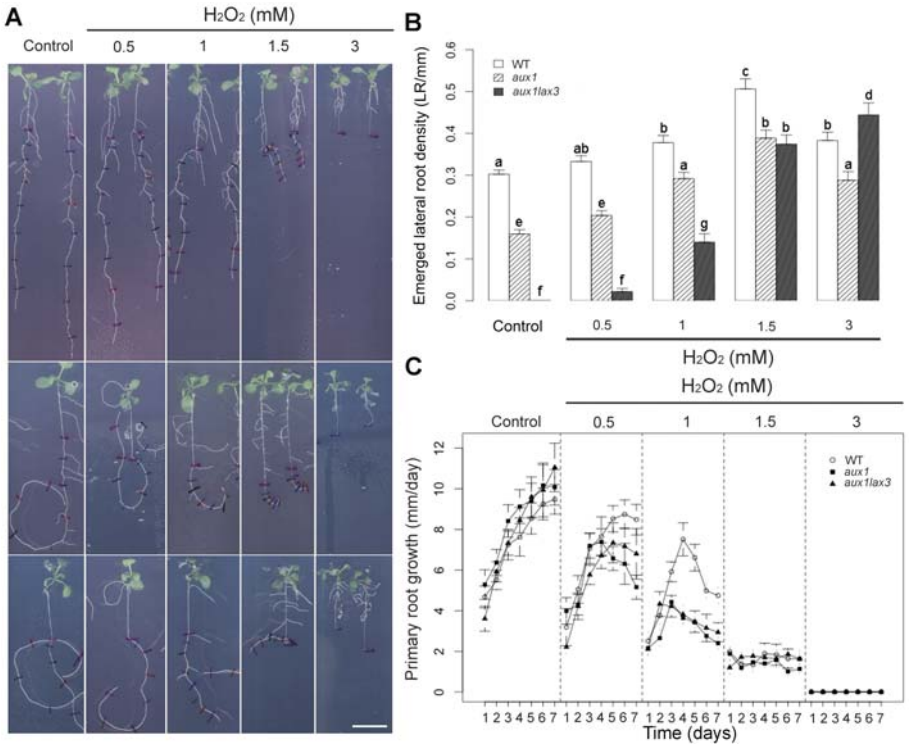

Figure 5-9: Effect of ROS on primary root growth and LR density of wild type (WT) *Arabidopsis* seedlings (Col-0) and auxin-influx mutans *aux1* and *aux1lax3*.

(A) Representatives of root phenotypes observed in three independent experiments. WT (top), *aux1* (middle), *aux1lax3* (bottom) seedlings. Bar = 1cm. **(B)** Lateral root (LR) density in WT, *aux1* and *aux1lax3* seedlings 12 dpg. Number of emerged LR in a transferred zone (n=30) was determined 7 d after the treatment of 5 d-old seedlings using binocular. **(C)** Primary root growth rates of WT, *aux1* and *aux1lax3* at 12dpg. Plants were germinated on MS agar plates for 5 d and then transferred into the fresh plates that were untreated (Control) or supplemented with various concentrations of H_2O_2 and grown for additional 7 d. The root tips of the seedlings were marked each day beginning from 1-d post-planting as shown on the photograph on the right. After 7 d, the distances between each mark were measured for each plant. The average root growth for each time period (n=15) is shown in the graph, with time point 2 indicating the average growth from d 1 to 2 and so on. Error bars = ±confidence interval. Data points represent averages ± confidence interval. Means not sharing subscripts differ at $p<.05$ according to Tukey HSD comparison.

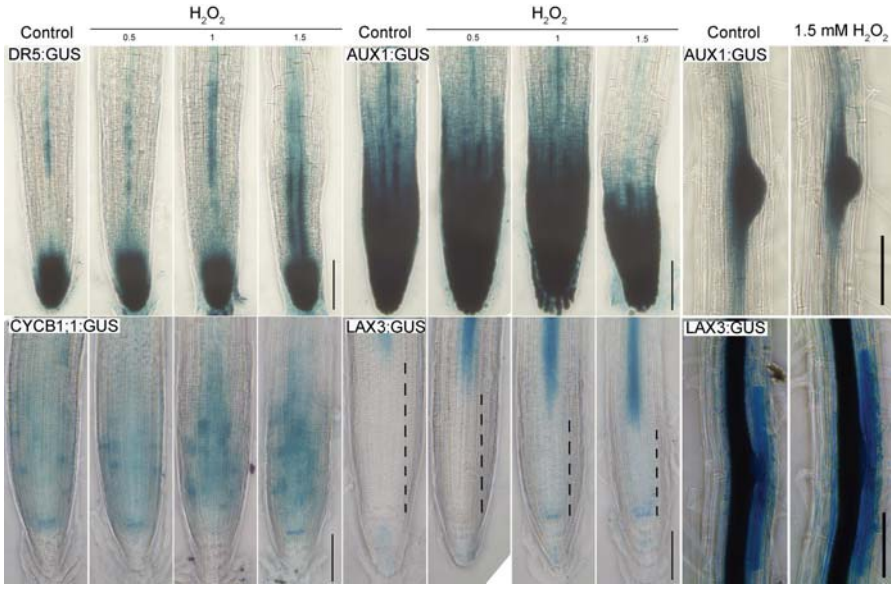

Figure 5-10: Effect of H_2O_2 treatment on promoter activities of DR5:GUS, AUX1:GUS, LAX3 and CYCB1;1.

5 dpg seedlings were transferred on standard media supplemented with growing concentrations of H_2O_2, as indicated. GUS staining was performed after 1 d of treatment. Dashed lines indicate shortening of the meristem. Bar = 100 µm.

To investigate the LR rescue by H_2O_2 in auxin influx mutants, we determined the LRP density in 5 dpg seedlings of *aux1, lax3* and *aux1lax3* exposed to various concentrations of H_2O_2 for 72 h. In the wild-type and the three mutants, the number of emerged LR at 72 hpt increased in a dose-dependent manner upon H_2O_2 treatment (Figure 5-11). In *aux1* and *lax3* backgrounds, H_2O_2 was able to bring the emerged LR number to the level of the wild-type. The number of non-ermerged LR increased in a dose-dependent manner upon H_2O_2 treatment in *aux1lax3* but did not respond to H_2O_2 in the wild type, *aux1* nor *lax3* mutants.

A refined analysis of the rescue by H_2O_2 was made in the *aux1lax3* background by determining the LRP stages in seedlings exposed to H_2O_2 for 24, 48 and 72 h (Suplementary Materials, Figure S-5). At 24 hpt, wild-type seedlings showed an increase in non-emerged LR number at stage I and II and an increase in emerged LRs. On the contrary, we found nearly no visible LRP in *aux1lax3*. At 48 hpt, the number of emerged LR progressively increase upon H_2O_2

treatment in wild-type, and emerged LRs were visible in *aux1lax3* mutant in addition to non-emerged LRP. At 72 hpt, the number of non-emerged and emerged LR in *aux1lax3* background was close to the number observed in the wild-type. We conclude that H_2O_2 can overcome defects in *aux1lax3* mutant background.

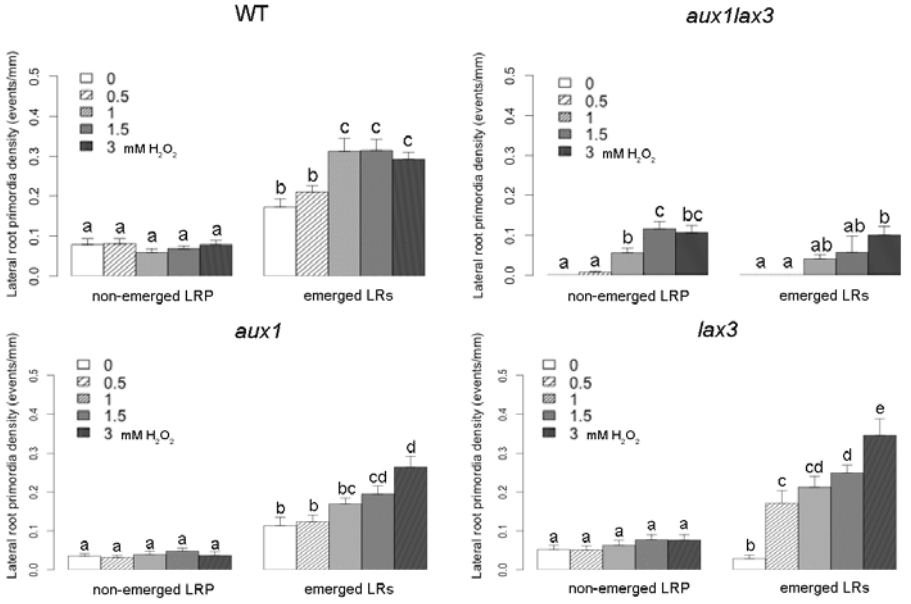

Figure 5-11: Effect of ROS on LRP density in auxin influx mutants.
Plants were germinated on standard MS media for 5 d and then transferred into the fresh plates that were untreated (Control) or supplemented with various concentrations of H_2O_2. LRP density per primary root length was determined 72 hpt by cleaning the tissue (n >15 per sample in two biological repetitions).

Finally, we analysed whether H_2O_2 may act downstream of polar auxin transport to promote LR development, by observing the effect of 7 d-long H_2O_2 treatments with 1.5 mM H_2O_2 on *gnom*^{R5}, which is involved in polar auxin transport (Geldner et al. 2004). The H_2O_2 treatment did not rescue the LR phenotype of the mutant (Figure 5-12), suggesting that the H_2O_2-mediated increase in LR number still depends on a proper directional efflux of auxin.

H_2O_2 contributes to cell wall remodelling downstream auxin signalling

During the early stages of LR formation, increased auxin levels perceived by TIR1/AFB receptors trigger the degradation of different AUX/IAA repressors of auxin response transcription factors (ARFs), which release the expression of auxin-responsive genes (De Smet 2011; Lavenus et al. 2013). Thus, mutants of genes that contribute to the early auxin-response modules that controls LR initiation often display LR-less phenotype (De Smet 2011; Lavenus et al. 2013), like *arf7arf19* (Okushima et al. 2007), *slr/iaa14* (Fukaki et al., 2002), *iaa28* (Rogg et al. 2001) and *shy2/iaa3* (Tian and Reed 1999). We therefore inspected the effect of H_2O_2 on the LR phenotype of loss-of-function mutant of *arf7arf19* and gain-of-function mutants of *iaa28* and *slr/iaa14*. Upon H_2O_2 treatment, no emerged or non-emerged LRP were observed in *iaa28, slr* and *arf7arf19* mutant backgrounds, which suggests that H_2O_2 doesn not act downstream of those auxin response modules (Figure 5-12). In agreement with the above observations, an increase in LR number was observed upon H_2O_2 in the auxin receptor mutants *abp1* (Sauer and Kleine-Vehn 2011) and *tir1* (Parry et al. 2009). We can therefore hypothesise that the response to H_2O_2 does not interfere with auxin perception.

Another auxin signalling module involving *shy2/iaa3* targets early auxin perception in the endodermis (Goh et al. 2012a; Vermeer et al. 2014; Hosmani et al. 2013). Auxin transported from the pericycle to the endodermis is thought to induce an early accommodation of the latter, which facilitates the expansion of the primed pericycle cells. Interestingly, the lignin-based Casparian strip network in the endodermis cannot be degraded by pectinases as in case of middle-lamella made of pectin, targeted by slr-ARF7-ARF19 module (Goh et al. 2012a; Vermeer et al. 2014; Hosmani et al. 2013). Treatment with H_2O_2 rescued the LR phenotype of a dominant mutation observed in *shy2* and of CASP:*shy2* backgrounds (Figure 5-12). This indicates that H_2O_2 is likely to contribute to the modulation of cell wall dynamics in

the endodermis and therefore, can bypass *shy2* gain-of-function mutation.

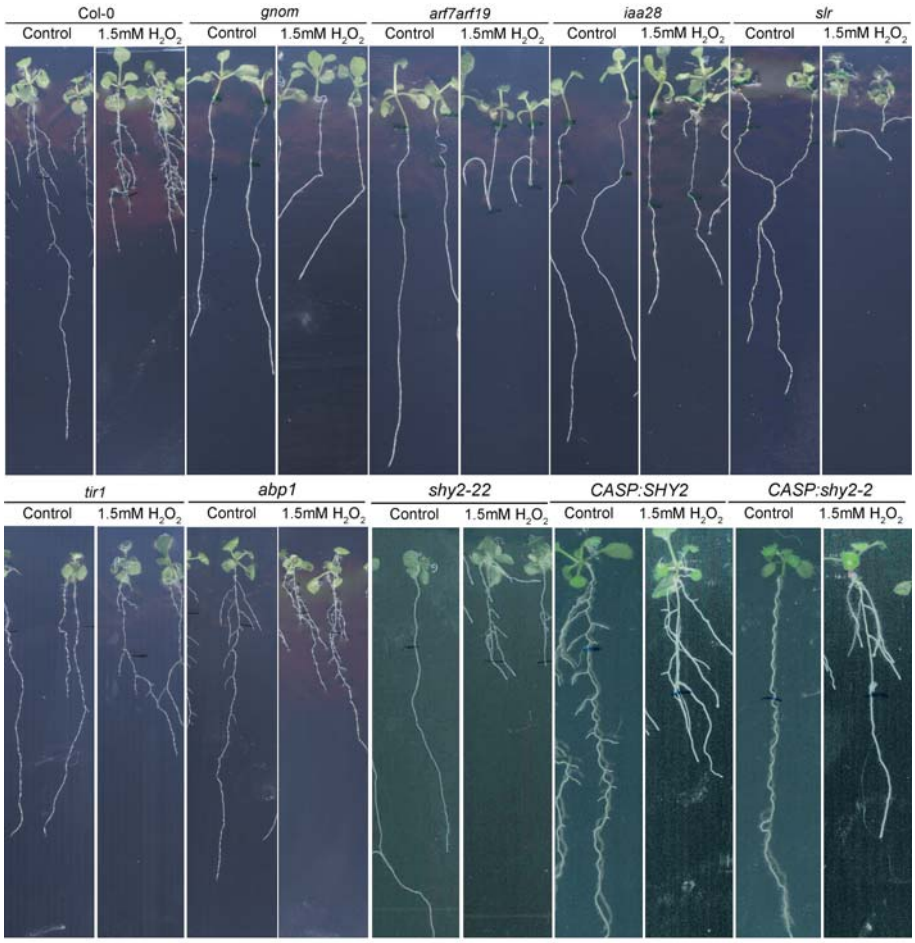

Figure 5-12: Effect of ROS on root phenotype of mutants involved in auxin response.

Plants were germinated on standard MS media for 5 d and then transferred into the fresh plates that were untreated (Control) or supplemented with 1.5 mM of H_2O_2 and photographed after 7 d. Representatives observed in at least two independent experiments are shown.

ROS decrease extracellular pH in parental root tissue

Changes in pH can affect the activity of numerous proteins and likely, cell wall stability (Monshausen et al. 2009). The acidification of a cell wall has been reported at the root hair initiation site, from the first

morphological indications of localized growth (Bibikova et al. 1998) and it has been suggested that the decrease in pH renders the apoplastic environment more in favour of cross-linking of specific components of the cell wall and counteracts cell wall-loosening enzymes (Staal et al. 2011). Using pHusion and apo-pHusion pH sensor lines (Gjetting et al. 2012), we investigated whether the reported effect of H_2O_2 on LR emergence interferes with intra- or extracellular pH. No differences were observed within one hour of treatment with 1 mM H_2O_2, however there was a remarkable acidification in the apoplast of a parental ground tissue after one day of treatment (Figure 5-13). Taken together, long exposure to H_2O_2 triggers acidification of the apoplast of a parental tissue that could potentially accelerate LR emergence, but further studies are needed to understand the underlying mechanism.

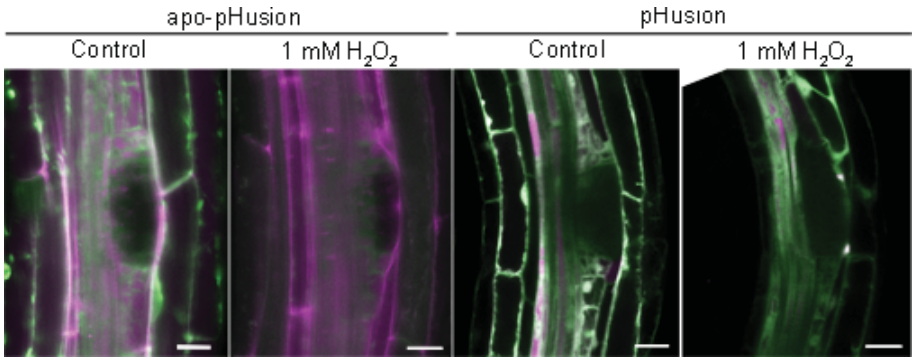

Figure 5-13: Effect of H_2O_2 on pH by using intracellular (pHusion) and extracellular (apo-pHusion) sensor lines.

5 dpg seedlings were transferred on standard MS media supplemented with 1 mM H_2O_2 for 16h. Green colour = alkaline environment, magenta = acidic environment (n>15). Bar = 50 µm.

Possible role of Rboh in LR formation

The *Arabidopsis* genome contains 10 *Rboh* genes, named from *RbohA* to *RbohJ* whose expression in various organs has been related to expansion, development and maturation (Muller et al. 2009; Foreman et al. 2003; Kwak et al. 2003; Torres et al. 2002; Lee et al. 2013; Boisson-Dernier et al. 2013). As LR development is affected by

change in ROS balance, we investigated the promoter activity of six *Rboh* genes in *Arabidopsis*. In junction (also called anchor) roots, *Rboh* genes were expressed at the root base (Figure 5-14, top panel).

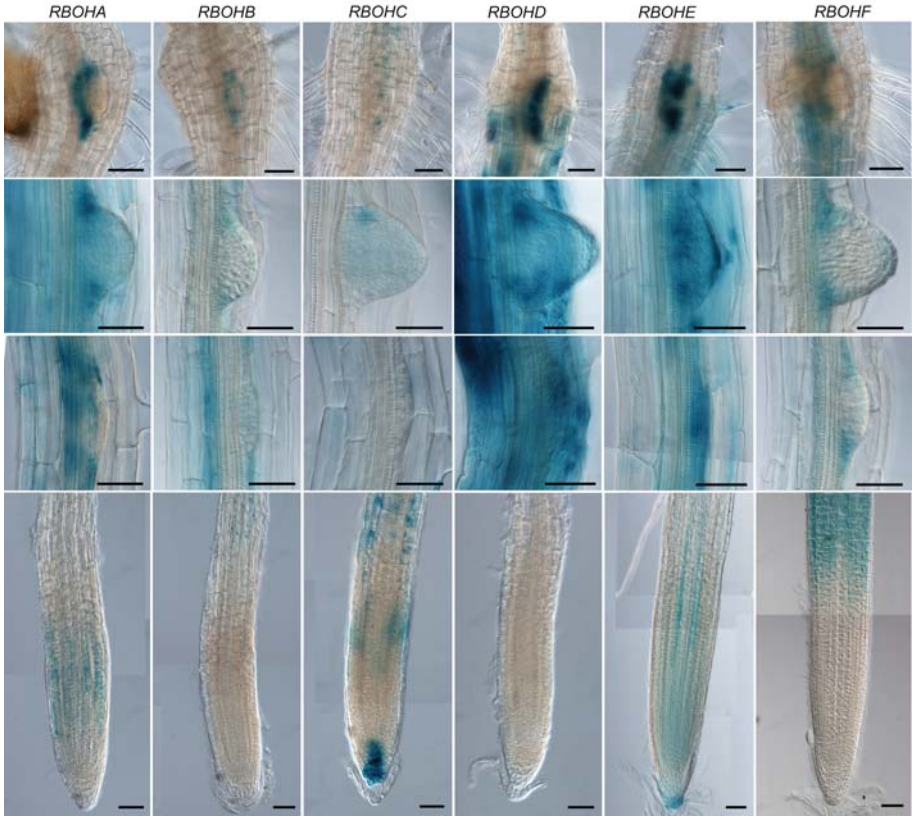

Figure 5-14: Promoter activity of *Rboh* genes in *Arabidopsis* root tissue.

7 dpg seedlings of each RBOH:nlsGFP:GUS line as indicated, were GUS-stained for 6h to overnight in order to visualise their promoter activity in the root tip (bottom panel), during LR formation (two middle panels) and during anchor root formation (upper panel). Bar = 50 µm.

In LRP, the expression of *Rboh* genes seems to be mainly restricted to the peripheral cells of the LRP. *RbohE* is also expressed in endodermis, cortex and epidermis cells that are in contact with or on the path of developing LRP (Figure 5-14 and Figure 5-15) and not depend on *AUX1* and *LAX3* function (Figure 5-15D). Interestingly, *RbohA, RbohC* and *RbohE* were also expressed in the basal meristem (Figure 5-14), where LR priming occurs (De Smet et al. 2007).

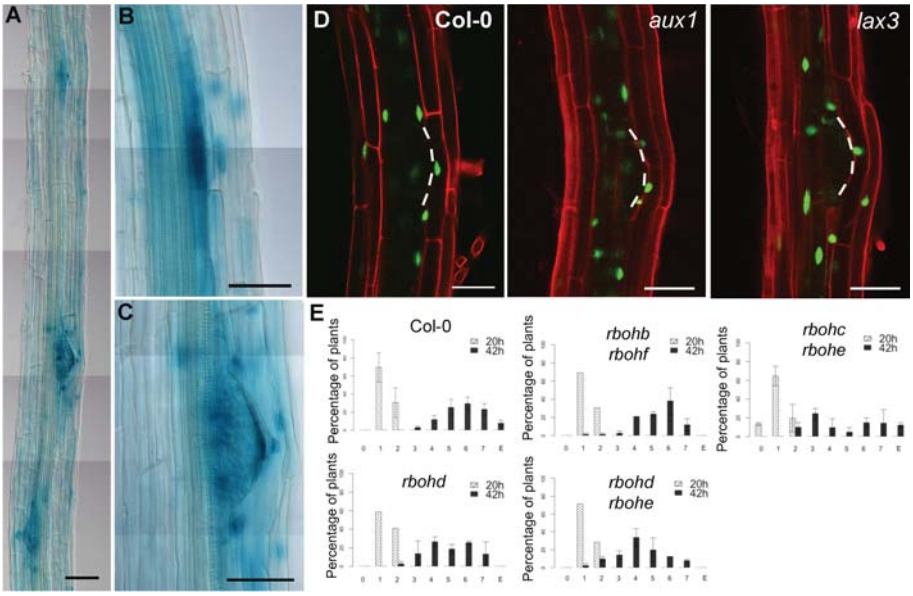

Figure 5-15: Characterisation of *RBOHE* in *Arabidopsis* root tissue.

(A through **C)** GUS-stained 7 dpg seedlings of RBOHE:nlsGFP:GUS in Col-0 line (8 h-long staining) in order to visualise in detail the promoter activity during LR formation upon optic microscopy. **(D)** Confocal images of RBOHE:nls:GFP:GUS in respectively, Col-0, *aux1* and *lax3* backgrounds. **(E)** LRE phenotype in WT and *rboh* single and double mutants, as indicated. 5 dpg seedlings were transferred on standard MS media supplemented with various compounds, as indicated above each graph. After 1 h, seedlings were gravistimulated by 90 degrees to achieve synchronization of LR formation. Primordia were grouped according to developmental stages at 20 h (grey bars) and 44 h (black bars) after the onset of gravistimulation (n > 15 in at least one biological replicate, analysis in progress). Bar = 50 μm.

Because there are several isoforms of the main subunit of the NADPH protein complex encoded by separate *Rboh* genes, it is difficult to assess the role of specific *Rboh* in LR formation. The preliminary analysis of LR emergence (LRE) phenotype of *Rboh* mutants revealed a moderate LRE phenotype in the *rbohe* background (Figure 5-15E). Furthermore, the initial analysis of 35S:RBOHD overexpression line was not conclusive, as seedlings showed many different developmental phenotypes (data not shown).

Taken together, we concluded that the promoter activities of *Rboh* family members inside the developing LRP and the *RbohE* expression in overlying endodermis, cortex and epidermis cells support the

hypothesis that *Rboh* are likely to contribute to LR development as an extracellular source of ROS for LR emergence, independently from *AUX1* and *LAX3*. Overlapping *Rboh* expression and ROS localisation in *Arabidopsis* and in maize further supports this notion (Figure 5-16).

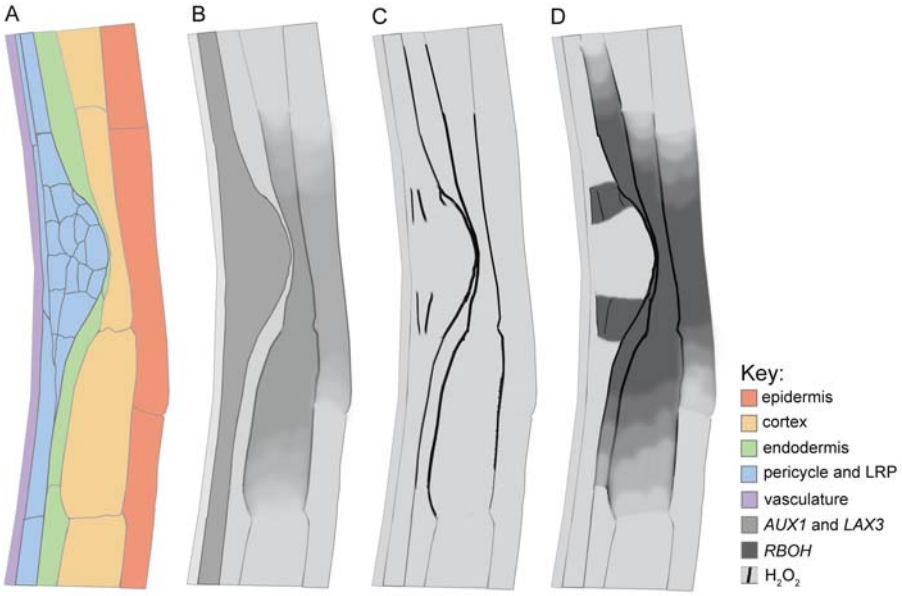

Figure 5-16: Auxin, ROS and *Rboh* during LR emergence.

(A) Schematic representation of root segment that contains emerging LR of *Arabidopsis*. **(B)** Promoter activity of *AUX1* and *LAX3* auxin influx carriers during LR emergence, based on (Swarup and Peret 2012; Swarup et al. 2008). *AUX1* is expressed inside LR primordia and in pericycle, whereas *LAX3* is expressed in cortex and epidermal cells in front of emerging LR primordia. The vascular localisation is omitted. **(C)** H_2O_2 localization during LR emergence. H_2O_2 accumulates in middle lamella of peripheral cells of LRP, generates a fine layer that sourrounds LRP and in endodermis and cortex cells sourrounding LRP. Epidermal localisation was not investigated in this study. **(D)** Expression of RBOH genes during LR emergence merged with H_2O_2 localization. The promoter of RBOH is active in peripheral cells of LRP and in cells surrounding the emerging LRP. The vascular promoter activity of *Rboh* is omitted. Expression of *Rboh* genes overlaps with H_2O_2 localization and promoter activities of auxin influx carriers during LR emergence.

Conclusions and perspectives

In the meta-analysis analysis, we have identified genes that are upregulated by auxin and ROS, indicating potential overlap of auxin and ROS signalling pathways during LR formation. Further experiments revealed that endogenous ROS are not equally distributed within LRP, but are deposited between an emerging LRP and the root parental tissues. Subsequent investigations revealed that H_2O_2 is progressively deposited from early stages of LRP development into the middle lamellae of the outer cell layer of the LRP, in the middle lamellae of endodermis and cortex cells adjacent to LRP and in outer cells inside of LRP. To address the possible crosstalk between auxin response and H_2O_2, we next exposed to 5 d-long H_2O_2 treatment the auxin-related mutants that display severe alterations in LR formation. We show that H_2O_2 can overcome defects in *aux1lax3, shy2* and *CASP:shy2-2* backgrounds. Together with a chemical analysis, those results indicate that deposition of ROS into extracellular spaces is likely to contribute to the modulation of cell wall dynamics downstream of auxin in the endodermis and in cortex cells and therefore, can bypass *aux1, lax3* loss-of-function and *shy2* gain-of-function mutations. One of the possible ways of doing so is by triggering the cleavage of pectin in the middle lamella of the cells overlaying the LR primordia. Interestingly, an increase in the pectin methylesterase (PME) activity and pectin demethylesterification known to contribute to cell wall separation has been recently reported upon H_2O_2 treatment (Xiong et al. 2015). PMEs are known to remove the methyl groups on pectin, making it susceptible to cleavage by polygalacturonases and/or pectate lyases. Thus, it is possible that H_2O_2 facilitates LR emergence through increase of PMEs activity and pectin demethylesterification in the middle lamella of the parental tissue in front of the emerging LR primordia.

We next investigated the promoter activities of the members of extracellular producers of ROS, the *Rboh* gene family, that showed the overlapping expression patterns during LR formation. Among

them, *RhohE* was found to be a good candidate to contribute to extracellular ROS balance during LR emergence.

Recently, a LR capacity assay was developed (Van Norman et al. 2014) that indicates the number of prebranch sites that are competent to produce a LR. In this assay, the root tip excision promotes the developmental progression and emergence of LR from nearly all LRP and prebranch sites. This analysis will be performed in *aux1lax3, shy2* and CASP:*shy2* backgrounds and compared with LR density upon H_2O_2 treatment.

The auxin-mediated regulation of aquaporins has been recently shown to contribute to LR emergence process (Peret et al. 2012a). Thus, it is possible that H_2O_2, known to cross plasma membrane through aquaporins (Bienert and Chaumont 2014), may act downstream of auxin or contribute to this regulation. Analysis of PIP2;1-overexpressing lines would shade a light on this hypothesis.

Tissue-targeted transactivation of *RBOH* driven by UAS promoter is currently underway. The use of several GAL4 lines (Suplementary Materials, Figure S-6) is motivated by the fact, that 35S:RBOHD line showed many different developmental phenotypes which makes it difficult to discern primary from secondary defects. The selection of *rbohd rbohe rbohf* triple mutant is also in progress.

Aknowledgements

We would like to thank Nico Geldner for Rboh:nls:GFP:GUS lines.

Materials and methods

Microarray retrieving and normalization

The following microarray hybridization files were retrieved from the Gene Expression Omnibus database: GEO series GSE3350 (GSM75508, GSM75509, GSM75512, GSM75513) for Vanneste et al. (Vanneste et al., 2005), series GSE42896 (GSM1053030, GSM1053031, GSM1053032, GSM1053036, GSM1053037,

GSM1053038) for De Rybel et al., 2012 (Rybel et al., 2012), series GSE41136 (GSM1009032, GSM1009033, GSM1009034, GSM1009029, GSM1009030, GSM1009031) for Ng et al. (Ng et al., 2013) and series GSE5530 (GSM128757, GSM128758, GSM128759, GSM128760, GSM128761, GSM128762) for Davletova et al., 2005 (Davletova et al., 2005). Each datasets have been normalized independently with the robust multi-array average method and the differential analysis performed using the moderated t-test using the vignettes affy (Gautier et al., 2004) and limma (Smyth, 2004; Smyth, 2005) within the R (www.r-project.org) bioconductor statistical package (www.bioconductor.org). Affymetrix probesets to AGI ID assignment was done using the affy_ATH1_array_elements-2010-12-20.txt file downloaded from TAIR (www.arabidopsis.org). A gene was considered as being differentially expressed if it fulfilled the following conditions: fold change ≥2 and p-value ≤0.01 in the two pairwise comparisons for the datasets related with NAA treatment, and at least in one of the two pairwise comparisons for the datasets related with H_20_2 treatment. 109 probesets satisfy this criteria, among which two are redundant, yielding a final list of 108 genes (see Suplementary Materials, Table S-6)

Plant material and growth conditions

Grains of maize (*Zea mays)* B83 inbred line were used in this study. Seed sterilization and growth conditions were as previously described in Chapter 4.

Seeds of *Arabidopsis* Col-0 were sterilized and grown as described in chapter 4. The scans of the plates were taken with V700 (Epson) or 3200 dpi (Medion). Figures were arranged in Photoshop CS3 and the brightness was increased equally, without further modifications.

LRE phenotype analysis

5 dpg *Arabidopsis* Col-O or mutant seedlings were transferred from standard MS media into fresh standard MS media (Control) or on standard MS media supplemented with various compounds, as indicated. After 1 h, seedlings were gravistimulated by 90 degrees to achieve synchronization of LR formation. After 20 h and 44 h seedlings were pre-fixed in 0.4 % formaldehyde in 50 mM phosphate buffer pH = 7 at 4 degrees upon a gentle vaccum for 30 min. Subsequently, 2.5 grams of chloral hydrate was dissolved per 1 ml of 30% glycerol and seedlings were left overnight in a cleaning solution. Primordia were observed Seedlings were analyzed in details with

BX53 microscope (Olympus) equipped with DS-Fi1 (Nicon) camera and grouped according to developmental stages at 20 h and 44 h after the onset of gravistimulation.

DAB and NBT staining

Arabidopsis DAB staining that indicates the presence of H_2O_2 in LRP of *Arabidopsis*. Control seedlings were pretreated for 1 h with 10 mM potassium iodide before DAB staining or for 1 h with 10 mM propyl gallate before NBT staining. Seedlings were DAB stained for 6 h (in 1 mg ml^{-1} DAB, Tween 20 (0.05% v/v) and 10 mM Na_2HPO_4, pH > 6.8) according to (Daudi and O'Brien 2012) and NBT stained for 1 h (in 0.1% nitroblue tetrazolium in 10 mM potassium phosphate buffer, pH = 7.8) according to (Kawai-Yamada et al. 2004). Seedlings were cleaned in chloral hydrate solution overnight or boiled for 5 min in bleaching solution (Ethanol:acetic acid:glycerol = 3:1:1) at ~90-95 °C. Maize root segments were embedded in 6 per cent agarose with 0.5 per cent gelatine and sections of 100 μm were cut with a vibratome. Sections were immediately transferred for 1h to NBT staining solution (NBT) or for 2 up to 3 h to DAB staining soluton (in DAB). Upon signal development, sections were mounted with distilled water and immediately imaged with an AxioCam (Zeiss).

Transmission electron microscopy

Cerium-hydroxide precipitates indicate H_2O_2 localization. 5 dpg seedlings were gravistimulated by 90 degrees to achieve synchronization of LR formation. After 22 h and 44 h, 2 mm fragments that were expected to contain early and late LRP were dissected under binocular (n > 50) and incubated for 1 h in 5 mM cerium chloride solution in 50 mM MOPS buffer at pH 7.2. Tissue embedding and electron probe x-rays were performed as described (D'Haeze et al. 2003).

GUS staining

Arabidopsis seedlings were GUS-stained as described in Chapter 4.

Statistical analyses

All data analyses were performed with R software package, v. 2.15. Bars are means ± CI, with different letters indicating significant differences according to Tukey's HSD test after ANOVA.

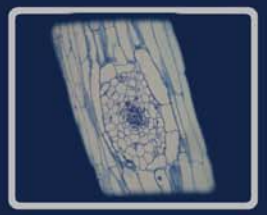

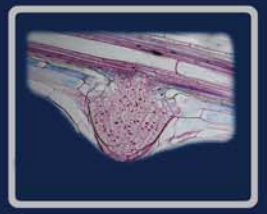

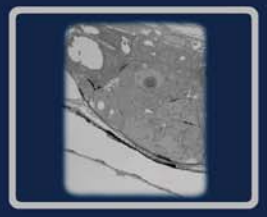

Chapter 9

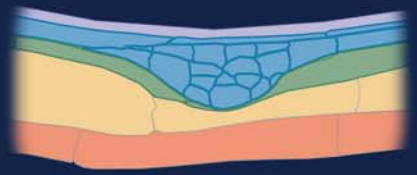

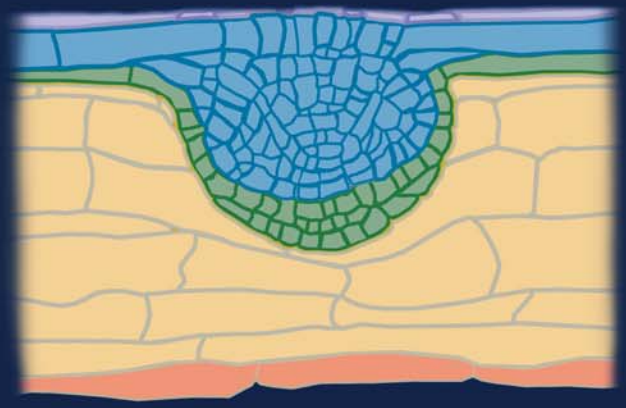

CHAPTER 6

General conclusions and perspectives

“Nothing in life is to be feared, it is only to be understood. Now is the time to understand more, so that we may fear less.”

Maria Skłodowska-Curie

Post-embryonic root formation in cereals is a composite process governed by the orchestrated action of intrinsic and external signals, that should be considered altogether (Figure 6-1). First, we focused on auxin response pathways during LR formation and we have shown that auxin-dependent components of LR formation are conserved between dicots and monocots (**Chapter 2**) and AUX1 and LAX3 function as auxin influx carriers in cereals **(Chapter 3)**. Secondly, we investigated how root branching is repressed upon transient WD episode and we reveal that ABA mediates this response **(Chapter 4)**. Finally, we addressed the crosstalk between auxin and ROS during root branching and we show that ROS conntribute to LR emergence **(Chapter 5)**. Studying not only hormonal response pathways, but also plant responses to external stimuli, allows merging these two separates worlds into one dynamic root system architecture.

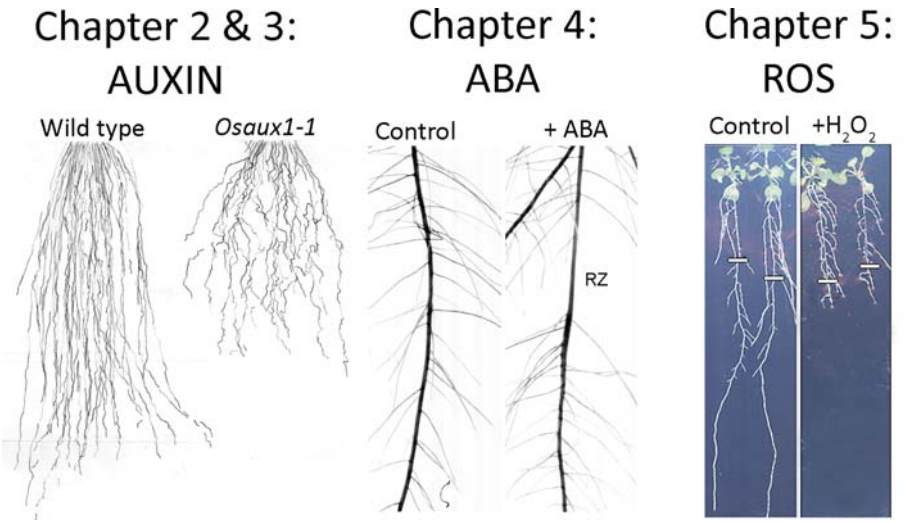

Figure 6-1: Intrinsic and external signals that shape root architecture investigated in this work.

This study was set out to investigate mechanisms that shape monocot root systems. We particularly focused on four aspects: **(1)** the conservation in monocots and dicots of the components of auxin-dependent pathway of LR formation, **(2)** the function of auxin influx

carriers in cereals, **(3)** the role of ABA in LR repression upon transient water deficit, and **(4)** the contribution of ROS to LR formation.

(1) Translational research as a tool to unlock the cereal genomes

The molecular bases of *Arabidopsis* root formation have been largery uncovered through genetic and chemical approaches in the past few decades by the use of Petri plates. Although not every gene regulatory pathway can be directly translated from *Arabidopsis* into cereals, some level of conservation is expected to be maintained. Currently, the majority of genes involved in lateral and crown root development in cereals have been discovered through time-consuming and expensive forward genetic screenings, which employed sophisticated phenotyping platforms. The translational approach offers the possibility to expicitly target genes of interest in cereals by using gene networks discovered in *Arabidopsis* and should help to orient and to accelerate cereal root research. This has been noticebly true for the *in silico* identification of genes in barley, that contribute to auxin-dependent pathway of LR formation in *Arabidopsis*, namely *TIR1, AFR7/ARF19, GNOM, AUX1* and *LAX3* (**Chapter 2**). A series of *in silico* analyses led us to the conclusion that the auxin-regulated pathway of LR formation is present in monocots, as the latter genes are conserved in barley and rice, in agreement with recent reports (**Chapter 1**). Conceptually, such translational strategy combining similarity, phylogeny and synteny analysis could be also employed to target genes in other plant species for which only partial sequence data are available, such as bread wheat (*Triticum aerstivum*). Furthermore, the number of developmental similarities between LR and crown root formation in cereals makes the translational studies even more attractive, as for the plant improvement programs. The formation of crown and lateral roots leads to an increased number of functional root meristems and allows to explore the soil more effectively. This has a profound impact on root system architecture and is therefore a key to optimizing the capture of soil resources (Fitter et al. 2002; Lynch 2011b).

Besides these obvious advantages, there are a few downsides, the largest difficulty being the gene redundancy within gene families in cereals. Although many approaches have been proposed in the litterature, an effective way of finding an equivalent gene in monocot plant species is a detailed bioinformatic analysis of all members belonging to the gene family of interest and subsequent functional characterisation of selected candidates.

The traditional marker-assisted QTL mapping in cereals is costly, time consuming and often hampered by the reduced accuracy of genomic localization (de Dorlodot et al. 2007). The cloning of a QTL to validate its function is also extremely complex and we are not aware of any successful root QTL cloning today in crops (Topp et al. 2013). The genes identified in barley (**Chapter 2**) are good candidates underlying root QTLs determined in cereals in the past decades, as they play a major role in auxin transport and signalling crucial for many aspects of root growth and development in *Arabidopsis*. Here, we have shown that *AUX1* loci known to govern root gravitropic response overlap with QTL intervals for morphological root traits and phosphorus uptake. We conclude that *AUX1* is a good candidate gene in this chromosomal region to stand behind those QTLs. The following step should be to validate the *AUX1* association with the phosphorus uptake efficiency.

The candidate gene-based strategy that we used might also prove useful to identify cereal genes corresponding to *Arabidopsis* genes involved in other target traits, such as disease and pests resistance and many others. These candidate genes, subsequently mapped on cereal genetic maps could be further combined with the positions of known cereal QTLs by meta-analysis. The resulting database could give a powerful data compendium of candidate genes in plants alongside known QTL positions (www.gramene.org/), leading to the identification of genes responsible for QTL effects, overcoming the need for marker-assisted mapping.

(2) Funcions of auxin influx carriers in cereals

So far, nothing was known in cereals about auxin influx carriers that are crucial for the formation of auxin gradients in *Arabidopsis*. In **Chapter 3**, a translational approach was employed in barley to address the function of AUX1 and LAX3 influx carriers involved in, respectively, LR initiation and emergence in *Arabidopsis*. We showed that the *AUX/LAX* gene family is conserved in monocots and that both *HvAUX1* and *HvLAX3* possess auxin influx activity, as they can rescue respectively, *aux1-22* and *lax3* in *Arabidopsis*. Furthermore, the expression pattern of the two auxin influx carriers in barley in most overlaps with the *Arabidopsis* equivalents and was observed during all stages of LR development. Together with the agravitropic root phenotype of *Osaux1* lines, these results led to the conclusion that *HvAUX1* and *HvLAX3* in barley are the equivalents of *AtAUX1* and *AtLAX3* in *Arabidopsis*. However, it is likely that AUX/LAX family members in cereals have diverged partially differently from those of the dicot *Arabidopsis*, as *Osaux1* lines did not show a decrease in LR number and *HvLAX3* is also expressed inside the LRP, unlike *AtLAX3*. Thus, we can not rule out that another member of AUX/LAX family also contributes to AUX1 and LAX3 protein function in monocots or that unknown pathways are involved in monocot LR development. Indeed, LRP needs to emerge through several cortex layers in cereals, unlike in *Arabidopsis*, where LRP passes through one cortex layer. It would be interesting to pursue the involvement of *HvLAX3* in cell divisions and/or cell wall separations that occure during LRP emergence in barley.

Adjusting the root angle driven by its gravitropic response has been proposed, among other root traits, as the basis for a second green revolution (Lynch 2007). However, very little is known about the consequences of agravitropic root growth on crop performance under water deficit. We showed that the cereal *AUX1* is a good potential target to modulate some aspects of nutrient and water uptake efficiency, as *Osaux1* roots tend to spend more time growing in the topsoil and their scattering seems to support water transfer from the

bulk soil to the root zone during a short drought episode (**Chapter 3**). The possible applications of the agravitropic root phenotype of *Osaux1* in phosphorus uptake efficiency is the topic of further study at the Center for Plant Integrative Biology (UNottingham).

(3) New role for ABA as an intrinsic mediator of transient changes in soil-water avaliability

Prior to the beginning of this study, ABA was only known to inhibit LR emergence. In **Chapter 4**, we propose that ABA response pathways stand behind the immediate plant responses to local depletions of soil-water content such as occur when a root meristem enters a macropore. It is in agreement with the recent findings that ABA signalling in the endodermis in essential for salt-regulated lateral root growth dynamics (Duan et al. 2013). By performing a microarray experiment, we showed that transient WD episode induces genes involved in ABA response. Furthermore, transient ABA treatment (**Chapter 4)** mimics LR repression at the LR initiation step or earlier that is observed upon transtient WD episode (Babé et al. 2012a). Our subsequent results lead to a general model where at least two ABA response pathways with different reaction times are involved in the regulation of LR formation in response to transient changes in soil-water content. Further experiments and exploration of candidate genes from WD microarray experiment may lead to a better understanding of the underlying mechanism of ABA-mediated LR repression. It would be interesting to investigate DR5 oscillations upon transient ABA treatment in 35S:bZIP and ABA signalling mutants backgrounds. Ultimatelly, knowledge of branching behaviour of ABA signalling mutants of *Arabidopsis* exposed to transient ABA treatment would further support the involvement of ABA signalling in LR repression at early stage of development. I would also be of interest to investigate the souce of ABA in LR repression upon transient WD episode.

(4) ROS contributes to LR development

The recent interest in ROS as signalling molecules has boosted our current understanding of the possible crosstalk between ROS and the intrinsic signalling pathways. However, very little is known about the interplay between ROS and auxin during LR formation. In **Chapter 5**, by performing a meta-analysis of LR- and H_2O_2-related microarrays, we first report a set of commmon genes induced upon auxin and H_2O_2 treatments. We subsequently show that H_2O_2 is deposited into middle lamellae of LRP cells in contact with parental tissue and explicitly in middle lamellae of endodermis and cortex cells that are known to contribute to LRP emergence. Together with the rescue of *aux1lax3* and *shy2* LR-less phenotypes, these results led to the conclusion that H_2O_2 is likely to contribute to the modulation of cell wall dynamics during LR emergence.

The endogenous source of extracellular ROS that appear progressively during LR formation and contribute to the formation of a fine ROS layer that separates LRP from the root parental tissues is still an open question. Although the contribution of *Rboh* family members to LR development remains to be elucidated, their expression patterns alongside the DPI-sensitivity of LR emergence suggest the possible link between *Rboh* genes and LR formation. It is of great interest to further address the role of *RbohE* in LR emergence, as the mutation in *RbohE* leads to delay in LR emergence.

SUPLEMENTARY MATERIALS

Suplementary Figures

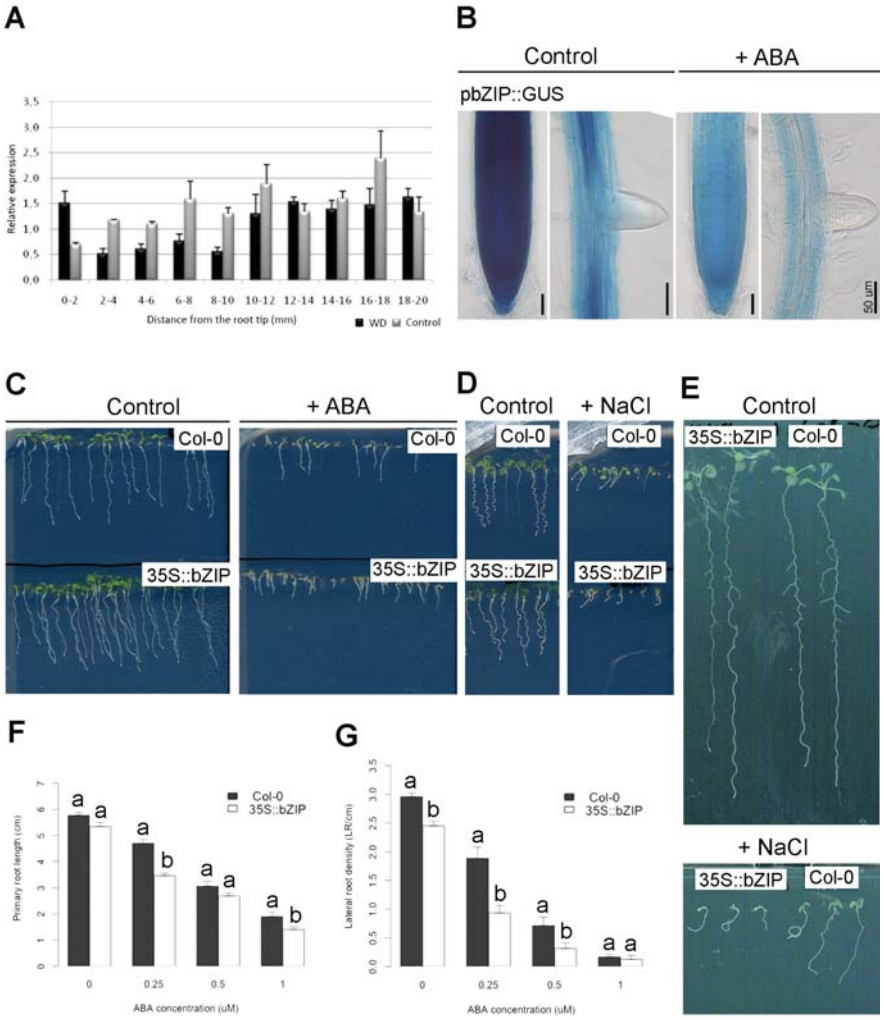

Figure S-1: WD microarray validation.

(A) Barley cv. Derkado bZIP expression levels in water deficit LR repression experiments as detected by quantitative PCR (qPCR). Plants grown in aeroponics were transferred into standard nutrient solution (Control) or exposed to water deficit for 2 h in the night phase. Primary seminal roots were then disected into 2 mm fragments up to 2 cm. bZIP mRNA levels were normalized by EFα expression. Values are presented as a mean ± SE (n = 3). **(B)** GUS staining of barley pbZIP:GUS in ABA-mediated LR repression experiments. Plants grown for 4 d on standard media were transferred for 1 d to DMSO (Control) or 50 µM ABA (+ABA) growth medium. **(C** through **E)** Inhibition of primary root growth of *Arabidopsis* bZIP overexpression lines on **(C)** 1 µM ABA for 5 dpg and on 100 µM NaCl after **(D)** 5 dpg and **(E)** 10 dpg. Seeds were sown on DMSO (Control) or 1 µM ABA growth media and imaged after 4 d **(C)** or 10 d **(D)** of growth. **(F)** Primary root length and **(G)** LR number were determined for 10 d-old seedlings. Bars are means ± CI, with different letters indicating significant differences according to Tukey's HSD test after ANOVA.

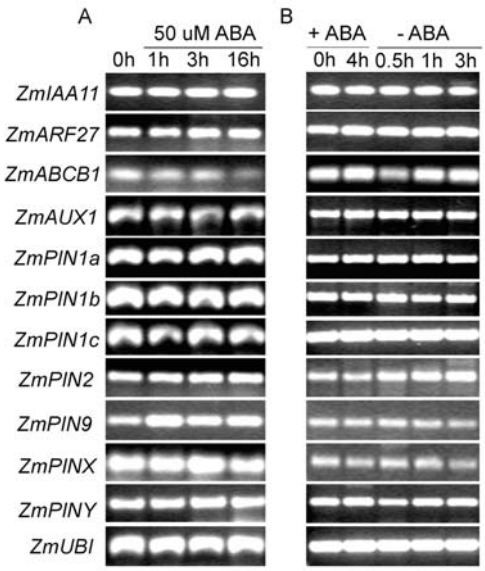

Figure S-2: Transcript abundance of auxin carriers in maize, as determined by reverse-transcription PCR (RT-PCR) analysis from B73 wild-type plants in LR repression experiments.

(A) Plants were exposed for to 50 μM ABA for times indicated. Maize ubiquitin signal was used as an equal loading control (n = 2). **(B)** Plants were exposed to 50 μM ABA for 4 h and then transferred to the standard nutrient solution (NS) for times indicated. Maize ubiquitin signal was used as an equal loading control (n = 2).

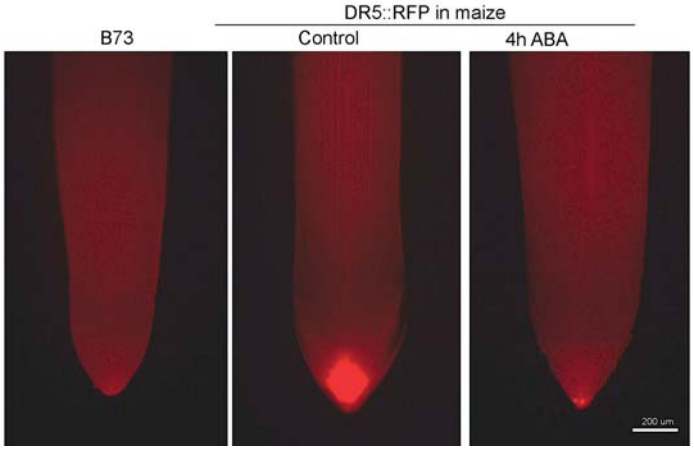

Figure S-3: DR5:RFP fluorescence in the root tip of maize in LR repression experiments.

Fluorescence was captured after 4h of DMSO (Control) or 50 μM ABA application in aeroponics. Wild-type B73 was used as a background control, n > 10.

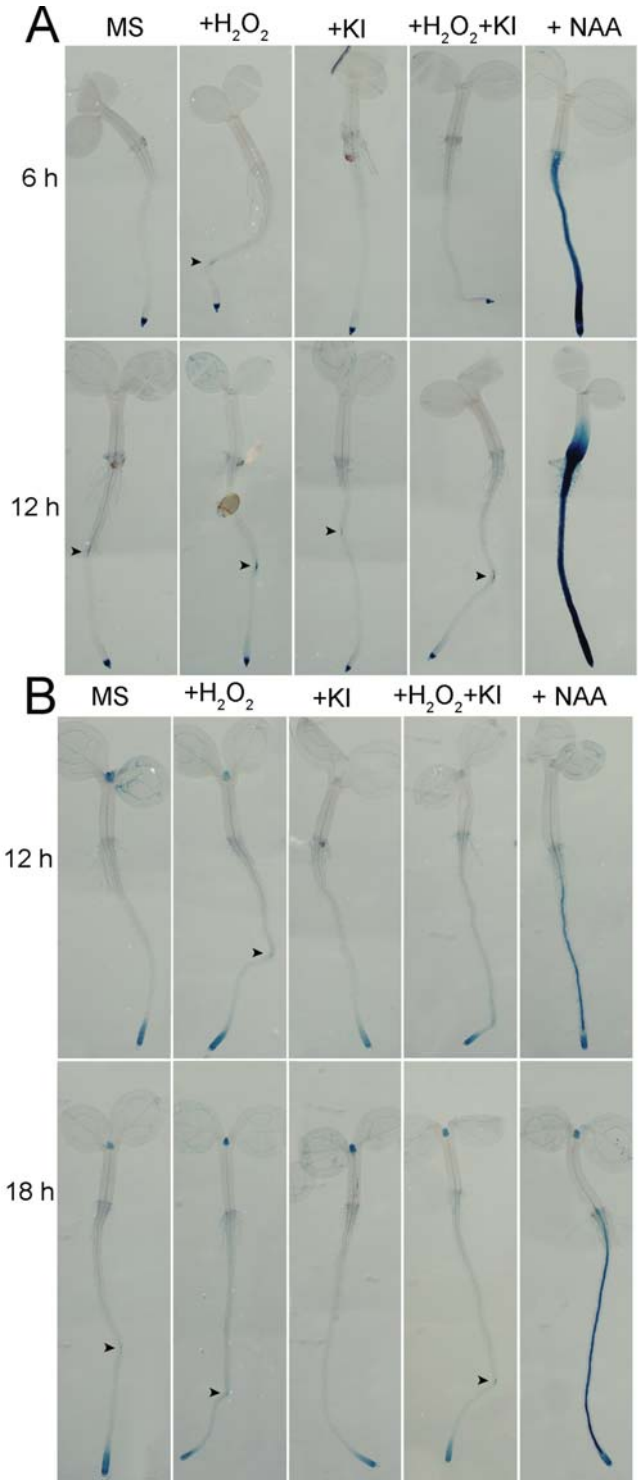
A
MS
+H2O2
+KI
+H2O2+KI
+ NAA
6 h
12 h
B
MS
+H2O2
+KI
+H2O2+KI
+ NAA
12 h
18 h

Figure S-4: Effect of H_2O_2 in Lateral Root Inducible System

(A) Visualisation of DR5 promoter activity. **(B)** Visualization of CYCB1;1 promoter activity. Briefly, 3 dpg were transferred from standard media supplemented with 10 uM NPA into fresh standard media as indicated (+H_2O_2 = 1.5 mM H_2O_2, +KI = 0.01 mM KI, + NAA = 10 uM NAA) . Black arrowheads marks the positions where the GUS signal appears. Seedlings (n > 20 per each sample) were prefixed with 0.5 % formaldehyde in 50 mM phosphate buffer for 30 min and GUS-stained for 6 h. Tissue was cleaned with chloral hydrate.

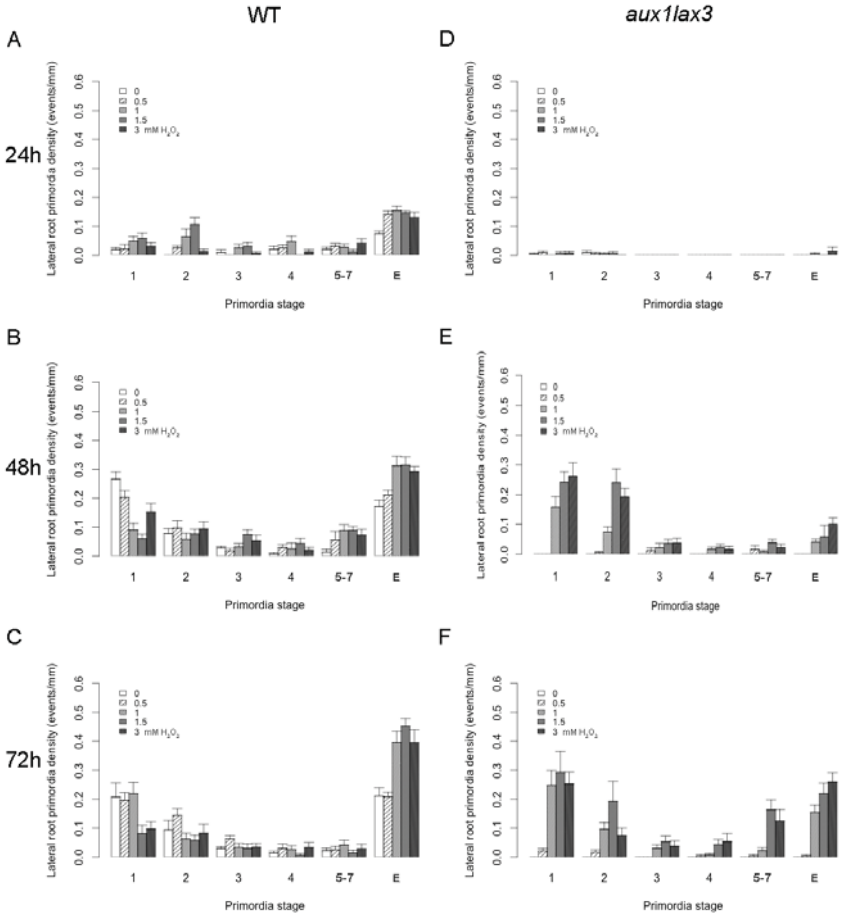

Figure S-5: Lateral root emergence phenotype of Col-0 and *aux1lax3* upon H_2O_2 treatment.

Plants were germinated on standard MS media for 5 days and then transferred into the fresh plates that were untreated (Control) or supplemented with various concentrations of H_2O_2. LRP density per primary root length was determined at **(A, D)** 24, **(B, E)** 48 and **(C, F)** 72 h after transfer by cleaning the tissue (n >15 per sample, 2 biological repetitions). E = emerged LR.

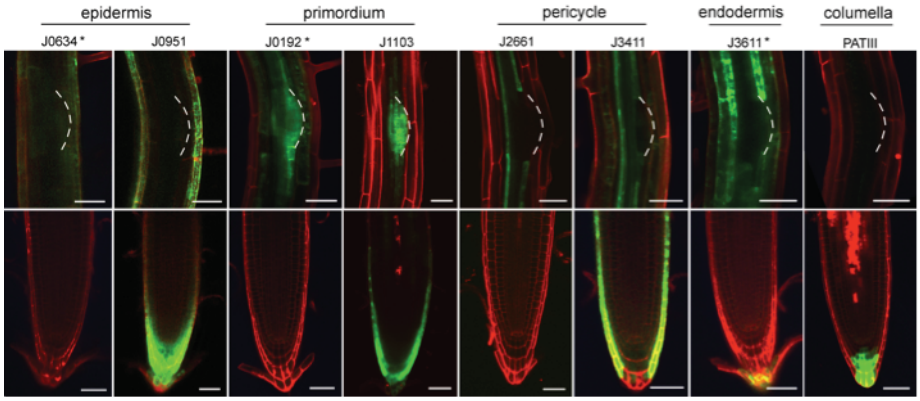

Figure S-6: Transactivation lines used in crosses with UAS:RbohD

Initial screening of transactivation lines. 5 dpg seedlings wee imaged with a confocal microscope. Homozygous lines were chosen for further crosses. Bar = 50 μm.

Suplementary Tables

Table S-1: Rice QTLs that span the region of *OsAUX1* location

Trait(s)	Marker(s) name	Position [cM]	LOD	REF
Root length on low Pi	RM1198	146.4 on IRMI 2003	-	Li et al., 2009
	RM5382	147.5 on IRMI 2003		
Yeld in low Pi conditions	RM414	191,1 on Cornell, 2004	-	Wang et al., 2009
Plant high under low N	RZ730	154,8 on Cornell 2001	5.12	Fang and Wu, 2001
	RZ801	189.6 on Cornell SSR 2001		
Plant high	RZ730	154,8 cM on Cornell 2001	2.53	Hemamalini et al., 2000
	RZ801	189.6 on Cornell SSR 2001		
Root length	RZ730	154,8 on Cornell 2001	3.81	de Dorlodot and Draye, unpublished
Root length	RG810	188,7 on Cornell 2001	3.55	
Root number and volume	RM472	171 on Cornell SSR 2001	6.13	Qu et al., 2008
	RM1198	146.4 on IRMI 2003	6.02	

Root weight, lenght and tickness	RZ19	97.3 on Cornell RFLP 2001	-	Yadav et al., 1997
	RZ801	189.6 on Cornell SSR 2001	-	
Crown root number	RM315	165.3 on Cornell SSR 2001	2.4	Zheng et al., 2003
	RG109B	97.3 on Cornell RFLP 2001		
Root tickness	RM5	146,4 on IRMI 2003	3.53	Li et al., 2005
	RM302	147,8 on Cornell SSR 2001		
Root volume	RM1003	136.75 on IRMI 2003	4.85	Qu et al., 2008
	RM1198	146.4 on IRMI 2003		
Root tickness	RZ730	154,8 on Cornell 2001	2.61	Zheng et al., 2000
	RZ801	189.6 on Cornell SSR 2001		
Root lenght	RG109B	97.3 on Cornell RFLP 2001	3.37	Zheng et al., 2001
	RG690	143.2 on Cornell SSR 2001		
Root weight	RZ730	154,8 on Cornell 2001	5.1	Shen et al.,2001
Dry weight under WD	RM212	148.7 on Cornell SSR 2001	4.2 3.0	Price et al., 2002
Root:shoot dry weight during WD	C86	103.8 on Cornell RFLP 2001	3.3	

Table S-2: Soybean QTLs that span the region of *SbAUX1* location

Trait(s)	Marker(s) name	Position [cM]	LOD	REF
Total root surface area at low P level	Satt295	42.5	2.72	Liang et al., 2010
	Satt436	63.1		
Total root length at low P level	Satt295	42.5	3.36	
	Satt436	63.1		
Enhanced fibrous root trait	Satt179	50.5	2.6	Abdel-Haleem et al., 2011

Table S-3: Maize QTLs that span the region of *ZmAUX1* location

Trait(s)	Marker name	Bins	LOD	REF
LR length at high P	bnl5.37	3.05	5.33	Zhou et al., 2005
	umc60	3.06		
Root exudations: upon low P	umc1400	3.05		Chen et al., 2008
	umc1148	3.07	2.95	
LR lenght	bnl8.01	3.06	3.5	Ruta et al., 2010
Root diameter	bnl8.01	3.06	-	Tuberosa et al., 2003 Ribaut et al., 1996
Root pulling force	bnl8.01	3.06	-	Tuberosa et al., 2003; Lebreton et al., 1995
	umc1844	3.08	-	
Grain N-uptake and content, grain yield	gsy224 sps2	3.05	-	Gallais et al., 2004
	gsy38a1	3.09	>2	
Root number on internodes	gsy224-sps2	3.05	-	Gauingo et al., 1998
	gsy38a1	3.09	3.1	
Fractal dimension of root system	MO372	3.06	7.62	Bohn et al., 2006
Seminal axile root length	UMC16A	3.09	3.9	Hund et al., 2004
Ear number	MO372	3.06	-	Austin and Lee, 1998 (Gramene)

Table S-4: Transcription factors that showed significant treatment vs time interaction and significant regulation over the drought treatment (respectively Two-Way ANOVA p-value ≤ 0.01 and FC≥1.5 FDR p-value ≤ 0.01) in WD experiment in barey.

Microarray probesets information		Contrast, FC			p value			Two-way Anova		
		Drought VS Control			Drought VS Control					
AGI	Description	2 VS 2	4 VS 4	6 VS 6	2 VS 2	4 VS 4	6 VS 6	Drought	Time	Interaction
		1	1	1	p.value.adj.F	p.value.adj.F	p.value.adj.F	Orig. p-value	Orig. p-value	Orig. p-values
AT3G23050	IAA7, AXR2 | indole-3-acetic acid 7	4,0444133	3,4863402	2,997903	1,01E-06	1,16E-06	1,74E-06	5,57E-08	5,069E-10	2,99519E-07
AT5G24930	ATCOL4, COL4 | CONSTANS-like 4	2,9687978	2,6736131	2,1264107	8,695E-06	1,51E-05	5,12E-05	1,17E-04	3,264E-08	1,45517E-05
AT5G44210	ERF9, ATERF9, ATERF-9 | erf domain protein 9	3,0523935	1,6828557	2,0632978	6,823E-06	1,12E-03	6,64E-05	8,25E-08	1,229E-07	2,04089E-05
AT2G40740	WRKY55, ATWRKY55 | WRKY DNA-binding protein	6,4632022	2,7959405	2,2542651	1,26E-06	4,02E-05	1,09E-04	7,92E-04	1,94E-07	2,17E-05
AT3G46640	PCL1 | Homeodomain-like superfamily protein	4,2682415	2,9639099	1,3003103	6,773E-06	4,58E-05	8,72E-02	5,00E-03	1,328E-06	4,13E-05
AT5G43700	ATAUX2-11, IAA4 | AUX/IAA transcriptional regula	6,611845	4,5003094	2,344247	2,39E-06	8,40E-06	2,13E-04	2,00E-05	3,859E-07	6,58E-05
AT4G34000	ABF3, DPBF5 | abscisic acid responsive elements-b	3,1789306	1,7471092	2,3113462	6,773E-06	7,87E-04	2,69E-05	8,25E-07	4,15E-07	7,77E-05
AT5G56960	basic helix-loop-helix (bHLH) DNA-binding family p	1,7935322	-1,920844	-3,012013	5,74E-03	0,0026102	4,282E-05	0,0041804	0,0024967	1,06E-04
AT1G58110	Basic-leucine zipper (bZIP) transcription factor fam	-1,969708	-1,376487	-1,083784	1,03E-04	1,15E-02	0,4613032	7,08E-05	1,234E-05	1,22E-04
AT1G01720	ATAF1, NAC (No Apical Meristem) domain transcrip	3,1547811	1,4258755	1,4549961	1,699E-05	2,61E-02	0,012582	8,76E-06	6,453E-06	0,000125345
AT1G80840	WRKY40, WRKY DNA-binding protein 40	2,4937232	1,03042	1,4285461	4,69E-05	8,77E-01	0,0106066	1,95E-07	4,849E-05	0,000165922
AT1G04250	AXR3, IAA17 | AUX/IAA transcriptional regulator fa	2,728527	1,7435742	1,4610019	3,32E-05	1,57E-03	9,40E-03	7,68E-08	2,923E-06	0,000219067
AT3G55980	SZF1, ATSZF1 | salt-inducible zinc finger 1	2,6352783	-1,251266	1,2694398	1,61E-04	2,20E-01	0,1402475	8,831E-06	0,0025019	0,00038993
AT2G22770	NAI1 | basic helix-loop-helix (bHLH) DNA-binding s	2,8530819	2,190028	1,4813438	5,963E-05	4,14E-04	1,57E-02	7,80E-06	5,383E-06	0,000520881
AT5G17260	NAC086 | NAC domain containing protein 86	1,1603332	-1,478475	-1,619675	2,52E-01	0,0051694	0,0008065	9,84E-05	8,35E-04	0,000547505
AT1G32640	JIN1 | Basic helix-loop-helix (bHLH) DNA-binding f	1,7282611	1,4260718	1,2777704	0,0004693	6,65E-03	0,0278812	2,78E-05	6,462E-06	0,000778431
AT5G48150	PAT1 | GRAS family transcription factor	2,0781174	1,1796928	-1,090573	0,0003712	2,93E-01	0,5492953	9,218E-05	0,0019402	0,000804971
AT2G03500	Homeodomain-like superfamily protein	1,5012427	1,7882031	2,0217488	0,0080418	0,000766	0,0001182	1,29E-04	3,77E-06	0,000891306
AT4G36930	SPT | basic helix-loop-helix (bHLH) DNA-binding su	2,7560858	1,459296	1,0995428	8,431E-05	3,21E-02	0,5587225	5,46E-05	1,76E-04	0,000907295
AT2G29660	zinc finger (C2H2 type) family protein | chr2:12675	3,331343	3,9082366	3,3620512	0,0001946	7,87E-05	9,44E-05	2,74E-04	2,367E-06	0,001006457
AT1G25280	AtTLP10, TLP10 | tubby like protein 10	-1,180707	1,2971578	1,2446271	1,59E-01	0,0280602	0,0393483	1,887E-07	0,0150101	0,00110126
AT3G46070	C2H2-type zinc finger family protein	2,91479	2,6642283	1,2419653	7,73E-05	1,35E-04	1,76E-01	1,23E-04	3,499E-05	0,001115073
AT5G39610	ATNAC2| NAC domain containing protein 6	1,1002767	-1,464478	-1,557984	0,5237709	0,0091296	0,0022317	8,053E-06	0,0012347	0,001922073
AT1G62990	KNAT7 | KNOTTED-like homeobox of Arabidopsis t	1,3725848	1,4728491	2,4784881	8,50E-02	0,0349457	0,0001238	3,26E-04	0,0001136	0,003615164
AT4G30080	ARF16 | auxin response factor 16	1,1702446	1,6772733	2,2148103	0,3778027	0,0056264	1,98E-04	3,01E-05	0,0001629	0,003833477
AT5G48150	PAT1 | GRAS family transcription factor	1,5077008	1,1231577	1,0643351	2,15E-03	0,3138298	0,5548729	0,0001512	0,0008623	0,004204868
AT3G24520	HSFC1 | heat shock transcription factor C1	1,9875568	2,0870601	1,9288245	0,0007699	4,43E-04	5,20E-04	5,01E-03	1,301E-05	0,00441883
AT3G54810	GATA8 | Plant-specific GATA-type zinc finger trans	-1,085517	1,4057037	1,7878763	0,6401359	0,0287735	0,0008045	0,0003786	0,003218	0,005594653
AT5G58900	Homeodomain-like transcriptional regulator	-2,982154	-2,122614	-1,698359	0,0003863	3,87E-03	1,68E-02	1,46E-02	5,846E-05	0,006498049
AT1G59750	ARF1 | auxin response factor 1	1,4307638	1,9719305	1,9771285	5,27E-02	0,0014629	8,31E-04	7,35E-04	5,846E-05	0,00745953
AT3G16500	PAP1, IAA26 | phytochrome-associated protein 1	1,6066589	1,475508	1,4812885	3,19E-03	0,0090541	0,0051962	5,15E-07	3,42E-05	0,008991247
AT1G52150	ICU4 | Homeobox-leucine zipper family protein	2,2032821	1,5871086	1,1859041	5,81E-04	1,39E-02	0,2839624	4,63E-03	0,0004369	0,009195969
AT1G04250	AXR3, IAA17 | AUX/IAA transcriptional regulator fa	1,2306678	1,3023275	1,0647914	7,14E-02	0,023132	0,5525731	9,929E-09	4,85E-04	0,013947771
AT2G35530	bZIP16 | basic region/leucine zipper transcription f	1,7094517	1,3257932	1,2224008	0,0014134	4,36E-02	0,104422	7,85E-03	0,000341	0,01407031
AT1G70000	myb-like transcription factor family protein	1,7487897	1,8866358	1,8036739	0,0092716	0,0038972	0,003673	1,65E-05	9,425E-05	0,021014145
AT3G48360	BT2 | BTB and TAZ domain protein 2	-1,992351	-2,133816	-1,863173	2,90E-03	1,38E-03	2,84E-03	7,95E-03	0,0001004	0,021202233

Table S-5: Primer pairs used in ZmPIN experiments

ZmPIN1a_F: ATAATCGCGTGCGGGAACAA
ZmPIN1a_R:TCCTGCTCCACATCCCCATC
ZmPIN1b_F: ATCATCGCGTGCGGGAACAA
ZmPIN1b_R:ACCCACGGGTCGGTCACAGG
ZmPIN1c_F: TCATCCCCATGGAGTCGAGGATGCCACC
ZmPIN1c_R:GGATCCACCCAGACCCAATCCCCATACCTACTTCT
ZmPIN2_F: AGGTGGCCAACAAGTTCGCGTCTGGG
ZmPIN2_R: CCTTCTTGCGCGGGGCCACGTACG
ZmPIN9_F: CACCGTCGCCTCGCTCTCCATGCTCC
ZmPIN9_R: AAGGCCCAACAGTATGTAGTAGACAATCG
ZmPINX_F: ATGGGTTTCTTCTCTCTATTTCTGGTGGCG
ZmPINX_R: GTCGCATACAGCCGGGACAATGATCAG
ZmPINY_F: ATGATGGAGAGATCGCTGCTGGAGGTGC
ZmPINY_R: GGCATGGAAGCAGAAGGGAAAACACAAG
ZmABCB1_F: GCCGCGTAGGACGGA ATG
ZmABCB1_R: TTGCGATCATGGAGTACCACCAT
ZMAUX1_F: GGATCCACCCAGACCCAATCCCCATACCTACTTCT
ZmAUX1_R: AGTCGAGGGAGAACGCCGTG
ZmUBI_F: TAAGCTGCCGATGTGCCTGCGTCG
ZmUBI_R: CTGAAAGACAGAACATAATGAGCACAG

Table S-6: Auxin and ROS overlapping genes.

Locus	Symbol	Vanneste et al., 2005		De Rybel et al., 2012		Ng et al., 2013		Davletova et al., 2005	
		Hit (+/-)	FC	Hit (+/-)	FC	Hit (+/-)	FC	Hit (+/-)	FC
AT1G80840	WRKY40	+	5,6	+	8,1	+	2,5	+	38,5
AT3G50930	BCS1	+	3,4	+	5,2	+	3,6	+	2,1
AT1G05680	UGT74E2	+	3,6	+	6,8	+	3,4	+	9,4
AT5G39670		+	2,8	+	3,3	+	2,4	+	3,2
AT1G72900		+	2,6	+	4,2	+	2,3	+	9,6
AT4G37370	CYP81D8	+	3,9	+	10,7	+	7,0	+	23,0
AT5G39050	PMAT1	+	3,5	+	3,9	+	2,1	+	10,2
AT2G30140	UGT87A2	+	2,8	+	2,6	+	2,3	+	3,6
AT3G28210	SAP12	+	2,8	+	5,3	+	14,0	+	7,2
AT2G41380		+	2,2	+	2,4	+	2,8	+	4,3
AT4G17490	ATERF6	+	2,2	+	2,1	+	2,5	+	20,2
AT1G21120	IGMT2	+	2,8	+	2,6	+	2,8	+	17,1
AT3G05360	AtRLP30	+	2,3	+	2,2	+	2,4	+	2,9
AT4G22530		+	5,9	+	6,0	+	2,7	+	5,3
AT2G38470	WRKY33	+	2,4	+	2,2	+	2,4	+	13,4
AT2G15490	UGT73B4	+	3,3	+	4,3	+	2,7	+	7,7
AT5G14730		+	3,2	+	3,7	+	2,5	+	9,0
AT1G76070		+	2,4	+	2,7	+	2,9	+	4,4
AT1G61340	AtFBS1	+	2,9	+	2,3	+	3,5	+	7,5
AT5G54490	PBP1	+	34,0	+	17,8	+	2,8	+	5,1
AT5G20230	SAG14	+	2,5	+	3,0	+	2,2	+	11,6
AT4G28085		+	2,5	+	2,1	+	2,8	+	4,8
AT4G33070		+	3,2	+	3,3	+	3,0		1,1
AT4G36430		+	2,6	+	2,8	+	2,1		1,3
AT2G02990	RNS1	+	4,5	+	4,2	+	4,1		-1,2
AT1G10370	GST30	+	2,5	+	2,5	+	2,1		-1,1

AT5G43450		+	2,3	+	2,2	+	3,6		1,9
AT5G62520	SRO5	+	2,2	+	2,1	+	4,1		1,3
AT2G29460	GST22	+	3,2	+	4,3	+	6,0		1,4
AT1G02850	BGLU11	+	2,6	+	3,1	+	2,1		1,3
AT3G11340	UGT76B1	+	2,2	+	2,8	+	2,8		-1,0
AT2G22470	AGP2	+	4,3	+	3,0	+	2,4		1,0
AT5G57910		+	2,5	+	2,2	+	2,5		1,5
AT5G02760		+	2,6	+	4,0	-	-3,0		-1,0
AT3G46280		+	3,0	+	4,2	-	-3,4		-1,5
AT5G48430		+	2,3	+	4,4	-	-2,6		-1,1
AT4G30140	CDEF1	+	8,0	+	9,6	-	-2,3		-1,3
AT4G12420	SKU5	+	5,1	+	4,8	-	-2,0		-1,5
AT3G12700	NANA	+	2,6	+	2,8	-	-2,0		-1,4
AT2G47140	SDR5	+	4,2	+	4,7		1,2	+	4,6
AT4G30280	XTH18	+	4,8	+	7,9		2,2	+	5,8
AT2G18690		+	2,3	+	2,5		1,8	+	3,3
AT3G07390	AIR12	+	15,8	+	19,0		-1,1	+	2,9
AT4G23180	RLK4	+	4,4	+	2,0		1,4	+	8,1
AT5G18470		+	6,9	+	5,7		1,4	+	5,4
AT3G59080		+	2,6	+	2,7		-1,0	+	3,5
AT5G64300	GCH1 RFD1	+	2,4	+	2,4		1,1	+	2,9
AT2G35710	PGSIP7	+	2,3	+	2,5		1,3	+	3,4
AT4G14680	APS3	+	3,7	+	5,0		-1,1	+	6,2
AT1G65390	PP2-A5	+	5,1	+	27,9		1,2	+	4,1
AT5G10830		+	3,8	+	3,6		-1,0	+	6,4
AT5G07870		+	2,7	+	3,4		1,0	+	4,0
AT4G01250	WRKY22	+	3,5	+	2,9		-1,0	+	2,5
AT2G39980		+	3,0	+	3,9		-1,8	+	2,9
AT3G59900	ARGOS	+	5,4	+	4,5		-1,7	+	2,1
AT4G21680	NRT1.8	+	11,1	+	16,0		-1,0	+	2,2

AT5G45340	CYP707A3	+	2,2	+	2,4	1,5	+	3,0
AT4G36500		+	4,8	+	3,3	1,6	+	4,6
AT2G18210		+	4,7	+	2,9	1,1	+	2,4
AT1G05560	UGT1	+	4,9	+	7,1	1,6	+	10,3
AT4G01870		+	2,4	+	2,6	1,6	+	21,7
AT4G31800	WRKY18	+	3,6	+	2,2	-1,3	+	3,6
AT1G18570	MYB51	+	3,4	+	2,5	1,5	+	4,1
AT1G62300	WRKY6	+	2,3	+	2,3	1,7	+	6,5
AT3G55980	SZF1	+	3,5	+	2,3	1,6	+	7,6
AT5G16970	AER	+	2,4	+	2,5	1,4	+	5,6
AT5G52810		+	4,1	+	3,1	1,6	+	2,7
AT5G51830		+	6,0	+	7,3	1,7	+	13,3
AT5G49480	CP1	+	2,2	+	2,5	1,4	+	5,7
AT4G27280		+	3,7	+	3,6	1,2	+	4,9
AT4G20830		+	2,2	+	2,3	1,7	+	7,3
AT4G13180		+	2,2	+	2,6	1,6	+	4,1
AT4G11280	ACS6	+	8,2	+	5,1	1,9	+	7,7
AT1G19180	JAZ1	+	3,0	+	2,1	1,3	+	4,9
AT3G02800	PFA-DSP3	+	2,1	+	2,4	2,0	+	6,7
AT3G23550		+	2,4	+	2,5	1,2	+	2,5
AT1G17170	GSTU24	+	2,9	+	3,2	1,4	+	33,8
AT1G30620	MUR4	+	2,9	+	2,9	1,3	+	2,2
AT2G41100	TCH3	+	17,4	+	16,6	1,8	+	6,8
AT5G27760		+	2,3	+	2,9	1,9	+	6,4
AT4G39230		+	2,8	+	2,0	-1,0	+	2,0
AT4G21990	PRH26	+	2,0	+	2,6	-1,1	+	23,4
AT4G18950		+	2,8	+	3,3	1,3	+	5,5
AT1G17180	GSTU25	+	6,6	+	6,2	2,1	+	13,3
AT1G33590		+	3,3	+	3,3	1,2	+	3,1
AT4G31550	WRKY11	+	2,3	+	2,0	1,2	+	4,1

AT1G04770		+	2,1	+	2,5		-1,5	+	2,8
AT2G36220		+	3,8	+	4,1		1,6	+	9,6
AT2G24500	FZF	+	2,2	+	2,5		-1,0	+	2,8
AT1G65390	PP2-A5	+	6,0	+	18,4		-1,0	+	3,8
AT4G15550	IAGLU	+	2,9	+	3,0		-1,1	+	4,5
AT5G48180	NSP5	+	2,3	+	2,5		1,2	+	2,3
AT5G13750	ZIFL1	+	2,5	+	3,5		1,2	+	2,6
AT3G44190		+	3,0	+	2,9		1,6	+	5,0
AT4G34710	ADC2 | SPE2	+	4,0	+	3,9		1,2	+	3,4
AT2G41820		+	3,9	+	3,2		-1,1	-	-2,0
AT3G62110		+	2,0	+	2,5		-1,4	-	-2,4
AT1G23480	CSLA03	+	3,3	+	2,7		-1,5	-	-2,8
AT5G49360	BXL1	-	-2,9	-	-10,5	+	2,6		-1,1
AT3G05640		-	-3,3	-	-4,1	+	2,3		1,0
AT1G76410	ATL8	-	-4,1	-	-7,0		1,0	+	2,1
AT3G20340		-	-2,3	-	-2,5		2,0	+	4,6
AT3G10985	SAG20	-	-2,5	-	-3,1		1,7	+	3,0
AT1G66180		-	-2,2	-	-2,3		-1,4	+	2,5
AT3G21070	NADK1	-	-2,3	-	-2,6		1,0	+	2,3
AT4G23700	CHX17	-	-3,6	-	-2,9		1,2	+	2,4
AT1G70420		-	-2,7	-	-2,2		1,6	+	4,2
AT1G32450	NRT1.5	-	-2,7	-	-4,4		1,3	-	-2,5
AT3G23430	PHO1	-	-2,6	-	-4,2		-1,4	-	-2,6

Aranda A, Sequedo L, Tolosa L, Quintas G, Burello E, Castell JV, Gombau L (2013) Dichloro-dihydro-fluorescein diacetate (DCFH-DA) assay: a quantitative method for oxidative stress assessment of nanoparticle-treated cells. Toxicology in vitro : an international journal published in association with BIBRA 27 (2):954-963. doi:10.1016/j.tiv.2013.01.016

Babe A, Lavigne T, Severin JP, Nagel KA, Walter A, Chaumont F, Batoko H, Beeckman T, Draye X (2012) Repression of early lateral root initiation events by transient water deficit in barley and maize. Philosophical Transactions of the Royal Society of London B Biological Sciences 367 (1595):1534-1541. doi:10.1098/rstb.2011.0240

Bahrun A, Jensen CR, Asch F, Mogensen VO (2002) Drought-induced changes in xylem pH, ionic composition, and ABA concentration act as early signals in field-grown maize (Zea mays L.). Journal of experimental botany 53 (367):251-263

Bailey-Serres J, Lee SC, Brinton E (2012) Waterproofing crops: effective flooding survival strategies. Plant physiology 160 (4):1698-1709. doi:10.1104/pp.112.208173

Bainbridge K, Guyomarc'h S, Bayer E, Swarup R, Bennett M, Mandel T, Kuhlemeier C (2008) Auxin influx carriers stabilize phyllotactic patterning. Genes & development 22 (6):810-823. doi:10.1101/gad.462608

Band LR, Wells DM, Fozard JA, Ghetiu T, French AP, Pound MP, Wilson MH, Yu L, Li W, Hijazi HI, Oh J, Pearce SP, Perez-Amador MA, Yun J, Kramer E, Alonso JM, Godin C, Vernoux T, Hodgman TC, Pridmore TP, Swarup R, King JR, Bennett MJ (2014) Systems analysis of auxin transport in the *Arabidopsis* root apex. The Plant cell 26 (3):862-875. doi:10.1105/tpc.113.119495

Bao Y, Aggarwal P, Robbins NE, 2nd, Sturrock CJ, Thompson MC, Tan HQ, Tham C, Duan L, Rodriguez PL, Vernoux T, Mooney SJ, Bennett MJ, Dinneny JR (2014) Plant roots use a patterning mechanism to position lateral root branches toward available water. Proceedings of the National Academy of Sciences of the United States of America 111 (25):9319-9324. doi:10.1073/pnas.1400966111

Baster P, Robert S, Kleine-Vehn J, Vanneste S, Kania U, Grunewald W, De Rybel B, Beeckman T, Friml J (2013) SCF(TIR1/AFB)-auxin signalling regulates PIN vacuolar trafficking and auxin fluxes during root gravitropism. The EMBO journal 32 (2):260-274. doi:10.1038/emboj.2012.310

Bates PJ, Sanderson G, Holgate ST, Johnston SL (1997) A comparison of RT-PCR, in-situ hybridisation and in-situ RT-PCR for the detection of rhinovirus infection in paraffin sections. Journal of virological methods 67 (2):153-160

Bates TR, Lynch JP (2000) The efficiency of Arabidopsis thaliana (Brassicaceae) root hairs in phosphorus acquisition. American journal of botany 87 (7):964-970

Baxter I, Hosmani PS, Rus A, Lahner B, Borevitz JO, Muthukumar B, Mickelbart MV, Schreiber L, Franke RB, Salt DE (2009) Root suberin forms an extracellular barrier that affects water relations and mineral nutrition in Arabidopsis. PLoS genetics 5 (5):e1000492. doi:10.1371/journal.pgen.1000492

Bell JK, McCully ME (1970) A histological study of lateral root initiation and development in Zea mays. Protoplasma 70:179-205

Benitez-Alfonso Y, Faulkner C, Pendle A, Miyashima S, Helariutta Y, Maule A (2013) Symplastic intercellular connectivity regulates lateral root patterning. Dev Cell 26 (2):136-147. doi:10.1016/j.devcel.2013.06.010

Benjamini Y, Hochberg Y (1995) Controlling the false discovery rate: a practical and powerful approach to multiple testing. J Roy Statist Soc Ser B (Methodological) 57:289-300

Benjamins R, Ampudia CS, Hooykaas PJ, Offringa R (2003) PINOID-mediated signaling involves calcium-binding proteins. Plant physiology 132 (3):1623-1630

Benkova E, Hejatko J (2009) Hormone interactions at the root apical meristem. Plant molecular biology 69 (4):383-396

Benkova E, Michniewicz M, Sauer M, Teichmann T, Seifertova D, Jurgens G, Friml J (2003) Local, efflux-dependent auxin gradients as a common module for plant organ formation. Cell 115 (5):591-602

Bent A (2006) Arabidopsis thaliana floral dip transformation method. Methods Mol Biol 343:87-103. doi:10.1385/1-59745-130-4:87

Berleth T, Jurgens G (1993) The role of monopteros in organizing the basal body region of the Arabidoposis embryo. . Development 118:575-587

Bernhardt C, Lee MM, Gonzalez A, Zhang F, Lloyd A, Schiefelbein J (2003) The bHLH genes GLABRA3 (GL3) and ENHANCER OF GLABRA3 (EGL3) specify epidermal cell fate in the Arabidopsis root. Development 130 (26):6431-6439. doi:10.1242/dev.00880

Bhattacharjee S (2012) The Language of Reactive Oxygen Species Signaling in Plants. Journal of Botany 2012:1-22

Bian H, Xie Y, Guo F, Han N, Ma S, Zeng Z, Wang J, Yang Y, Zhu M (2012) Distinctive expression patterns and roles of the miRNA393/TIR1 homolog module in regulating flag leaf inclination and primary and crown root growth in rice (Oryza sativa). New Phytologist 196 (1):149-161. doi:10.1111/j.1469-8137.2012.04248.x

Bibikova TN, Jacob T, Dahse I, Gilroy S (1998) Localized changes in apoplastic and cytoplasmic pH are associated with root hair development in Arabidopsis thaliana. Development 125 (15):2925-2934

Bienert GP, Chaumont F (2014) Aquaporin-facilitated transmembrane diffusion of hydrogen peroxide. Biochimica et biophysica acta 1840 (5):1596-1604. doi:10.1016/j.bbagen.2013.09.017

Bingham IJ, Blackwood JM (1997) Site, scale and time-course for adjustments in lateral root initiation in wheat following changes in C and N supply. Annals of Botany (London) 80:97-106

Blilou I, Xu J, Wildwater M, Willemsen V, Paponov I, Friml J, Heidstra R, Aida M, Palme K, Scheres B (2005) The PIN auxin efflux facilitator network controls growth and patterning in Arabidopsis roots. Nature 433 (7021):39-44. doi:10.1038/nature03184

Bocca SN, Magioli C, Mangeon A, Junqueira RM, Cardeal V, Margis R, Sachetto-Martins G (2005) Survey of glycine-rich proteins (GRPs) in the Eucalyptus expressed sequence tag database (ForEST). . Genetics and Molecular Biology 28:608-624

REFERENCES

Boerjan W, Cervera MT, Delarue M, Beeckman T, Dewitte W, Bellini C, Caboche M, Van Onckelen H, Van Montagu M, Inze D (1995) Superroot, a recessive mutation in Arabidopsis, confers auxin overproduction. The Plant cell 7 (9):1405-1419

Boisson-Dernier A, Lituiev DS, Nestorova A, Franck CM, Thirugnanarajah S, Grossniklaus U (2013) ANXUR receptor-like kinases coordinate cell wall integrity with growth at the pollen tube tip via NADPH oxidases. PLoS biology 11 (11):e1001719. doi:10.1371/journal.pbio.1001719

Brady SM, Sarkar SF, Bonetta D, McCourt P (2003) The ABSCISIC ACID INSENSITIVE 3 (ABI3) gene is modulated by farnesylation and is involved in auxin signaling and lateral root development in Arabidopsis. The Plant journal : for cell and molecular biology 34 (1):67-75

Bramley H, Turner NC, Turner DW, Tyerman SD (2009) Roles of morphology, anatomy, and aquaporins in determining contrasting hydraulic behavior of roots. Plant physiology 150 (1):348-364. doi:10.1104/pp.108.134098

Brunoud G, Wells DM, Oliva M, Larrieu A, Mirabet V, Burrow AH, Beeckman T, Kepinski S, Traas J, Bennett MJ, Vernoux T (2012) A novel sensor to map auxin response and distribution at high spatio-temporal resolution. Nature 482 (7383):103-106. doi:10.1038/nature10791

Buchanan CD, Lim S, Salzman RA, Kagiampakis I, Morishige DT, Weers BD, Klein RR, Pratt LH, Cordonnier-Pratt MM, Klein PE, Mullet JE (2005) Sorghum bicolor's transcriptome response to dehydration, high salinity and ABA. Plant molecular biology 58 (5):699-720. doi:10.1007/s11103-005-7876-2

Byrne JM, Pesacreta TC, Fox JA (1977) Development and structure of the vascular connection between the primary and secondary root of Glycine max (L.) Merr. . American journal of botany 64:946–959

Calderon Villalobos LI, Lee S, De Oliveira C, Ivetac A, Brandt W, Armitage L, Sheard LB, Tan X, Parry G, Mao H, Zheng N, Napier R, Kepinski S, Estelle M (2012) A combinatorial TIR1/AFB-Aux/IAA co-receptor system for differential sensing of auxin. Nature Chemical Biology 8 (5):477-485. doi:10.1038/nchembio.926

Campoli C, Drosse B, Searle I, Coupland G, von Korff M (2012) Functional characterisation of HvCO1, the barley (Hordeum vulgare) flowering time ortholog of CONSTANS. The Plant journal : for cell and molecular biology 69 (5):868-880. doi:10.1111/j.1365-313X.2011.04839.x

Carol RJ, Takeda S, Linstead P, Durrant MC, Kakesova H, Derbyshire P, Drea S, Zarsky V, Dolan L (2005) A RhoGDP dissociation inhibitor spatially regulates growth in root hair cells. Nature 438 (7070):1013-1016. doi:10.1038/nature04198

Casero PJ, Casimiro I, Lloret PG (1995) Lateral root initiation by asymmetrical transverse divisions of pericycle cells in four plant species: Raphanus sativus, Helianthus annuus, Zea mays, and Daucus carota. Protoplasma 188 49-58

Casero PJ, Casimiro I, Lloret PG (1996) Pericycle proliferation pattern during the lateral root initiation in adventitious roots of Allium cepa. Protoplasma 191:136-147

Casimiro I, Beeckman T, Graham N, Bhalerao R, Zhang H, Casero P, Sandberg G, Bennett MJ (2003) Dissecting Arabidopsis lateral root development. Trends in plant science 8 (4):165-171. doi:10.1016/S1360-1385(03)00051-7

Casimiro I, Marchant A, Bhalerao RP, Beeckman T, Dhooge S, Swarup R, Graham N, Inze D, Sandberg G, Casero PJ, Bennett M (2001) Auxin transport promotes Arabidopsis lateral root initiation. The Plant cell 13 (4):843-852

Causin HF, Roqueiro G, Petrillo E, Lainez V, Pena LB, Marchetti CF, Gallego SM, Maldonado SI (2012) The control of root growth by reactive oxygen species in Salix nigra Marsh. seedlings. Plant Science 183:197-205. doi:10.1016/j.plantsci.2011.08.012

Cernac A, Lincoln C, Lammer D, Estelle M (1997) The SAR1 gene of Arabidopsis acts downstream of the AXR1 gene in auxin response. Development 124 (8):1583-1591

Chen Y-H, Chao Y-Y, Hsu Y, Hong C-Y, Kao C (2012) Heme oxygenase is involved in nitric oxide- and auxin-induced lateral root formation in rice. Plant cell reports 31 (6):1085-1091. doi:10.1007/s00299-012-1228-x

Clark DG, Gubrium EK, Barrett JE, Nell TA, Klee HJ (1999) Root formation in ethylene-insensitive plants. Plant physiology 121 (1):53-60

Clark RT, MacCurdy RB, Jung JK, Shaff JE, McCouch SR, Aneshansley DJ, Kochian LV (2011) Three-dimensional root phenotyping with a novel imaging and software platform. Plant physiology 156 (2):455-465. doi:10.1104/pp.110.169102

Close TJ, Bhat PR, Lonardi S, Wu Y, Rostoks N, Ramsay L, Druka A, Stein N, Svensson JT, Wanamaker S, Bozdag S, Roose ML, Moscou MJ, Chao S, Varshney RK, Szucs P, Sato K, Hayes PM, Matthews DE, Kleinhofs A, Muehlbauer GJ, DeYoung J, Marshall DF, Madishetty K, Fenton RD, Condamine P, Graner A, Waugh R (2009) Development and implementation of high-throughput SNP genotyping in barley. BMC genomics 10:582. doi:10.1186/1471-2164-10-582

Clough SJ, Bent AF (2008) Floral dip: a simplified method forAgrobacterium-mediated transformation of Arabidopsis thaliana. The Plant Journal 16 (6):735-743

Correa-Aragunde N, Foresi N, Delledonne M, Lamattina L (2013) Auxin induces redox regulation of ascorbate peroxidase 1 activity by S-nitrosylation/denitrosylation balance resulting in changes of root growth pattern in Arabidopsis. Journal of experimental botany 64 (11):3339-3349. doi:10.1093/jxb/ert172

Coudert Y, Bes M, Le Thi VA, Pre M, Guiderdoni E, Gantet P (2011) Transcript profiling of *crown root less* 1 stem base reveals new elements associated with crown root development in rice. BMC genomics 12:e387

Coudert Y, Dievart A, Droc G, Gantet P (2012) ASL/LBD phylogeny suggests that genetic mechanisms of root initiation downstream of auxin are distinct in lycophytes and euphyllophytes. Molecular biology and evolution. doi:10.1093/molbev/mss250

Coudert Y, Perin C, Courtois B, Khong NG, Gantet P (2010a) Genetic control of root development in rice, the model cereal. Trends in plant science 15 (4):219-226

Coudert Y, Perin C, Courtois B, Khong NG, Gantet P (2010b) Genetic control of root development in rice, the model cereal. Trends in plant science 15 (4):219-226. doi:10.1016/j.tplants.2010.01.008

D'Haeze W, De Rycke R, Mathis R, Goormachtig S, Pagnotta S, Verplancke C, Capoen W, Holsters M (2003) Reactive oxygen species and ethylene play a positive role in lateral root base nodulation of a semiaquatic legume. Proceedings of the National Academy of Sciences of the United States of America 100 (20):11789-11794. doi:10.1073/pnas.1333899100

Dalton TP, Shertzer HG, Puga A (1999) Regulation of gene expression by reactive oxygen. Annual review of pharmacology and toxicology 39:67-101. doi:10.1146/annurev.pharmtox.39.1.67

Daudi A, O'Brien JA (2012) Detection of Hydrogen Peroxide by DAB Staining in Arabidopsis Leaves. Bio-protocol 2 (18)

Davletova S, Schlauch K, Coutu J, Mittler R (2005) The zinc-finger protein Zat12 plays a central role in reactive oxygen and abiotic stress signaling in Arabidopsis. Plant physiology 139 (2):847-856. doi:10.1104/pp.105.068254

De Diego N, Rodriguez JL, Dodd IC, Perez-Alfocea F, Moncalean P, Lacuesta M (2013) Immunolocalization of IAA and ABA in roots and needles of radiata pine (Pinus radiata) during drought and rewatering. Tree physiology 33 (5):537-549. doi:10.1093/treephys/tpt033

de Dorlodot S, Forster B, Pages L, Price A, Tuberosa R, Draye X (2007) Root system architecture: opportunities and constraints for genetic improvement of crops. Trends in plant science 12 (10):474-481. doi:10.1016/j.tplants.2007.08.012

De Rybel B, Audenaert D, Xuan W, Overvoorde P, Strader LC, Kepinski S, Hoye R, Brisbois R, Parizot B, Vanneste S, Liu X, Gilday A, Graham IA, Nguyen L, Jansen L, Njo MF, Inze D, Bartel B, Beeckman T (2012) A role for the root cap in root branching revealed by the non-auxin probe naxillin. Nat Chem Biol 8 (9):798-805. doi:10.1038/nchembio.1044

De Rybel B, Vassileva V, Parizot B, Demeulenaere M, Grunewald W, Audenaert D, Van Campenhout J, Overvoorde P, Jansen L, Vanneste S, Moller B, Wilson M, Holman T, Van Isterdael G, Brunoud G, Vuylsteke M, Vernoux T, De Veylder L, Inze D, Weijers D, Bennett MJ, Beeckman T (2010) A novel aux/IAA28 signaling cascade activates GATA23-dependent specification of lateral root founder cell identity. Current biology : CB 20 (19):1697-1706. doi:10.1016/j.cub.2010.09.007

De Smet I (2011) Lateral root initiation: one step at a time. New Phytologist 193:867–873

De Smet I, Signora L, Beeckman T, Inze D, Foyer CH, Zhang H (2003) An abscisic acid-sensitive checkpoint in lateral root development of Arabidopsis. The Plant journal : for cell and molecular biology 33 (3):543-555

De Smet I, Tetsumura T, De Rybel B, Frey NF, Laplaze L, Casimiro I, Swarup R, Naudts M, Vanneste S, Audenaert D, Inze D, Bennett MJ, Beeckman T (2007) Auxin-dependent regulation of lateral root positioning in the basal meristem of Arabidopsis. Development 134 (4):681-690

De Smet I, Vassileva V, De Rybel B, Levesque MP, Grunewald W, Van Damme D, Van Noorden G, Naudts M, Van Isterdael G, De Clercq R, Wang JY, Meuli N, Vanneste S, Friml J, Hilson P, Jurgens G, Ingram GC, Inze D, Benfey PN, Beeckman T (2008) Receptor-like kinase ACR4 restricts formative cell divisions in the Arabidopsis root. Science 322 (5901):594-597. doi:10.1126/science.1160158

Deak KI, Malamy J (2005) Osmotic regulation of root system architecture. The Plant journal : for cell and molecular biology 43 (1):17-28. doi:10.1111/j.1365-313X.2005.02425.x

Delbarre A, Muller P, Imhoff V, Guern J (1996) Comparison of mechanisms controlling uptake and accumulation of 2,4-dichlorophenoxy acetic acid, naphthalene-1-acetic acid, and indole-3-acetic acid in suspension-cultured tobacco cells. Planta 198 (4):532-541

Dello Ioio R, Linhares FS, Scacchi E, Casamitjana-Martinez E, Heidstra R, Costantino P, Sabatini S (2007) Cytokinins determine Arabidopsis root-meristem size by controlling cell differentiation. Current biology : CB 17 (8):678-682. doi:10.1016/j.cub.2007.02.047

Dello Ioio R, Nakamura K, Moubayidin L, Perilli S, Taniguchi M, Morita MT, Aoyama T, Costantino P, Sabatini S (2008) A genetic framework for the control of cell division and differentiation in the root meristem. Science 322 (5906):1380-1384

Demchenko NP, Demchenko KN (2001) Resumption of DNA synthesis and cell division in wheat roots as related to lateral root initiation. Russian Journal of Plant Physiology 48 (6):755-764

Depuydt S, Hardtke CS (2011) Hormone signalling crosstalk in plant growth regulation. Current Biology 21 (9):R365-373. doi:10.1016/j.cub.2011.03.013

Desnos T (2008) Root branching responses to phosphate and nitrate. Current opinion in plant biology 11 (1):82-87. doi:10.1016/j.pbi.2007.10.003

Dharmasiri S, Dharmasiri N, Hellmann H, Estelle M (2003) The RUB/Nedd8 conjugation pathway is required for early development in Arabidopsis. The EMBO journal 22 (8):1762-1770. doi:10.1093/emboj/cdg190

Dhondt S, Wuyts N, Inze D (2013) Cell to whole-plant phenotyping: the best is yet to come. Trends in plant science 18 (8):428-439. doi:10.1016/j.tplants.2013.04.008

Dodd IC, Davies WJ (2006) The relationship between leaf growth and ABA accumulation in the grass leaf elongation zone. Plant, cell & environment 19 (9):1047-1056

Draye X (2002) Influence of root growth and vascular structure on the distribution of lateral roots. Plant Cell and Environment, vol 25.

Draye X, Delvaux B, Swennen R (1999) Distribution of lateral root primordia in root tips of Musa. Annals of Botany (London) 84:393-400

Draye X, Kim Y, Lobet G, Javaux M (2010) Model-assisted integration of physiological and environmental constraints affecting the dynamic and spatial patterns of root water uptake from soils. Journal of experimental botany 61 (8):2145-2155. doi:10.1093/jxb/erq077

Drew MC (1975) Comparison of the Effects of a Localized Supply of Phosphate, Nitrate, Ammonium and Potassium on the Growth of the Seminal Root System, and the Shoot, in Barley. New Phytologist 75:479-490

Drew MC, He CJ, Morgan PW (1989) Decreased Ethylene Biosynthesis, and Induction of Aerenchyma, by Nitrogen- or Phosphate-Starvation in Adventitious Roots of Zea mays L. Plant physiology 91 (1):266-271

Drew MC, He CJ, Morgan PW (2000) Programmed cell death and aerenchyma formation in roots. Trends in plant science 5 (3):123-127

Duan L, Dietrich D, Ng CH, Chan PM, Bhalerao R, Bennett MJ, Dinneny JR (2013) Endodermal ABA signaling promotes lateral root quiescence during salt stress in Arabidopsis seedlings. The Plant cell 25 (1):324-341. doi:10.1105/tpc.112.107227

Duarte JM, Cui L, Wall PK, Zhang Q, Zhang X, Leebens-Mack J, Ma H, Altman N, dePamphilis CW (2006) Expression pattern shifts following duplication indicative of subfunctionalization and neofunctionalization in regulatory genes of Arabidopsis. Molecular biology and evolution 23 (2):469-478. doi:10.1093/molbev/msj051

Dubcovsky J, Ramakrishna W, SanMiguel PJ, Busso CS, Yan L, Shiloff BA, Bennetzen JL (2001) Comparative sequence analysis of colinear barley and rice bacterial artificial chromosomes. Plant physiology 125 (3):1342-1353

Dubrovsky JG, Gambetta GA, Hernandez-Barrera A, Shishkova S, Gonzalez I (2006a) Lateral root initiation in Arabidopsis: developmental window, spatial patterning, density and predictability. Annals of Botany (London) 97 (5):903-915. doi:10.1093/aob/mcj604

Dubrovsky JG, Gambetta GA, Hernandez-Barrera A, Shishkova S, Gonzalez I (2006b) Lateral root initiation in Arabidopsis: developmental window, spatial patterning, density and predictability. Annals of botany 97 (5):903-915. doi:10.1093/aob/mcj604

Fetter K, Van Wilder V, Moshelion M, Chaumont F (2004) Interactions between plasma membrane aquaporins modulate their water channel activity. The Plant cell 16 (1):215-228. doi:10.1105/tpc.017194

Fisher K, Turner S (2007) PXY, a receptor-like kinase essential for maintaining polarity during plant vascular-tissue development. Current biology : CB 17 (12):1061-1066. doi:10.1016/j.cub.2007.05.049

Fitter A (2002) Characteristics and functions of roots systems. In: Waisel Y, Eshel A, Kafkafi U (eds) Plant roots: the hidden half, 3rd Edit. Marcel Dekker Pub, New York, pp 15–32

Fitter A, Williamson L, Linkohr B, Leyser O (2002) Root system architecture determines fitness in an Arabidopsis mutant in competition for immobile phosphate ions but not for nitrate ions. Proceedings Biological sciences / The Royal Society 269 (1504):2017-2022. doi:10.1098/rspb.2002.2120

Fitter AH (1982) Morphometric analysis of root systems: application of the technique and influence of soil fertility on root system development in two herbaceous species. . Plant, Cell and Environment 5:313–322

Foreman J, Demidchik V, Bothwell JH, Mylona P, Miedema H, Torres MA, Linstead P, Costa S, Brownlee C, Jones JD, Davies JM, Dolan L (2003) Reactive oxygen species produced by NADPH oxidase regulate plant cell growth. Nature 422 (6930):442-446. doi:10.1038/nature01485

Forestan C, Farinati S, Varotto S (2012) The Maize PIN Gene Family of Auxin Transporters. Frontiers in plant science 3:16. doi:10.3389/fpls.2012.00016

Fu C, Wehr DR, Edwards J, Hauge B (2008) Rapid one-step recombinational cloning. Nucleic acids research 36 (9):e54. doi:10.1093/nar/gkn167

Gale MD, Devos KM (1998) Comparative genetics in the grasses. Proceedings of the National Academy of Sciences of the United States of America 95 (5):1971-1974

Gallavotti A, Yang Y, Schmidt RJ, Jackson D (2008a) The Relationship between auxin transport and maize branching. Plant physiology 147 (4):1913-1923. doi:10.1104/pp.108.121541

Gallavotti A, Yang Y, Schmidt RJ, Jackson D (2008b) The Relationship between auxin transport and maize branching. Plant physiology 147 (4):1913-1923.

Garay-Arroyo A, De La Paz Sanchez M, Garcia-Ponce B, Azpeitia E, Alvarez-Buylla ER (2012) Hormone symphony during root growth and development. Developmental dynamics : an official publication of the American Association of Anatomists 241 (12):1867-1885. doi:10.1002/dvdy.23878

Gautier L, Cope L, Bolstad BM, Irizarry RA (2004) affy--analysis of Affymetrix GeneChip data at the probe level. Bioinformatics 20 (3):307-315. doi:10.1093/bioinformatics/btg405

Geiger D, Maierhofer T, Al-Rasheid KA, Scherzer S, Mumm P, Liese A, Ache P, Wellmann C, Marten I, Grill E, Romeis T, Hedrich R (2011) Stomatal closure by fast abscisic acid signaling is mediated by the guard cell anion channel SLAH3 and the receptor RCAR1. Science signaling 4 (173):ra32. doi:10.1126/scisignal.2001346

Geldner N, Richter S, Vieten A, Marquardt S, Torres-Ruiz RA, Mayer U, Jurgens G (2004) Partial loss-of-function alleles reveal a role for GNOM in auxin transport-related, post-embryonic development of Arabidopsis. Development 131 (2):389-400. doi:10.1242/dev.00926

Geng Y, Wu R, Wee CW, Xie F, Wei X, Chan PM, Tham C, Duan L, Dinneny JR (2013) A spatio-temporal understanding of growth regulation during the salt stress response in Arabidopsis. The Plant cell 25 (6):2132-2154. doi:10.1105/tpc.113.112896

Ghanem ME, Hichri I, Smigocki AC, Albacete A, Fauconnier ML, Diatloff E, Martinez-Andujar C, Lutts S, Dodd IC, Perez-Alfocea F (2011) Root-targeted biotechnology to mediate hormonal signalling and improve crop stress tolerance. Plant cell reports 30:807-823. doi:10.1007/s00299-011-1005-2

Gill SS, Tuteja N (2010) Reactive oxygen species and antioxidant machinery in abiotic stress tolerance in crop plants. Plant physiology and biochemistry : PPB / Societe francaise de physiologie vegetale 48 (12):909-930. doi:10.1016/j.plaphy.2010.08.016

Gjetting KS, Ytting CK, Schulz A, Fuglsang AT (2012) Live imaging of intra- and extracellular pH in plants using pHusion, a novel genetically encoded biosensor. Journal of experimental botany 63 (8):3207-3218. doi:10.1093/jxb/ers040

Goh T, Kasahara H, Mimura T, Kamiya Y, Fukaki H (2012a) Multiple AUX/IAA-ARF modules regulate lateral root formation: the role of Arabidopsis SHY2/IAA3-mediated auxin signalling. Philosophical transactions of the Royal Society of London Series B, Biological sciences 367 (1595):1461-1468. doi:10.1098/rstb.2011.0232

Goh T, Kasahara H, Mimura T, Kamiya Y, Fukaki H (2012b) Multiple AUX/IAA-ARF modules regulate lateral root formation: the role of Arabidopsis SHY2/IAA3-mediated auxin signalling. Philosophical Transactions of the Royal Society of London B Biological Sciences 367 (1595):1461-1468. doi:10.1098/rstb.2011.0232

Gonzalez-Carranza ZH, Elliott KA, Roberts JA (2007) Expression of polygalacturonases and evidence to support their role during cell separation processes in Arabidopsis thaliana. Journal of experimental botany 58 (13):3719-3730. doi:10.1093/jxb/erm222

Gottwald S, Bauer P, Komatsuda T, Lundqvist U, Stein N (2009) TILLING in the two-rowed barley cultivar 'Barke' reveals preferred sites of functional diversity in the gene HvHox1. BMC research notes 2:258. doi:10.1186/1756-0500-2-258

Gowda V, Henry A, Yamauchi A, Shashidhar HE, R. S (2011a) Root biology and genetic improvement for drought avoidance in rice. Field Crops Research 122 (1):1–13

Gowda VRP, Henry A, Yamauchi A, Shashidhar HE, Serraj R (2011b) Root biology and genetic improvement for drought avoidance in rice. Field Crops Research 1:1-13

Gregory PJ, Hutchison DJ, Read DB, Jenneson PM, Gilboy WB, Morton EJ (2003) Non-invasive imaging of roots with high resolution X-ray micro-tomography. Plant and Soil 255 (1):351-359

Grierson CS, Roberts K, Feldmann KA, Dolan L (1997) The COW1 locus of arabidopsis acts after RHD2, and in parallel with RHD3 and TIP1, to determine the shape, rate of elongation, and number of root hairs produced from each site of hair formation. Plant physiology 115 (3):981-990

Grunewald W, Vanholme B, Pauwels L, Plovie E, Inze D, Gheysen G, Goossens A (2009) Expression of the Arabidopsis jasmonate signalling repressor JAZ1/TIFY10A is stimulated by auxin. EMBO reports 10 (8):923-928. doi:10.1038/embor.2009.103

Guyomarc'h S, Leran S, Auzon-Cape M, Perrine-Walker F, Lucas M, Laplaze L (2012) Early development and gravitropic response of lateral roots in Arabidopsis thaliana. Philosophical transactions of the Royal Society of London Series B, Biological sciences 367 (1595):1509-1516. doi:10.1098/rstb.2011.0231

Hachez C, Moshelion M, Zelazny E, Cavez D, Chaumont F (2006) Localization and quantification of plasma membrane aquaporin expression in maize primary root: a clue to understanding their role as cellular plumbers. Plant molecular biology 62 (1-2):305-323. doi:10.1007/s11103-006-9022-1

Haga K, Takano M, Neumann R, Iino M (2005) The Rice COLEOPTILE PHOTOTROPISM1 gene encoding an ortholog of Arabidopsis NPH3 is required for phototropism of coleoptiles and lateral translocation of auxin. The Plant cell 17 (1):103-115. doi:10.1105/tpc.104.028357

Hamburger D, Rezzonico E, MacDonald-Comber Petetot J, Somerville C, Poirier Y (2002) Identification and characterization of the Arabidopsis PHO1 gene involved in phosphate loading to the xylem. The Plant cell 14 (4):889-902

Han B, Xu S, Xie YJ, Huang JJ, Wang LJ, Yang Z, Zhang CH, Sun Y, Shen WB, Xie GS (2012) ZmHO-1, a maize haem oxygenase-1 gene, plays a role in determining lateral root development. Plant Science 184:63-74. doi:10.1016/j.plantsci.2011.12.012

Hauser M, Morikami A, Benfey PN (1995) Conditional root expansion mutants of Arabidopsis. Development 121:1237–1252

Heisler MG, Ohno C, Das P, Sieber P, Reddy GV, Long JA, Meyerowitz EM (2005) Patterns of auxin transport and gene expression during primordium development revealed by live imaging of the Arabidopsis inflorescence meristem. Current biology : CB 15 (21):1899-1911. doi:10.1016/j.cub.2005.09.052

Helariutta Y, Fukaki H, Wysocka-Diller J, Nakajima K, Jung J, Sena G, Hauser MT, Benfey PN (2000) The SHORT-ROOT gene controls radial patterning of the Arabidopsis root through radial signaling. Cell 101 (5):555-567

Henry A, Cal AJ, Batoto TC, Torres RO, Serraj R (2012) Root attributes affecting water uptake of rice (Oryza sativa) under drought. Journal of experimental botany 63 (13):4751-4763. doi:10.1093/jxb/ers150

Hernandez I, Martynowicz D, Rodriguez A, PÃrez-Morales MB, Graether SP, Jimenez BJF (2014) A dehydrin-dehydrin interaction: the case of SK3 from Opuntia streptacantha. Frontiers in plant science 5:1664-1462

Hetz W, Hochholdinger F, Schwall M, Feix G (1996) Isolation and characterization of rtcs, a maize mutant deficient in the formation of nodal roots. Plant Journal 10 (5):845-857. doi:10.1046/j.1365-313X.1996.10050845.x

Hewitt EJ (1966) Sand and water culture methods used in the study of plant nutrition. . Commonw – Bur Hortic Tech Com 22:431-446

Himanen K, Boucheron E, Vanneste S, de Almeida Engler J, Inze D, Beeckman T (2002) Auxin-mediated cell cycle activation during early lateral root initiation. The Plant cell 14 (10):2339-2351

Himanen K, Vuylsteke M, Vanneste S, Vercruysse S, Boucheron E, Alard P, Chriqui D, Van Montagu M, Inzé D, Beeckman T (2004) Transcript profiling of early lateral root initiation. Proc Natl Acad Sci USA 101 (14):5146-5151

Hirose N, Makita N, Kojima M, Kamada-Nobusada T, Sakakibara H (2007) Overexpression of a type-A response regulator alters rice morphology and cytokinin metabolism. Plant and Cell Physiology 48 (3):523-539. doi:10.1093/pcp/pcm022

Hochholdinger F, Park WJ, Sauer M, Woll K (2004a) From weeds to crops: genetic analysis of root development in cereals. Trends in plant science 9 (1):42-48. doi:10.1016/j.tplants.2003.11.003

Hochholdinger F, Park WJ, Sauer M, Woll K (2004b) From weeds to crops: genetic analysis of root development in cereals. Trends in plant science 9 (1):42-48. doi:10.1016/j.tplants.2003.11.003

Hochholdinger F, Tuberosa R (2009) Genetic and genomic dissection of maize root development and architecture. Current opinion in plant biology 12 (2):172-177. doi:10.1016/j.pbi.2008.12.002

Hose E, Clarkson DT, Steudle E, Schreiber L, Hartung W (2001) The exodermis: a variable apoplastic barrier. Journal of experimental botany 52 (365):2245-2264

Hosmani PS, Kamiya T, Danku J, Naseer S, Geldner N, Guerinot ML, Salt DE (2013) Dirigent domain-containing protein is part of the machinery required for formation of the lignin-based Casparian strip in the root.

Proceedings of the National Academy of Sciences of the United States of America 110 (35):14498-14503. doi:10.1073/pnas.1308412110

Hsu YY, Chao YY, Kao CH (2013) Methyl jasmonate-induced lateral root formation in rice: The role of heme oxygenase and calcium. Journal of Plant Physiology 170 (1):63-69. doi:10.1016/j.jplph.2012.08.015

Hu Y, Xie Q, Chua NH (2003) The Arabidopsis auxin-inducible gene ARGOS controls lateral organ size. The Plant cell 15 (9):1951-1961

Huang BR, Taylor HM, McMichael BL (1991) Behavior of lateral roots in winter wheat as affected by temperature. Environmental and Experimental Botany 31:187-192

Huffaker A, Dafoe NJ, Schmelz EA (2011) ZmPep1, an ortholog of Arabidopsis elicitor peptide 1, regulates maize innate immunity and enhances disease resistance. Plant physiology 155 (3):1325-1338. doi:10.1104/pp.110.166710

Ilegems M, Douet V, Meylan-Bettex M, Uyttewaal M, Brand L, Bowman JL, Stieger PA (2010) Interplay of auxin, KANADI and Class III HD-ZIP transcription factors in vascular tissue formation. Development 137 (6):975-984. doi:10.1242/dev.047662

International Rice Genome Sequencing P (2005) The map-based sequence of the rice genome. Nature 436 (7052):793-800. doi:10.1038/nature03895

Inukai Y, Sakamoto T, Ueguchi-Tanaka M, Shibata Y, Gomi K, Umemura I, Hasegawa Y, Ashikari M, Kitano H, Matsuoka M (2005) Crown rootless1, which is essential for crown root formation in rice, is a target of an AUXIN RESPONSE FACTOR in auxin signaling. The Plant cell 17 (5):1387-1396

Irizarry RA, Hobbs B, Collin F, Beazer-Barclay YD, Antonellis KJ, Scherf U, Speed TP (2003) Exploration, normalization, and summaries of high density oligonucleotide array probe level data. Biostatistics 4 (2):249-264. doi:10.1093/biostatistics/4.2.249

Ishibashi Y, Tawaratsumida T, Kondo K, Kasa S, Sakamoto M, Aoki N, Zheng SH, Yuasa T, Iwaya-Inoue M (2012) Reactive oxygen species are involved in gibberellin/abscisic acid signaling in barley aleurone cells. Plant physiology 158 (4):1705-1714. doi:10.1104/pp.111.192740

Ivanchenko MG, Muday GK, Dubrovsky JG (2008) Ethylene-auxin interactions regulate lateral root initiation and emergence in Arabidopsis thaliana. Plant Journal 55 (2):335-347

Jackson MB, Armstrong W (1999) Formation of Aerenchyma and the Processes of Plant Ventilation in Relation to Soil Flooding and Submergence. Plant Biology 1 (3):274–287

Jahn L, Mucha S, Bergmann S, Horn C, Staswick S, Steffens B, Siemens J, Ludwig-Müller J (2013) The Clubroot Pathogen (Plasmodiophora brassicae) Influences Auxin Signaling to Regulate Auxin Homeostasis in Arabidopsis. Plants 2:726-749. doi:10.3390/plants2040726

Jain M, Kaur N, Garg R, Thakur JK, Tyagi AK, Khurana JP (2006) Structure and expression analysis of early auxin-responsive Aux/IAA gene family in rice (Oryza sativa). Functional & Integrative Genomics 6 (1):47-59. doi:10.1007/s10142-005-0005-0

Jansen L, Parizot B, Beeckman T (2013) Inducible system for lateral roots in Arabidopsis thaliana and maize. Methods Mol Biol 959:149-158. doi:10.1007/978-1-62703-221-6_9

Jansen L, Roberts I, De Rycke R, Beeckman T (2012) Phloem-associated auxin response maxima determine radial positioning of lateral roots in maize. Philosophical Transactions of the Royal Society of London B Biological Sciences 367 (1595):1525-1533. doi:10.1098/rstb.2011.0239

Joo JH, Bae YS, Lee JS (2001) Role of auxin-induced reactive oxygen species in root gravitropism. Plant physiology 126 (3):1055-1060

Joshi R, Kumar P (2012) Lysigenous aerenchyma formation involves non-apoptotic programmed cell death in rice (Oryza sativa L.) roots. Physiology and molecular biology of plants : an international journal of functional plant biology 18 (1):1-9. doi:10.1007/s12298-011-0093-3

Kang B, Zhang Z, Wang L, Zheng L, Mao W, Li M, Wu Y, Wu P, Mo X (2013) OsCYP2, a chaperone involved in AUX/IAA degradation, plays crucial roles in rice lateral root initiation. Plant Journal. doi:10.1111/tpj.12106

Karve A, Moore BD (2009) Function of Arabidopsis hexokinase-like1 as a negative regulator of plant growth. Journal of experimental botany 60 (14):4137-4149. doi:10.1093/jxb/erp252

Kawai-Yamada M, Ohori Y, Uchimiya H (2004) Dissection of Arabidopsis Bax inhibitor-1 suppressing Bax-, hydrogen peroxide-, and salicylic acid-induced cell death. The Plant cell 16 (1):21-32. doi:10.1105/tpc.014613

Kennedy S, Wang D, Ruvkun G (2004) A conserved siRNA-degrading RNase negatively regulates RNA interference in C. elegans. Nature 427 (6975):645-649. doi:10.1038/nature02302

Keyes SD, Daly KR, Gostling NJ (2013) High resolution synchrotron imaging of wheat root hairs growing in soil and imaged based modelling of phosphate uptake. . New Phytologist 198:1023-1029

Kim TH, Kunz HH, Bhattacharjee S, Hauser F, Park J, Engineer C, Liu A, Ha T, Parker JE, Gassmann W, Schroeder JI (2012) Natural variation in small molecule-induced TIR-NB-LRR signaling induces root growth arrest via EDS1- and PAD4-complexed R protein VICTR in Arabidopsis. The Plant cell 24 (12):5177-5192. doi:10.1105/tpc.112.107235

King J, Gay A, Sylvester-Bradley R, Bingham I, Foulkes J, Gregory P, Robinson D (2003) Modelling cereal root systems for water and nitrogen capture: towards an economic optimum. Annals of botany 91 (3):383-390

Kitomi Y, Inahashi H, Takehisa H, Sato Y, Inukai Y (2012) OsIAA13-mediated auxin signaling is involved in lateral root initiation in rice. Plant Science 190:116-122. doi:10.1016/j.plantsci.2012.04.005

Kitomi Y, Ito H, Hobo T, Aya K, Kitano H, Inukai Y (2011a) The auxin responsive AP2/ERF transcription factor CROWN ROOTLESS5 is involved in crown root initiation in rice through the induction of OsRR1, a type-A response regulator of cytokinin signaling. The Plant journal : for cell and molecular biology 67 (3):472-484. doi:10.1111/j.1365-313X.2011.04610.x

Kitomi Y, Kitano H, Inukai Y (2011b) Molecular mechanism of crown root initiation and the different mechanisms between crown root and radicle in rice. Plant signaling & behavior 6 (9):1270-1278

Kitomi Y, Ogawa A, Kitano H, Inukai Y (2008) *CRL4* regulates crown root formation through auxin transport in rice. Plant Root 2:19-28

Kojima S, Takahashi Y, Kobayashi Y, Monna L, Sasaki T, Araki T, Yano M (2002) Hd3a, a rice ortholog of the Arabidopsis FT gene, promotes transition to flowering downstream of Hd1 under short-day conditions. Plant & cell physiology 43 (10):1096-1105

Kwak JM, Mori IC, Pei ZM, Leonhardt N, Torres MA, Dangl JL, Bloom RE, Bodde S, Jones JD, Schroeder JI (2003) NADPH oxidase AtrbohD and AtrbohF genes function in ROS-dependent ABA signaling in Arabidopsis. The EMBO journal 22 (11):2623-2633. doi:10.1093/emboj/cdg277

Lamb C, Dixon RA (1997) The Oxidative Burst in Plant Disease Resistance. Annual review of plant physiology and plant molecular biology 48:251-275. doi:10.1146/annurev.arplant.48.1.251

Laplaze L, Benkova E, Casimiro I, Maes L, Vanneste S, Swarup R, Weijers D, Calvo V, Parizot B, Herrera-Rodriguez MB, Offringa R, Graham N, Doumas P, Friml J, Bogusz D, Beeckman T, Bennett M (2007) Cytokinins act directly on lateral root founder cells to inhibit root initiation. The Plant cell 19 (12):3889-3900

Larkin PJ, Gibson JM, Mathesius U, Weinman JJ, Gartner E, Hall E, Tanner GJ, Rolfe BG, Djordjevic MA (1996) Transgenic white clover. Studies with the auxin-responsive promoter, GH3, in root gravitropism and lateral root development. Transgenic research 5 (5):325-335

Laskowski M, Biller S, Stanley K, Kajstura T, Prusty R (2006) Expression profiling of auxin-treated Arabidopsis roots: toward a molecular analysis of lateral root emergence. Plant & cell physiology 47 (6):788-792. doi:10.1093/pcp/pcj043

Lavenus J, Goh T, Roberts I, Guyomarc'h S, Lucas M, De Smet I, Fukaki H, Beeckman T, Bennett M, Laplaze L (2013) Lateral root development in Arabidopsis: fifty shades of auxin. Trends in plant science 18 (8):450-458. doi:10.1016/j.tplants.2013.04.006

Lee KH, Piao HL, Kim HY, Choi SM, Jiang F, Hartung W, Hwang I, Kwak JM, Lee IJ, Hwang I (2006) Activation of glucosidase via stress-induced polymerization rapidly increases active pools of abscisic acid. Cell 126 (6):1109-1120. doi:10.1016/j.cell.2006.07.034

Lee Y, Rubio MC, Alassimone J, Geldner N (2013) A mechanism for localized lignin deposition in the endodermis. Cell 153 (2):402-412. doi:10.1016/j.cell.2013.02.045

Levine A, Tenhaken R, Dixon R, Lamb C (1994) H2O2 from the oxidative burst orchestrates the plant hypersensitive disease resistance response. Cell 79 (4):583-593

Lewis DR, Olex AL, Lundy SR, Turkett WH, Fetrow JS, Muday GK (2013) A kinetic analysis of the auxin transcriptome reveals cell wall remodeling proteins that modulate lateral root development in Arabidopsis. The Plant cell 25 (9):3329-3346. doi:10.1105/tpc.113.114868

Li J, Jia H (2013) Hydrogen peroxide is involved in cGMP modulating the lateral root development of Arabidopsis thaliana. Plant signaling & behavior 8 (8)

Li YJ, Fu YR, Huang JG, Wu CA, Zheng CC (2011) Transcript profiling during the early development of the maize brace root via Solexa sequencing. The FEBS journal 278 (1):156-166. doi:10.1111/j.1742-4658.2010.07941.x

Li Z, Xu C, Li K, Yan S, Qu X, Zhang J (2012) Phosphate starvation of maize inhibits lateral root formation and alters gene expression in the lateral root primordium zone. BMC plant biology 12:89. doi:10.1186/1471-2229-12-89

Lin SH, Kuo HF, Canivenc G, Lin CS, Lepetit M, Hsu PK, Tillard P, Lin HL, Wang YY, Tsai CB, Gojon A, Tsay YF (2008) Mutation of the Arabidopsis NRT1.5 nitrate transporter causes defective root-to-shoot nitrate transport. The Plant cell 20 (9):2514-2528. doi:10.1105/tpc.108.060244

Liu H, Wang S, Yu X, Yu J, He X, Zhang S, Shou H, Wu P (2005) ARL1, a LOB-domain protein required for adventitious root formation in rice. Plant Journal 43 (1):47-56

Liu J, An X, Cheng L, Chen F, Bao J, Yuan L, Zhang F, Mi G (2010) Auxin transport in maize roots in response to localized nitrate supply. Annals of Botany (London) 106 (6):1019-1026. doi:10.1093/aob/mcq202

Liu S, Wang J, Wang L, Wang X, Xue Y, Wu P, Shou H (2009) Adventitious root formation in rice requires OsGNOM1 and is mediated by the OsPINs family. Cell research 19 (9):1110-1119. doi:10.1038/cr.2009.70

Liu ZB, Ulmasov T, Shi X, Hagen G, Guilfoyle TJ (1994) Soybean GH3 promoter contains multiple auxin-inducible elements. The Plant cell 6 (5):645-657. doi:10.1105/tpc.6.5.645

Lloret PG, Casero PJ, Pulgarin A, Navascues J (1989) The behaviour of two cell populations in the pericycle of Allium cepa, Pisum sativum, and Daucus carota during early lateral root development. . Annals of Botany (London) 63 (4): 465-475

Lobet G, Couvreur V, Meunier F, Javaux M, Draye X (2014) Plant water uptake in drying soils. Plant physiology 164 (4):1619-1627. doi:10.1104/pp.113.233486

Lobet G, Draye X (2013) Novel scanning procedure enabling the vectorization of entire rhizotron-grown root systems. Plant methods 9 (1):1. doi:10.1186/1746-4811-9-1

Lopez-Bucio J, Cruz-Ramirez A, Herrera-Estrella L (2003) The role of nutrient availability in regulating root architecture. Current opinion in plant biology 6 (3):280-287

Ludwig-Muller J (2011) Auxin conjugates: their role for plant development and in the evolution of land plants. Journal of experimental botany 62 (6):1757-1773. doi:10.1093/jxb/erq412

Luschnig C, Gaxiola RA, Grisafi P, Fink GR (1998) EIR1, a root-specific protein involved in auxin transport, is required for gravitropism in Arabidopsis thaliana. Genes & development 12 (14):2175-2187

Lynch J (1995) Root Architecture and Plant Productivity. Plant Physiol 109:7-13

Lynch JP (2007) Roots of the second green revolution. Australian Journal of Botany 55 (5):493–512

Lynch JP (2011a) Root phenes for enhanced soil exploration and phosphorus acquisition: tools for future crops. Plant physiology 156 (3):1041-1049. doi:10.1104/pp.111.175414

Lynch JP (2011b) Root phenes for enhanced soil exploration and phosphorus acquisition: tools for future crops. . Plant physiology 156:1041-1049

Ma B, Chen S, Zhang J (2010) Ethylene signaling in rice. Chin Sci Bull 55 (21):2204-2210. doi:10.1007/s11434-010-3192-2

Ma F, Wang L, Li J, Samma MK, Xie Y, Wang R, Wang J, Zhang J, Shen W (2014) Interaction between HY1 and H2O2 in auxin-induced lateral root formation in Arabidopsis. Plant molecular biology 85 (1-2):49-61. doi:10.1007/s11103-013-0168-3

MacLeod RD (1990) Lateral root primordium inception in Zea mays L. Environmental and Experimental Botany 30:225–229

Majer C, Xu C, Berendzen KW, Hochholdinger F (2012) Molecular interactions of ROOTLESS CONCERNING CROWN AND SEMINAL ROOTS, a LOB domain protein regulating shoot-borne root initiation in maize (Zea mays L.). Philosophical Transactions of the Royal Society of London B Biological Sciences 367 (1595):1542-1551

Malamy JE, Benfey PN (1997) Organization and cell differentiation in lateral roots of Arabidopsis thaliana. Development 124 (1):33-44

Mallory TE, Chiang SH, Cutter EG, Gifford EM (1970) Sequence and pattern of lateral root formation in five selected species. American journal of botany 57:800-809

Manzano C, Pallero-Baena M, Casimiro I, De Rybel B, Orman-Ligeza B, Van Isterdael G, Beeckman T, Draye X, Casero P, Del Pozo JC (2014) The Emerging Role of Reactive Oxygen Species Signaling during Lateral Root Development. Plant physiology 165 (3):1105-1119. doi:10.1104/pp.114.238873

Marchant A, Bhalerao R, Casimiro I, Eklof J, Casero PJ, Bennett M, Sandberg G (2002) AUX1 promotes lateral root formation by facilitating indole-3-acetic acid distribution between sink and source tissues in the Arabidopsis seedling. The Plant cell 14 (3):589-597

Marchant A, Kargul J, May ST, Muller P, Delbarre A, Perrot-Rechenmann C, Bennett MJ (1999) AUX1 regulates root gravitropism in Arabidopsis by facilitating auxin uptake within root apical tissues. The EMBO journal 18 (8):2066-2073. doi:10.1093/emboj/18.8.2066

Mason MG, Jha D, Salt DE, Tester M, Hill K, Kieber JJ, Schaller GE (2010) Type-B response regulators ARR1 and ARR12 regulate expression of AtHKT1;1 and accumulation of sodium in Arabidopsis shoots. The Plant journal : for cell and molecular biology 64 (5):753-763. doi:10.1111/j.1365-313X.2010.04366.x

Mayer KF, Martis M, Hedley PE, Simkova H, Liu H, Morris JA, Steuernagel B, Taudien S, Roessner S, Gundlach H, Kubalakova M, Suchankova P, Murat F, Felder M, Nussbaumer T, Graner A, Salse J, Endo T, Sakai H, Tanaka T, Itoh T, Sato K, Platzer M, Matsumoto T, Scholz U, Dolezel J, Waugh R, Stein N (2011) Unlocking the barley genome by chromosomal and comparative genomics. The Plant cell 23 (4):1249-1263. doi:10.1105/tpc.110.082537

Mhamdi A, Queval G, Chaouch S, Vanderauwera S, Van Breusegem F, Noctor G (2010) Catalase function in plants: a focus on Arabidopsis mutants as stress-mimic models. Journal of experimental botany 61 (15):4197-4220. doi:10.1093/jxb/erq282

Michniewicz M, Brewer PB, Friml JI (2007) Polar auxin transport and asymmetric auxin distribution. The Arabidopsis book / American Society of Plant Biologists 5:e0108. doi:10.1199/tab.0108

Mikkelsen MD, Pedas P, Schiller M, Vincze E, Mills RF, Borg S, Moller A, Schjoerring JK, Williams LE, Baekgaard L, Holm PB, Palmgren MG (2012) Barley HvHMA1 is a heavy metal pump involved in mobilizing organellar Zn and Cu and plays a role in metal loading into grains. PloS one 7 (11):e49027. doi:10.1371/journal.pone.0049027

Mittler R (2002) Oxidative stress, antioxidants and stress tolerance. Trends in plant science 7 (9):405-410

Mochizuki S, Harada A, Inada S, Sugimoto-Shirasu K, Stacey N, Wada T, Ishiguro S, Okada K, Sakai T (2005) The Arabidopsis WAVY GROWTH 2 protein modulates root bending in response to environmental stimuli. The Plant cell 17 (2):537-547. doi:10.1105/tpc.104.028530

Monroe-Augustus M, Zolman BK, Bartel B (2003) IBR5, a dual-specificity phosphatase-like protein modulating auxin and abscisic acid responsiveness in Arabidopsis. The Plant cell 15 (12):2979-2991. doi:10.1105/tpc.017046

Monshausen GB, Bibikova TN, Messerli MA, Shi C, Gilroy S (2007) Oscillations in extracellular pH and reactive oxygen species modulate tip growth of Arabidopsis root hairs. Proceedings of the National Academy of Sciences of the United States of America 104 (52):20996-21001. doi:10.1073/pnas.0708586104

Monshausen GB, Bibikova TN, Weisenseel MH, Gilroy S (2009) Ca2+ regulates reactive oxygen species production and pH during mechanosensing in Arabidopsis roots. The Plant cell 21 (8):2341-2356. doi:10.1105/tpc.109.068395

Moreno-Risueno MA, Van Norman JM, Moreno A, Zhang J, Ahnert SE, Benfey PN (2010) Oscillating gene expression determines competence for periodic Arabidopsis root branching. Science 329 (5997):1306-1311. doi:10.1126/science.1191937

Mori IC, Pinontoan R, Kawano T, Muto S (2001) Involvement of superoxide generation in salicylic acid-induced stomatal closure in Vicia faba. Plant & cell physiology 42 (12):1383-1388

Moriwaki T, Miyazawa Y, Fujii N, Takahashi H (2012) Light and abscisic acid signalling are integrated by MIZ1 gene expression and regulate hydrotropic response in roots of Arabidopsis thaliana. Plant, cell & environment 35 (8):1359-1368. doi:10.1111/j.1365-3040.2012.02493.x

Mostajeran A, Rahimi-Eichi V (2008) Drought stress effects on root anatomical characteristics of rice cultivars (Oryza sativa L.). Pakistan journal of biological sciences: PJBS 11 (18):2173-2183

Mravec J, Kubes M, Bielach A, Gaykova V, Petrasek J, Skupa P, Chand S, Benkova E, Zazimalova E, Friml J (2008) Interaction of PIN and PGP transport mechanisms in auxin distribution-dependent development. Development 135 (20):3345-3354. doi:10.1242/dev.021071

Muhlenbock P, Plaszczyca M, Plaszczyca M, Mellerowicz E, Karpinski S (2007) Lysigenous aerenchyma formation in Arabidopsis is controlled by LESION SIMULATING DISEASE1. The Plant cell 19 (11):3819-3830. doi:10.1105/tpc.106.048843

Mullen JL, Hangarter RP (2003) Genetic analysis of the gravitropic set-point angle in lateral roots of Arabidopsis. Adv Space Res 31 (10):2229-2236

Muller K, Carstens AC, Linkies A, Torres MA, Leubner-Metzger G (2009) The NADPH-oxidase AtrbohB plays a role in Arabidopsis seed after-ripening. The New phytologist 184 (4):885-897. doi:10.1111/j.1469-8137.2009.03005.x

Navarre C, Sallets A, Gauthy E, Maitrejean M, Magy B, Nader J, Pety de Thozee C, Crouzet J, Batoko H, Boutry M (2011) Isolation of heat shock-induced Nicotiana tabacum transcription promoters and their potential as a tool for plant research and biotechnology. Transgenic research 20 (4):799-810. doi:10.1007/s11248-010-9459-5

Negi S, Ivanchenko MG, Muday GK (2008) Ethylene regulates lateral root formation and auxin transport in Arabidopsis thaliana. Plant Journal 55 (2):175-187. doi:10.1111/j.1365-313X.2008.03495.x

Neuteboom LW, Veth-Tello LM, Clijdesdale OR, Hooykaas PJ, van der Zaal BJ (1999) A novel subtilisin-like protease gene from Arabidopsis thaliana is expressed at sites of lateral root emergence. DNA research : an international journal for rapid publication of reports on genes and genomes 6 (1):13-19

Ng S, Ivanova A, Duncan O, Law SR, Van Aken O, De Clercq I, Wang Y, Carrie C, Xu L, Kmiec B, Walker H, Van Breusegem F, Whelan J, Giraud E (2013) A membrane-bound NAC transcription factor, ANAC017, mediates mitochondrial retrograde signaling in Arabidopsis. The Plant cell 25 (9):3450-3471. doi:10.1105/tpc.113.113985

Nishimura C, Ohashi Y, Sato S, Kato T, Tabata S, Ueguchi C (2004) Histidine kinase homologs that act as cytokinin receptors possess overlapping functions in the regulation of shoot and root growth in Arabidopsis. The Plant cell 16 (6):1365-1377. doi:10.1105/tpc.021477

Novak O, Henykova E, Sairanen I, Kowalczyk M, Pospisil T, Ljung K (2012) Tissue-specific profiling of the Arabidopsis thaliana auxin metabolome. The Plant journal : for cell and molecular biology 72 (3):523-536. doi:10.1111/j.1365-313X.2012.05085.x

Ohashi Y, Oka A, Rodrigues-Pousada R, Possenti M, Ruberti I, Morelli G, Aoyama T (2003) Modulation of phospholipid signaling by GLABRA2 in root-hair pattern formation. Science 300 (5624):1427-1430. doi:10.1126/science.1083695

Okumura K, Goh T, Toyokura K, Kasahara H, Takebayashi Y, Mimura T, Kamiya Y, Fukaki H (2013) GNOM/FEWER ROOTS is required for the establishment of an auxin response maximum for arabidopsis lateral root initiation. Plant & cell physiology 54 (3):406-417. doi:10.1093/pcp/pct018

Okushima Y, Fukaki H, Onoda M, Theologis A, Tasaka M (2007) ARF7 and ARF19 regulate lateral root formation via direct activation of LBD/ASL genes in Arabidopsis. The Plant cell 19 (1):118-130. doi:10.1105/tpc.106.047761

Orman-Ligeza B, Parizot B, Gantet PP, Beeckman T, Bennett MJ, Draye X (2013) Post-embryonic root organogenesis in cereals: branching out from model plants. Trends in plant science 18 (8):459-467. doi:10.1016/j.tplants.2013.04.010

Oztur ZN, Talame V, Deyholos M, Michalowski CB, Galbraith DW, Gozukirmizi N, Tuberosa R, Bohnert HJ (2002) Monitoring large-scale changes in transcript abundance in drought- and salt-stressed barley. Plant molecular biology 48 (5-6):551-573

Paponov IA, Teale WD, Trebar M, Blilou I, Palme K (2005) The PIN auxin efflux facilitators: evolutionary and functional perspectives. Trends in plant science 10 (4):170-177. doi:10.1016/j.tplants.2005.02.009

Parker JS, Cavell AC, Dolan L, Roberts K, Grierson CS (2000) Genetic interactions during root hair morphogenesis in Arabidopsis. . The Plant cell 12:1961–1974

Parry G, Calderon-Villalobos LI, Prigge M, Peret B, Dharmasiri S, Itoh H, Lechner E, Gray WM, Bennett M, Estelle M (2009) Complex regulation of the TIR1/AFB family of auxin receptors. Proceedings of the National Academy of Sciences of the United States of America 106 (52):22540-22545. doi:10.1073/pnas.0911967106

Passaia G, Spagnolo Fonini L, Caverzan A, Jardim-Messeder D, Christoff AP, Gaeta ML, de Araujo Mariath JE, Margis R, Margis-Pinheiro M (2013) The mitochondrial glutathione peroxidase GPX3 is essential for H2O2 homeostasis and root and shoot development in rice. Plant science : an international journal of experimental plant biology 208:93-101. doi:10.1016/j.plantsci.2013.03.017

Paterson AH, Bowers JE, Bruggmann R, Dubchak I, Grimwood J, Gundlach H, Haberer G, Hellsten U, Mitros T, Poliakov A, Schmutz J, Spannagl M, Tang H, Wang X, Wicker T, Bharti AK, Chapman J, Feltus FA, Gowik U, Grigoriev IV, Lyons E, Maher CA, Martis M, Narechania A, Otillar RP, Penning BW, Salamov AA, Wang Y, Zhang L, Carpita NC, Freeling M, Gingle AR, Hash CT, Keller B, Klein P, Kresovich S, McCann MC, Ming R, Peterson DG, Mehboob ur R, Ware D, Westhoff P, Mayer KF, Messing J, Rokhsar DS (2009) The Sorghum bicolor genome and the diversification of grasses. Nature 457 (7229):551-556. doi:10.1038/nature07723

Peeters AJM, Cox MCH, Benschop JJ, Vreeburg RAM, Bou J, Voesenek LACJ (2002) Submergence research using Rumex palustris as a model; looking back and going forward. Journal of experimental botany 53 (368):391-398. doi:10.1093/jexbot/53.368.391

Peret B, De Rybel B, Casimiro I, Benkova E, Swarup R, Laplaze L, Beeckman T, Bennett MJ (2009) Arabidopsis lateral root development: an emerging story. Trends in plant science 14 (7):399-408. doi:10.1016/j.tplants.2009.05.002

Peret B, Li G, Zhao J, Band LR, Voss U, Postaire O, Luu DT, Da Ines O, Casimiro I, Lucas M, Wells DM, Lazzerini L, Nacry P, King JR, Jensen OE, Schaffner AR, Maurel C, Bennett MJ (2012a) Auxin regulates aquaporin function to facilitate lateral root emergence. Nature cell biology 14 (10):991-998. doi:10.1038/ncb2573

Peret B, Swarup K, Ferguson A, Seth M, Yang Y, Dhondt S, James N, Casimiro I, Perry P, Syed A, Yang H, Reemmer J, Venison E, Howells C, Perez-Amador MA, Yun J, Alonso J, Beemster GT, Laplaze L, Murphy A, Bennett MJ, Nielsen E, Swarup R (2012b) AUX/LAX genes encode a family of auxin influx transporters that perform distinct functions during Arabidopsis development. The Plant cell 24 (7):2874-2885. doi:10.1105/tpc.112.097766

Peret B, Swarup R, Jansen L, Devos G, Auguy F, Collin M, Santi C, Hocher V, Franche C, Bogusz D, Bennett M, Laplaze L (2007) Auxin influx activity is associated with Frankia infection during actinorhizal nodule formation in Casuarina glauca. Plant physiology 144 (4):1852-1862. doi:10.1104/pp.107.101337

Perez-Amador MA, Leon J, Green PJ, Carbonell J (2002) Induction of the arginine decarboxylase ADC2 gene provides evidence for the involvement of polyamines in the wound response in Arabidopsis. Plant physiology 130 (3):1454-1463. doi:10.1104/pp.009951

Petrov VD, Van Breusegem F (2012) Hydrogen peroxide-a central hub for information flow in plant cells. AoB plants 2012:pls014. doi:10.1093/aobpla/pls014

Pitzschke A, Forzani C, Hirt H (2006) Reactive oxygen species signaling in plants. Antioxidants & redox signaling 8 (9-10):1757-1764. doi:10.1089/ars.2006.8.1757

Postma JA, Lynch JP (2011) Root cortical aerenchyma enhances the growth of maize on soils with suboptimal availability of nitrogen, phosphorus, and potassium. Plant physiology 156 (3):1190-1201. doi:10.1104/pp.111.175489

Prasad ME, Schofield A, Lyzenga W, Liu H, Stone SL (2010) Arabidopsis RING E3 ligase XBAT32 regulates lateral root production through its role in ethylene biosynthesis. Plant Physiol 153 (4):1587-1596.

Rani Debi B, Taketa S, Ichii M (2005) Cytokinin inhibits lateral root initiation but stimulates lateral root elongation in rice (Oryza sativa). Journal of Plant Physiology 162 (5):507-515

Rastogi S, Liberles DA (2005) Subfunctionalization of duplicated genes as a transition state to neofunctionalization. BMC evolutionary biology 5:28. doi:10.1186/1471-2148-5-28

Rebouillat A, Dievart A, Verdeil JL, Escoute J, Giese G, Breitler JC, Gantet P, Espeout S, Guiderdoni E, Périn C (2009) Molecular genetic of rice root development. Rice 2:15-34

Regina A, Kosar-Hashemi B, Ling S, Li Z, Rahman S, Morell M (2010) Control of starch branching in barley defined through differential RNAi suppression of starch branching enzyme IIa and IIb. Journal of experimental botany 61 (5):1469-1482. doi:10.1093/jxb/erq011

Remy E, Baster P, Friml J, Duque P (2013) ZIFL1.1 transporter modulates polar auxin transport by stabilizing membrane abundance of multiple PINs in Arabidopsis root tip. Plant signaling & behavior 8 (10):doi: 10 4161/psb 25688

Richards RA, Passioura JB (1989) A breeding program to reduce the diameter of the major xylem vessel in the seminal roots of wheat and its effect on grain yield in rain-fed environments. Australian Journal of Agricultural Research 40 (5):943 - 950

Robertson JM, Pharis RP, Huang YY, Reid DM, Yeung EC (1985) Drought-induced increases in abscisic Acid levels in the root apex of sunflower. Plant physiology 79 (4):1086-1089

Rogg LE, Lasswell J, Bartel B (2001) A gain-of-function mutation in IAA28 suppresses lateral root development. The Plant cell 13 (3):465-480

Ros Barcelo A (2005) Xylem parenchyma cells deliver the H2O2 necessary for lignification in differentiating xylem vessels. Planta 220 (5):747-756. doi:10.1007/s00425-004-1394-3

Roycewicz PS, Malamy JE (2014) Cell wall properties play an important role in the emergence of lateral root primordia from the parent root. Journal of experimental botany 65 (8):2057-2069. doi:10.1093/jxb/eru056

Ruiz-Sola MA, Arbona V, Gomez-Cadenas A, Rodriguez-Concepcion M, Rodriguez-Villalon A (2014) A root specific induction of carotenoid biosynthesis contributes to ABA production upon salt stress in arabidopsis. PloS one 9 (3):e90765. doi:10.1371/journal.pone.0090765

Rutschow HL, Baskin TI, Kramer EM (2011) Regulation of solute flux through plasmodesmata in the root meristem. Plant physiology 155 (4):1817-1826. doi:10.1104/pp.110.168187

Ryan E, Grierson CS, Cavell A, Steer M, Dolan L (1998) TIP1 is required for tip growth and non-tip growth in Arabidopsis. . New Phytol 138:49–58

Sato Y, Antonio BA, Namiki N, Takehisa H, Minami H, Kamatsuki K, Sugimoto K, Shimizu Y, Hirochika H, Nagamura Y (2011) RiceXPro: a platform for monitoring gene expression in japonica rice grown under natural field conditions. Nucleic acids research 39:1141-1148

Sauer M, Kleine-Vehn J (2011) AUXIN BINDING PROTEIN1: the outsider. The Plant cell 23 (6):2033-2043. doi:10.1105/tpc.111.087064

Scarpella E, Rueb S, Meijer AH (2003) The RADICLELESS1 gene is required for vascular pattern formation in rice. Development 130 (4):645-658

Scheres B, Laurenzio LD, Willemsen V, Hauser MT, Janmaat K, Weisbeek Pa, Benfey PN (1995) Mutations affecting the radial organisation of the Arabidopsis root display specific defects throughout the embryonic axis. Development 121:53-62

Schiefelbein JW, Somerville C (1990) Genetic Control of Root Hair Development in Arabidopsis thaliana. The Plant cell 2 (3):235-243. doi:10.1105/tpc.2.3.235

Schnable JC, Freeling M, Lyons E (2012) Genome-wide analysis of syntenic gene deletion in the grasses. Genome biology and evolution 4 (3):265-277. doi:10.1093/gbe/evs009

Schroeder JI, Kwak JM, Allen GJ (2001) Guard cell abscisic acid signalling and engineering drought hardiness in plants. Nature 410 (6826):327-330. doi:10.1038/35066500

Sedbrook JC, Carroll KL, Hung KF, Masson PH, Somerville CR (2002) The Arabidopsis SKU5 gene encodes an extracellular glycosyl phosphatidylinositol-anchored glycoprotein involved in directional root growth. The Plant cell 14 (7):1635-1648

Segal E, Kushnir T, Mualem Y, Shani U (2008) Water uptake and hydraulics of the root hair rhizosphere. Vandose Zone Journal 7:1027-1034

Shapiguzov A, Vainonen JP, Wrzaczek M, Kangasjarvi J (2012) ROS-talk - how the apoplast, the chloroplast, and the nucleus get the message through. Frontiers in plant science 3:292. doi:10.3389/fpls.2012.00292

Shen C, Bai Y, Wang S, Zhang S, Wu Y, Chen M, Jiang D, Qi Y (2010) Expression profile of PIN, AUX/LAX and PGP auxin transporter gene families in Sorghum bicolor under phytohormone and abiotic stress. The FEBS journal 277 (14):2954-2969. doi:10.1111/j.1742-4658.2010.07706.x

Shinozaki K, Yamaguchi-Shinozaki K, Seki M (2003) Regulatory network of gene expression in the drought and cold stress responses. Current opinion in plant biology 6 (5):410-417

Shkolnik-Inbar D, Bar-Zvi D (2010) ABI4 mediates abscisic acid and cytokinin inhibition of lateral root formation by reducing polar auxin transport in Arabidopsis. The Plant cell 22 (11):3560-3573. doi:10.1105/tpc.110.074641

Signora L, De Smet I, Foyer CH, Zhang H (2001) ABA plays a central role in mediating the regulatory effects of nitrate on root branching in Arabidopsis. The Plant journal : for cell and molecular biology 28 (6):655-662

Siyiannis VF, Protonotarios VE, Zechmann B, Chorianopoulou SN, Muller M, Hawkesford MJ, Bouranis DL (2012) Comparative spatiotemporal analysis of root aerenchyma formation processes in maize due to sulphate, nitrate or phosphate deprivation. Protoplasma 249 (3):671-686. doi:10.1007/s00709-011-0309-y

Smit AL, George E, Groenwold J (2000) Root observation and measurements at (transparent) interfaces with soil. In: Smit AL, Bengough AG, Engels C (eds) Root methods. A handbook. Springer, Berlin, Heidelberg, pp 235–272

Smith S, De Smet I (2012) Root system architecture: insights from Arabidopsis and cereal crops. Philosophical transactions of the Royal Society of London Series B, Biological sciences 367 (1595):1441-1452. doi:10.1098/rstb.2011.0234

Smyth GK (2004) Linear models and empirical bayes methods for assessing differential expression in microarray experiments. Statistical Applications in Genetics and Molecular Biology 3:Article 3. doi:10.2202/1544-6115.1027

Smyth GK, Michaud J, Scott HS (2005) Use of within-array replicate spots for assessing differential expression in microarray experiments. Bioinformatics 21 (9):2067-2075. doi:10.1093/bioinformatics/bti270

Sperry JS, Ikeda T (1997) Xylem cavitation in roots and stems of Douglas-fir and white fir. Tree physiology 17 (4):275-280

Sperry JS, Stiller V, Hacke U (2002) Soil water uptake and water transport through root systems. In: Waisel Y EA, Kafkafi U ((ed) Plant roots: the hidden half. Marcel Dek. , New York, pp 663–681

Sreevidya VS, Hernandez-Oane RJ, Gyaneshwar P, Lara-Flores M, Ladha JK, Reddy PM (2010) Changes in auxin distribution patterns during lateral root development in rice. Plant Science 178:531–538

Staal M, De Cnodder T, Simon D, Vandenbussche F, Van der Straeten D, Verbelen JP, Elzenga T, Vissenberg K (2011) Apoplastic alkalinization is instrumental for the inhibition of cell elongation in the Arabidopsis root by the ethylene precursor 1-aminocyclopropane-1-carboxylic acid. Plant physiology 155 (4):2049-2055. doi:10.1104/pp.110.168476

Steffens B, Kovalev A, Gorb SN, Sauter M (2012) Emerging Roots Alter Epidermal Cell Fate through Mechanical and Reactive Oxygen Species Signaling. The Plant Cell Online 24 (8):3296-3306. doi:10.1105/tpc.112.101790

Steffens B, Sauter M (2005) Epidermal Cell Death in Rice Is Regulated by Ethylene, Gibberellin, and Abscisic Acid. Plant physiology 139 (2):713-721. doi:10.1104/pp.105.064469

Steffens B, Sauter M (2009) Epidermal cell death in rice is confined to cells with a distinct molecular identity and is mediated by ethylene and H2O2 through an autoamplified signal pathway. The Plant cell 21 (1):184-196. doi:10.1105/tpc.108.061887

Steffens B, Wang J, Sauter M (2006) Interactions between ethylene, gibberellin and abscisic acid regulate emergence and growth rate of adventitious roots in deepwater rice. Planta 223 (3):604-612. doi:10.1007/s00425-005-0111-1

Steinmann T, Geldner N, Grebe M, Mangold S, Jackson CL, Paris S, Galweiler L, Palme K, Jurgens G (1999) Coordinated polar localization of auxin efflux carrier PIN1 by GNOM ARF GEF. Science 286 (5438):316-318

Strohm AK, Baldwin KL, Masson PH (2012) Multiple roles for membrane-associated protein trafficking and signaling in gravitropism. Frontiers in plant science 3:274. doi:10.3389/fpls.2012.00274

Swarup K, Benkova E, Swarup R, Casimiro I, Peret B, Yang Y, Parry G, Nielsen E, De Smet I, Vanneste S, Levesque MP, Carrier D, James N, Calvo V, Ljung K, Kramer E, Roberts R, Graham N, Marillonnet S, Patel K, Jones JD, Taylor CG, Schachtman DP, May S, Sandberg G, Benfey P, Friml J, Kerr I, Beeckman T, Laplaze L, Bennett MJ (2008) The auxin influx carrier LAX3 promotes lateral root emergence. Nature cell biology 10 (8):946-954. doi:10.1038/ncb1754

Swarup R, Friml J, Marchant A, Ljung K, Sandberg G, Palme K, Bennett M (2001) Localization of the auxin permease AUX1 suggests two functionally distinct hormone transport pathways operate in the Arabidopsis root apex. Genes & development 15 (20):2648-2653. doi:10.1101/gad.210501

Swarup R, Kargul J, Marchant A, Zadik D, Rahman A, Mills R, Yemm A, May S, Williams L, Millner P, Tsurumi S, Moore I, Napier R, Kerr ID, Bennett MJ (2004) Structure-function analysis of the presumptive Arabidopsis auxin permease AUX1. The Plant cell 16 (11):3069-3083. doi:10.1105/tpc.104.024737

Swarup R, Kramer EM, Perry P, Knox K, Leyser HM, Haseloff J, Beemster GT, Bhalerao R, Bennett MJ (2005) Root gravitropism requires lateral root cap and epidermal cells for transport and response to a mobile auxin signal. Nature cell biology 7 (11):1057-1065. doi:10.1038/ncb1316

Swarup R, Peret B (2012) AUX/LAX family of auxin influx carriers-an overview. Frontiers in plant science 3:225. doi:10.3389/fpls.2012.00225

Takehisa H, Sato Y, Igarashi M, Abiko T, Antonio BA, Kamatsuki K, Minami H, Namiki N, Inukai Y, Nakazono M, Nagamura Y (2012) Genome-wide transcriptome dissection of the rice root system: implications for developmental and physiological functions. Plant Journal 69 (1):126-140. doi:10.1111/j.1365-313X.2011.04777.x

Tamura K, Dudley J, Nei M, Kumar S (2007) MEGA4: Molecular Evolutionary Genetics Analysis (MEGA) software version 4.0. Molecular biology and evolution 24 (8):1596-1599. doi:10.1093/molbev/msm092

Taramino G, Sauer M, Stauffer JL, Jr., Multani D, Niu X, Sakai H, Hochholdinger F (2007) The maize (*Zea mays* L.) RTCS gene encodes a LOB domain protein that is a key regulator of embryonic seminal and post-embryonic shoot-borne root initiation. Plant Journal 50 (4):649-659

Terenius O, Papanicolaou A, Garbutt JS, Eleftherianos I, Huvenne H, Kanginakudru S, Albrechtsen M, An C, Aymeric JL, Barthel A, Bebas P, Bitra K, Bravo A, Chevalier F, Collinge DP, Crava CM, de Maagd RA, Duvic B, Erlandson M, Faye I, Felfoldi G, Fujiwara H, Futahashi R, Gandhe AS, Gatehouse HS, Gatehouse LN, Giebultowicz JM, Gomez I, Grimmelikhuijzen CJ, Groot AT, Hauser F, Heckel DG, Hegedus DD, Hrycaj S, Huang L, Hull JJ, Iatrou K, Iga M, Kanost MR, Kotwica J, Li C, Li J, Liu J, Lundmark M, Matsumoto S, Meyering-Vos M, Millichap PJ, Monteiro A, Mrinal N, Niimi T, Nowara D, Ohnishi A, Oostra V, Ozaki K, Papakonstantinou M, Popadic A, Rajam MV, Saenko S, Simpson RM, Soberon M, Strand MR, Tomita S, Toprak U, Wang P, Wee CW, Whyard S, Zhang W, Nagaraju J, Ffrench-Constant RH, Herrero S, Gordon K, Swevers L, Smagghe G (2011) RNA interference in Lepidoptera: an overview of successful and unsuccessful studies and implications for experimental design. Journal of insect physiology 57 (2):231-245. doi:10.1016/j.jinsphys.2010.11.006

Tian Q, Reed JW (1999) Control of auxin-regulated root development by the Arabidopsis thaliana SHY2/IAA3 gene. Development 126 (4):711-721

Tominaga-Wada R, Ishida T, Wada T (2011) New insights into the mechanism of development of Arabidopsis root hairs and trichomes. International review of cell and molecular biology 286:67-106. doi:10.1016/B978-0-12-385859-7.00002-1

Topp CN, Iyer-Pascuzzi AS, Anderson JT, Lee CR, Zurek PR, Symonova O, Zheng Y, Bucksch A, Mileyko Y, Galkovskyi T, Moore BT, Harer J, Edelsbrunner H, Mitchell-Olds T, Weitz JS, Benfey PN (2013) 3D phenotyping and quantitative trait locus mapping identify core regions of the rice genome controlling root architecture. Proceedings of the National Academy of Sciences of the United States of America 110 (18):E1695-1704. doi:10.1073/pnas.1304354110

Torres MA, Dangl JL, Jones JD (2002) Arabidopsis gp91phox homologues AtrbohD and AtrbohF are required for accumulation of reactive oxygen intermediates in the plant defense response. Proceedings of the National Academy of Sciences of the United States of America 99 (1):517-522. doi:10.1073/pnas.012452499

Trubat R, Cortina J, Vilagrosa A (2012) Root architecture and hydraulic conductance in nutrient deprived Pistacia lentiscus L. seedlings. Oecologia 170 (4):899-908. doi:10.1007/s00442-012-2380-2

Tsai YC, Weir NR, Hill K, Zhang W, Kim HJ, Shiu SH, Schaller GE, Kieber JJ (2012) Characterization of genes involved in cytokinin signaling and metabolism from rice. Plant physiology 158 (4):1666-1684. doi:10.1104/pp.111.192765

Ulmasov T, Murfett J, Hagen G, Guilfoyle TJ (1997) Aux/IAA proteins repress expression of reporter genes containing natural and highly active synthetic auxin response elements. The Plant cell 9 (11):1963-1971

Van Norman JM, Zhang J, Cazzonelli CI, Pogson BJ, Harrison PJ, Bugg TD, Chan KX, Thompson AJ, Benfey PN (2014) Periodic root branching in Arabidopsis requires synthesis of an uncharacterized carotenoid derivative. Proceedings of the National Academy of Sciences of the United States of America 111 (13):E1300-1309. doi:10.1073/pnas.1403016111

Vandenabeele S, Van Der Kelen K, Dat J, Gadjev I, Boonefaes T, Morsa S, Rottiers P, Slooten L, Van Montagu M, Zabeau M, Inze D, Van Breusegem F (2003) A comprehensive analysis of hydrogen peroxide-induced gene expression in tobacco. Proceedings of the National Academy of Sciences of the United States of America 100 (26):16113-16118. doi:10.1073/pnas.2136610100

Vandenbussche F, Petrasek J, Zadnikova P, Hoyerova K, Pesek B, Raz V, Swarup R, Bennett M, Zazimalova E, Benkova E, Van Der Straeten D (2010) The auxin influx carriers AUX1 and LAX3 are involved in auxin-ethylene interactions during apical hook development in Arabidopsis thaliana seedlings. Development 137 (4):597-606. doi:10.1242/dev.040790

Vanderauwera S, Zimmermann P, Rombauts S, Vandenabeele S, Langebartels C, Gruissem W, Inze D, Van Breusegem F (2005) Genome-wide analysis of hydrogen peroxide-regulated gene expression in Arabidopsis reveals a high light-induced transcriptional cluster involved in anthocyanin biosynthesis. Plant physiology 139 (2):806-821. doi:10.1104/pp.105.065896

Vanneste S, De Rybel B, Beemster GT, Ljung K, De Smet I, Van Isterdael G, Naudts M, Iida R, Gruissem W, Tasaka M, Inze D, Fukaki H, Beeckman T (2005) Cell cycle progression in the pericycle is not sufficient for SOLITARY ROOT/IAA14-mediated lateral root initiation in Arabidopsis thaliana. The Plant cell 17 (11):3035-3050. doi:10.1105/tpc.105.035493

Vartanian N, Marcotte L, Giraudat J (1994) Drought Rhizogenesis in Arabidopsis thaliana (Differential Responses of Hormonal Mutants). Plant physiology 104 (2):761-767

Vermeer JE, von Wangenheim D, Barberon M, Lee Y, Stelzer EH, Maizel A, Geldner N (2014) A spatial accommodation by neighboring cells is required for organ initiation in Arabidopsis. Science 343 (6167):178-183. doi:10.1126/science.1245871

Vilches-Barro A, Maizel A (2014) Talking through walls: mechanisms of lateral root emergence in Arabidopsis thaliana. Current opinion in plant biology 23C:31-38. doi:10.1016/j.pbi.2014.10.005

von Behrens I, Komatsu M, Zhang Y, Berendzen KW, Niu X, Sakai H, Taramino G, Hochholdinger F (2011) Rootless with undetectable meristem 1 encodes a monocot-specific AUX/IAA protein that controls embryonic seminal and post-embryonic lateral root initiation in maize. Plant Journal 66 (2):341-353. doi:10.1111/j.1365-313X.2011.04495.x

Walker AR, Davison PA, Bolognesi-Winfield AC, James CM, Srinivasan N, Blundell TL, Esch JJ, Marks MD, Gray JC (1999) The TRANSPARENT TESTA GLABRA1 locus, which regulates trichome differentiation and anthocyanin biosynthesis in Arabidopsis, encodes a WD40 repeat protein. The Plant cell 11 (7):1337-1350

Wang D, Pei K, Fu Y, Sun Z, Li S, Liu H, Tang K, Han B, Tao Y (2007) Genome-wide analysis of the auxin response factors (ARF) gene family in rice (*Oryza sativa*). Gene 394 (1-2):13-24

Wang H, Xiao W, Niu Y, Jin C, Chai R, Tang C, Zhang Y (2012) Nitric oxide enhances development of lateral roots in tomato (Solanum lycopersicum L.) under elevated carbon dioxide. Planta 237:137-144. doi:10.1007/s00425-012-1763-2

Wang JR, Hu H, Wang GH, Li J, Chen JY, Wu P (2009) Expression of PIN genes in rice (Oryza sativa L.): tissue specificity and regulation by hormones. Molecular Plant 2 (4):823-831. doi:10.1093/mp/ssp023

Wang S, Bai Y, Shen C, Wu Y, Zhang S, Jiang D, Guilfoyle TJ, Chen M, Qi Y (2010) Auxin-related gene families in abiotic stress response in Sorghum bicolor. Functional & Integrative Genomics 10 (4):533-546. doi:10.1007/s10142-010-0174-3

Wang S, Ichii M, Taketa S, Xu L, Xia Kai, Zhou Xie (2002a) Lateral root formation in rice (Oryza sativa): promotion effect of jasmonic acid. Journal of Plant Physiology 159 (8):827-832. doi:http://dx.doi.org/10.1078/0176-1617-00825

Wang W, Zheng H, Fan C, Li J, Shi J, Cai Z, Zhang G, Liu D, Zhang J, Vang S, Lu Z, Wong GK, Long M, Wang J (2006) High rate of chimeric gene origination by retroposition in plant genomes. The Plant cell 18 (8):1791-1802. doi:10.1105/tpc.106.041905

Wang X, Wu P, Xia M, Wu Z, Chen Q, Liu F (2002b) Identification of genes enriched in rice roots of the local nitrate treatment and their expression patterns in split-root treatment. Gene 297 (1-2):93-102

Wang X-F, He F-F, Ma X-X, Mao C-Z, Hodgman C, Lu C-G, Wu P (2011) OsCAND1 Is Required for Crown Root Emergence in Rice. Molecular Plant 4 (2):289-299. doi:10.1093/mp/ssq068

Waters MT, Brewer PB, Bussell JD, Smith SM, Beveridge CA (2012) The Arabidopsis ortholog of rice DWARF27 acts upstream of MAX1 in the control of plant development by strigolactones. Plant physiology 159 (3):1073-1085. doi:10.1104/pp.112.196253

Wei B, Zhang RZ, Guo JJ, Liu DM, Li AL, Fan RC, Mao L, Zhang XQ (2014) Genome-wide analysis of the MADS-box gene family in *Brachypodium* distachyon. PloS one 9 (1):e84781. doi:10.1371/journal.pone.0084781

Wei-Biao L, Mei-Ling Z., Gao-Bao H., Ji-Hua Y. (2012) Ca2+ and CaM are Involved in NO- and H2O2-Induced Adventitious Root Development in Marigold. J Plant Growth Regul 31:253–264

Weil CF (2009) TILLING in grass species. Plant physiology 149 (1):158-164. doi:10.1104/pp.108.128785

Werner T, Motyka V, Laucou V, Smets R, Van Onckelen H, Schmulling T (2003) Cytokinin-deficient transgenic Arabidopsis plants show multiple developmental alterations indicating opposite functions of cytokinins in the regulation of shoot and root meristem activity. The Plant cell 15 (11):2532-2550. doi:10.1105/tpc.014928

Whalen MC (1988) The effect of mechanical impedance on ethylene production by maize roots. Canadian Journal of Botany 66 (11):2139-2142

White RG, Kirkegaard JA (2010) The distribution and abundance of wheat roots in a dense, structured subsoil--implications for water uptake. Plant, cell & environment 33 (2):133-148. doi:10.1111/j.1365-3040.2009.02059.x

Williamson LC, Ribrioux SP, Fitter AH, Leyser HM (2001) Phosphate availability regulates root system architecture in Arabidopsis. Plant physiology 126 (2):875-882

Wilmoth JC, Wang S, Tiwari SB, Joshi AD, Hagen G, Guilfoyle TJ, Alonso JM, Ecker JR, Reed JW (2005) NPH4/ARF7 and ARF19 promote leaf expansion and auxin-induced lateral root formation. Plant Journal 43 (1):118-130

Woll K, Borsuk LA, Stransky H, Nettleton D, Schnable PS, Hochholdinger F (2005) Isolation, Characterization, and Pericycle-Specific Transcriptome Analyses of the Novel Maize Lateral and Seminal Root Initiation Mutant rum1. Plant physiology 139 (3):1255-1267. doi:10.1104/pp.105.067330

Wu Y, Messing J (2012) RNA interference can rebalance the nitrogen sink of maize seeds without losing hard endosperm. PloS one 7 (2):e32850. doi:10.1371/journal.pone.0032850

Xia K, Wang R, Ou X, Fang Z, Tian C, Duan J, Wang Y, Zhang M (2012) OsTIR1 and OsAFB2 downregulation via OsmiR393 overexpression leads to more tillers, early flowering and less tolerance to salt and drought in rice. PloS one 7 (1):e30039. doi:10.1371/journal.pone.0030039

Xiong J, Yang Y, Fu G, Tao L (2015) Novel roles of hydrogen peroxide (H O) in regulating pectin synthesis and demethylesterification in the cell wall of rice (Oryza sativa) root tips. The New phytologist. doi:10.1111/nph.13285

Xiong L, Wang RG, Mao G, Koczan JM (2006) Identification of drought tolerance determinants by genetic analysis of root response to drought stress and abscisic Acid. Plant physiology 142 (3):1065-1074. doi:10.1104/pp.106.084632

Xu J, Scheres B (2005) Dissection of Arabidopsis ADP-RIBOSYLATION FACTOR 1 function in epidermal cell polarity. The Plant cell 17 (2):525-536. doi:10.1105/tpc.104.028449

Yamada M, Sawa S (2012) The roles of peptide hormones during plant root development. Current opinion in plant biology. doi:10.1016/j.pbi.2012.11.004

Yamamoto Y, Kamiya N, Morinaka Y, Matsuoka M, Sazuka T (2007) Auxin biosynthesis by the YUCCA genes in rice. Plant physiology 143 (3):1362-1371. doi:10.1104/pp.106.091561

REFERENCES

Yang X, Li Y, Ren B, Ding L, Gao C, Shen Q, Guo S (2012) Drought-induced root aerenchyma formation restricts water uptake in rice seedlings supplied with nitrate. Plant & cell physiology 53 (3):495-504. doi:10.1093/pcp/pcs003

Yang Y, Hammes UZ, Taylor CG, Schachtman DP, Nielsen E (2006) High-affinity auxin transport by the AUX1 influx carrier protein. Current biology : CB 16 (11):1123-1127. doi:10.1016/j.cub.2006.04.029

Yoshida S, Forno DA, Cock JH, Gomez KA (1976) Laboratory Manual for Physiological Studies of Rice. . IRRI, Las Banos, Laguna

Young TE, Gallie DR (2000) Regulation of programmed cell death in maize endosperm by abscisic acid. Plant molecular biology 42 (2):397-414

Zadnikova P, Petrasek J, Marhavy P, Raz V, Vandenbussche F, Ding Z, Schwarzerova K, Morita MT, Tasaka M, Hejatko J, Van Der Straeten D, Friml J, Benkova E (2010) Role of PIN-mediated auxin efflux in apical hook development of Arabidopsis thaliana. Development 137 (4):607-617. doi:10.1242/dev.041277

Zalewski W, Galuszka P, Gasparis S, Orczyk W, Nadolska-Orczyk A (2010) Silencing of the HvCKX1 gene decreases the cytokinin oxidase/dehydrogenase level in barley and leads to higher plant productivity. Journal of experimental botany 61 (6):1839-1851. doi:10.1093/jxb/erq052

Zhang H, Han W, De Smet I, Talboys P, Loya R, Hassan A, Rong H, Jurgens G, Paul Knox J, Wang MH (2010) ABA promotes quiescence of the quiescent centre and suppresses stem cell differentiation in the Arabidopsis primary root meristem. The Plant journal : for cell and molecular biology 64 (5):764-774. doi:10.1111/j.1365-313X.2010.04367.x

Zhang W, Zhou X, Wen CK (2012) Modulation of ethylene responses by OsRTH1 overexpression reveals the biological significance of ethylene in rice seedling growth and development. Journal of experimental botany 63 (11):4151-4164. doi:10.1093/jxb/ers098

Zhang X, Zhang L, Dong F, Gao J, Galbraith DW, Song CP (2001) Hydrogen peroxide is involved in abscisic acid-induced stomatal closure in Vicia faba. Plant physiology 126 (4):1438-1448

Zhao R, Moriau L, M. B (1999) Expression analysis of the plasma membrane H+-ATPase pma4 transcription promoter from Nicotiana plumbaginifolia activated by the CaMV 35S promoter enhancer. Plant Science 149 (2):157-165

Zhao Y, Hu Y, Dai M, Huang L, Zhou DX (2009) The WUSCHEL-related homeobox gene WOX11 is required to activate shoot-borne crown root development in rice. The Plant cell 21 (3):736-748. doi:10.1105/tpc.108.061655

Zhao Y, Xing L, Wang X, Hou YJ, Gao J, Wang P, Duan CG, Zhu X, Zhu JK (2014) The ABA receptor PYL8 promotes lateral root growth by enhancing MYB77-dependent transcription of auxin-responsive genes. Science signaling 7 (328):ra53. doi:10.1126/scisignal.2005051

Zhu J, Ingram PA, Benfey PN, Elich T (2011) From lab to field, new approaches to phenotyping root system architecture. Current opinion in plant biology 14 (3):310-317. doi:10.1016/j.pbi.2011.03.020

Zhu ZX, Liu Y, Liu SJ, Mao CZ, Wu YR, Wu P (2012) A gain-of-function mutation in OsIAA11 affects lateral root development in rice. Molecular Plant 5 (1):154-161. doi:10.1093/mp/ssr074

Zou J, Zhang S, Zhang W, Li G, Chen Z, Zhai W, Zhao X, Pan X, Xie Q, Zhu L (2006) The rice HIGH-TILLERING DWARF1 encoding an ortholog of Arabidopsis MAX3 is required for negative regulation of the outgrowth of axillary buds. The Plant journal : for cell and molecular biology 48 (5):687-698. doi:10.1111/j.1365-313X.2006.02916.x

Zuchi S, Cesco S, Gottardi S, Pinton R, Romheld V, Astolfi S (2011) The root-hairless barley mutant brb used as model for assessment of role of root hairs in iron accumulation. Plant physiology and biochemistry : PPB / Societe francaise de physiologie vegetale 49 (5):506-512. doi:10.1016/j.plaphy.2010.12.005